Aix*Marseille université
Socialement engagée

NNT : 0000AIXM0000

THÈSE DE DOCTORAT

Soutenue à Aix-Marseille Université
le 13 septembre 2024 par

Gaëlle CAPITAINE

Etablir la traçabilité métrologique des mesures de l'acidification des eaux marines

Discipline
Sciences de l'environnement

Spécialité
Océanographie

École doctorale
ED251 : Sciences de l'environnement

Laboratoire/Partenaires de recherche
Institut Méditerranéen d'Océanologie – MIO
Laboratoire National de Métrologie et d'Essais - LNE

Composition du jury

Dr. Marta ÁLVAREZ Chargée de recherche, IEO	Rapporteuse
Pr. Andrew DICKSON Professeur émérite, UCSD	Rapporteur
Pr. Jean-François DOUSSIN Professeur des universités, UPEC CNRS	Examinateur
Pr. Sabrina SPEICH Professeure des universités, ENS Paris	Examinatrice
Pr. Thierry MOUTIN Professeur des universités, AMU	Président
Dr. Paola FISICARO Cadre scientifique des EPIC, LNE	Co-directrice de thèse
Dr. Thibaut WAGENER Maître de conférence, AMU	Directeur de thèse Non membre du jury
Dr. Regina EASLEY Chargée de recherche, NIST	Membre invitée
Pr. Simon CLEGG Professeur émérite, UEA	Membre invité

mio Institut Méditerranéen d'Océanologie

LABORATOIRE NATIONAL DE MÉTROLOGIE ET D'ESSAIS LNE

Affidavit

I, undersigned, Gaëlle Capitaine, hereby declare that the work presented in this manuscript is my own work, carried out under the scientific supervision of Thibaut Wagener and Paola Fisicaro, in accordance with the principles of honesty, integrity and responsibility inherent to the research mission. The research work and the writing of this manuscript have been carried out in compliance with both the French national charter for Research Integrity and the Aix-Marseille University charter on the fight against plagiarism.

This work has not been submitted previously either in this country or in another country in the same or in a similar version to any other examination body.

Paris, 17/06/2024

This thesis is dedicated in memory of Eunice Newton Foote, in tribute to her pioneering work on the greenhouse effect of carbon dioxide, which has been overlooked for too long, and for her activism for women's rights and equality, constituting a source of inspiration.

Scientific activities conducted during the thesis

Publications

Capitaine, G., Demeyer, S., Stoica, D., Alliouane, S., Petton, S., Rimmelin-Maury, P., Savoye, N., Wagener, T., Fisicaro, P., 2023a. Inter-laboratory comparison on a reference material for seawater spectrophotometric pHT measurements. Presented at the 2023 IEEE International Workshop on Metrology for the Sea; Learning to Measure Sea Health Parameters (MetroSea), La Valletta, Malta, pp. 11–15. https://doi.org/10.1109/MetroSea58055.2023.10317274

Capitaine, G., Stoica, D., Wagener, T., Fisicaro, P., 2023b. Production of a reference material for seawater pHT measurements by a National Metrology Institute. Marine Chemistry 252, 104244. https://doi.org/10.1016/j.marchem.2023.104244

Capitaine, G., Schäfer, R., Bastkowski, F., Pellegrino, O., Quendera, R., Achterberg, E., Wagener, T., Stoica, S.L. Clegg, D., Seitz, S., Fisicaro, P., In preparation. pHT measurements of TRIS buffer solutions in artificial seawater matrix in the salinity range 5–40 and temperature range 5–40 °C. Measurements and data fitting.

Capitaine, G., Alliouane, S., Cariou, T., Comeau, S., Fin, J., Gazeau, F., Fisicaro, P., Wagener, T., In preparation. Metrological tools applied to the measurement of Total Alkalinity of seawater.

Oral communications in conferences and workshops

1. Capitaine, G., Stoica, D., Demeyer, S., Fisicaro, P., 2022. Application des matériaux de référence pour les mesures de pHT. National scientific expertise consortium of ODATIS CO_2/pH marin, March 31st 2022, Paris.
2. Capitaine, G., Stoica, D., Fisicaro, P., Wagener, T., 2022. The role of quality control into the value chain of ocean carbon observations. ICOS International Conference, September 13th - 15th 2022, Utrecht.
3. Capitaine, G., Wagener T., 2022. Mesures de CO_2 océanique en Méditerranée : Exemple du pH, intérêt de la métrologie pour une meilleure qualité des données. Scientific presentation during the oceanographic cruise MOOSE-GE 2022, September 23rd 2022, on board of the *Pourquoi Pas ?*.
4. Capitaine, G., Stoica, D., Petit, S., Demeyer, S., Wagener, T., Fisicaro, P., 2022. Matériaux de référence pour la mesure du pHT : Exploitation des résultats obtenus sur le matériau distribué lors de l'intercomparaison SOMLIT 2021. Scientific workshop of the 2022 SOMLIT inter-laboratory comparison, October 20th 2022, Marseille.
5. Capitaine, G., Fisicaro, P., Wagener, T., 2023. L'intérêt de la métrologie pour le suivi de l'Alcalinité Totale des eaux marines. 30th Congress of the Environmental Sciences Doctoral School of Aix-Marseille University, May 3rd - 4th 2023, Marseille.

6. Capitaine, G., 2023. Le système des carbonates océanique : La qualité des mesures d'Alcalinité Totale et de pH pour le suivi de l'acidification des océans. Scientific presentation during the oceanographic cruise MOOSE-GE 2023, August 4th 2023, on board of the *Thalassa*.
7. Capitaine, G., Demeyer, S., Stoica, D., Alliouane, S., Petton, S., Rimmelin-Maury, P., Savoye, N., Wagener, T., Fisicaro, P., 2023. Inter-laboratory comparison on a reference material for seawater spectrophotometric pHT measurements. IEEE International Workshop on Metrology for the Sea (MetroSea), October 4th – 6th 2023, La Valletta.
8. Capitaine, G., Fisicaro, P., Wagener, T., 2023. Metrology for pHT and total alkalinity measurements results in assessing ocean acidification. Scientific workshop of the MINKE project inter-laboratory comparison, November 13th - 17th 2023, Marseille.
9. Capitaine, G., Fisicaro, P., Wagener, T., 2024. Quantification of seawater total alkalinity measurement uncertainty to support the evaluation of ocean alkalinity enhancement. EGU General Assembly 2024, April 15th - 19th 2024, Vienna.
10. Capitaine, G., Alasonati, E., Fisicaro, P., 2024. Results of the EMPIR project SapHTies : Metrology for standardised seawater pHT measurements in support of international and European climate strategies. CCQM Working Group on Electrochemical Analysis annual meeting, April 22nd 2024, Sèvres.
11. Capitaine, G., Fisicaro, P., Wagener, T., 2024. Metrological concepts applied to total alkalinity measurements in support of ocean alkalinity enhancement assessment. ICOS International Conference, September 10th - 13th 2024, Versailles.

Oceanographic cruises

Participation to MOOSE-GE (Mediterranean Ocean Observing System for the Environment – Grande Echelle) cruises in 2022, 2023 and 2024, each time for two weeks. Sampling for pH_T, dissolved oxygen and TA/DIC were performed as well as on board pH_T and dissolved oxygen analyses.

Collaborations

- Participations to the BIPM and EURAMET annual meetings with the electrochemical analyses working group.
- Hosting of Ukrainian counterpart Anton Petrenko for two months in the electrochemistry laboratory to work on primary measurements of TRIS buffers.
- Part I of the work presented, relative to the pH_T measurement method, was conducted within the Joint Research Project EMPIR 20NRM06 SApHTIES (https://projects.lne.eu/jrp-saphties/).
- Collaboration with the French community performing total alkalinity measurements and organisation of an inter-laboratory comparison for TA.

Outreach and public engagement

- Participation in the “Fête de la Science” (2021) with the presentation of LNE’s activities to the public
- Video of presentation of the thesis with the organization "l’Exploratoire" for their YouTube channel "99SEC.La dose de Science" (https://www.youtube.com/watch?v=uLO0C5hMqoY)
- Video of presentation of the thesis with LNE Communication Service (https://www.youtube.com/watch?v=uLGxvGZFigo)
- Participation in the “Fête de la Science” (2024) with a YouTube video about ocean acidification (https://www.youtube.com/watch?v=NNL4Zz9YUH0)

Additional training and courses

- Biogeochemical Cycles of the Ocean, ENS Paris (27 hours)
- ME13 – Evaluation of Measurement Uncertainties, LNE (21 hours)
- Summer School: Marine Protected Areas: Current Issues and Challenges, Ocean Sciences Institute (AMU) (35 hours)
- Scientific Publication: 1, General Issues & 2, Writing a Scientific Article (14 hours)
- European Research and Postdoctoral Funding (16 hours)
- MOOC: Research Ethics (10 hours)
- MOOC: Scientific Integrity in Research Professions (10 hours)
- Gender Equality in Academic and Professional Environments: The Effects of Gender Stereotypes (1.5 hours)

Résumé

Depuis le début de la révolution industrielle, la concentration en dioxyde de carbone (CO_2) dans l'atmosphère a augmenté de 50% en raison des activités humaines. L'océan absorbe chaque année environ 26% des émissions de CO_2. Cependant, cette absorption entraîne l'acidification des océans et la modification du système des carbonates. Ce qui, en affectant la stabilité des formes minérales du carbonate de calcium, impacte la biodiversité marine.

Les mesures océanographiques sont essentielles pour l'observation du système des carbonates océanique, soutenant la prise de décision en matière de stratégies d'atténuation et d'adaptation. La surveillance de l'acidification repose sur des mesures précises de variables comme le pH_T et l'alcalinité totale (AT). Pour garantir la qualité des données, des recommandations internationales et des guides de bonnes pratiques ont été établis, comme ceux du Réseau mondial d'observation de l'acidification des océans (GOA-ON), qui fixe des objectifs de qualité des données.

Les travaux de thèse visent à soutenir les océanographes avec des outils métrologiques permettant de garantir la comparabilité des résultats de mesure du pH_T et de l'AT. La métrologie, incluant la traçabilité, la validation des procédures de mesure et l'évaluation des incertitudes, est cruciale pour obtenir des résultats fiables et comparables, permettant une évaluation des tendances à long terme de l'acidification des océans.

Pour les deux paramètres, des matériaux de référence ont été développés et testés dans le cadre de comparaisons inter-laboratoires, permettant d'évaluer la précision et la justesse des méthodes de mesures. Les bilans d'incertitudes des mesures de pH_T et d'AT ont également été étudiés en suivant deux approches de quantification des incertitudes. Enfin l'amélioration des chaînes de traçabilité est présentée.

Mots-clés : Acidification des océans, système des carbonates, pH total, alcalinité totale, métrologie, traçabilité

Abstract

Since the beginning of the industrial revolution, the mole fraction of carbon dioxide (CO_2) in the atmosphere has increased by 50% due to human activities. Each year, the ocean absorbs around 26% of CO_2 emissions. However, this absorption leads to ocean acidification and changes in the carbonate system. This, by affecting the stability of calcium carbonate mineral forms, affects marine biodiversity.

Oceanographic measurements are essential for observing the oceanic carbonate system, supporting decision-making regarding mitigation and adaptation strategies. Monitoring acidification relies on accurate measurements of variables such as pH_T and total alkalinity (TA). To ensure data quality, international recommendations and best practice guidelines have been established, such as those from the Global Ocean Acidification Observing Network (GOA-ON), which sets data quality objectives.

The thesis work aims to support oceanographers with metrological tools to ensure the comparability of pH_T and TA measurement results. Metrology, including traceability, validation of measurement procedures, and uncertainty assessment, is crucial for obtaining reliable and comparable results, enabling the evaluation of long-term trends in ocean acidification.

For both parameters, reference materials have been developed and tested in inter-laboratory comparisons, allowing the evaluation of the precision and trueness of measurement methods. The uncertainty budgets of pH_T and TA measurements have also been studied using two approaches of uncertainty quantification. Finally, improvements to the traceability chains are presented.

Keywords: Ocean acidification, carbonate system, total pH, total alkalinity, metrology, traceability

Acknowledgments

De nombreuses personnes ont contribué à l'aboutissement de cette thèse, par leurs conseils et leur soutien, et je tiens à les en remercier.

Je tiens tout d'abord à remercier mes directrice et directeur de thèse, Paola Fisicaro et Thibaut Wagener. Merci à tous les deux pour votre générosité dans le partage de votre savoir et pour votre bienveillance. Paola, merci pour toute la confiance que tu m'accordes, pour ta disponibilité, et pour tes conseils précieux. Thibaut, merci de m'avoir fait découvrir ce monde merveilleux de l'océanographie, de m'avoir permis d'embarquer sur les missions MOOSE, et pour ta bonne humeur constante. Je suis très reconnaissante d'avoir réalisé cette thèse sous votre direction.

Merci à Daniela Stoica pour m'avoir accompagnée dans les débuts de cette thèse, pour m'avoir guidée au laboratoire et pour m'avoir partagé son gout pour la métrologie et pour l'électrochimie.

I am grateful to all the members of the thesis committee, Marta Álvarez, Simon Clegg, Andrew Dickson, Jean-François Doussin, Regina Easley, Thierry Moutin and Sabrina Speich, for agreeing to evaluate my work and be part of the jury.

Merci aux membres de mon comité de suivi de thèse : David Nerini, Bruno Lansard et Florence Salvetat, pour vos conseils et les échanges toujours constructifs.

Many thanks to all the partners of the SapHTies project and to the community of metrologists working on electrochemical measurements, with special acknowledgments to Steffen Seitz, and Anton Petrenko. Merci également à la communauté océanographique française travaillant sur le système des carbonates : les membres du service d'observation SOMLIT pour le pH ; Samir Alliouane, Thierry Cariou, Steeve Comeau, Jonathan Fin et Frédéric Gazeau pour la partie alcalinité ; et aux collègues du MIO. La collaboration avec toutes ces personnes fut absolument essentielle dans l'obtention des résultats présentés.

Merci aux équipes scientifiques et aux équipages que j'ai eu l'occasion de côtoyer lors des missions MOOSE. Avec une pensée spéciale pour Louise, Luther, Sandra, Théo, Thibault, Yves et Elisabeth.

Au LNE, il y a également de nombreuses personnes à remercier : Romy, Isabel, Hélène, Chloé, Samy, Maxence, merci infiniment pour tous les très chouettes moments partagés ; Caro et Véro pour votre bienveillance, votre écoute et pour me faire toujours rire ; Enrica pour ton soutien ; Vincent pour ton aide au laboratoire. Merci aussi à Béatrice, Amandine, Chiara, Johanna et à tous·tes les collègues de la chimie. Merci à Jabran, Nicolas, Séverine et Sébastien pour votre aide sur les traitements statistiques et les budgets d'incertitudes.

Un immense merci à mes ami·e·s de l'ENSCM, pour tous nos week-ends de retrouvailles, avec une mention spéciale pour Justine et Antoine pour les

décompressions autour de pressions, et encore plus particulièrement à Morgane, la meilleure coloc qui soit. Votre présence aura été essentielle.

Clément, merci de m'avoir encouragée à me lancer dans cette aventure qu'est la thèse, et de m'avoir soutenue.

Je tiens également à remercier tous·tes mes camarades écologistes, et plus particulièrement mes ami·e·s : Margot, Corentin, Robin, Olivia, Clément, Clémence, Guillaume... Car tous les moments partagés avec vous depuis trois ans furent des moments où la thèse n'existait plus, et je crois que ça fait du bien, ça, des fois. Et puis pour ces causes que nous portons ensemble, qui donnent espoir en ces temps troublés.

Lila, Kilian, Guilhem, Julien, vous revoir lors de mes passages en Bretagne est toujours un réel plaisir, merci d'être toujours là après toutes ces années.

Merci à Quentin pour ta présence et ton incroyable soutien durant ces derniers mois importants.

Papa, Maman, merci pour tout, merci de m'avoir toujours encouragée et soutenue. Et puis aussi pour les bons petits plats et les balades en bord de mer lors de mes passages en Bretagne. Merci aussi à mes grands-parents, pour l'intérêt et la curiosité dont vous faites preuve pour tout ce qui est important pour nous, et pour croire en nous.

Il reste une personne que je souhaite remercier particulièrement. Merci Anna, car je pense que ma passion pour la chimie m'a en partie été transmise par toi, car tu m'as montré que la thèse, en plus d'être épanouissante scientifiquement, pouvait aussi être de très belles années. Merci de m'avoir accueillie si souvent chez toi à Marseille et enfin merci pour ton soutien constant, depuis toujours.

Contents

List of figures

General Introduction

1. From the XIXth century to nowadays: studies of a world increasingly rich in CO_2 and the role of the ocean

1.1. The origin of the Anthropocene

The term "Anthropocene", introduced by Crutzen and Stoermer (2000), designates the current geological epoch for which the impacts of human activities on earth and atmosphere have led to distinct changes in geology and ecology. Human activities started to have a significant impact on climate and on ecosystems, on a commonly accepted basis, at the industrial revolution around 1800, also described as the origin of the "Great Acceleration" (Steffen et al., 2015, 2011). Some studies link the roots of the Anthropocene to an older origin, when humans started mastering their environment. The agricultural revolution about 8000 years ago was thus also proposed as the origin of the Anthropocene (Gowdy and Krall, 2013; Ruddiman, 2003).

The beginning of the industrial revolution is associated to the spread of James Watt's steam engine, mainly in Great Britain's cotton mills. The steam engine, using coal as power source, widely replaced water wheels in these industries in the first half of the XIXth century (Malm, 2013). This turning point in industrial history led to the exponential amount of carbon dioxide (CO_2) emitted into the atmosphere. CO_2 mole fraction in the atmosphere has increased by 50 % since that time, going from about 280 parts per million (ppm) prior to the industrial revolution up to 421 ppm in 2022 (NOAA, 2022).

1.2. Discovery of the greenhouse effect and establishment of the impact of human activities on climate

Eunice Newton Foote published in 1856 a paper entitled "Circumstances affecting the heat of sun's rays" in the American Journal of Art and Science (Newton Foote, 1856). She was the first one to demonstrate the relation between carbon dioxide concentration and atmosphere temperature rising, later described as greenhouse effect. In the next years, John Tyndall demonstrated the heat radiation absorbing power of water vapour, carbon dioxide and ozone gases (Jackson, 2019; Tyndall, 1861).

In 1896, Svante Arrhenius published a first estimation of carbon dioxide gas contribution to the greenhouse effect (Arrhenius, 1896; Fleming, 1998). However, it would take until 1938 and the work of Guy Callendar to actually quantify the impact of fossil fuels burning coming from human activities on the increase in atmospheric carbon dioxide concentration, and on the increase in mean temperature (Callendar, 1938). At that time, he estimated a temperature increase rate of 0.003°C per year due to fuel combustion of that time, and quantified a temperature increase rate of 0.005°C per year in the preceding half century. The major novelty of Callendar's work compared

to the one of Arrhenius relied on scaling down the estimation of the amount of CO_2 taken up by the ocean, as discussed in the next section.

1.3. Recognition of the ocean CO_2 uptake and physico-chemical characterization of the marine CO_2 system

In the first half of the XX^{th} century, the ocean was already recognised for its important capacity to absorb carbon dioxide from the atmosphere (Gruber et al., 2023). By measuring radioactive ^{14}C, Revelle and Suess were able to estimate CO_2 air-sea exchange in 1957 (Revelle and Suess, 1957). Their study allowed them to realize that the importance of the ocean in absorbing part of atmospheric carbon dioxide was overestimated by Arrhenius, whereas it was underestimated in later studies by Callendar.

In the meantime, studies were conducted in order to describe the marine CO_2 system. The understanding of solution chemistry concepts such as the dissociation of ionic species in solution have initiated the work leading to the description of carbonic acid dissociation constants by Kurt Buch and co-workers in 1932 (Dickson, 1992; Schneider and Matthäus, 2023).

1.4. Current state

Since the first work of Eunice Newton Foote to the present day, many researchers, including the ones aforementioned, contributed to assess the impact CO_2 emitted from human activities has on the climate and ecosystems, and the important role of the ocean acting as a carbon sink.

The last report of the Working Group I of the Intergovernmental Panel on Climate Change (IPCC) established a mean increase in global surface temperature of 1.1°C since the industrial revolution due to human activities (fossil fuel burning, cement industry and land-use change) (IPCC, 2021). 2023 alone has broken records and is now the warmest year, with a temperature of 1.4 ± 0.12°C above the 1850-1900 baseline (World Meteorological Organization, 2023). The increase of temperature leads to several impacts on the climate system such as occurrence of droughts and precipitations, lower snow cover extent, proportion of intense tropical cyclones and sea level rise. These phenomena have direct impacts on both human society and ecosystems (IPCC, 2022).

Among the 10.9 gigatonnes of carbon (GtC) emitted each year on average in the atmosphere in the last decade (2013-2022), it is estimated that 48% remained in the atmosphere, acting as greenhouse gas, and contributing to the effects aforementioned (Friedlingstein et al., 2023). The remaining emissions were partitioned between land uptake, driven by plant photosynthesis (about 30%) and ocean uptake, driven by air-sea surface disequilibrium (about 26%). The ocean plays a major role as a carbon sink allowing climate change attenuation.

2. The Ocean Carbon Cycle

2.1. The physical and biological pumps

Chemistry, physics and biology drive the transport of carbon into the ocean. The vertical transport of carbon is described by the term "Carbon Pump". Two types of carbon pumps are identified: the physical pump and the biological pump (Figure 1) (Bopp et al., 2019; Emerson and Hedges, 2008).

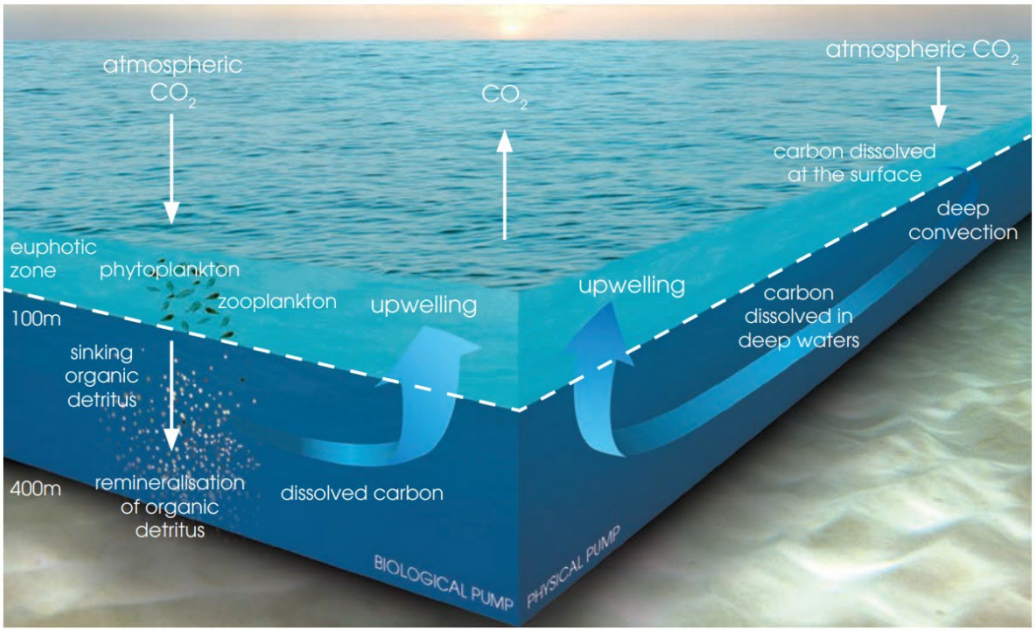

Figure 1: The two oceanic carbon pumps: the biological pump and the physical pump. From Bopp *et al.,* 2019.

The physical pump is driven by seawater salinity and temperature. The temperature directly affects the carbon dioxide solubility. Carbon dioxide solubility in seawater indeed decreases with temperature, which, combined with variation in salinity, total carbon and total alkalinity of seawater from artic to tropics, lead to less CO_2 absorption at the tropics than at higher latitudes. Salinity and temperature of seawater also directly act on its density, driving the vertical gradient of the physical pump and thermohaline circulation of the ocean, leading to sinking of enriched CO_2 water for example in the North Atlantic. Whereas in upwelling regions as Northern Pacific and Indian Ocean, CO_2 can diffuse back to the atmosphere (Gruber et al., 2009).

The biological pump, also called soft tissue pump, is driven by photosynthesis and the transfer of organic carbon through the trophic levels. Phytoplankton need both nutrients and dissolved inorganic carbon to produce organic matter by photosynthetic activity in the euphotic layer. This process leads to the production of particulate organic carbon. A small portion of these particles sink down to the sediments while the

remainder is remineralized through respiration process. A linked process is the carbonate pump, or hard-tissue pump, where calcium carbonate ($CaCO_3$) produced by biological activity sinks vertically in the ocean.

The physical and biological pumps of the ocean carbon cycle both lead to the regulation of carbon circulation in the oceans. They also rely on one another to ensure the sequestration of carbon and the supply of nutrients to marine ecosystems. The two pumps are subject to important seasonal and regional variabilities (Rustogi et al., 2023; Wimart-Rousseau et al., 2021). Inter-annual variabilities also come from other forces such as the El Nino – Southern Oscillation (ENSO) phenomenon, which reduces the upwelling process in the Pacific Ocean, leading to less inorganic supply of carbon at the ocean surface.

2.2. Anthropogenic perturbation of the carbon cycle

Climate change resulting from human activities directly affects the ocean carbon cycle (IPCC, 2019). The solubility of CO_2 and thus its absorption in seawater is impacted with rising temperatures. Simultaneously, the vertical mixing and the global ocean circulation is slowing down, conducting to a sharper stratification and reducing the sinking of inorganic carbon in the ocean depths. Perturbation of biological activity is hard to predict as it also depends on other environmental factors and compensating effects, it is however predicted that the net primary productivity (representing an increase in biomass), will decline by 4% to 11% by 2100 relative to the decade 2006-2015 (IPCC, 2019).

A recent study from Müller and co-workers (Müller et al., 2023) showed that the global amount of stored anthropogenic CO_2 grew at a lesser extent than had been predicted from the increase in atmospheric CO_2, showing the vulnerability of the ocean carbon sink to climate change.

2.3. The oceanic carbonate system

The carbonate system is a major concept for the ocean carbon cycle as it affects the buffer capacity of the ocean, the partial pressure of carbon dioxide and the amount of calcium carbonate formation (Emerson and Hedges, 2008).

Four independently measurable variables can be used for the subsequent description of the ocean carbonate system: the dissolved inorganic carbon, the total alkalinity, pH and the partial pressure of carbon dioxide (Dickson *et al.*, 2007). It is defined by the chemical equilibria below (Figure 2), considering dissolved carbon dioxide, bicarbonate (HCO_3^-) and carbonate ions (CO_3^{2-}).

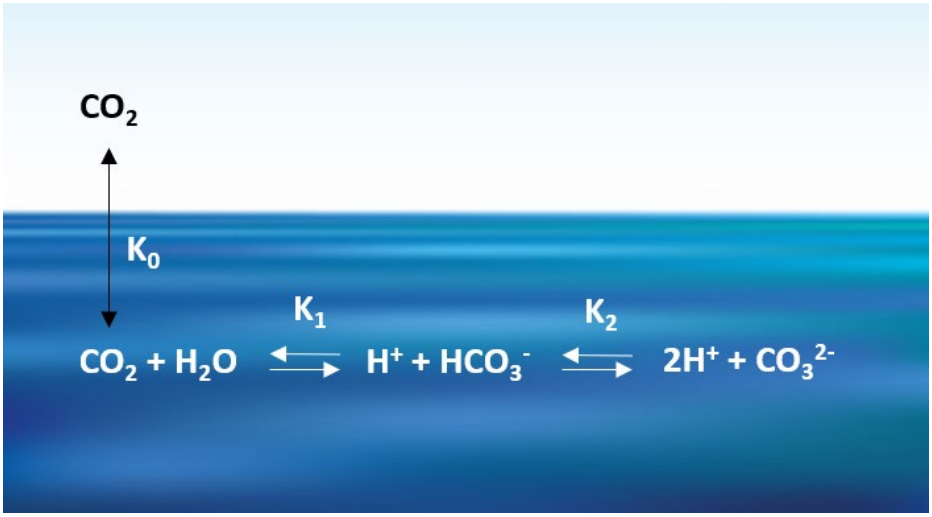

Figure 2: Oceanic carbonate system equilibrium, where K_0 represents CO_2 solubility and K_1 and K_2 the dissociation constants of the bicarbonate and carbonate ions.

Dissolved Inorganic Carbon

The dissolved inorganic carbon (DIC) variable is defined as the sum of the amount contents of the chemical species considered in the ocean carbonate system (equation I.1).

$$\mathrm{DIC} = [{CO_2}^*] + [{HCO_3}^-] + [{CO_3}^{2-}] \quad \text{(I.1)}$$

where ${CO_2}^*$ represents dissolved carbon dioxide, either present as H_2CO_3 or CO_2. Amount contents [i] are expressed in moles per kilogram of solution (noted mol/kg-sol).

Total Alkalinity

The Total Alkalinity (TA) can be understood as the ability of seawater to mitigate variations in acidity. It is defined as being the amount content of excess proton acceptors over proton donors in seawater (equation I.2).

$$\begin{aligned}\mathrm{TA} = {} & [{HCO_3}^-] + 2[{CO_3}^{2-}] + [{B(OH)_4}^-] + [{OH}^-] + [{HPO_4}^{2-}] \\ & + 2[{PO_4}^{3-}] + [{SiO(OH)_3}^-] + [{NH_3}] + [{HS}^-] + [\dots] - [{H^+}]_F - \\ & [{HSO_4}^-] - [HF] - [H_3PO_4] - [\dots]\end{aligned} \quad \text{(I.2)}$$

where ellipses represent minor species unidentified or negligible.

pH on the total scale

The pH on the total scale, noted pH_T, is based on a reference state in a constant ionic medium. It considers amount contents of free hydrogen ions, $[H^+]_F$, and hydrogen ions

combined with sulphate ions, [HSO_4^-], involved in the following equilibria, and defined according to equations I.3.a and I.3.b.

$$SO_4^{2-} + H^+ \rightleftharpoons HSO_4^-$$

$$pH_T = -\lg [H^+]_T \quad \text{(I.3.a)}$$

$$[H^+]_T = [H^+]_F \ (1 + S_T/K_S) \approx [H^+]_F + [HSO_4^-] \quad \text{(I.3.b)}$$

where S_T is the total sulphate amount content ($[HSO_4^-] + [SO_4^{2-}]$) and K_S is the dissociation constant of HSO_4^-.

Partial pressure of carbon dioxide

The partial pressure of carbon dioxide, noted pCO_2, is defined for a gas phase, i.e. air, in equilibrium with a sample of seawater (equation I.4).

$$pCO_2 = x(CO_2) \times p \quad \text{(I.4)}$$

where x represents the mole fraction of CO_2 in the equilibrated air, and p the pressure at which the equilibration is made (in atm).

These measurements allow estimation of air-sea CO_2 fluxes from differences in pCO_2.

For a particular seawater sample, two of these four variables depend on temperature and pressure: pH_T and pCO_2, while the two others do not. The knowledge of two measurable carbonate system variables, combined with the dissociation constants and information on salinity, temperature and pressure, allows to compute the two others, as well as other variables describing the carbonate system.

The various processes coming from the ocean carbon cycle physical and biological pumps (CO_2 fluxes, photosynthesis, $CaCO_3$ formation...) affect the different variables of the carbonate system. These can be well described by representing changes in DIC, TA and pH coming from these processes (Figure 3, Zeebe and Wolf-Gladrow, 2001).

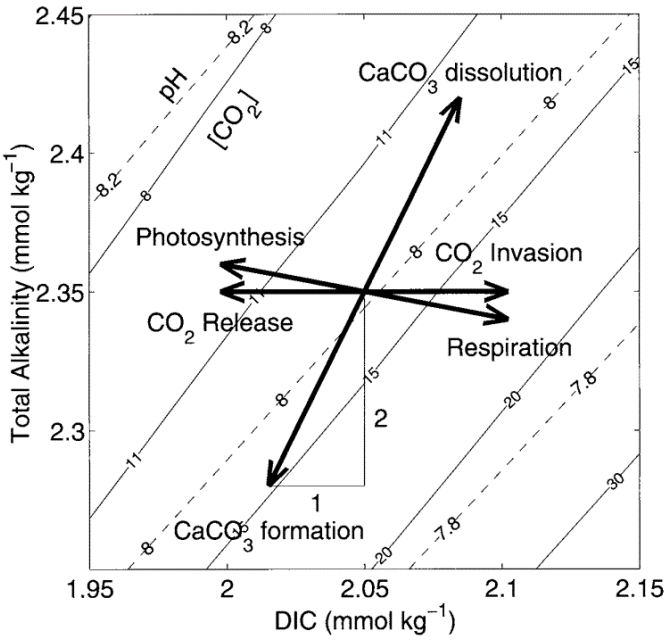

Figure 3: Effects of the various processes (except mixing) that constitute the ocean carbon cycles on changes in DIC, TA and pH. From Zeebe and Wolg-Gadrow, 2001.

3. Ocean acidification and its impacts

3.1. Chemical phenomenon and carbonate system perturbation

The increasing amount of carbon dioxide dissolved in the ocean, induced by the increasing anthropogenic CO_2 emissions, modifies the carbonate system equilibrium. Which results in the release of hydrogen ions in the marine environment, and thus to the decrease of seawater pH_T (equation I.3.a; Figure 4). This chemical phenomenon is described as anthropogenic ocean acidification (OA). In addition, the modification of the carbonate system equilibrium results in the consumption of carbonate ions, acting as a buffer to limit acidification. It reduces the stability of mineral forms of calcium carbonate, mainly present in the form of aragonite and calcite (IPCC, 2019).

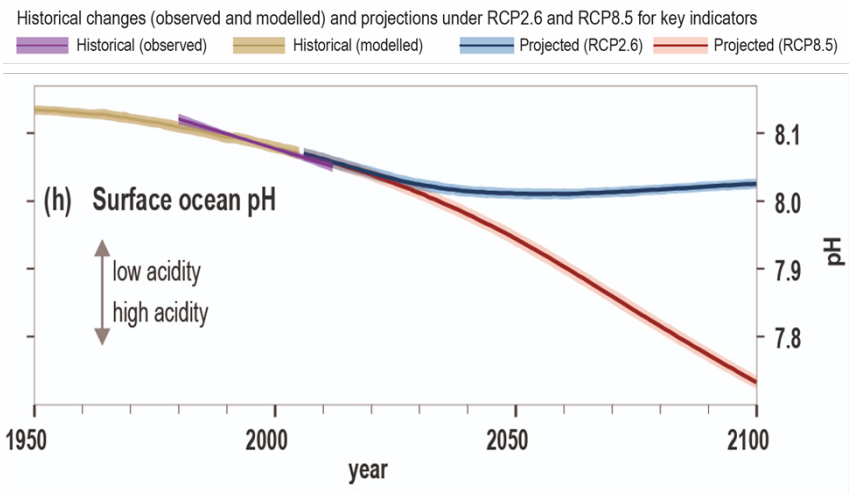

Figure 4: Observed and modelled changes in the global mean surface pH on the total scale (i.e. pH_T). Where RCP2.6 and RCP8.5 corresponds, respectively, to low and high greenhouse gas emissions scenarios of the IPCC. From IPCC, 2019.

It is estimated that the pH_T of the ocean has decreased by at least 0.1 since the preindustrial time and that the pH_T continues to decrease at a rate between 0.017 and 0.027 per decade since 1980s (Figure 4, IPCC, 2019).

3.2. Impacts on the biodiversity

The carbonate ion decrease in the marine environment hinders the calcification process of many marine species with $CaCO_3$ shells and skeletons, such as molluscs or corals. It leads to a lower calcification rate, but also to malformation or dissolution of the carbonate structure (Rastelli et al., 2020).

By affecting coral reefs, as well as other marine animals able to build calcareous seabed, ocean acidification influences their ability of homing various other species. This results in less complex, rich and extensive biogenic reefs (Hall-Spencer and Harvey, 2019).

The decrease of seawater pH_T also leads to a harsher environment for the renewal of marine species by affecting early life stages, such as the larval settlement of corals, echinoderms or fishes (Albright, 2011; Espinel Velasco et al., 2018).

The impact of ocean acidification on marine species is highly dependent on taxonomic groups and on several other factors, as life stage, nutrient supply or adaptation ability. However, it is globally observed that a decrease in survival, calcification, growth, development and abundance is caused by OA (Kroeker et al., 2013).

3.3. Socio-economic impacts

The ocean has a great social and economic importance for humankind. Coastal and marine ecosystems, being affected by ocean acidification, results in direct and indirect socio-economic impacts.

The main impact is on the fishery and aquaculture sectors around the world, affecting the largest economies, such as the United States or Canada (Cooley and Doney, 2009; Wilson et al., 2020), but also small island developing states (Schmutter et al., 2017). Different regions of the world face specific problems. As an example, the red coral of the Mediterranean Sea is an important and emblematic species for both jewellery and tourism. Income losses are predicted in these sectors due to the impact of ocean acidification on red coral development (Rodrigues et al., 2013). These phenomena have direct social implications in terms of job availability in fisheries, aquaculture and tourism industries but also for food security.

Other anthropogenic induced climatic phenomenon, such as sea-level rise and occurrence of extreme events, combined to the higher vulnerability of coral reefs, partly caused by ocean acidification, lead to a higher exposure of coastal communities to floods and erosion (Lam et al., 2019).

Several of these impacts can be monetarily quantified in terms of income loss or restoration investments. The loss in the world economy is estimated to be US $1 trillion per year by 2100 if ocean acidification isn't mitigated (Secretariat of the Convention on Biological Diversity, 2014). However, the ties that bind people to their habitat from a cultural point of view, such as spiritual enrichment and aesthetic appreciation, are also important and the implications of OA are more difficult to assess.

4. International governance system and recommendations to address and monitor ocean acidification

4.1. A governance system for international action

The international scope of both causes and impacts of ocean acidification requires an international governance system in order to address this problem with policy actions. This falls under the scope of various organizations governed by the United Nations, as the United Nations Framework Convention for Climate Change (UNFCCC), the Convention on Biological Diversity (CBD) or the Intergovernmental Oceanographic Commission (IOC) (Harrould-Kolieb and Hoegh-Guldberg, 2019; Turley and Gattuso, 2012).

In 2015, the United Nations Member States adopted the 2030 Agenda for Sustainable Development, including 17 Sustainable Development Goals (SDGs). One indicator of the SDG 14, "Conserve and sustainably use the oceans, seas and marine resources for sustainable development", aims to minimize and address ocean acidification through enhanced scientific cooperation at all levels (SDG 14.3) (United Nations, 2015). Harrould-Kolieb and Hoegh-Guldberg (2019), proposed a governing framework with three main objectives to drive international ocean acidification policy: mitigation, adaptation and redress.

4.2. Control variables for monitoring ocean acidification

In-situ oceanographic observations and measurements are the first step of the value chain aiming at tracking seawater CO_2. Treatment and analysis of collected data, with the use of models, enable climate assessments. It constitutes the basis for the preparation of United Nations reports and influences decision making on mitigation and adaptation strategies (Jiang et al., 2023).

Ocean acidification can be studied based on the monitoring of different parameters, such as the concentration of the carbonate ions and the calcium carbonate mineral saturation state (under the form of either aragonite or calcite), noted Ω (equation I.5) (GOA-ON, 2019; Rockström et al., 2009).

$$\Omega = \frac{[Ca^{2+}]_T \times [CO_3^{2-}]_T}{K_{sp}^*} \quad \text{(I.5)}$$

where $[Ca^{2+}]_T$ and $[CO_3^{2-}]_T$ represent the total amount contents of calcium and carbonate ions in seawater respectively, and K_{sp}^* the solubility product of the aragonite or calcite at the in-situ temperature, salinity and pressure conditions (Zeebe and Wolf-Gladrow, 2001).

These two variables can be computed from the knowledge of two of the four independently measurable variables of the ocean carbonate system, as well as from dissociation constants and information on salinity, temperature and pressure.

The calcium carbonate mineral saturation state decreases with ocean acidification, towards the threshold value of one, which describes the under-saturation of calcium carbonate and the closeness to a corrosive environment. This parameter gives direct information over the ability of calcifying organisms to form $CaCO_3$ in the studied seawater. This threshold value has already been reached for aragonite in summer surface waters of the Canada Basin of the Arctic Ocean (Yamamoto-Kawai et al., 2009).

4.3. International data quality requirements

One main objective for monitoring ocean acidification is the assessment of long-term trends. In order to do so, several metrological challenges have to be faced to ensure data comparability and to reduce measurement uncertainties. This latter aspect is even more important given the seasonal variability of variables measured for OA monitoring.

In order to establish significant long term-trends with high confidence, international recommendations and best practices guides have been made available in recent decades. Below are listed four of the main international recommendations concerning ocean acidification monitoring:

(1) One task of the SDG 14.3, aiming to coordinate seawater pH_T measurements, gives a methodology and recommendations for the conduction of the measurements and their report in the databases (IOC-UNESCO, 2019).
(2) The Global Ocean Acidification Observing Network (GOA-ON) has fixed a data quality objective for the monitoring of ocean acidification, called the "climate" quality objective, with maximum uncertainties target in each of the input variables in order to have a standard uncertainty of 1% in the carbonate ion's amount content (GOA-ON, 2019).
(3) The World Meteorological Organization (WMO) reports the need to sustain and extend ocean CO_2 observations (WMO, 2015).
(4) The Global Climate Observing System, a programme sustained by different organizations of the United Nations, also acts to improve data quality and fill gaps of data (WMO et al., 2022).

Requirements for high data quality become even more stringent as data shared in international databases are collected over diverse spatial and temporal scales, from many sources and with a large variety of instruments (Pearlman et al., 2019). This also makes standardisation of data management a priority (Jiang et al., 2022).

The computation, from two measured variables, of other variables, is also a metrological challenge as it can be an additional source of error. Indeed, discrepancies have been reported between observed and calculated values (Carter et al., 2023; Takeshita et al., 2020). This highlights the importance of in-situ measurements, as required by the WMO, and a greater metrological focus on measurement techniques.

5. Thesis objectives

The work hereafter presented addresses this need for high data quality for the monitoring of ocean acidification. The overall objective of the thesis is to support oceanographers with metrological tools to guarantee the comparability of measurement

results. The thesis focuses on the measurements of two of the four independently measurable variables: pH_T and total alkalinity (TA). These two parameters have been selected among the four possible because they are already widely studied using benchtop devices. pH_T observations have also been enhanced by the development of in-situ sensors (Seidel et al., 2008; Yin et al., 2021). For these two variables, several metrological issues still remain.

Metrology is essential to meet the data quality objective required by the GOA-ON. Among the metrological principles, metrological traceability is the notion according to which measurement results can be linked to a single reference ("JCGM 200:2012," 2012). In addition, the validation of measurement procedures, achieved through inter-laboratory comparisons (ILCs) or the use of reference materials, as well as the evaluation of measurement uncertainties, are essential principles. The application of these three main principles guarantees reliable measurement results that are comparable over time and space, allowing for the assessment of long-term trends. The aim of the thesis is to apply these three principles to the measurement of both pH_T and total alkalinity of seawater.

The first chapter details the scientific basis on which the present work relies, the state of the art of metrology applied to ocean acidification monitoring, and remaining issues that the thesis work aims to address. This integrates measurement and data treatment methods for the study of both pH_T and total alkalinity.

The conducted work is presented in two main parts. Part I presents the studies conducted on pH_T measurements:

- Chapter 2 introduces reference material production for seawater spectrophotometric pH_T measurement, which is the standard measurement method for pH_T. It includes batch homogeneity, long-term stability assessments and a detailed uncertainty budget attributed to the characterized pH_T value. An inter-laboratory comparison conducted with 13 laboratories on this reference material is presented.
- Chapter 3 presents the characterization of equimolal TRIS buffers in the salinity range 5-40 and temperature range 5-40°C. This provides for a fit function for the pH_T of TRIS buffers dependant on salinity and temperature, consistent for the whole salinity and temperature ranges that are most relevant for oceanographic measurements. This function is suitable for the characterization of the indicator dye used for pH_T spectrophotometric measurement. Traceability of pH_T measurement results is also discussed in this chapter.
- Chapter 4 details the uncertainty sources of the spectrophotometric pH_T measurement method and presents the uncertainty quantification of absorbance values, in the context of achieving a complete uncertainty budget of spectrophotometric pH_T values.

Part II focuses on seawater total alkalinity measurements:

- Chapter 5 focuses on the application of the different metrological tools for TA. Two reference materials have been produced and tested in an inter-laboratory comparison conducted with five participants. The uncertainty budget of the standardized measurement method (i.e. potentiometric titration) together with Gran's data treatment is assessed following two approaches for uncertainty quantification. Finally, a route for better traceability of TA results, including the two materials developed, is proposed.

The chapter "Conclusion and perspectives" summarizes the major results obtained during the thesis. The levels of uncertainty estimated for pH_T and total alkalinity measurements are combined and propagated to estimate uncertainties of other variables of the oceanic carbonate system. Remaining metrological issues are exposed. Finally, the contribution of the work presented to the evaluation of currently developing marine Carbon Dioxide Removal methods such as the Ocean Alkalinity Enhancement is further discussed.

References

Albright, R., 2011. Reviewing the Effects of Ocean Acidification on Sexual Reproduction and Early Life History Stages of Reef-Building Corals. Hindawi Publishing Corporation Journal of Marine Biology 14. https://doi.org/10.1155/2011/473615

Arrhenius, S., 1896. On the Influence of Carbonic Acid in the Air upon the Temperature of the Ground. Philosophical Magazine and Journal of Science, Series 5 41, 237–276.

Bopp, L., Bowler, C., Guidi, L., Karsenti, E., de Vargas, C., 2019. The Ocean: a Carbon Pump.

Callendar, G.S., 1938. The artificial production of carbon dioxide and its influence on temperature. Quarterly Journal of the Royal Meteorological Society 64, 223–240. https://doi.org/10.1002/qj.49706427503

Carter, B.R., Sharp, J.D., Dickson, A.G., Álvarez, M., Fong, M.B., García-Ibáñez, M.I., Woosley, R.J., Takeshita, Y., Barbero, L., Byrne, R.H., Cai, W.-J., Chierici, M., Clegg, S.L., Easley, R.A., Fassbender, A.J., Fleger, K.L., Li, X., Martín-Mayor, M., Schockman, K.M., Wang, Z.A., 2023. Uncertainty sources for measurable ocean carbonate chemistry variables. Limnology and Oceanography n/a. https://doi.org/10.1002/lno.12477

Cooley, S.R., Doney, S.C., 2009. Anticipating ocean acidification's economic consequences for commercial fisheries. Environ. Res. Lett. 4, 024007. https://doi.org/10.1088/1748-9326/4/2/024007

Crutzen, P.J., Stoermer, E.F., 2000. The "Anthropocene." IGBP Newsletter The International Geosphere–Biosphere Programme (IGBP): A Study of Global Change of the International Council for Science (ICSU).

Dickson, A.G., 1992. The development of the alkalinity concept in marine chemistry. Marine Chemistry, Progress in Marine Chemistry 40, 49–63. https://doi.org/10.1016/0304-4203(92)90047-E

Dickson, A.G., Sabine, C.L., Christian, J.R. (Eds.), 2007. Guide to Best Practices for Ocean CO2 Measurements PICES Special Publication 3, 191.

Emerson, S., Hedges, J., 2008. Chemical Oceanography and the Marine Carbon Cycle. Cambridge University Press, Cambridge. https://doi.org/10.1017/CBO9780511793202

Espinel Velasco, N., Hoffmann, L., Agüera, A., Byrne, M., Dupont, S., Uthicke, S., Webster, N., Lamare, M., 2018. Effects of ocean acidification on the settlement and metamorphosis of marine invertebrate and fish larvae: A review. Marine Ecology Progress Series 606. https://doi.org/10.3354/meps12754

Fleming, J.R., 1998. Arrhenius and current climate concerns: Continuity or a 100-year gap? Eos, Transactions American Geophysical Union 79, 405–410. https://doi.org/10.1029/98EO00310

Friedlingstein, P., O'Sullivan, M., Jones, M.W., Andrew, R.M., Bakker, D.C.E., Hauck, J., Landschützer, P., Le Quéré, C., Luijkx, I.T., Peters, G.P., Peters, W., Pongratz, J., Schwingshackl, C., Sitch, S., Canadell, J.G., Ciais, P., Jackson, R.B., Alin, S.R., Anthoni, P., Barbero, L., Bates, N.R., Becker, M., Bellouin, N., Decharme, B., Bopp, L., Brasika, I.B.M., Cadule, P., Chamberlain, M.A., Chandra, N., Chau, T.-T.-T., Chevallier, F., Chini, L.P., Cronin, M., Dou, X., Enyo, K., Evans, W., Falk, S., Feely, R.A., Feng, L., Ford, D.J., Gasser, T., Ghattas, J., Gkritzalis, T., Grassi, G., Gregor, L., Gruber, N., Gürses, Ö., Harris, I., Hefner, M., Heinke, J., Houghton, R.A., Hurtt, G.C., Iida, Y., Ilyina, T., Jacobson, A.R., Jain, A., Jarníková, T., Jersild, A., Jiang, F., Jin, Z., Joos, F., Kato, E., Keeling, R.F., Kennedy, D., Klein Goldewijk, K., Knauer, J., Korsbakken, J.I., Körtzinger, A., Lan, X., Lefèvre, N., Li, H., Liu, J., Liu, Z., Ma, L., Marland, G., Mayot, N., McGuire, P.C., McKinley, G.A., Meyer, G., Morgan, E.J., Munro, D.R., Nakaoka, S.-I., Niwa, Y., O'Brien, K.M., Olsen, A., Omar, A.M., Ono, T., Paulsen, M., Pierrot, D., Pocock, K., Poulter, B., Powis, C.M., Rehder, G., Resplandy, L., Robertson, E., Rödenbeck, C., Rosan, T.M., Schwinger, J., Séférian, R., Smallman, T.L., Smith, S.M., Sospedra-Alfonso, R., Sun, Q., Sutton, A.J., Sweeney, C., Takao, S., Tans, P.P., Tian, H., Tilbrook, B., Tsujino, H., Tubiello, F., van der Werf, G.R., van Ooijen, E., Wanninkhof, R., Watanabe, M., Wimart-Rousseau, C., Yang, D., Yang, X., Yuan, W., Yue, X., Zaehle, S., Zeng, J., Zheng, B., 2023. Global Carbon Budget 2023. Earth System Science Data 15, 5301–5369. https://doi.org/10.5194/essd-15-5301-2023

GOA-ON, 2019. Global Ocean Acidification Observing Network (GOA-ON): Implementation Strategy.

Gowdy, J., Krall, L., 2013. The ultrasocial origin of the Anthropocene. Ecological Economics 95, 137–147. https://doi.org/10.1016/j.ecolecon.2013.08.006

Gruber, N., Bakker, D.C.E., DeVries, T., Gregor, L., Hauck, J., Landschützer, P., McKinley, G.A., Müller, J.D., 2023. Trends and variability in the ocean carbon sink. Nat Rev Earth Environ 4, 119–134. https://doi.org/10.1038/s43017-022-00381-x

Gruber, N., Gloor, M., Mikaloff Fletcher, S.E., Doney, S.C., Dutkiewicz, S., Follows, M.J., Gerber, M., Jacobson, A.R., Joos, F., Lindsay, K., Menemenlis, D., Mouchet, A., Müller, S.A., Sarmiento, J.L., Takahashi, T., 2009. Oceanic sources, sinks, and transport of atmospheric CO2. Global Biogeochemical Cycles 23. https://doi.org/10.1029/2008GB003349

Hall-Spencer, J.M., Harvey, B.P., 2019. Ocean acidification impacts on coastal ecosystem services due to habitat degradation. Emerging Topics in Life Sciences 3, 197–206. https://doi.org/10.1042/ETLS20180117

Harrould-Kolieb, E.R., Hoegh-Guldberg, O., 2019. A governing framework for international ocean acidification policy. Marine Policy 102, 10–20. https://doi.org/10.1016/j.marpol.2019.02.004

IOC-UNESCO, 2019. Indicator Methodology for SDG 14.3.1 (Report). International Oceanographic Commission of UNESCO.

IPCC, 2022. 2022: Summary for Policymakers In: Climate Change 2022: Impacts, Adaptation and Vulnerability. Contribution of Working Group II to the Sixth Assessment Report of the Intergovernmental Panel on Climate Change [H.-O. Pörtner, D.C. Roberts, M. Tignor, E.S. Poloczanska, K. Mintenbeck, A. Alegría, M. Craig, S. Langsdorf, S. Löschke, V. Möller, A. Okem, B. Rama (eds.)]. Cambridge University Press, Cambridge, UK and New York, NY, USA, pp. 3–33. https://doi.org/10.1017/9781009325844.001

IPCC, 2021. 2021: Technical Summary In Climate Change 2021: The Physical Science Basis. Contribution of Working Group I to the Sixth Assessment Report of the Intergovernmental Panel on Climate Change [Masson-Delmotte, V., P. Zhai, A. Pirani, S.L. Connors, C. Péan, S. Berger, N. Caud, Y. Chen, L. Goldfarb, M.I. Gomis, M. Huang, K. Leitzell, E. Lonnoy, J.B.R. Matthews, T.K. Maycock, T. Waterfield, O. Yelekçi, R. Yu, and B. Zhou (eds.)]. Cambridge University Press, Cambridge, United Kingdom and New York, NY, USA, p. 33–144. https://doi.org/10.1017/9781009157896.002

IPCC, 2019. 2019: Technical Summary In: IPCC Special Report on the Ocean and Cryosphere in a Changing Climate [H.-O. Pörtner, D.C. Roberts, V. Masson-Delmotte, P. Zhai, M. Tignor, E. Poloczanska, K. Mintenbeck, A. Alegría, M. Nicolai, A. Okem, J. Petzold, B. Rama, N.M. Weyer (eds.)]. Cambridge University Press, Cambridge, UK and New York, NY, USA, pp. 39–69. https://doi.org/10.1017/9781009157964.002

Jackson, R., 2019. Eunice Foote, John Tyndall and a question of priority. Notes and Records: the Royal Society Journal of the History of Science 74, 105–118. https://doi.org/10.1098/rsnr.2018.0066

JCGM 200:2012, 2012. International vocabulary of metrology (VIM) — Basic and general concepts and associated terms.

Jiang, L.-Q., Kozyr, A., Relph, J.M., Ronje, E.I., Kamb, L., Burger, E., Myer, J., Nguyen, L., Arzayus, K.M., Boyer, T., Cross, S., Garcia, H., Hogan, P., Larsen, K., Parsons, A.R., 2023. The Ocean Carbon and Acidification Data System. Sci Data 10, 136. https://doi.org/10.1038/s41597-023-02042-0

Jiang, L.-Q., Pierrot, D., Wanninkhof, R., Feely, R.A., Tilbrook, B., Alin, S., Barbero, L., Byrne, R.H., Carter, B.R., Dickson, A.G., Gattuso, J.-P., Greeley, D., Hoppema, M., Humphreys, M.P., Karstensen, J., Lange, N., Lauvset, S.K., Lewis, E.R., Olsen, A., Pérez, F.F., Sabine, C., Sharp, J.D., Tanhua, T., Trull, T.W., Velo, A., Allegra, A.J., Barker, P., Burger, E., Cai, W.-J., Chen, C.-T.A., Cross, J., Garcia, H., Hernandez-Ayon, J.M., Hu, X., Kozyr, A., Langdon, C., Lee, K., Salisbury, J., Wang, Z.A., Xue, L., 2022. Best Practice Data Standards for Discrete Chemical Oceanographic Observations. Frontiers in Marine Science 8.

Kroeker, K.J., Kordas, R.L., Crim, R., Hendriks, I.E., Ramajo, L., Singh, G.S., Duarte, C.M., Gattuso, J.-P., 2013. Impacts of ocean acidification on marine organisms: quantifying sensitivities and

interaction with warming. Global Change Biology 19, 1884–1896. https://doi.org/10.1111/gcb.12179

Lam, V.W.Y., Chavanich, S., Djoundourian, S., Dupont, S., Gaill, F., Holzer, G., Isensee, K., Katua, S., Mars, F., Metian, M., Hall-Spencer, J.M., 2019. Dealing with the effects of ocean acidification on coral reefs in the Indian Ocean and Asia. Regional Studies in Marine Science 28, 100560. https://doi.org/10.1016/j.rsma.2019.100560

Malm, A., 2013. The Origins of Fossil Capital: From Water to Steam in the British Cotton Industry. Historical Materialism.

Müller, J.D., Gruber, N., Carter, B., Feely, R., Ishii, M., Lange, N., Lauvset, S.K., Murata, A., Olsen, A., Pérez, F.F., Sabine, C., Tanhua, T., Wanninkhof, R., Zhu, D., 2023. Decadal Trends in the Oceanic Storage of Anthropogenic Carbon From 1994 to 2014. AGU Advances 4, e2023AV000875. https://doi.org/10.1029/2023AV000875

Newton Foote, E., 1856. Circumstances Affecting the Heat of Sun's Rays. American Journal of Art and Science, 2nd Series XXII, 382–383.

NOAA, 2022. Carbon dioxide now more than 50% higher than pre-industrial levels [WWW Document]. noaa.gov. URL https://www.noaa.gov/news-release/carbon-dioxide-now-more-than-50-higher-than-pre-industrial-levels (accessed 11.18.22).

Pearlman, J., Bushnell, M., Coppola, L., Karstensen, J., Buttigieg, P.L., Pearlman, F., Simpson, P., Barbier, M., Muller-Karger, F.E., Munoz-Mas, C., Pissierssens, P., Chandler, C., Hermes, J., Heslop, E., Jenkyns, R., Achterberg, E.P., Bensi, M., Bittig, H.C., Blandin, J., Bosch, J., Bourles, B., Bozzano, R., Buck, J.J.H., Burger, E.F., Cano, D., Cardin, V., Llorens, M.C., Cianca, A., Chen, H., Cusack, C., Delory, E., Garello, R., Giovanetti, G., Harscoat, V., Hartman, S., Heitsenrether, R., Jirka, S., Lara-Lopez, A., Lantéri, N., Leadbetter, A., Manzella, G., Maso, J., McCurdy, A., Moussat, E., Ntoumas, M., Pensieri, S., Petihakis, G., Pinardi, N., Pouliquen, S., Przeslawski, R., Roden, N.P., Silke, J., Tamburri, M.N., Tang, H., Tanhua, T., Telszewski, M., Testor, P., Thomas, J., Waldmann, C., Whoriskey, F., 2019. Evolving and Sustaining Ocean Best Practices and Standards for the Next Decade. Frontiers in Marine Science 6, 277. https://doi.org/10.3389/fmars.2019.00277

Rastelli, E., Petani, B., Corinaldesi, C., Dell'Anno, A., Lo Martire, M., Cerrano, C., Danovaro, R., 2020. A high biodiversity mitigates the impact of ocean acidification on hard-bottom ecosystems. Sci Rep 10, 2948. https://doi.org/10.1038/s41598-020-59886-4

Revelle, R., Suess, H.E., 1957. Carbon Dioxide Exchange Between Atmosphere and Ocean and the Question of an Increase of Atmospheric CO2 during the Past Decades. Tellus 9, 18–27. https://doi.org/10.1111/j.2153-3490.1957.tb01849.x

Rockström, J., Steffen, W., Noone, K., Persson, Å., Chapin, F.S.I., Lambin, E., Lenton, T., Scheffer, M., Folke, C., Schellnhuber, H.J., Nykvist, B., de Wit, C., Hughes, T., van der Leeuw, S., Rodhe, H., Sörlin, S., Snyder, P., Costanza, R., Svedin, U., Falkenmark, M., Karlberg, L., Corell, R., Fabry, V., Hansen, J., Walker, B., Liverman, D., Richardson, K., Crutzen, P., Foley, J., 2009. Planetary Boundaries: Exploring the Safe Operating Space for Humanity. Ecology and Society 14 (2), art32. https://doi.org/10.5751/ES-03180-140232

Rodrigues, L.C., van den Bergh, J.C.J.M., Ghermandi, A., 2013. Socio-economic impacts of ocean acidification in the Mediterranean Sea. Marine Policy 38, 447–456. https://doi.org/10.1016/j.marpol.2012.07.005

Ruddiman, W., 2003. The Anthropogenic Greenhouse Era Began Thousands of Years Ago. Climatic Change 61, 261-293, https://doi.org/10.1023/B:CLIM.0000004577.17928.fa

Rustogi, P., Landschützer, P., Brune, S., Baehr, J., 2023. The impact of seasonality on the annual air-sea carbon flux and its interannual variability. npj Clim Atmos Sci 6, 1–8. https://doi.org/10.1038/s41612-023-00378-3

Schmutter, K., Nash, M., Dovey, L., 2017. Ocean acidification: assessing the vulnerability of socioeconomic systems in Small Island Developing States. Reg Environ Change 17, 973–987. https://doi.org/10.1007/s10113-016-0949-8

Schneider, B., Matthäus, W., 2023. The history of chemical concepts and field studies of CO2 in seawater: A tribute to Kurt Buch (1881–1967). Marine Chemistry 248, 104204. https://doi.org/10.1016/j.marchem.2022.104204

Secretariat of the Convention on Biological Diversity, 2014. An Updated Synthesis of the Impacts of Ocean Acidification on Marine Biodiversity.

Seidel, M.P., DeGrandpre, M.D., Dickson, A.G., 2008. A sensor for in situ indicator-based measurements of seawater pH. Marine Chemistry 109, 18–28. https://doi.org/10.1016/j.marchem.2007.11.013

Steffen, W., Broadgate, W., Deutsch, L., Gaffney, O., Ludwig, C., 2015. The trajectory of the Anthropocene: The Great Acceleration. The Anthropocene Review 2, 81–98. https://doi.org/10.1177/2053019614564785

Steffen, W., Grinevald, J., Crutzen, P., McNeill, J., 2011. The Anthropocene: conceptual and historical perspectives. Philosophical Transactions of the Royal Society A: Mathematical, Physical and Engineering Sciences 369, 842–867. https://doi.org/10.1098/rsta.2010.0327

Takeshita, Y., Johnson, K.S., Coletti, L.J., Jannasch, H.W., Walz, P.M., Warren, J.K., 2020. Assessment of pH dependent errors in spectrophotometric pH measurements of seawater. Marine Chemistry 223, 103801. https://doi.org/10.1016/j.marchem.2020.103801

Turley, C., Gattuso, J.-P., 2012. Future biological and ecosystem impacts of ocean acidification and their socioeconomic-policy implications. Current Opinion in Environmental Sustainability, Aquatic and marine systems 4, 278–286. https://doi.org/10.1016/j.cosust.2012.05.007

Tyndall, J., 1861. The Bakerian Lecture: On the Absorption and Radiation of Heat by Gases and Vapours, and on the Physical Connexion of Radiation, Absorption, and Conduction. Philosophical Transactions of the Royal Society of London 151, 1–36.

United Nations, 2015. Transforming our world: the 2030 Agenda for Sustainable Development A/RES/70/1.

Wilson, T.J.B., Cooley, S.R., Tai, T.C., Cheung, W.W.L., Tyedmers, P.H., 2020. Potential socioeconomic impacts from ocean acidification and climate change effects on Atlantic Canadian fisheries. PLOS ONE 15, e0226544. https://doi.org/10.1371/journal.pone.0226544

Wimart-Rousseau, C., Wagener, T., Álvarez, M., Moutin, T., Fourrier, M., Coppola, L., Niclas-Chirurgien, L., Raimbault, P., D'Ortenzio, F., Durrieu de Madron, X., Taillandier, V., Dumas, F., Conan, P., Pujo-Pay, M., Lefèvre, D., 2021. Seasonal and Interannual Variability of the CO2 System in the Eastern Mediterranean Sea: A Case Study in the North Western Levantine Basin. Frontiers in Marine Science 8.

WMO, 2015. Monitoring Ocean Carbon and Ocean Acidification. Bulletin p.48-51.

WMO, United Nations Environment Programme (UNEP), International Science Council (ISC), Scientific and Cultural Organization (IOC-UNESCO) Intergovernmental Oceanographic Commission of the United Nations Educational, 2022. The 2022 GCOS Implementation Plan (GCOS-244) [WWW Document]. URL https://library.wmo.int/records/item/58104-the-2022-gcos-implementation-plan-gcos-244 (accessed 1.4.24).

World Meteorological Organization, 2023. 2023 shatters climate records, with major impacts.

Yamamoto-Kawai, M., McLaughlin, F.A., Carmack, E.C., Nishino, S., Shimada, K., 2009. Aragonite Undersaturation in the Arctic Ocean: Effects of Ocean Acidification and Sea Ice Melt. Science 326, 1098–1100. https://doi.org/10.1126/science.1174190

Yin, T., Papadimitriou, S., Rérolle, V.M.C., Arundell, M., Cardwell, C.L., Walk, J., Palmer, M.R., Fowell, S.E., Schaap, A., Mowlem, M.C., Loucaides, S., 2021. A Novel Lab-on-Chip Spectrophotometric pH Sensor for Autonomous In Situ Seawater Measurements to 6000 m Depth on Stationary and Moving Observing Platforms. Environ. Sci. Technol. 55, 14968–14978. https://doi.org/10.1021/acs.est.1c03517

Zeebe, R.E., Wolf-Gladrow, D.A., 2001. CO2 in Seawater: Equilibrium, Kinetics, Isotopes Elsevier Oceanography Series 65, Amsterdam.

Chapter I: Scientific context and methods

1. Introduction

The comparability of measurement results is the intrinsic purpose of metrology. It makes sense especially in comparison to a reference value, to a regulatory threshold or in establishing long-term trends such as for climate assessments. In order to ensure the comparability of measurement results over time and space, integrating metrological concepts, such as clear definition of the measurand, validation of measurement procedure, uncertainty estimation, establishment of metrological traceability and standardisation, are required.

In the monitoring of ocean acidification and the study of the oceanic carbon cycle, there has been, for decades, a real recognition of the importance of observational data quality (Dickson, 2010). The ambition for the application of metrological concepts to ocean carbon observation has emerged from the oceanographic community, and metrology institutions are now working together with oceanographers to pursue this goal.

This chapter details, in a first part, the metrological concepts needed to ensure the comparability of measurement results. The state of the art of metrological concepts applied, on one hand to the measurement of seawater total pH, and on the other hand to Total Alkalinity measurements, is then presented.

2. Metrology and metrological concepts in guarantying comparability of measurement results

2.1. Definition, brief history and international governance

The etymology of the word "Metrology" comes from the ancient Greek "meter" and the suffix "-logy", literally meaning "science of measurements". Measuring is defined in the International Vocabulary of Metrology (VIM, from the French Vocabulaire international de métrologie) as a "process of experimentally obtaining one or more quantity values that can reasonably be attributed to a quantity" ("JCGM 200:2012", 2012). It is important to note that this definition, and thus the concepts presented in this chapter, do not refer to non-numerical and nominal measurement results that are generally used in areas of science other than physics and chemistry, such as taxonomic identification in biology or quantification of societal phenomena as in economy or psychology studies (White, 2011).

The most ancient civilisations such as China, India, Egypt and Mesopotamia, had a knowledge of metrology, as shown by the early use of a decimal metric system, or impressive constructions relying on accurate dimensioning (Fanton, 2019). However, it would take until after the French Revolution of 1789 to establish for the first time a

generalized system of weights and measures with a decimal notation, with the underlying idea of having a stable and universal unit system (Himbert, 2009; Sant'Ambrogio and Dejours, 1995). The French law of the 18 Germinal an III (7th of April 1795) introduced the decimal metric system, relying on a single definition for the dimension unit: the meter. Other units (e.g. liter, gram) ensue from this definition. The decree of the 19 Frimaire an VIII (10th of December 1799), organized the dissemination of this unit by means of standards based on a reference meter: the platinum meter standard (French Government, 2017).

The Metre Convention signed in Paris in 1875 by seventeen states, acted the creation of the International Bureau of Weights and Measures (BIPM – from the French "Bureau International des Poids et Mesures"), aiming to coordinate international metrology, to assure the international unification and to improve the metric system (BIPM, 1921). The meter-kilogram-second (MKS) international system was then adopted (Fanton, 2019).

Over more than a hundred years since the Meter convention, four other units joined the International System of Units (SI): the ampere, the kelvin and the candela in 1954, later followed by the mole in 1971. In 2018, during the 26th General Conference of Weights and Measures (CGPM – from the French "Conférence Générale des Poids et Mesures"), the redefinition of the units were adopted in order to link all of the seven base units to natural constants, ensuring the stability of the units (Figure 5, BIPM, 2019; Fanton, 2019).

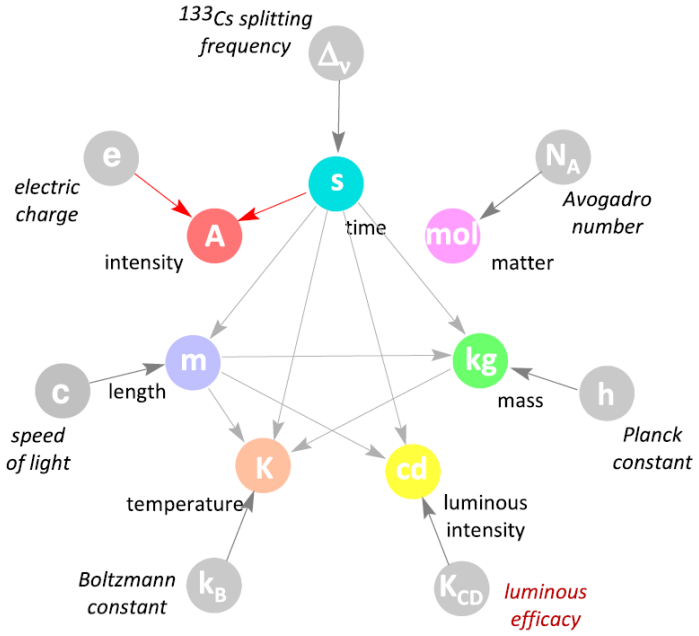

Figure 5: The seven units of the International System of Units relying on seven general natural constants, and relationships between units. From Fanton (2019).

Nowadays, the BIPM accounts for 64 Member States and 36 associate States and Economies. Intermediate level, between National Metrology Institutes (NMIs) and BIPM, exists through Regional Metrology Organizations (RMOs). The French NMI: Laboratoire National de Métrologie et d'Essais (LNE) is thus part of the RMO "European Association of National Metrology Institutes" (EURAMET). Annual meetings of the BIPM and RMOs allow the gathering of metrologists around the world. Working groups and tasks groups are created within these institutions, allowing for metrologists working on a same research area to coordinate advancements and demonstrate the equivalence of the national standards via the participation to inter-laboratory comparisons.

Metrology aims, by developing tools allowing the application of the metrological concepts mentioned in Section 1, to ensure the comparability of measurement results over time and space.

2.2. Metrological traceability

Metrological traceability is defined in the VIM as the "property of a measurement result whereby the result can be related to a reference through a documented unbroken chain of calibrations, each contributing to the measurement uncertainty" (Figure 6, "JCGM 200:2012", 2012).

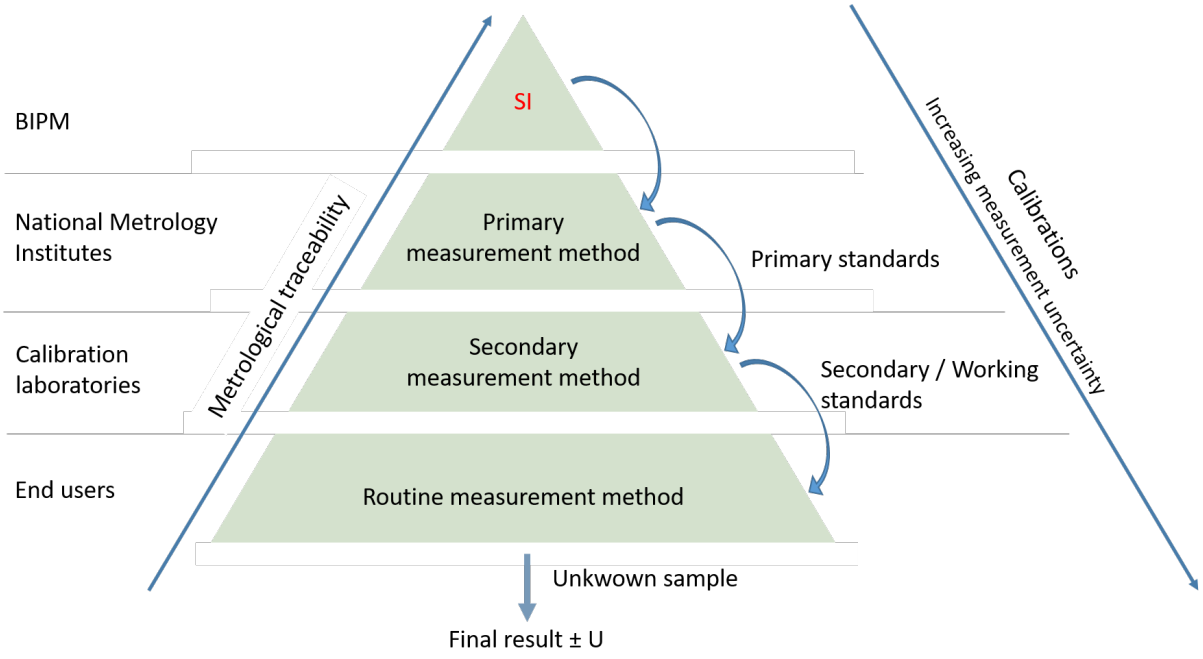

Figure 6: Metrological traceability chain allowing connection of end-users' measurement results to internationally agreed reference.

National Metrology Institutes have mission to develop, characterize and maintain primary standards. Primary standards are references of the highest metrological quality to be used in calibrations (Wright, 2000). They are characterized using a primary

reference measurement procedure, defined in the VIM as a "reference measurement procedure used to obtain a measurement result without relation to a measurement standard for a quantity of the same kind" ("JCGM 200:2012", 2012).

NMIs' primary measurement procedures seek to provide traceability to the SI as it is the highest order and most stable reference. International comparability and the equivalence of NMIs' measurement procedures is verified through their validation by participating in inter-NMIs comparisons organised at the BIPM level.

However, traceability to the SI requires a complete mastering of the measurement mathematical model with thorough quantification of uncertainties. There are certain cases where this cannot be achieved, for example, when the measurement procedure requires making approximations that are not fully mastered nor have a quantified uncertainty. In this case, the reference to which final measurements are traceable can either be a reference material or a harmonized measurement procedure, such as the standard methods of the International Organization of Standardisation (ISO) or the European Committee for Standardisation (CEN).

End-user's measurement results have to be linked to the primary standard, through calibration made with measurement standards from intermediate calibration laboratories. These standards are called secondary, or working, measurement standards. In chemistry, measurement standards are often reference materials that are stable, homogeneous and with a matrix and parameters close to the unknown sample being analysed.

Each step added between the final measurement results and the highest reference adds a contribution to the final uncertainty budget. Thus, it is essential that each step involved in the traceability chain achieves the lowest uncertainty practical.

2.3. Definition of the measurand

The measurand is defined in the VIM as "the quantity intended to be measured" ("JCGM 200:2012", 2012). This implies that the studied quantity may differ from the actual measured quantity, meaning it is necessary to have a measurement model linking the quantity of interest to the measured quantity (Mari, 2006). The measurement model is defined in the VIM as the "mathematical relation among all quantities known to be involved in a measurement". This of course adds complexity in assessing metrological traceability and uncertainty of the measurand. Moreover, influence quantities that are not the measurand itself but yet influence the measurement result, such as environmental conditions, must be stated. As an example, for the density measurand, measurement results must be given together with the temperature to which it is applied.

The measurand under evaluation must be very carefully defined, and agreed among the scientific community.

2.4. Procedure validation

Ensuring the comparability of measurement results involves measurement procedure validation. It aims to validate all the conditions intervening in a measurement process, by checking the accuracy of the measurement results (i.e. both trueness and precision). This can mainly be achieved by two means: the use of a reference material and by participation to an inter-laboratory comparison (Figure 7). By using these tools, it is possible not only to check the measurement procedure trueness, but also to correct, if needed, a systematic bias.

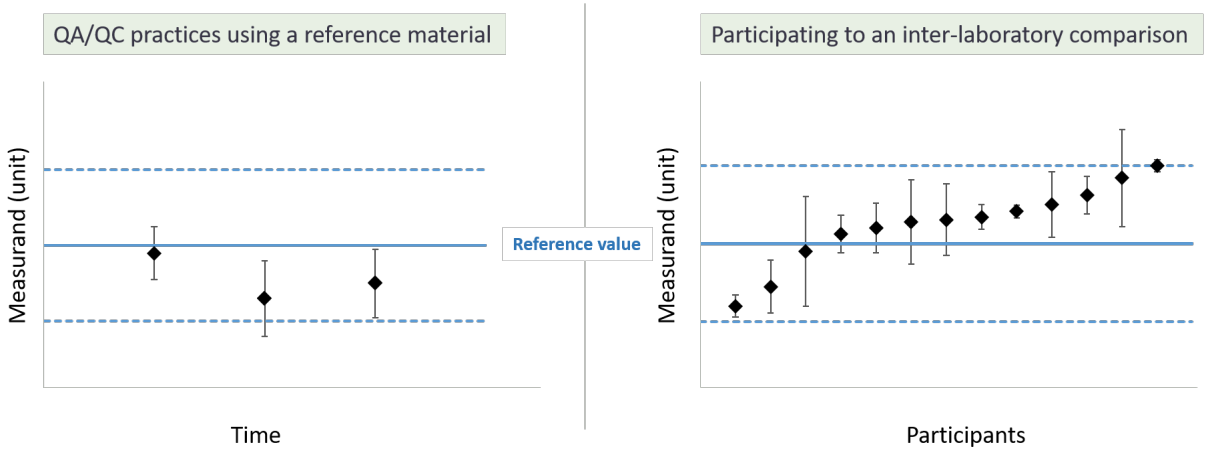

Figure 7: Means for procedure validation

Reference Materials

Reference Materials (RMs) are materials "sufficiently homogeneous and stable with reference to specified properties, which has been established to be fit for its intended use in measurement or in examination of nominal properties" ("JCGM 200:2012", 2012). A reference material whose reference value is given with an associated uncertainty and traceability using valid procedures is described as a Certified Reference Material (CRM).

Reference materials can be used to calibrate a measurement method or in Quality Assurance and Quality Control (QA/QC) practices. Reference materials are characterized using a reference measurement procedure, which differs from the measurement procedure being under evaluation. Producing reference materials falls under strict requirements detailed in the ISO standard 17034:2016 "General requirements for the competence of reference material producers" (2016).

By comparing a measurement result, obtained with a routine measurement procedure on a reference material, to the reference value given, one can establish the trueness of the measurement procedure. In addition, by applying QA/QC practices and using reference materials on a regular basis with repeatability measurements, it is possible to

assess not only the trueness, but also the precision of a measurement procedure, as well as any eventual deviation over time. Reference materials can also be used in qualifying a new operator or testing a new device.

Inter-laboratory comparison

The accuracy of a measurement method can also be determined with an inter-laboratory experiment if a sufficient amount of laboratories perform measurements on the same stable material using a standardized measurement method ("ISO 5725-1", 2023). Each laboratory performs repeatability measurements under constant operating conditions to allow the evaluation of the precision of the method. The trueness is estimated in comparison with a reference value that is preferably known from characterization of the sample with a reference method. If the inter-laboratory comparison is performed without a well characterized reference value, only the precision of the method can be assessed.

The first step of data processing from inter-laboratory comparison results is to identify eventual outliers. To do so, two statistical tests are recommended in the ISO standard 5725-2 "basic method for the determination of repeatability and reproducibility of a standard measurement method" (2020). Grubbs' test is used to identify an outlying observation compared to the mean observation while Cochran's test is used to identify inter-laboratory variances that are too large. Once inter-laboratory results have been checked with these two tests, bias of the measurement is obtained from the difference between the mean measurement result of the participants and the reference value. The precision of the measurement method is obtained from knowledge of the standard deviation of repeatability (intra-laboratory) and of reproducibility (inter-laboratory) data.

Inter-laboratory comparisons can also be used to assign a reference value to a material or to check for individual laboratories performances. In these cases, the inter-laboratory comparisons must be performed under specific conditions together with an adequate data treatment. As an example, the performances of a laboratory can be determined using the Z-score as well as a Youden plot ("ISO 13528", 2022). The Z-score is a standardized measure of a laboratory performance calculated based on the participant result, the assigned value of the item analysed and the standard deviation of the result obtained by the participant. Youden plot consists in representing measurements results obtained by participants to an inter-laboratory comparison on two different samples (Martín et al., 2017). This representation allows one to determine if the discrepancy of a laboratory comes from systematic or random errors, which is valuable information on the methodology that can be applied to lower the discrepancies.

2.5. Uncertainty estimation

When reporting a measurement result of one parameter, it is required to give a quantitative information on the quality of the result so that users of the measurement result can assess its reliability. Without this information, comparing measurement results is impossible. This quantitative information is called uncertainty, whose exact definition from the VIM is a "non-negative parameter characterizing the dispersion of the quantity values being attributed to a measurand, based on the information used" ("JCGM 200:2012", 2012).

Two methods can be applied to quantify the uncertainty of a measurement result (Figure 8). The preferred one is the bottom-up approach, relying on the detailed identification and quantification of every source of uncertainty involved in a measurement process. This method leads to a thorough evaluation of a measurement uncertainty but can be cumbersome to achieve. To overcome this, a second approach exists: the top-down approach, relying on experimental data to compute the uncertainty budget (Meyer, 2007).

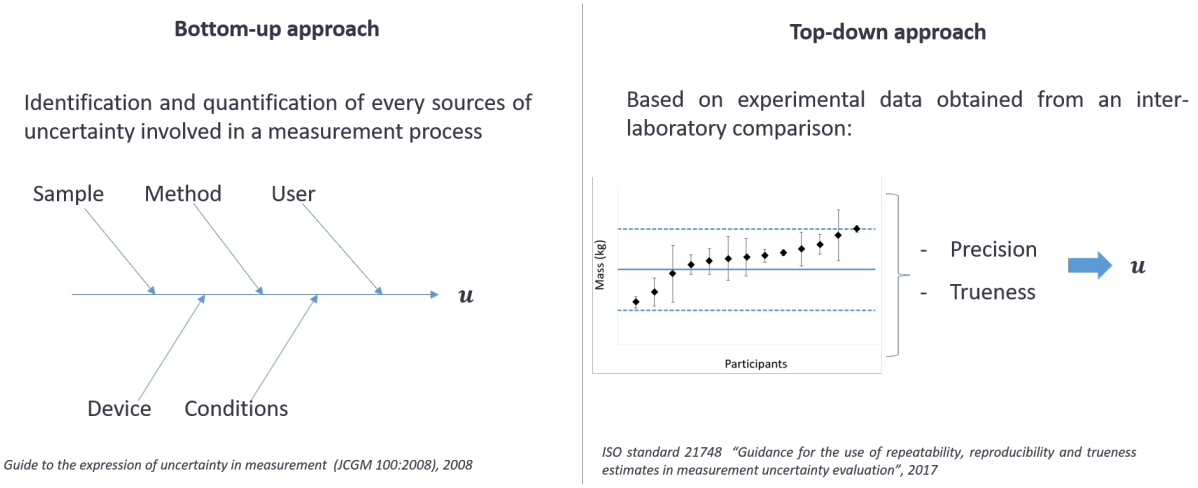

Figure 8: The two methods to quantify the uncertainty of a measurement result

Bottom-up approach

The bottom-up approach is detailed in the Guide to the expression of uncertainty in measurement (GUM) (JCGM 100:2008, 2008). Achieving the quantification of the uncertainty of a measurement result relies on a multi-step process (Figure 9, Allard and Fischer, 2015).

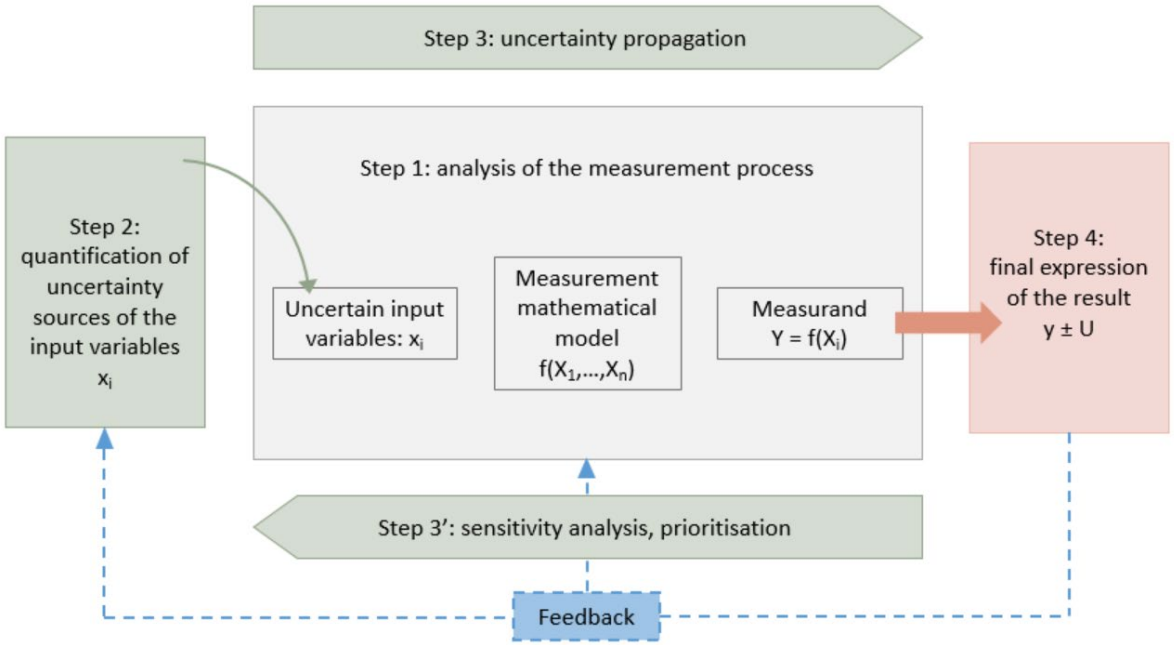

Figure 9: Schematic representation of the process leading to the assessment of a measurement uncertainty following the GUM.

The first step is the analysis of the measurement process. It consists in defining the measurand (Y), identifying the quantities involved in the measurement process and influence quantities (x_i), as well as establishing the mathematical relation between the measurand and these quantities ($f(X_1,...X_n)$). The identification of the input quantities is often realised with the help of an Ishikawa diagram, which regroups the potential factors of influence under five categories: Device, Sample, Method, Conditions, and User (Liliana, 2016).

The second step corresponds to the quantification of the uncertainty sources. Firstly, the input quantities are quantified by assessing the mean value of the quantity as well as its associated standard uncertainty ($u(x_i)$). Two categories can be distinguished for the standard uncertainty of an input quantity. The type A uncertainty is obtained from experimental repeatability values. The type B uncertainty is obtained from the choice of a probability law corresponding to a form of distribution, and from ranges of possible variation. The latter requires experience, expertise or auxiliary information to define the distribution form and the range of variation. This can be, for example, information about a device resolution that is known from the manufacturer's specification. If there is a correlation between two or more input quantities in the measurement model, meaning that variations of input quantities are linked, their covariance must be taken into account.

The third step consist in propagating the uncertainties associated with the input quantities through the mathematical model in order to deduce the best estimate of the measurand together with its associated standard uncertainty. The uncertainty propagation is obtained using partial derivatives as expressed in equation 1.1. The second term in equation 1.1 is involved only when covariances are present.

$$u^2(y) = \sum_{i=1}^{N} \left[\frac{\partial f}{\partial x_i}\right]^2 u^2(x_i) + 2\sum_{i=1}^{N-1}\sum_{j=i+1}^{N} \frac{\partial f}{\partial x_i}\frac{\partial f}{\partial x_j} u(x_i, x_j) \quad (1.1)$$

The step 3' corresponds to a sensitivity analysis that can be applied in order to prioritise the input quantities according to their estimated contribution to the final budget.

Finally, step 4 corresponds to the final expression of the result. Uncertainty budgets are generally expressed by expanded uncertainties. This requires the introduction of a coverage factor, which provides an interval corresponding to a particular level of confidence. In chemistry, the level of confidence chosen is often 95 percent, corresponding to a coverage factor of 2. The expanded uncertainty is obtained by multiplying the standard uncertainty by the chosen coverage factor.

The first estimation of the uncertainty, as well as the estimated contribution of each of the input quantities allows, by a feedback process, modification of the different parameters to adjust the final uncertainty budget. For example, if the final uncertainty is too high compared to what is expected, a work can be done to reduce the uncertainty of the input parameter corresponding to the major contribution to the final uncertainty budget.

The GUM approach is suitable for most uncertainty quantifications; however, it relies on some assumptions. If these assumptions don't hold, the Monte-Carlo approach, described as a method of propagation of the distributions obtained by simulation, can be used to determine the final uncertainty budget (Allard and Fischer, 2015; "JCGM 101:2008," 2008). It relies on propagating the complete distribution of all input quantities in the mathematical model in order to obtain directly the distribution of the measurand value. It is useful for example if the partial derivatives of the measurement mathematical model are difficult to compute for their application in the propagation law, or if the distribution of the input quantities aren't Gaussian.

Top-down approach

The top-down approach relies on experimental data to determine the uncertainty of a measurement results (Magnusson et al., 2017; Meyer, 2007). It can be computed either for a measurement method, from data of an inter-laboratory comparison made with a standardized method, or for one laboratory, using its quality control data over a large period of time. In both cases, the value of the bias between the mean measured value and the reference material value can either be integrated in the uncertainty calculation or corrected. Either way, the uncertainty on the bias has to be taken into account in the uncertainty budget.

Only the uncertainty budget with the correction of the bias is presented hereafter as it is the method that can achieve the lowest uncertainties and thus, better data quality.

The ISO standard 21748 "Guidance for the use of repeatability, reproducibility and trueness estimates in measurement uncertainty evaluation" (2017) can be used to

establish an uncertainty budget with the results for an inter-laboratory comparison that follows the conditions given in the ISO standard 5725-2 (2020). The uncertainty budget is calculated using equation 1.2.

$$u^2(y) = s_L^2 + s_r^2 + u^2(\hat{\delta}) \quad (1.2)$$

where $u(y)$ is the estimated measurement result uncertainty, s_L the inter-laboratory standard deviation, s_r the intra-laboratory standard deviation divided by the square root of the mean number of replicates, and $u(\hat{\delta})$ the uncertainty associated with the estimated bias of the measurement method.

The uncertainty coming from the estimation of the bias, $u(\hat{\delta})$, is calculated with equation 1.3 and takes into account both the estimated standard deviation of the bias, and the standard uncertainty associated with the reference material value, used for trueness estimation in the inter-laboratory comparison. The bias itself is calculated as being the difference between the mean value of the participants and the assigned reference value of the reference material.

$$u^2(\hat{\delta}) = \frac{(s_L^2 + s_r^2) - \left(1 - \frac{1}{n}\right)s_r^2}{p} + u^2(\hat{\mu}) \quad (1.3)$$

where n is the number of replicates in each laboratory, p the number of laboratories and $\hat{\mu}$ the certified value.

Following a similar methodology to the one described above, it is possible to compute the uncertainty budget of measurement results for one laboratory. s_L in equation 1.2 then corresponds to the within-laboratory intermediate precision, i.e. the estimated variation from differences in calibration over time. $u(\hat{\delta})$ is in this case calculated from equation 1.4.

$$u^2(\hat{\delta}) = \left(\frac{s_\delta}{\sqrt{n}}\right)^2 + u^2(\hat{\mu}) \quad (1.4)$$

where s_δ is the standard deviation of the measured values of the reference material and n is the number of reference material used (i.e. number of calibration) (Magnusson et al., 2017).

Even though both top-down and bottom-up approaches allow the quantification of the uncertainties of a measurement result, only the bottom-up approach enables having a thorough identification and quantification of each source of uncertainty involved in a measurement process, thus allowing one to identify which parameter it is possible to work on to reduce the final uncertainty.

3. Metrological concepts applied to the measurement of pH on the total scale

3.1. Definition of the measurand

The pH scale, first described by Soren Peter Lauritz Sørensen in 1909, is defined by the International Union of Pure and Applied Chemistry (IUPAC) as a function of free hydrogen ion activity (Buck et al., 2002), also known as the NBS scale (National Bureau of Standards). However, the Bates-Guggenheim convention used to define chemical activity does not accurately estimate activity coefficients for solutions with ionic strengths above 0.1 mol/kg (Stoica et al., 2014). Natural seawater is a multi-electrolyte solution with a high ionic strength, around 0.7 mol/kg for a salinity of 35. Therefore, the NBS scale isn't suitable for seawater pH measurements. Marine chemists introduced, since the late 60s, alternative pH scales more adequate for the study of seawater (Dickson, 1993; Wedborg et al., 1999):

- The free hydrogen ion scale:

$$\mathrm{pH} = -\lg [\mathrm{H}^+]_\mathrm{F} \tag{1.5}$$

where brackets represent amount contents, expressed in moles per kilogram of solution and noted mol/kg-sol.

- The total hydrogen ion concentration scale, $\mathrm{pH_T}$, which takes into account the free hydrogen ions and hydrogen ions associated to sulphate ions (equations 1.6.a and 1.6.b, equivalent to equation I.3 of the General Introduction).

$$\mathrm{pH_T} = -\lg [\mathrm{H}^+]_\mathrm{T} \tag{1.6.a}$$

$$[\mathrm{H}^+]_\mathrm{T} = [\mathrm{H}^+]_\mathrm{F} \, (1 + S_T/K_S) \approx [\mathrm{H}^+]_\mathrm{F} + [\mathrm{HSO_4}^-] \tag{1.6.b}$$

where S_T is the total sulphate amount content ($[\mathrm{HSO_4^-}] + [\mathrm{SO_4^{2-}}]$) (mol/kg-sol), and K_S is the dissociation constant of $\mathrm{HSO_4^-}$. This is appropriate only for the range of $\mathrm{pH_T}$ for which $[\mathrm{HSO_4^-}] << [\mathrm{SO_4^{2-}}]$.

- The seawater scale, $\mathrm{pH_{sws}}$, taking into account both sulphate and fluoride ions present in the seawater media:

$$\mathrm{pH}_{sws} = -\lg [\mathrm{H}^+]_\mathrm{sws} \tag{1.7.a}$$

$$[\mathrm{H}^+]_\mathrm{sws} = [\mathrm{H}^+]_\mathrm{F} \, (1 + \frac{\mathrm{S_T}}{K_S} + \frac{\mathrm{F_T}}{K_F}) \tag{1.7.b}$$

where $\mathrm{F_T}$ is the total fluoride ion amount content (mol/kg-sol) and K_F the dissociation constant of hydrogen fluoride.

It should be noted that the various equilibrium constants are stoichiometric ones, that is to say the values applied in the equations are those for the particular temperature and salinity (or, more generally, composition) of interest.

After considerable work and discussion within the community regarding the choice of pH scale for seawater analyses, the total pH scale (c.f. total hydrogen ion concentration scale above) has become established and is now the one mainly used by the oceanographic community.

The free hydrogen scale has been set aside by the majority of oceanographers due to the difficulty in accurately determining its amount content as hydrogen ions can bind to sulphate and fluoride ions, although Waters and Millero (2013) recommended the use of that scale. Indeed, there is still use of the free hydrogen scale, mainly from sensors on autonomous platforms. Conversion between the scales might thus be important for oceanographers, as well as the calibration of the free scale, which both may draw metrological attention.

The seawater scale has also been abandoned, primarily because fluoride ions are a minor component of seawater. Additionally, adopting the total pH scale helps to mitigate errors stemming from uncertainties in the stability constant for hydrogen fluoride ion (Wedborg et al., 1999).

When reporting seawater pH data, it is mandatory to specify the scale to which it refers, as discrepancies between the scales are not negligible. As pH data is dependent on temperature, it is also mandatory to state the temperature to which the given pH_T refers (generally in-situ temperature or pH_T normalized to 25°C).

3.2. Spectrophotometric measurement method

pH_T measurements are widespread in the oceanographic field, this has been achieved thanks to the development of the spectrophotometric measurement method (Byrne and Breland, 1989; Clayton and Byrne, 1993), followed by the introduction of spectrophotometric in-situ autonomous sensors (Seidel et al., 2008; Yin et al., 2021).

The spectrophotometric pH_T measurement method relies on the addition of an indicator dye, whose absorbance spectra depends on the acidity of the analysed sample. For suitability in seawater analyses, the pKa of the indicator dye must be similar in value with the pH_T of seawater. Ideally the dye is chosen so that absorbance peaks are approximately equal in the required pH range. Three sulfonephthalein dyes have been studied for this use: the meta Cresol Purple (mCP), the Thymol Blue and the Cresol Red (Byrne and Breland, 1989; Mosley, Husheer and Hunter, 2004; Liu, Patsavas and Byrne, 2011; Patsavas, Byrne and Liu, 2013; Loucaides *et al.*, 2017; Douglas and Byrne, 2017; Hudson-Heck and Byrne, 2019). The mCP is the dye mostly used among the oceanographic community for the conduction of these measurements, and thus the one we will focus on in the rest of this manuscript.

Measuring the ratio of absorbance values R at the wavelengths corresponding to the basic and acid form of the indicator dye in the sample allows the calculation of pH_T using equation 1.8 (Clayton and Byrne, 1993; Dickson et al., 2007).

$$pH_T = -\lg(K_2^T e2) + \lg\left(\frac{R-e1}{1-R\times\frac{e3}{e2}}\right) \quad (1.8)$$

where K_2^T is the second dissociation constant of the indicator dye, R the ratio of the absorbance at 578 nm (i.e. mCP basic form absorbance wavelength, noted A_{578}) to the absorbance at 434 nm (i.e. mCP acid form absorbance wavelength, noted A_{434}), obtained with equations 1.9, and $e1$, $e2$ and $e3$ are ratios of the dye molar extinction coefficients (Liu et al., 2011).

$$R = 2\times R'_{(1st\ dye\ addition)} - R'_{(2nd\ dye\ addition)} \quad (1.9.a)$$

$$R' = \frac{(A_{578,dye}-A_{578,blank})-(A_{730,dye}-A_{730,blank})}{(A_{434,dye}-A_{434,blank})-(A_{730,dye}-A_{730,blank})} \quad (1.9.b)$$

A third absorbance acquisition at a non-absorbing wavelength, 730 nm, is performed to adjust for any baseline shift that may be occurring during the measurement process. The absorbance acquisition is performed first for the background (i.e. without any dye, noted "blank"), then with the added dye (noted "dye"). A double dye addition can be performed to correct for perturbation of the sample pH_T coming from the addition of the dye. Indeed, differences between parameters of the dye solution (i.e. pH_T, salinity, alkalinity) and the analysed sample can slightly change the pH_T value (Li et al., 2020). The ratio R is thus calculated using the equations 1.9.a and 1.9.b (Dickson et al., 2007; "ISO 18191:2015", 2015).

Routine measurements rely on the acquisition of the absorbance values allowing to compute the ratio R, while the terms $K_2^T e2$, $e1$, and $e3/e2$ are determined for the relevant salinity and temperature from the empirical characterizations of the indicator dye available in the literature (Liu et al., 2011; Loucaides et al., 2017; Müller and Rehder, 2018). The accurate control and measurement of the temperature, as well as knowledge of the sample salinity, are required.

The dye purity is another important parameter to take into account while performing spectrophotometric pH_T measurements of seawater. Impurities contained in the mCP can affect the pH_T of the analysed sample. To overcome this, purification techniques using chromatography, as well as a correction methodology have been developed (Douglas and Byrne, 2017b; Fong, 2021; Liu et al., 2011; Patsavas et al., 2013; Takeshita et al., 2021).

3.3. Metrological traceability of the spectrophotometric method results

The traceability of pH_T spectrophotometric measurement results is not established to the International System of units. It is, at present, established to an agreed primary measurement method: the potentiometric pH_T measurement method, conducted with Harned cells.

The characterization of the indicator dye used for the spectrophotometric measurement requires the use of solutions of known pH_T, themselves characterized with this potentiometric method (Figure 10). The Harned cell is the primary standard for

aqueous pH measurements, it allows having the lowest standard uncertainty on pH results, typically below 0.002 (Buck et al., 2002).

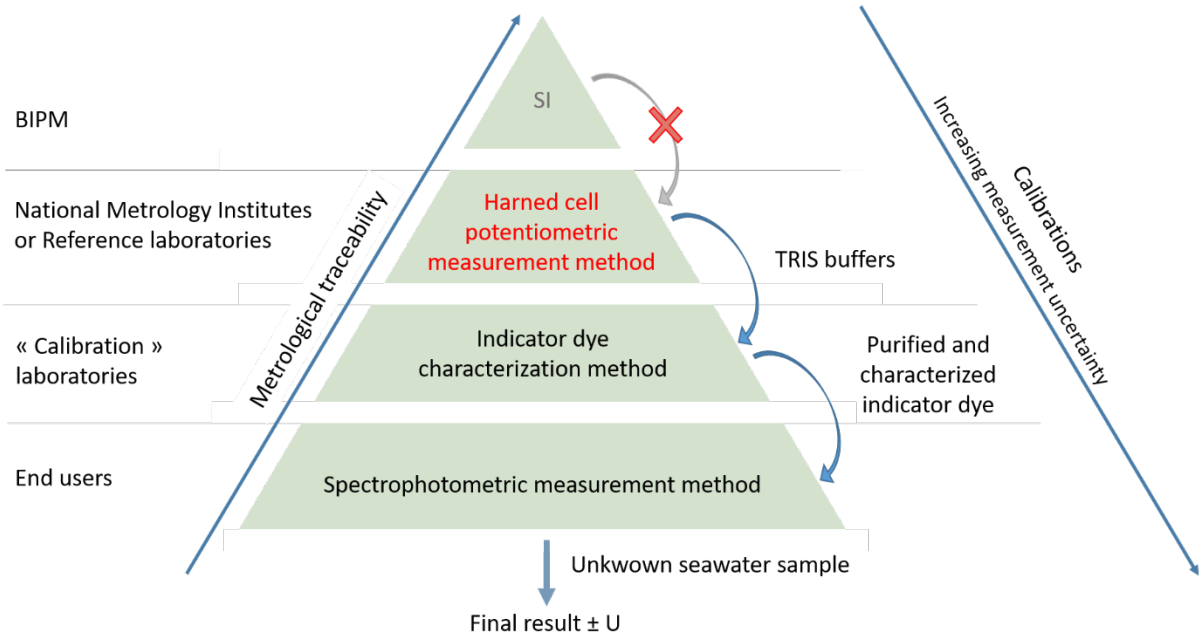

Figure 10: Schematized traceability route of seawater pH_T spectrophotometric measurements to the Harned cell potentiometric measurement method.

The characterization of $e1$ and $\frac{e3}{e2}$ terms in equation 1.8 relies on spectrophotometric measurements (1) in a solution of pH 4.5 at different temperatures for $e1$, and (2) in solutions of pH 12 at different salinities and temperatures for $\frac{e3}{e2}$ (Liu et al., 2011; Loucaides et al., 2017). The characterization of $K_2^T e2$ at different salinities and temperature is somewhat less direct. By isolating $K_2^T e2$ in equation 1.8, and once the $e1$ and $\frac{e3}{e2}$ terms have been characterized, $K_2^T e2$ is determined by spectrophotometric measurements at different temperatures on solutions of known pH_T, prepared in an artificial seawater matrix of different salinities (Liu et al., 2011; Müller and Rehder, 2018).

The solutions used for that purpose are equimolal TRIS buffers (buffer of 2-Amino-2-(hydroxymethyl)-1,3-propanediol (TRIS) and TRIS hydrochloride (TRIS.HCl)) made in artificial seawater of the desired salinities. The TRIS molecule is suitable for its buffering effect in the pH range 7 to 9, explaining its use for seawater analyses (Hansson, 1973). The pH_T of these solutions are characterized with the potentiometric Harned cell measurement method (DelValls and Dickson, 1998; Dickson, 1993; Millero et al., 1993a; Müller et al., 2018). The pH_T value, relying on Harned cell potentiometric measurement procedure on TRIS buffers, itself relies on approximations whose magnitudes, which vary with temperature and salinity, are not yet fully quantified. These approximations arise because of the combination of Harned cell results for two

solutions (TRIS buffer vs artificial seawater only) that differ slightly in composition and therefore acid-base thermodynamic properties (Clegg et al., 2022). This is further discusses in Chapter III. Even if the approximations are considered negligible, the definition of the potentiometric pH_T obtained experimentally differs from the thermodynamic definition, and can be traceable to the SI only if an uncertainty is assigned to the assumptions. The highest reference of spectrophotometric pH_T measurement traceability chain is thus the Harned cell potentiometric measurement method. This measurement method has been studied through inter-NMIs comparison.

3.4. Potentiometric Harned cell measurement method

Figure 11 shows the description of the Harned cell, also called junction-free cell, set-up. The potential difference is acquired between a silver-silver chloride (Ag/AgCl) reference electrode (Figure 11.a) and a standard hydrogen electrode (Pt, H_2) (Figure 11.b). A Harned cell is used as it allows the humidity saturation of hydrogen before it enters the measurement compartment (Figure 11.c) and eliminates errors due to residual junction potentials thanks to a junction-free measurement compartment (Figure 11.d).

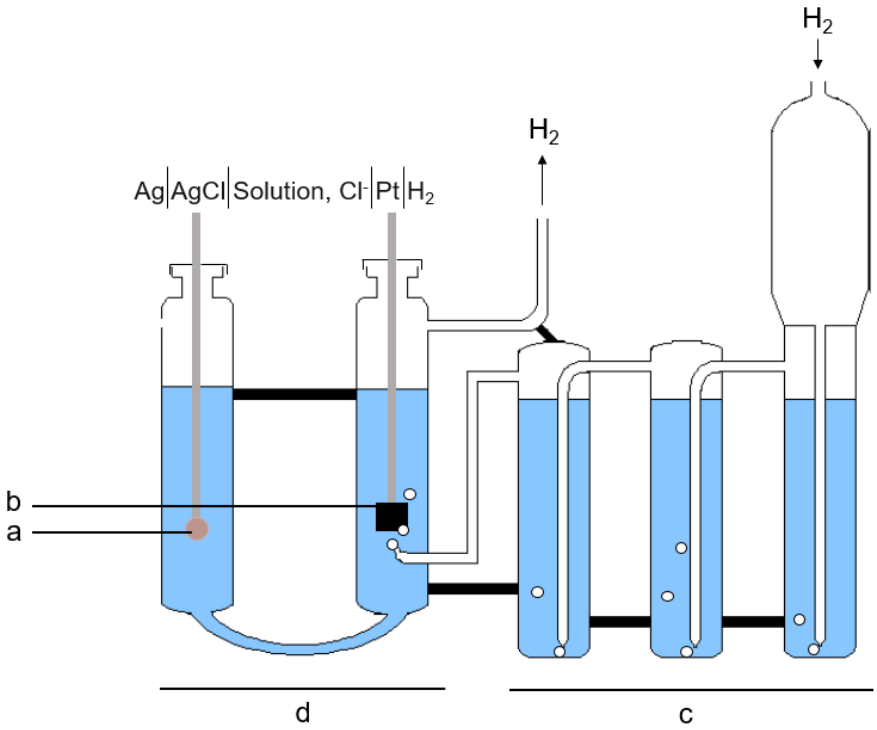

Figure 11: Harned cell set-up description. (a) silver-silver chloride electrode; (b) standard hydrogen electrode; (c) hydrogen humidity saturation system; (d) junction-free measurement compartment.

The determination of the operational pH_T, in an amount-content basis, by the potentiometric method is well described in the literature (DelValls and Dickson, 1998;

Dickson, 1990, 1993; Millero et al., 1993a; Müller et al., 2018; Papadimitriou et al., 2016; Pratt, 2014) and is obtained by equation 1.10.a.

$$\mathrm{pH_T} = \frac{E-E^{\circ *}}{k} + lg(b_{Cl}) - lg\ (\omega_{H2O}) \qquad (1.10.a)$$

where E is the potential difference corrected to a fugacity of H_2 equal to 1 atm (V) (equation 1.10.b), E°* the standard potential of the silver-silver chloride (Ag/AgCl) electrode in saline media (V), k the Nernstian term (equation 1.10.c), b_{Cl} the molality of chloride ions in the TRIS buffer solution (expressed in moles per kilogram of solvent, here water, noted mol/kg-H_2O) and ω_{H2O} the water mass fraction (g/kg-sol).

$$E = E_{mes} - \frac{k}{2} lg\left(\frac{P-p_{vap}+0.4\times\rho\times g\times h}{p^{\circ}}\right) \qquad (1.10.b)$$

where E_{mes} is the measured potential difference (V), P the measured ambient pressure (Pa), p_{vap} the saturation vapour pressure of the solution (Pa), ρ the density of the solution (kg/m^3), g the standard gravity (m/s^2), h the liquid height (m) and p° the standard pressure (101 325 Pa).

$$k = \frac{RTln(10)}{F} \qquad (1.10.c)$$

where F is the Faraday constant (C/mol), R the Gas constant (J/mol.K), and T the measured temperature (K).

The term ω_{H2O} in equation 1.10.a, representing the mass fraction of water in seawater, enables to express the calculated $\mathrm{pH_T}$ value in amount content (i.e. mol/kg-sol) and to align with spectrophotometric $\mathrm{pH_T}$ values.

The determination of the terms E and E°* in equation 1.10.a requires two Harned cell measurements steps described below.

(1) The first step consists in the determination of the E°* term in equation 1.10.a. Potential measurements are performed with a batch of Ag/AgCl electrodes in solutions of HCl molalities varying between 0.005 and 0.05 mol/kg-H_2O in the artificial seawater matrix of the desired salinity (ASW), while conserving a constant ionic strength. The electrochemical cell can be written as:

$\mathrm{Pt}\,|\,\mathrm{H_2(g)}\,|$ HCl ($0.005 < b < 0.05$ mol/kg-H_2O) in ASW solution $|\,\mathrm{AgCl}\,|\,\mathrm{Ag}$ *cell I*

These measurements - noted E' (V) - allow the determination of the standard potential of the Ag/AgCl electrodes in saline media for the studied chloride molalities. The extrapolation of these E' values to an HCl molality of zero mol/kg-H_2O using a quadratic polynomial function gives the E°* value.

(2) The second step is the determination of E_{mes} in equation 1.10.b, measured in the TRIS buffer solution itself. The electrochemical cell can be written as:

$\mathrm{Pt}\,|\,\mathrm{H_2(g)}\,|$ TRIS buffer solution $|\,\mathrm{AgCl}\,|\,\mathrm{Ag}$ *cell II*

Based on measurements carried out with *cell I* and *cell II*, pH_T values are calculated using the equation 1.10.a. Terms b_{Cl} in equation 1.10.a is determined from the TRIS buffer gravimetric preparation while k is determined from constants and temperature measurements. ω_{H2O} is used to convert the pH_T from molality to amount content for sake of practicality for end-users. It must correspond to the water mass fraction of the reference natural seawater composition of the relevant salinity (more details are given in Chapter III, section 2.3).

The determination of E°* is made simultaneously with different Ag/AgCl electrodes. In order to attribute the extrapolated E°* value to each of these electrodes respectively, their homogeneity must be studied. This can be achieved by the determination of the standard deviation of their standard potential, noted E°, in a solution of HCl at a molality of 0.01 mol/kg-H_2O.

3.5. Metrological tools: current state and needs

Reference materials

TRIS buffers in artificial seawater matrix, needed for the characterization of the indicator dye as described in Section 3.3, can also be considered as reference materials that can be used directly as a quality control standard in the validation of end-user procedures. These buffers have been studied for seawater analysis since the 60's (Hansson, 1973; Smith and Hood 1964). In the following decades, a substantial amount of work has been done on the development of these buffers (DelValls and Dickson, 1998; Dickson, 1993; Millero, 1986; Millero et al., 1993a; Nemzer and Dickson, 2005). All this effort conducted to the production of TRIS buffers as reference materials for the measurement of seawater pH_T. Since 2010, the Scripps Institution of Oceanography of the University of California San Diego (UCSD), produces this buffer for the worldwide oceanographic community on a regular basis (Dickson, 2010). The GOA-ON is working to organize the production and certification of reference materials dedicated to the seawater carbonate that would be centered on regional hubs, and would involve NMIs. This should create a more resilient system for the distribution of reference materials that is, to date, relying on a single laboratory (GOA-ON, 2023).

Measurement procedure standardization and comparisons

Standard operating procedures detailing the spectrophotometric measurement method have also been made available, and led, in 2015, to the standardization of this method by the ISO body (Dickson et al., 2007; "ISO 18191:2015", 2015). The procedure is currently under revision within the ISO standardization body in order to expand the application of the method to lower salinities, down to 5, as opposed to the current lower limit of 20. This work is conducted within the Joint Research Project EMPIR

"SApHTIES: Metrology for standardised seawater pH_T measurements in support of international and European climate strategies". EMPIR (European metrology programme for innovation and research) is EURAMET's research and innovation programme.

Inter-laboratory comparisons performed on the spectrophotometric measurement method are reported in the literature (Bockmon and Dickson, 2015; Lamandé et al., 2015; Takeshita et al., 2021). Ocean observatories as the French National Observation Service SOMLIT (for "Service d'Observation en Milieu Littoral", meaning Coastal Observation Service) perform pH_T spectrophotometric measurement on a regular basis. To ensure comparability of every members' results, they perform an inter-laboratory comparison once a year on natural seawater samples (Breton et al., 2023).

The inter-laboratory comparison conducted by Bockmon and Dickson showed quite scattered results, with spectrophotometric pH_T results within 0.04 pH_T units of the assigned value, even though many were within 0.02. The participants who used purified mCP showed results within 0.004 pH_T units from the assigned value, which is encouraging. The reference value was assigned using the same method (i.e. spectrophotometry). Takeshita et al. (2021) presented an inter-laboratory comparison study on TRIS buffers with four laboratories, aiming to evaluate different batches of mCP. Results shown good agreement, with a maximum discrepancy being around 0.005 pH_T units.

Uncertainties

The quantification of the spectrophotometric pH_T results is of major importance to ensure the comparability of the results. The GOA-ON has fixed a climate data quality objective with a standard uncertainty target of 0.003 pH_T units (GOA-ON, 2019).

The sources of uncertainty involved in the measurement process have been investigated (Carter et al., 2013; DeGrandpre et al., 2014). The main source of errors is found to be the presence of impurities in the dye. Nevertheless, the purification methods published and the purified dye provided by Robert H. Byrne laboratory (University of South Florida) enable a reduction in this source of uncertainty. Other sources of uncertainties are absorbance and wavelength accuracy of the spectrophotometer used, the temperature control and the characterization of the indicator dye (DeGrandpre et al., 2014). Achieving their thorough quantification remains a challenge. Advancement have been fulfilled, however, to assess the uncertainty by the mean of the GUM, the re-evaluation of the indicator dye characterization together with its uncertainty is needed (Fong, 2021). The current state of research estimates the standard uncertainty of spectrophotometric pH_T results to be in the range 0.005 to 0.02 pH_T units (Carter et al., 2013; DeGrandpre et al., 2014; Loucaides et al., 2017). Standard uncertainties of pH_T data computing from a pair of other parameters of the carbonate system is also evaluated to be close to 0.01 pH_T units (Álvarez et al., 2020; Orr et al., 2018). However,

observed and calculated pH_T present discrepancies ranging from -0.018 to 0.014 at pH_T 7.4 and 8.2, respectively (Fong and Dickson, 2019; Takeshita et al., 2020).

Important and significant metrological advancements in establishing comparability of seawater pH_T spectrophotometric results have been made. This, by the development and distribution of TRIS buffers, the conduction of inter-laboratory comparisons, standardization of procedures and preliminary estimate of routine pH_T measurement results uncertainties. In order to fully guarantee the comparability of these results over time and space, the thorough establishment of the uncertainty budgets of (1) the pH_T value attributed to the reference material, taking into account its homogeneity and stability, and (2) the pH_T value attributed to unknown seawater samples with the spectrophotometric method, is required. Moreover, metrological work is also needed to seek for the establishment of traceability of the spectrophotometric method to the SI. The work conducted during this thesis relative to the metrological needs aforementioned is detailed in chapters II, III and IV.

4. Metrological concepts applied to the measurement of Total Alkalinity

4.1. Definition of the measurand

The concept of alkalinity has evolved throughout the years and is inherently linked to the understanding of acid-base equilibria. Different terms standing for alkalinity emerged in the first half of the XX^{th} century as "buffer capacity of seawater", "alkaline reserve" or "titrable bases" (Dickson, 1992; Thompson and Bonnar, 1931).

A common definition, referring to the analytical measurement method, was adopted by the International Association of Physical Oceanography in 1939, being the number of milliequivalents of hydrogen ion neutralized by one litre of water at 20°C, (Dickson, 1992). Rakestraw (1949) clarified this definition by expressing that "the alkalinity of the water is the result of the predominance of base effectiveness over acid effectiveness". In other terms, it can be described as the excess of proton acceptors over proton donors (Dickson, 1981).

Definitions of total alkalinity (TA) are often related either to the measurement method (i.e. titration by an acid) or to the ionic chemical model. Dickson (1981) proposed a precise definition combining both approaches: the number of moles of hydrogen ion equivalent to the excess of proton acceptors (bases formed from weak acids with a dissociation constant $K \leq 10^{-4.5}$, at 25°C and zero ionic strength) over proton donors (acids with $K > 10^{-4.5}$, same conditions) in one kilogram of sample. This definition is still, up to date, the one commonly accepted and is represented in terms of ionic

chemical model by equation 1.11 (equivalent to the equation I.2 of the General Introduction).

$$TA = [HCO_3^-] + 2[CO_3^{2-}] + [B(OH)_4^-] + [OH^-] + [HPO_4^{2-}] + 2[PO_4^{3-}] + [SiO(OH)_3^-] + [NH_3] + [HS^-] + [\dots] - [H^+]_F - [HSO_4^-] - [HF] - [H_3PO_4] - [\dots] \quad (1.11)$$

where brackets represent amount contents (mol/kg-sol) and ellipses represent minor species unidentified or negligible, [HNO_2] (a minor proton donor) may be added at the end of the equation (Wolf-Gladrow et al., 2007).

Based on the statement that seawater obeys the electroneutrality condition, total alkalinity can also be described as the explicitly conservative form of total alkalinity (TA_{ec}) (Wolf-Gladrow et al., 2007). TA_{ec} is another manner of writing TA that takes into account all of the species in seawater, including the ones that are not involved in proton exchanges, defined by equation 1.12. The two definitions TA and TA_{ec} are equivalent.

$$TA_{ec} = [Na^+] + 2[Mg^{2+}] + 2[Ca^{2+}] + [K^+] + 2[Sr^{2+}] + \cdots - [Cl^-] - [Br^-] - [NO_3^-] - \cdots + TPO_4 + TNH_3 - 2TSO_4 - THF - THNO_2 \quad (1.12)$$

where TPO_4, TNH_3, TSO_4, THF and $THNO_2$ are total amount contents (mol/kg-sol) for, respectively, phosphate, ammonia, sulphate, fluoride and nitrite.

Another definition of alkalinity, described as the charge balance alkalinity (CBA) has recently been introduced. CBA, or excess negative charge, is defined as "the sum of nonconservative ions involved in proton exchange reactions that account for the difference between the sum of conservative cations and anions" (Middelburg et al., 2020).

TA_{ec} and CBA are useful definitions allowing us to highlight changes due to biogeochemical processes. As an example, they make clear that the alkalinity of seawater isn't affected by the absorption of CO_2. However, TA and TA_{ec} can differ from CBA. This, due to the charge of minor components at the reference pH of 4.5. It is of major importance to specify to which definition ones refers when talking about alkalinity.

The rest of the manuscript refers to the definition of TA given by Dickson (1981) (equation 1.11).

4.2. Potentiometric titration measurement method

The titration method has always been the measurement method of choice for the determination of seawater total alkalinity (Greenberg et al., 1932). It consists in monitoring the pH of the analysed seawater sample being titrated with a strong acid in order to identify the equivalence point, taking into account the matrix and acid-base systems of the solution (Figure 12, Wolf-Gladrow *et al.*, 2007). At this equivalence

point, the concentration of proton acceptors is therefore equal to that of proton donors and the total alkalinity equals zero. Total alkalinity is related to the amount of acid added to reach the equivalence point.

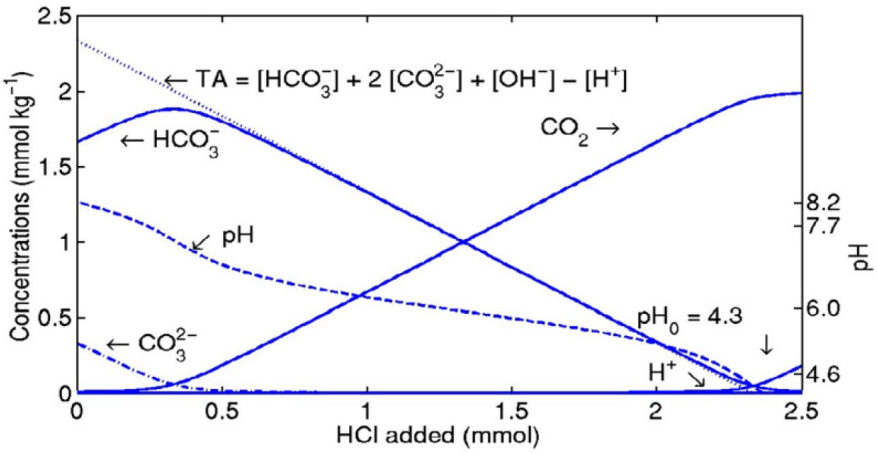

Figure 12: Total Alkalinity titration determination represented for a simple system. From Wolf-Gladrow et al., (2007).

Choice of the method

Two main procedures for the realisation of the titration method have been developed (Millero et al., 1993b).

(1) A multi-step addition of acid, with algorithmic determination of the equivalence point from potentiometric data titration curve (Dickson, 1981; Edmond, 1970). This method either can be used in an open or closed cell.

(2) A single-step acid addition with a potentiometric or spectrophotometric determination of the excess of acid added (Breland and Byrne, 1993; Culberson et al., 1970; Perez and Fraga, 1987).

The single-step method consists of an addition of hydrochloric acid that passes the endpoint. The sample is then purged of CO_2 before measuring the pH that will allow the determination of the excess of acid added. This is an important intermediate step as the dissociation of carbonic acid (H_2CO_3) affects the determination of the endpoint (Martz, 2005). This is a fast and precise method, easier to automate (Liu et al., 2015; Watanabe et al., 2004), however, it is highly dependent on the accurate determination of $[H^+]$ in order to have correct estimation of the excess hydrogen ion concentration (Breland and Byrne, 1993). Potentiometric measurements of $[H^+]$ require a very accurate electrode calibration, which is not easily achievable, while the spectrophotometric measurement relies on the bromo-Cresol Green dye calibration, which adds complexity in achieving metrological traceability.

The multi-step titration is recognized as the best-practice method for measurements in seawater (Dickson et al., 2007).

In the past, the closed-cell multi-step method has been the method of choice as it allows the simultaneous determination of Dissolved Inorganic Carbon (Edmond, 1970). However, since the development of the accurate coulometric determination of DIC, the latter approach is considered as the standard procedure (Dickson et al., 2007). An open-cell method has been introduced, offering a more straightforward way to know accurately the amount of sample being analysed by gravimetry (Dickson et al., 2003). This point is important and affects the trueness of TA results.

Therefore, the procedure chosen and thus the one to referred to in the rest of this manuscript is the open-cell mutli-step potentiometric titration.

The standard procedure as well as the data treatment method for the open-cell multi-step titration has been well described in the literature (Dickson et al., 2007, 2003; Okamura et al., 2014), and is presented below.

Procedure

A known amount of sample, measured by gravimetry, is placed in an open-cell thermostated at 25°C. The sample is titrated by an HCl solution of known amount content and density. It is often recommended that the HCl solution is prepared in an NaCl matrix in order to keep the ionic strength, and thus the activity coefficients, constant during the titration. However, Okamura *et al.* (2014) has indicated that using HCl solution containing no NaCl has a negligible effect on the TA results (about -0.2 µmol/kg).

A glass electrode allows the monitoring of the potential during the titration. The glass electrode is first calibrated in pH_T using a TRIS buffer.

The titration is then carried out in two stages. The first stage consists in adding enough HCl to reach a pH_T situated just beyond the endpoint (between pH_T 4 and 3.5). At this pH_T, the predominant weak bases, HCO_3^- and CO_3^{2-}, are converted to CO_2. This CO_2 is removed by agitation and by bubbling of air through the solution for around 6 minutes. A further addition of HCl, in a series of small increments, allows reaching a pH_T of about 3. At this pH_T, all proton acceptors are consumed (Figure 12). The data given by the titration (i.e. measured potential, temperature and volume of HCl added) during the second stage is used to compute the total alkalinity. Data are taken only for this range of pH_T as it is low enough to neglect residual bicarbonate ions and high enough so that the Nernst equation still holds true (Dickson et al., 2007).

Calculation

An initial estimate of the total alkalinity is obtained from the titration curve using Gran's method (Gran, 1952). This is a highly effective method for the determination of the equivalence point in potentiometric titrations.

At each point of the titration, the amount content of hydrogen ions C_H can be described by equation 1.13.

$$C_H = \frac{m_{HCl}\, C_{HCl} - m_{init}\, TA}{m_{HCl} + m_{init}} \tag{1.13}$$

where m_{HCl} is the mass of acid added (g), C_{HCl} the acid amount content (mol/kg-sol), and m_{init} the mass of sample analysed (g).

In the range of pH_T corresponding to the second stage of the titration, the following equation is valid (equation 1.14):

$$\frac{m_{HCl}\, C_{HCl} - m_{init}\, TA}{m_{HCl} + m_{init}} = [H^+] + [HSO_4^-] + [HF] \approx [H^+]_T \tag{1.14}$$

The glass electrode has been calibrated in total pH:

$$[H^+]_T = \exp\left(\frac{E - E^\circ}{\frac{RT}{F}}\right) = cst \exp\left(\frac{E}{\frac{RT}{F}}\right) \tag{1.15}$$

where E is the potential measured by the glass electrode (V), E° its reference potential (V) and *cst* and undefined constant.

From equations 1.14 and 1.15, the equation 1.16 is computed.

$$(m_{init} + m_{HCl}) \times \exp\left(\frac{E}{\frac{RT}{F}}\right) = \frac{-TA\, m_{init} + m_{HCl}\, C_{HCl}}{cst} \tag{1.16}$$

The left-hand side of this equation defines the Gran function F1. By plotting F1 as a function of the amount of HCl added for each point of the second stage of the titration, a graph illustrated by Figure 13 is obtained.

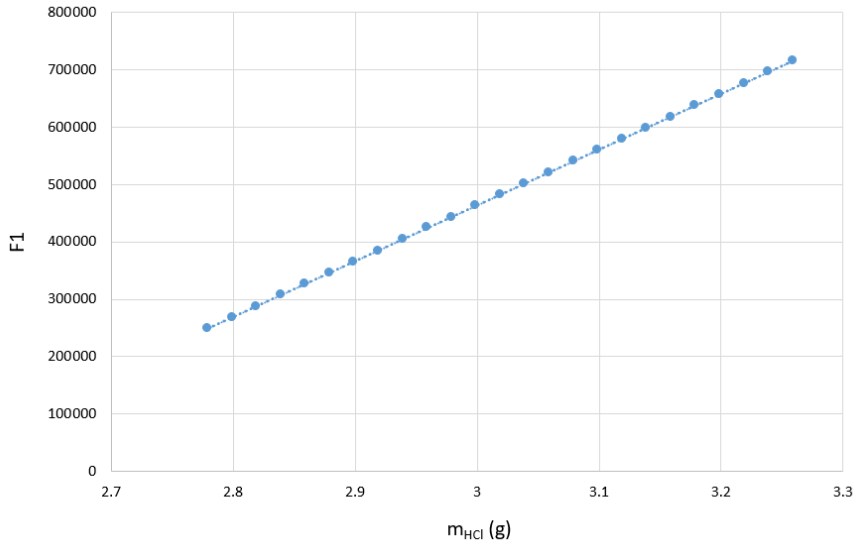

Figure 13: Gran's method illustrated for the estimation of total alkalinity of seawater from potentiometric data titration curve.

For F1 equals to zero, the total alkalinity is obtained with equation 1.17. At least 20 titration points are required in order to obtain a robust total alkalinity estimation.

$$AT = \frac{m_{HCl\_GRAN}\, C_{HCl}}{m_{init}} \tag{1.17}$$

where m_{HCl_GRAN} is the mass of HCl added for which F1 is equal to zero (g), determined with Gran's method.

This method gives a first estimation of the total alkalinity. However, errors are introduced when using the Gran's method for seawater analysis due to competing acid-base equilibria in seawater. A method allowing to solve the equivalence point by curve fitting has thus been developed (Dickson, 1981; Martz, 2005). This method consists in an iterative process where the standard potential of the glass electrode (E°) is calculated from the estimation of TA obtained by the Gran's method. A nonlinear least-squares (NLLS) regression is then used to refine the values of E° and TA. The refinement in E° first allows the calculation of the factor $f = [\mathrm{H}^+]_\mathrm{T}/[\mathrm{H}']_\mathrm{T}$, where $[\mathrm{H}']_\mathrm{T}$ is obtained from the refinement in E° and equation 1.15. f is then itself used to determine a new value of TA using equation 1.18.

$$TA + \frac{S_T}{1+\frac{K_S Z}{f\,[H^{+\prime}]_T}} + \frac{F_T}{1+\frac{K_F}{f\,[H^{+\prime}]_T}} + \frac{m_{init}+m_{HCl}}{m_{init}}\,\frac{f\,[H^{+\prime}]_T}{Z} - \frac{m_{HCl}\,C_{HCl}}{m_{init}} = 0 \tag{1.18}$$

where $Z = 1 + \frac{S_T}{K_s}$

The nonlinear least-squares regression consists in computing how much the left-hand side of equation 1.18 differs from zero. The residuals are squared and the sum of squares is minimized by adjusting f and TA using an algorithm. By applying this method, the errors in Ks are negligible (Dickson et al., 2007).

4.3. Metrological traceability and metrological tools: current state and needs

Metrological traceability and reference materials

Scripps Institution of Oceanography, in addition to producting TRIS buffers as reference materials for the validation of spectrophotometric pH_T measurements, also produces reference materials for the measurements of CO_2 in seawater (Dickson, 2010). These materials consist of natural seawater, stabilized through filtration, UV radiation and mercuric chloride poisoning. They are bottled in ground neck borosilicate bottles with greased stoppers. The natural seawater is characterized for total alkalinity and dissolved inorganic carbon with the open-cell multi-step potentiometric and vacuum extraction/manometric methods, respectively (Dickson, 2022, 2010). It is the only laboratory producing reference materials for total alkalinity measurements on a regular basis (Acquafredda et al., 2022).

The method used to assign a total alkalinity value to the natural seawater is sought to be validated with (1) an HCl titrant solution whose amount content is assessed by coulometry and (2) synthetic solution with a TA value known from the composition of the solution (i.e. purity of the salts used and gravimetric information). These two solutions are potentially traceable to the SI units (Figure 14). However, the synthetic solution is a simple system made of either TRIS, borax or sodium carbonate bases in an NaCl matrix. This should allow obtaining a known value of TA from the exact composition, but no acid-base equilibria coming from sulphate or fluoride ions are at stake, meaning the data treatment is achieved directly with the Gran's method and NLLS regression isn't required. Thus, only the accuracy of the experimental procedure is validated but not the entire data treatment.

Traceability is, as yet, not completely fulfilled between the validation of the calibration laboratory method and the assignment of the reference material TA value.

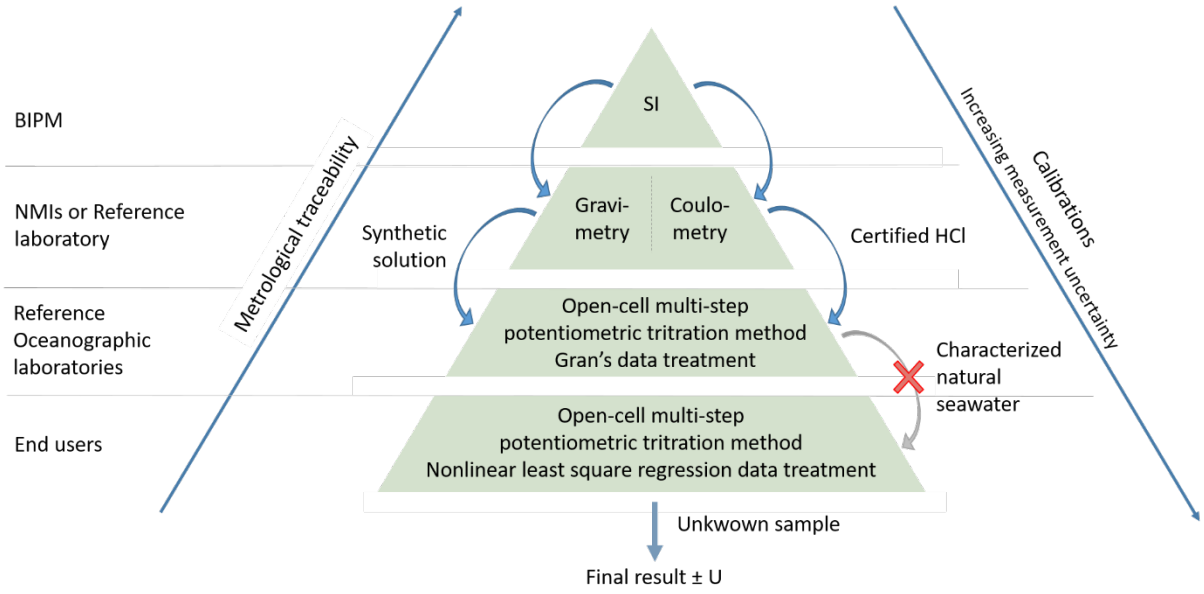

Figure 14: Schematized traceability route of seawater total alkalinity open-cell mutli-step titration measurement method.

Procedures for in-house preparation of reference materials have been made available. However, it is difficult to guarantee a sufficient quality of these in-house reference materials and it is thus recommended to use them only when the supply of commercially available reference materials is difficult (Moras et al., 2023).

Scripps also makes characterized HCl solution available. It could be useful to additionally distribute synthetic solution in order for end-users to be able to validate the measurement protocol independently from the entire data treatment, or to assign a molality to the end-user's HCl solution, with a traceable reference material. This requires also having a thorough evaluation of the uncertainty budgets associated.

Uncertainty budget

The reference material distributed by Scripps for TA measurements is given with an uncertainty estimated from standard deviation (i.e. precision) obtained from a definite number of analyses performed to assign a TA value to the material. A significant number of analyses are performed (typically around 30 from 9 different bottles), which allows having confidence in the value given. A complete uncertainty budget assessed with a bottom-up approach would allow controlling the trueness of end-user's procedures in a more robust manner. Up to date, no thorough uncertainty estimation of the open-cell multi-step potentiometric titration procedure following the bottom-up approach is reported in the literature. Anes *et al.* (2018) have conducted a work heading in that direction. They identified and quantified uncertainty sources for a simple endpoint potentiometric detection method, where they used derivative-based technique to locate the two titration inflexion points, for the measurement of carbonate alkalinity.

Carbonate alkalinity is a slightly different measurand from TA as reported in Section 4.1, which takes into account only alkalinity coming from carbonate and bicarbonate ions, neglecting other acid-base equilibria from seawater media. The major sources identified are the identification of the endpoint and the acid titrant concentration. They obtained a standard uncertainty for carbonate TA ranging from 25 to 40 µmol/kg-sol, which seems very high. This may be due to the fact that the concentration of acid is obtained from titration over TRIS solution instead of coulometrically. No other studies, to my knowledge, report bottom-up uncertainty quantification of TA measurements results. However, experimental studies seems to indicate very good precision of the measurement method, typically in the range 2-4 µmol/kg-sol (Bockmon and Dickson, 2015; Millero et al., 1998). This is encouraging in approaching the climate standard uncertainty objective fixed by the GOA-ON, being of 2 µmol/kg-sol for total alkalinity measurement results (GOA-ON, 2019). The Global Carbon Observation System (GCOS) implementation plan specifies a lower standard uncertainty, of 1 µmol/kg-sol (WMO et al., 2022).

Carter *et al.* (2023), pay attention to a particular source of uncertainty that shouldn't be omitted, being the contribution to alkalinity coming from unidentified total alkalinity. Unidentified total alkalinity refers to unknown or unconsidered acid-bases systems, such as the ones coming from organic bases. This seems important especially in coastal areas.

In assessing the uncertainties of TA measurement results on natural seawater (end-user's measurements or characterization of reference materials), it is necessary to take into account the uncertainty brought by the NLLS regression. This involves quantifying uncertainties from salinity and temperature, from the assumptions leading to the estimation of fluoride and sulphate amount contents, dissociation constants, and from the mathematical model, in addition to uncertainties in the volume and potential measurements comprising the titration.

In the computation of variables of the carbonate system from two input variables, the uncertainty can be propagated following the GUM from (1) input variables uncertainties and (2) equilibrium constants uncertainties. Orr *et al.* (2018) estimated that the major source comes from the input quantities. It is thus of major importance to thoroughly quantify these uncertainties.

Inter-laboratory comparisons

An inter-laboratory comparison was conducted in 1990 (Poisson et al., 1990) for several batches of seawater at different salinities. From 12 sets of results obtained by potentiometric titration and calculated for seawater without silicate and phosphate, a maximum difference of 29 µmol/kg-sol was obtained for the salinity 35. This early work showed a discrepancy more than ten times larger than the climate quality objective of

the GOA-ON. A more recent study (Bockmon and Dickson, 2015) conducted an inter-laboratory comparison and obtained 61 sets of results for total alkalinity measurements conducted with a variety of instruments and methods. The majority of the laboratory obtained results within 10 µmol/kg-sol of the assigned value and a few obtained results within 2 µmol/kg-sol. This improvement is encouraging in achieving a good data quality and comparability of measurement results. Moreover, it was shown in this study that the simple endpoint method seems to give lower values while small samples analysis (around 20 ml) gave larger uncertainties. A better agreement than the one obtained might thus be achievable with the conduction of open cell multi-step titrations and using sample volumes of at least 50 ml.

The development of reference materials by the Scripps Institution of Oceanography has now achieved a robust organization for the production, characterization and distribution of RMs that support the oceanographic community around the world in improving the data quality and comparability of total alkalinity measurement results. However, the RMs distributed aren't fully traceable and aren't given with a rigorously assessed uncertainty. Developing a reference material made in artificial seawater, characterized with a traceable reference method, and with a thoroughly quantified uncertainty that could be distributed together with a natural seawater such as the one from Scripps, might help in improving the trueness of the results. Moreover, the uncertainty budget of the measurement method results is required to ensure the comparability of total alkalinity measurements. The work relative to these metrological challenges conducted during the thesis are presented in Chapter V.

References

Acquafredda, M., Cochran, C., Busch, D.S., Jewett, L., Edmonds, H., Dickson, A.G., 2022. Understanding the Current Use and Future Needs of CO2 in Seawater Certified Reference Materials NOAA Technical Memorandum OAR-OAP-5. https://doi.org/10.25923/ANC4-GJ33

Allard, A., Fischer, N., 2015. Note technique n°002 : Guide pour l'évaluation des incertitudes de mesure LNE internal document.

Álvarez, M., Fajar, N.M., Carter, B.R., Guallart, E.F., Pérez, F.F., Woosley, R.J., Murata, A., 2020. Global Ocean Spectrophotometric pH Assessment: Consistent Inconsistencies. Environ. Sci. Technol. 54, 10977–10988. https://doi.org/10.1021/acs.est.9b06932

Anes, B., Bettencourt da Silva, R.J.N., Oliveira, C., Filomena Camões, M., 2018. Uncertainty evaluation of alkalinity measurements on seawater samples. Measurement 129, 395–404. https://doi.org/10.1016/j.measurement.2018.07.042

BIPM, 2019. The International System of Units (SI) 9th edition.

BIPM, 1921. The Metre Convention and Annexed Regulations.

Bockmon, E.E., Dickson, A.G., 2015. An inter-laboratory comparison assessing the quality of seawater carbon dioxide measurements. Marine Chemistry 171, 36–43. https://doi.org/10.1016/j.marchem.2015.02.002

Breland, J.A., Byrne, R.H., 1993. Spectrophotometric procedures for determination of sea water alkalinity using bromocresol green. Deep Sea Research Part I: Oceanographic Research Papers 40, 629–641. https://doi.org/10.1016/0967-0637(93)90149-W

Breton, E., Savoye, N., Rimmelin-Maury, P., Sautour, B., Goberville, E., Lheureux, A., Cariou, T., Ferreira, S., Agogué, H., Alliouane, S., Aubert, F., Aubin, S., Berthebaud, E., Blayac, H., Blondel, L., Boulart, C., Bozec, Y., Bureau, S., Caillo, A., Cauvin, A., Cazes, J.-B., Chasselin, L., Claquin, P., Conan, P., Cordier, M.-A., Costes, L., Crec'hriou, R., Crispi, O., Crouvoisier, M., David, V., Del Amo, Y., De Lary, H., Delebecq, G., Devesa, J., Domeau, A., Durozier, M., Emery, C., Feunteun, E., Fauchot, J., Gentilhomme, V., Geslin, S., Giraud, M., Grangeré, K., Grégori, G., Grossteffan, E., Gueux, A., Guillaudeau, J., Guillou, G., Harrewyn, M., Jolly, O., Jude-Lemeilleur, F., Labatut, P., Labourdette, N., Lachaussée, N., Lafont, M., Lagadec, V., Lambert, C., Lamoureux, J., Lanceleur, L., Lebreton, B., Lecuyer, E., Lemeille, D., Leredde, Y., Leroux, C., Leynaert, A., L'Helguen, S., Liénart, C., Macé, E., Maria, E., Marie, B., Marie, D., Mas, S., Mendes, F., Mornet, L., Mostajir, B., Mousseau, L., Nowaczyk, A., Nunige, S., Parra, R., Paulin, T., Pecqueur, D., Petit, F., Pineau, P., Raimbault, P., Rigaut-Jalabert, F., Salmeron, C., Salter, I., Sauriau, P.-G., Seuront, L., Sultan, E., Valdès, R., Vantrepotte, V., Vidussi, F., Voron, F., Vuillemin, R., Zudaire, Laurent., Garcia, N., 2023. Data quality control considerations in multivariate environmental monitoring: experience of the French coastal network SOMLIT. Frontiers in Marine Science 10.

Buck, R.P., Rondinini, S., Covington, A.K., Baucke, F.G.K., Brett, C.M.A., Camoes, M.F., Milton, M.J.T., Mussini, T., Naumann, R., Pratt, K.W., Spitzer, P., Wilson, G.S., 2002. Measurement of pH. Definition, standards, and procedures (IUPAC Recommendations 2002). Pure Appl. Chem. 74, 2169–2200. https://doi.org/10.1351/pac200274112169

Byrne, R.H., Breland, J.A., 1989. High precision multiwavelength pH determinations in seawater using cresol red. Deep Sea Research Part A. Oceanographic Research Papers 36, 803–810. https://doi.org/10.1016/0198-0149(89)90152-0

Carter, B.R., Radich, A., Doyle, H.L., Dickson, A.G., 2013. An automated system for spectrophotometric seawater pH measurements. Limnology and Oceanography: methods 16–27. https://doi.org/10.4319/lom.2013.11.16

Carter, B.R., Sharp, J.D., Dickson, A.G., Álvarez, M., Fong, M.B., García-Ibáñez, M.I., Woosley, R.J., Takeshita, Y., Barbero, L., Byrne, R.H., Cai, W.-J., Chierici, M., Clegg, S.L., Easley, R.A., Fassbender, A.J., Fleger, K.L., Li, X., Martín-Mayor, M., Schockman, K.M., Wang, Z.A., 2023. Uncertainty sources for measurable ocean carbonate chemistry variables. Limnology and Oceanography n/a. https://doi.org/10.1002/lno.12477

Clayton, T.D., Byrne, R.H., 1993. Spectrophotometric seawater pH measurements: total hydrogen ion concentration scale calibration of m-cresol purple and at-sea results. Deep Sea Research Part I: Oceanographic Research Papers 40, 2115–2129. https://doi.org/10.1016/0967-0637(93)90048-8

Culberson, C., Pytkowicz, R., Hawley, J., 1970. Seawater alkalinity determination by the pH method. Journal of Marine Research 28.

DeGrandpre, M.D., Spaulding, R.S., et al., 2014. Considerations for the measurement of spectrophotometric pH for ocean acidification and other studies. Limnology and Oceanography: Methods 12, 830–839. https://doi.org/10.4319/lom.2014.12.830

DelValls, T.A., Dickson, A.G., 1998. The pH of buffers based on 2-amino-2-hydroxymethyl-1,3-propanediol ('tris') in synthetic sea water. Deep Sea Research Part I: Oceanographic Research Papers 45, 1541–1554. https://doi.org/10.1016/S0967-0637(98)00019-3

Dickson, A.G., 2022. Certificate of Analysis, Reference material for oceanic CO2 measurements. University of California, San Diego Scripps Institution of Oceanography-Marine Physical Laboratory.

Dickson, A.G., 2010. Standards for Ocean Measurements. Oceanography 23, 34–47. https://www.jstor.org/stable/24860884

Dickson, A.G., 1993. pH buffers for sea water media based on the total hydrogen ion concentration scale. Deep Sea Research Part I: Oceanographic Research Papers 40, 107–118. https://doi.org/10.1016/0967-0637(93)90055-8

Dickson, A.G., 1992. The development of the alkalinity concept in marine chemistry. Marine Chemistry, Progress in Marine Chemistry 40, 49–63. https://doi.org/10.1016/0304-4203(92)90047-E

Dickson, A.G., 1990. Standard potential of the reaction: AgCl(s) + 12H2(g) = Ag(s) + HCl(aq), and and the standard acidity constant of the ion HSO4− in synthetic sea water from 273.15 to 318.15 K. The Journal of Chemical Thermodynamics 22, 113–127. https://doi.org/10.1016/0021-9614(90)90074-Z

Dickson, A.G., 1981. An exact definition of total alkalinity and a procedure for the estimation of alkalinity and total inorganic carbon from titration data. Deep Sea Research Part A. Oceanographic Research Papers 28, 609–623. https://doi.org/10.1016/0198-0149(81)90121-7

Dickson, A.G., Afghan, J.D., Anderson, G.C., 2003. Reference materials for oceanic CO2 analysis: a method for the certification of total alkalinity. Marine Chemistry 80, 185–197. https://doi.org/10.1016/S0304-4203(02)00133-0

Dickson, A.G., Sabine, C.L., Christian, J.R. (Eds.), 2007. Guide to Best Practices for Ocean CO2 Measurements PICES Special Publication 3, 191.

Douglas, N.K., Byrne, R.H., 2017a. Spectrophotometric pH measurements from river to sea: Calibration of mCP for 0 ≤S≤ 40 and 278.15 ≤T≤ 308.15 K. Marine Chemistry 197, 64–69. https://doi.org/10.1016/j.marchem.2017.10.001

Douglas, N.K., Byrne, R.H., 2017b. Achieving accurate spectrophotometric pH measurements using unpurified meta-cresol purple. Marine Chemistry 190, 66–72. https://doi.org/10.1016/j.marchem.2017.02.004

Edmond, J.M., 1970. High precision determination of titration alkalinity and total carbon dioxide content of sea water by potentiometric titration. Deep Sea Research and Oceanographic Abstracts 17, 737–750. https://doi.org/10.1016/0011-7471(70)90038-0

Fanton, J.-P., 2019. A brief history of metrology: past, present, and future. Int. J. Metrol. Qual. Eng. 10, 5. https://doi.org/10.1051/ijmqe/2019005

Fong, M.B., Dickson, A.G., 2019. Insights from GO-SHIP hydrography data into the thermodynamic consistency of CO2 system measurements in seawater. Marine Chemistry 211, 52-63. https://doi.org/10.1016/j.marchem.2019.03.006.

Fong, M.B., 2021. Uncertainty of spectrophotometric pH measurements in seawater and implications for ocean carbon chemistry. PhD dissertation, UC San Diego.

French Government, 2017. Adoption du système métrique décimal [WWW Document]. Gouvernement.fr. URL https://www.gouvernement.fr/partage/9103-adoption-du-systeme-metrique-decimal (accessed 2.28.24).

GOA-ON, 2023. Multinational Effort in the Search for a Global Solution for the Production and Certification of Reference Materials for Measurements of the Seawater Carbonate System.

GOA-ON, 2019. Global Ocean Acidification Observing Network (GOA-ON): Implementation Strategy.

Gran, G., 1952. Determination of the equivalence point in potentiometric titrations. Part II. Analyst 77, 661–671. https://doi.org/10.1039/AN9527700661

Greenberg, D.M., Moberg, E.G., Allen, E.C., 1932. Determination of carbon dioxide and titratable base in sea water. Ind. Eng. Chem. Anal. Ed. 4, 309–313. https://doi.org/10.1021/ac50079a031

Hansson, I., 1973. A new set of pH-scales and standard buffers for sea water. Deep Sea Research and Oceanographic Abstracts 20, 479–491. https://doi.org/10.1016/0011-7471(73)90101-0

Himbert, M.E., 2009. A brief history of measurement. Eur. Phys. J. Spec. Top. 172, 25–35. https://doi.org/10.1140/epjst/e2009-01039-1

Hudson-Heck, E., Byrne, R.H., 2019. Purification and characterization of thymol blue for spectrophotometric pH measurements in rivers, estuaries, and oceans. Anal Chim Acta 1090, 91–99. https://doi.org/10.1016/j.aca.2019.09.009

ISO 5725-1, 2023. Accuracy (trueness and precision) of measurement methods and results — Part 1: General principles and definitions.

ISO 5725-2, 2020. Accuracy (trueness and precision) of measurement methods and results-Part 2 : basic method for the determination of repeatability and reproducibility of a standard measurement method.

ISO 13528, 2022. Statistical methods for use in proficiency testing by interlaboratory comparison.

ISO 17034, 2016. General requirements for the competence of reference material producers.

ISO 18191, 2015. Water quality-Determination of pHt in sea water-Method using the indicator dye m-cresol purple.

ISO 21748, 2017. Guidance for the use of repeatability, reproducibility and trueness estimates in measurement uncertainty evaluation.

JCGM 100:2008, 2008. Evaluation of Measurement Data-Guide to the Expression of Uncertainty in Measurement.

JCGM 101:2008, 2008. Evaluation of measurement data — Supplement 1 to the "Guide to the expression of uncertainty in measurement" — Propagation of distributions using a Monte Carlo method.

JCGM 200:2012, 2012. International vocabulary of metrology (VIM) — Basic and general concepts and associated terms.

Lamandé, N., Salvetat, F., Bihan, C.L., Delauney, L., 2015. Spectrophotometric method for the determination of the pHT of sea water, in: 17th International Congress of Metrology. Presented at the 17th International Congress of Metrology, EDP Sciences, p. 07007. https://doi.org/10.1051/metrology/20150007007

Li, X., García-Ibáñez, M.I., Carter, B.R., Chen, B., Li, Q., Easley, R.A., Cai, W.-J., 2020. Purified meta-Cresol Purple dye perturbation: How it influences spectrophotometric pH measurements. Marine Chemistry 225, 103849. https://doi.org/10.1016/j.marchem.2020.103849

Liliana, L., 2016. A new model of Ishikawa diagram for quality assessment. IOP Conf. Ser.: Mater. Sci. Eng. 161, 012099. https://doi.org/10.1088/1757-899X/161/1/012099

Liu, X., Byrne, R.H., Lindemuth, M., Easley, R., Mathis, J.T., 2015. An automated procedure for laboratory and shipboard spectrophotometric measurements of seawater alkalinity: Continuously monitored single-step acid additions. Marine Chemistry 174, 141–146. https://doi.org/10.1016/j.marchem.2015.06.008

Liu, X., Patsavas, M.C., Byrne, R.H., 2011. Purification and Characterization of meta-Cresol Purple for Spectrophotometric Seawater pH Measurements. Environmental science & Technology 4862–4868.

Loucaides, S., Rèrolle, V.M.C., Papadimitriou, S., Kennedy, H., Mowlem, M.C., Dickson, A.G., Gledhill, M., Achterberg, E.P., 2017. Characterization of meta-Cresol Purple for spectrophotometric pH measurements in saline and hypersaline media at sub-zero temperatures. Sci Rep 7, 2481. https://doi.org/10.1038/s41598-017-02624-0

Magnusson, B., Näykki, T., Hovind, H., Krysell, M., Sahlin, E., 2017. Nordtest NT TR 537 - Edition 4 Handbook for calculation of measurement uncertainty in environmental laboratories.

Mari, L., 2006. On the measurand definition. XVIII IMEKO WORLD CONGRESS Metrology for a Sustainable Development September 17 – 22, 2006, Rio de Janeiro, Brazil.

Martín, J., Velázquez, N., Asuero, A.G., 2017. Youden Two-Sample Method Quality Control and Assurance-An Ancient Greek Term Re-Mastered. https://doi.org/10.5772/66397

Martz, T., 2005. A tracer monitored titration for seawater total alkalinity Graduate Student Theses, Dissertations, Professional Papers.

Meyer, V.R., 2007. Measurement uncertainty. Journal of Chromatography A, Data Analysis in Chromatography 1158, 15–24. https://doi.org/10.1016/j.chroma.2007.02.082

Middelburg, J.J., Soetaert, K., Hagens, M., 2020. Ocean Alkalinity, Buffering and Biogeochemical Processes. Rev. Geophys. 58. https://doi.org/10.1029/2019RG000681

Millero, F.J., 1986. The pH of estuarine waters. Limnology and Oceanography 31, 839–847. https://doi.org/10.4319/lo.1986.31.4.0839

Millero, F.J., Lee, K., Roche, M., 1998. Distribution of alkalinity in the surface waters of the major oceans. Marine Chemistry 60, 111–130. https://doi.org/10.1016/S0304-4203(97)00084-4

Millero, F.J., Zhang, J.-Z., Fiol, S., Sotolongo, S., Roy, R.N., Lee, K., Mane, S., 1993a. The use of buffers to measure the pH of seawater. Marine Chemistry 44, 143–152. https://doi.org/10.1016/0304-4203(93)90199-X

Millero, F.J., Zhang, J.-Z., Lee, K., Campbell, D.M., 1993b. Titration alkalinity of seawater. Marine Chemistry 44, 153–165. https://doi.org/10.1016/0304-4203(93)90200-8

Moras, C.A., Bach, L.T., Cyronak, T., Joannes-Boyau, R., Schulz, K.G., 2023. Preparation and quality control of in-house reference materials for marine dissolved inorganic carbon and total alkalinity measurements. Limnology and Oceanography: Methods 21, 637–644. https://doi.org/10.1002/lom3.10570

Mosley, L.M., Husheer, S.L.G., Hunter, K.A., 2004. Spectrophotometric pH measurement in estuaries using thymol blue and m-cresol purple. Marine Chemistry 91, 175–186. https://doi.org/10.1016/j.marchem.2004.06.008

Müller, J.D., Bastkowski, F., Sander, B., Seitz, S., Turner, D.R., Dickson, A.G., Rehder, G., 2018. Metrology for pH Measurements in Brackish Waters—Part 1: Extending Electrochemical pHT Measurements of TRIS Buffers to Salinities 5–20. Front. Mar. Sci. 5, 176. https://doi.org/10.3389/fmars.2018.00176

Müller, J.D., Rehder, G., 2018. Metrology of pH Measurements in Brackish Waters—Part 2: Experimental Characterization of Purified meta-Cresol Purple for Spectrophotometric pHT Measurements. Front. Mar. Sci. 0. https://doi.org/10.3389/fmars.2018.00177

Nemzer, B.V., Dickson, A.G., 2005. The stability and reproducibility of Tris buffers in synthetic seawater. Marine Chemistry 96, 237–242. https://doi.org/10.1016/j.marchem.2005.01.004

Okamura, K., Kimoto, H., Hatta, M., Noguchi, T., Nakaoka, A., Suzue, T., Kimoto, T., 2014. Potentiometric open-cell titration for seawater alkalinity considering temperature dependence of titrant density and Nernst response of pH electrode. Geochem. J. 48, 153–163. https://doi.org/10.2343/geochemj.2.0296

Orr, J.C., Epitalon, J.-M., Dickson, A.G., Gattuso, J.-P., 2018. Routine uncertainty propagation for the marine carbon dioxide system. Marine Chemistry 207, 84–107. https://doi.org/10.1016/j.marchem.2018.10.006

Papadimitriou, S., Loucaides, S., Rérolle, V., Achterberg, E.P., Dickson, A.G., Mowlem, M., Kennedy, H., 2016. The measurement of pH in saline and hypersaline media at sub-zero temperatures: Characterization of Tris buffers. Marine Chemistry 184, 11–20. https://doi.org/10.1016/j.marchem.2016.06.002

Patsavas, M.C., Byrne, R.H., Liu, X., 2013. Purification of meta-cresol purple and cresol red by flash chromatography: Procedures for ensuring accurate spectrophotometric seawater pH measurements. Marine Chemistry 150, 19–24. https://doi.org/10.1016/j.marchem.2013.01.004

Perez, F.F., Fraga, F., 1987. A precise and rapid analytical procedure for alkalinity determination. Marine Chemistry 21, 169–182. https://doi.org/10.1016/0304-4203(87)90037-5

Poisson, A., Culkin, F., Ridout, P., 1990. Intercomparison of total alkalinity and total inorganic carbon determinations in seawater. UNESCO: United Nations Educational, Scientific and Cultural Organisation UNESCO technical papers in marine science, 59.

Pratt, K.W., 2014. Measurement of pHT values of Tris buffers in artificial seawater at varying mole ratios of Tris:Tris·HCl. Marine Chemistry 162, 89–95. https://doi.org/10.1016/j.marchem.2014.03.003

Rakestraw, N., 1949. The conception of alkalinity of excess base of sea water. Journal of Marine Research 8.

Sant'Ambrogio, G., Dejours, P., 1995. On the Origin of the Metric System. Physiology 10, 46–49. https://doi.org/10.1152/physiologyonline.1995.10.1.46

Seidel, M.P., DeGrandpre, M.D., Dickson, A.G., 2008. A sensor for in situ indicator-based measurements of seawater pH. Marine Chemistry 109, 18–28. https://doi.org/10.1016/j.marchem.2007.11.013

Smith Jr., W.H., Hood, D.W., 1964. pH measurement in the ocean: a sea water secondary buffer system. In: Y. Miyake, Y., Koyama, T. (Eds), Recent Researches in the Fields of Hydrosphere, Atmosphere and Nuclear Geochemistry. Published by Editorial Committee for Sugawara Volume, distributed by Maruzen Company, Ltd, Tokyo, Japan, pp. 185–202.

Stoica, D., Ben-Achour, M., Spitzer, P., Fisicaro, P., Vaslin-Reimann, S., 2014. pH measurement of seawater: a present day challenge. R. franç. métrol. 23–30. https://doi.org/10.1051/rfm/2014006

Takeshita, Y., Johnson, K.S., Coletti, L.J., Jannasch, H.W., Walz, P.M., Warren, J.K., 2020. Assessment of pH dependent errors in spectrophotometric pH measurements of seawater. Marine Chemistry 223, 103801. https://doi.org/10.1016/j.marchem.2020.103801

Takeshita, Y., Warren, J.K., Liu, X., Spaulding, R.S., Byrne, R.H., Carter, B.R., DeGrandpre, M.D., Murata, A., Watanabe, S., 2021. Consistency and stability of purified meta-cresol purple for spectrophotometric pH measurements in seawater. Marine Chemistry 236, 104018. https://doi.org/10.1016/j.marchem.2021.104018

Thompson, T.G., Bonnar, R.U., 1931. The Buffer Capacity of Sea Water. Industrial and Engineering Chemistry - Analytical Edition 3, 393–395. https://doi.org/10.1021/ac50076a029

Watanabe, A., Kayanne, H., Nozaki, K., Kato, K., Negishi, A., Kudo, S., Kimoto, H., Tsuda, M., Dickson, A.G., 2004. A rapid, precise potentiometric determination of total alkalinity in seawater by a newly developed flow-through analyzer designed for coastal regions. Marine Chemistry 85, 75–87. https://doi.org/10.1016/j.marchem.2003.09.004

Wedborg, M., Turner, D.R., Anderson, L.G., Dyrssen, D., 1999. Determination of pH. Methods of Seawater Analysis 109–125. https://doi.org/10.1002/9783527613984.ch7

White, R., 2011. The meaning of measurement in metrology. Accred Qual Assur 16, 31–41. https://doi.org/10.1007/s00769-010-0698-1

WMO, United Nations Environment Programme (UNEP), International Science Council (ISC), Scientific and Cultural Organization (IOC-UNESCO) Intergovernmental Oceanographic Commission of the United Nations Educational, 2022. The 2022 GCOS Implementation Plan (GCOS-244) [WWW Document]. URL https://library.wmo.int/records/item/58104-the-2022-gcos-implementation-plan-gcos-244 (accessed 1.4.24).

Wolf-Gladrow, D.A., Zeebe, R.E., Klaas, C., Körtzinger, A., Dickson, A.G., 2007. Total alkalinity: The explicit conservative expression and its application to biogeochemical processes. Marine Chemistry 106, 287–300. https://doi.org/10.1016/j.marchem.2007.01.006

Wright, J.D., 2000. Laboratory Primary Standards Flow Measurement, ISA, Research Triangle Park, NC.

Yin, T., Papadimitriou, S., Rérolle, V.M.C., Arundell, M., Cardwell, C.L., Walk, J., Palmer, M.R., Fowell, S.E., Schaap, A., Mowlem, M.C., Loucaides, S., 2021. A Novel Lab-on-Chip Spectrophotometric pH Sensor for Autonomous In Situ Seawater Measurements to 6000 m Depth on Stationary and Moving Observing Platforms. Environ. Sci. Technol. 55, 14968–14978. https://doi.org/10.1021/acs.est.1c03517

Part I: Development of metrological tools for the measurement of pH_T in seawater

Chapter II: Production of a reference material for seawater spectrophotometric pH_T measurements and its use in an inter-laboratory comparison

1. Introduction

Measurements of seawater pH_T contribute to the assessment of ocean acidification and to the study of the oceanic carbonate system, if a sufficient data quality is achieved. To be able to highlight significant trends in ocean acidification, the Global Ocean Acidification Observing Network (GOA-ON) has fixed the data quality objective for the monitoring of ocean acidification, called the "climate" quality objective, for which pH_T measurement uncertainties must be less than 0.003 (GOA-ON, 2019). The aforementioned "climate" data quality objective of the GOA-ON differs from the "weather" quality objective, for which an uncertainty of only 0.02 in pH_T is required. As data from diverse sources, spatial and temporal scales, and various instruments are shared internationally, ensuring high data quality becomes increasingly critical (Pearlman et al., 2019).

The number and frequency of seawater pH measurements have increased significantly through the development of the highly-reproducible spectrophotometric measurement method (Byrne and Breland, 1989) together with the introduction of the concept of pH on a total scale. Although spectrophotometric analyses are readily implemented and straightforward, there are several aspects that can affect the quality of pH_T measurements (e.g. the purity of the indicator dye, the perturbation of adding dye on the pH_T of the sample, the temperature control, the performance characteristics of the instrument, etc.). Assessing the reliability of pH_T measurements requires the availability of appropriate reference materials. Reference materials with assigned value and quantified uncertainty play an important role in the implementation and maintenance of a robust quality assurance system and represent key elements in assuring the comparability of measurement results. As such, they can be used for the spectrophotometric pH_T measurement method validation, the calibration of the indicator dye or the estimation of routine measurement uncertainty by following a top-down approach.

The metrological traceability chain of pH_T spectrophotometric measurements requires the TRIS buffer reference material. In order to obtain the lowest uncertainty on routine pH_T measurements, it is mandatory to have previously obtained the lowest uncertainty on the pH_T value assigned to the reference material. A particular attention is thus being paid to the uncertainty estimates, which should consider the contribution of the homogeneity and stability of the reference material. The ISO Guide 35, "Reference materials – Guidance for characterization and assessment of homogeneity and stability" ("ISO Guide 35," 2017) provides technical recommendations for the assessment of these components.

The commonly accepted reference material for seawater pH_T is an equimolal buffer of 2-Amino-2-(hydroxymethyl)-1,3-propanediol (TRIS) and TRIS hydrochloride (TRIS.HCl) in artificial seawater of salinity 35 (Wolfe et al., 2021). The studied buffer is thus a solution at $b(\text{TRIS}) = b(\text{TRIS.HCl}) = 0.04$ mol/kg-H_2O (where b expresses

molality in moles per kilogram of solvent, i.e. water in this study, noted mol/kg-H_2O) ; which equals a pH_T of 8.1 at 25°C (DelValls and Dickson, 1998; Müller et al., 2018; Pratt, 2014). This buffer has been developed and is now distributed on a regular basis by Scripps Institution of Oceanography (Dickson, 2010). It can be characterized in terms of pH_T by potentiometric measurements made using a Harned cell.

The aim of the study presented in this chapter is to describe the production of a reference material for oceanic pH_T measurements at the Laboratoire National de Métrologie et d'Essais (LNE), according to the ISO guide 35 and ISO standard 17034, "General requirements for the competence of reference material producers" guidelines ("ISO 17034", 2016; "ISO Guide 35", 2017). It includes a thorough uncertainty budget evaluation carried out following the Guide to the expression of Uncertainty in Measurement (GUM). Characterization with Harned Cell at three temperatures as well as homogeneity and long-term stability assessments are performed and taken into account in the final uncertainty budget. Critical parameters: the TRIS buffer water mass fraction definition and pH_T measurement traceability are identified and discussed.

The use of an equivalent reference material in an inter-laboratory comparison of spectrophotometric pH_T measurements is presented. It was performed with the laboratories involved in the French coastal observation service SOMLIT (Service d'Observation en Milieu Littoral), which carries out temporal data series and annual inter-laboratory comparisons (Breton et al., 2023; Lheureux et al., 2021) and laboratories involved in the project CocoriCO_2 (La Conchyliculture dans un monde riche en CO_2). In addition to the results of the comparison themselves, this study allowed us to establish an uncertainty budget from experimental data (i.e. following the top-down approach) and to demonstrate the applicability of the reference material used to maintain a robust quality assurance system of routine pH_T measurements.

This work has been published under the following references:

- Capitaine, G., Demeyer, S., Stoica, D., Alliouane, S., Petton, S., Rimmelin-Maury, P., Savoye, N., Wagener, T., Fisicaro, P., 2023a. Inter-laboratory comparison on a reference material for seawater spectrophotometric pHT measurements. Presented at the 2023 IEEE International Workshop on Metrology for the Sea; Learning to Measure Sea Health Parameters (MetroSea), La Valletta, Malta, pp. 11–15. https://doi.org/10.1109/MetroSea58055.2023.10317274
- Capitaine, G., Stoica, D., Wagener, T., Fisicaro, P., 2023b. Production of a reference material for seawater pHT measurements by a National Metrology Institute. Marine Chemistry 252, 104244. https://doi.org/10.1016/j.marchem.2023.104244

2. Materials and methods

2.1. Instrumentation

The LNE has a quality system that follows the principles of the ISO standard 17025, "General requirements for the competence of testing and calibration laboratories" ("ISO 17025", 2017). All measurements presented in this manuscript comply with the requirements of the aforementioned ISO standard.

2.1.1. pH_T Harned cell measurements

Each Harned cell measurement was carried out at 15°C, 25°C and 30 °C. The setup is described in Figure 15. The cells were placed in a TAMSON thermostatic bath regulated within ± 0.01°C and connected to a recirculating chiller Agilent G3292A, allowing measurements to be carried out at a known, stable and reproducible temperature. Five calibrated 4-wire resistance Pt100 probes were placed at different locations in the bath to check for temperature stability and homogeneity. The potential difference between the two electrodes in the Harned cell was measured with an Agilent 34972A, a high input-impedance data acquisition system. It was recorded using the Agilent Benchlink Data Logger software along with the bath temperature measurement. Standard measurement uncertainties were respectively of 10 µV and 0.01°C. The Agilent 34972A was equipped with two multiplexers allowing for six potentiometric measurements. Atmospheric pressure was measured with a Druck DPI 740 sensor having a resolution of 1 Pa and an uncertainty of 100 Pa. Pressure was recorded with Acquisit, an LNE in-house software. All data (i.e. potential difference, temperature and pressure) were collected every 2 minutes. The pH_T calculations were carried out using data collected during one hour of acquisition (i.e. 30 points), after achieving a stable potential signal (i.e. standard deviation below 20 µV).

The Pt,H_2 and Ag/AgCl electrodes were prepared at LNE according to the methods described by Bates (Bates, 1973) for primary pH measurements.

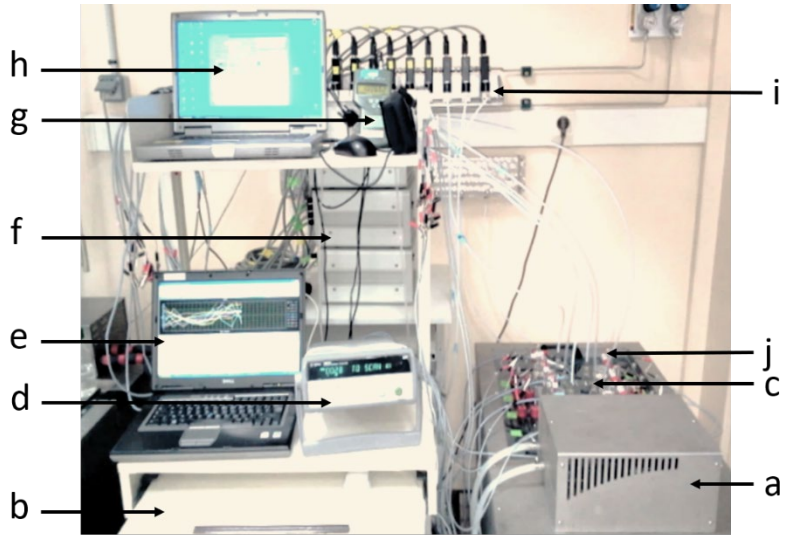

Figure 15: Description of the Harned cell measurement setup. a) TAMSON thermostatic bath. b) Agilent G3292A recirculating chiller. c) Pt100 probes. d) Agilent 34972A high input-impedance data acquisition system. e) Agilent Benchlink Data Logger software. f) Multiplexers. g) Druck DPI 740 atmospheric pressure sensor. h) Acquisit LNE in-house software. i) Hydrogen flow entrance. j) Harned cells.

2.1.2. pH_T spectrophotometric measurements

The pH_T spectrophotometric measurements were carried out with an Agilent Cary 60 UV-visible spectrophotometer. The description of the setup is showed by Figure 16. The internal support of the spectrophotometer can accommodate a cylindrical cell of 10 cm path-length. Starna quartz cells, with a 10 cm optical path-length, two opening chimneys and PTFE plugs, were used.

The cells were pre-thermostated in a LAUDA ECO GOLD RE 2025 GN recirculating chiller. A Lauda Loop L100 circulation thermostat was also connected to the internal support by two heat-insulated tubes allowing the stabilisation and control of the temperature inside the cell. The two PTFE plugs of the spectrophotometric cell contained a calibrated temperature probe allowing for precise measurements of the temperature inside the cell during the pH_T measurement. Both the recirculating chiller and the circulation thermostat were set in order to obtain a temperature of 25.0 $\pm$ 0.1°C inside the cell.

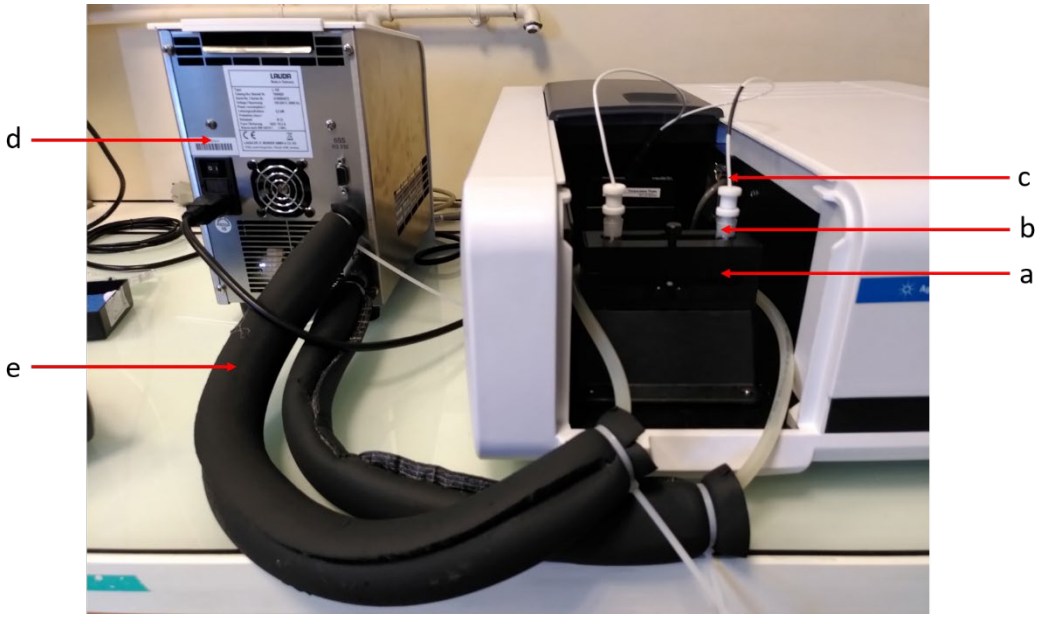

Figure 16: Description of the spectrophotometric measurement setup. a) Thermostated internal support. b) Starna quartz cell of 10 cm path-length. c) PTFE plugs of the spectrophotometric cell containing calibrated temperature probes. d) Lauda Loop L100 circulation thermostat. e) heat-insulated tubes.

The indicator dye used is a concentrated solution of purified meta cresol purple (2mmol/L) with a pH, checked with a glass electrode, approximating that of marine waters. It was prepared following the recommendations of Dickson et al. (2007). A micropipette with a volume of 50µL-1000µL was used to inject 60µL of the indicator dye solution into the sample.

The Cary WinUV software was used for the acquisition of absorbances. The acquisition was carried out in the "Kinetics" or “Scan” modes, which allows the acquisition of absorbances at individual wavelengths, or the acquisition of the entire spectrum between 300nm and 800nm, respectively.

The pH_T results are obtained following the method described in Chapter I, Section 3.2 and computed using equations 1.8, 1.9.a and 1.9.b.

The terms corresponding to the dye characterization were calculated using the functions given in Liu et al. (2011).

The spectrophotometer was checked in linearity and wavelength accuracy using optical density and holmium filters, respectively. The filters were calibrated at Danmarks Nationale Metrologiinstitut (DFM, Danish Metrology Institute).

2.2. Reference material preparation

Artificial seawater matrix

In order to simulate natural seawater, an artificial seawater matrix was chosen as defined by the International Association for the Physical Sciences of the

Oceans (IAPSO) for a practical salinity of 35 (Millero et al., 2008). For simplicity, the anions CO_3^{2-}, $B(OH)_4^-$, OH^-, F^- and HCO_3^- were replaced by chloride ions and Sr^{2+} were replaced by calcium ions (Pratt, 2014). Moreover, as Br- ions can damage silver-silver chloride electrodes (Sandifer, 1981), they were substituted with chloride ions in the composition to allow the use of the potentiometric system for pH_T measurements.

Preparation procedure and Materials

Reference materials should be prepared in such a way that they are homogeneous and stable (i.e. have constant characteristics over a sufficiently long period). The production of the reference material included the gravimetric preparation from reagents easily weighable and of known composition together with the use of a protocol that enables to reproduce the composition between different batches.

The products used for the preparation of the TRIS buffer in the artificial seawater matrix are TRIS (NIST Standard Reference Material 723e), NaCl (VWR chemicals, 99.945%), KCl (VWR chemicals, 99.928%), Na_2SO_4 (VWR chemicals, 99.994%), $CaCl_2.2H_2O$ (VWR chemicals), $MgCl_2.6H_2O$ (Merck), HCl (Slovak Institute of Metrology (SMU) Standard Reference Material, amount content of 1 mol/kg-sol) and Milli-Q water.

As calcium chloride and magnesium chloride are highly hygroscopic salts, they are dissolved independently in two separate solutions in order to facilitate weighing.

Great care was taken on the quality of the products used. To this respect, all the purchased salts and solutions used for the preparation of the artificial seawater were characterized in term of mass fraction based on halide content, except for Na_2SO_4 for which mass fraction of anion content has been determined. The characterization was carried out by the Slovak Institute of Metrology (SMU) using coulometric assay. The Milli-Q water used to prepare the buffer was boiled then left overnight under Argon bubbling to get rid of oxygen and limit bacterial development.

The TRIS buffer was prepared gravimetrically from stock solutions of the different components: NaCl, minor salts (KCl, $CaCl_2$, $MgCl_2$), Na_2SO_4, HCl and TRIS (Table 1, Table 2).

Table 1: Stock solutions molalities (mol/kg-H_2O) used for the TRIS buffer preparation.

		b (mol/kg-H_2O)
Minor salts	KCl	0.054511
	$CaCl_2$	0.055392
	$MgCl_2$	0.282045
HCl		1.047969
NaCl		2.137023
Na_2SO_4		0.410475
TRIS		0.827402

Table 2: Detailed information from gravimetric data of the TRIS buffer preparation.

	Stock solution weighed (g)	*v* (mol/kg-sol)	*b* (mol/kg-H_2O)	Target *b* (mol/kg-H_2O)	Delta *b* (mol/kg-H_2O)
HCl	363.6014	0.038272	0.040000	0.040000	0.000000
NaCl	1871.7003	0.370789	0.387529	0.387531 =0.427531-*b*(HCl)	-0.000002
KCl	1846.8833	0.010123	0.010580	0.010580	0.000000
Na_2SO_4	692.2908	0.028000	0.029264	0.029264	0.000000
$CaCl_2$	1846.8833	0.010287	0.010751	0.010751	0.000000
$MgCl_2$	1846.8833	0.052377	0.054742	0.054742	0.000000
TRIS	976.0824	0.076544	0.080000	0.080000	0.000000
Final buffer solution mass (g)	**9589.7545**				

In order to maintain the same nominal ionic strength as natural seawater, the 0.04 mol/kg-H_2O of HCl added were subtracted from the targeted NaCl molality during TRIS buffer solution preparation (Table 2, Dickson et al., 2007).

After being prepared, the 9 litres of buffer solution were bottled in 125 mL borosilicate-33 glass bottles with screw caps and sealed using Parafilm to minimize evaporation and gas exchanges with the atmosphere, especially for carbon dioxide. The bottles are filled to the brim with a peristaltic pump, which delivers the same volume in all bottles; the final volume contained in each bottle is of approximately 160 ml. Bottles were stored in the dark in a temperature and humidity-controlled room.

2.3. Reference material characterization method

The characterization was performed following the method detailed in Chapter I, Section 3.4 and with instrumentation detailed in Section 2.1.1.

Figure 17 schematizes the measurement steps performed for the pH_T determination of the reference material. The determination of the terms in boxes in the equation 1.10.a (Figure 17) requires two Harned cell measurement steps (1) and (2), that are presented in Chapter I, Section 3.4. Other terms are known from gravimetric information or from temperature and pressure measurements. Each of the steps described in Figure 17 was performed at 15°C, 25°C and 30°C.

The final pH_T value is the mean of the pH_T calculated from six distinct potentials E measured for the step (2) in Figure 17.

The additional step conducted with the Harned cell setup stands for the evaluation of the homogeneity within the batch of Ag/AgCl electrodes used (Figure 17). This step corresponds to the determination of their standard potential, noted E°, in a solution of HCl at a molality of 0.01 mol/kg-H_2O. It was performed at the three studied temperatures. This step isn't involved in the determination of the pH_T absolute value but remains important as it will be included in the final uncertainty budget. Indeed, to be able to attribute the E°* value obtained by extrapolation during step (1) in Figure 17, to each of the six Ag/AgCl electrodes used, the discrepancy between these electrodes must be taking into account. To do so, the standard deviation between the E° values of the batch of six Ag/AgCl electrodes is included in the uncertainty budget of the E°* value.

$$pH_T = \frac{E - E^{\circ *}}{k} + log(b_{Cl}) - log(\omega_{H2O}) \qquad (1.10.a)$$

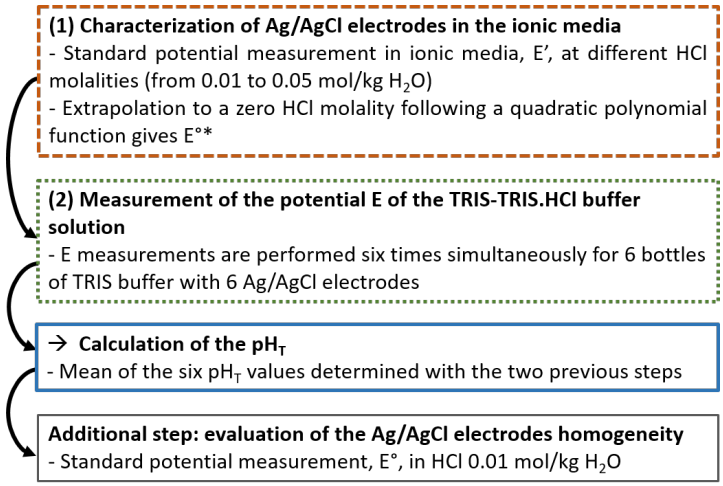

Figure 17: Harned cell measurements steps allowing the determination of the pH_T.

ω_{H2O} (equation 1.10.a, Figure 17) is used to convert the pH_T from molality to amount content for sake of practicality for end-users. It must correspond to the water mass fraction of the reference natural seawater composition of the relevant salinity (more details in Chapter III, section 2.3). However, in this chapter, ω_{H2O} is calculated from the actual buffer composition ignoring the TRIS and considering the molality of HCl as part of the NaCl amount, in order to represent a pure artificial seawater (equation 2.1). This allows us to correctly assess the uncertainty of this term based on gravimetric preparation of the buffer, while it leads to a difference in pH_T compared to the correct definition of only 0.0002. The definition given to this term has not yet reached a consensus and is thus discussed in more details in Section 4.2.

$$\omega_{H2O} = \frac{1000 - ((\nu_{HCl} + \nu_{NaCl}) \times M_{NaCl} + \sum(\nu_i \times M_i))}{1000} \qquad (2.1)$$

where ω_{H2O} is the water mass fraction (g/kg-sol) of pure artificial seawater, ν the amount content of stock solutions that make up the pure artificial seawater composition

(i.e. TRIS is removed and HCl is added to the NaCl amount) (mol/kg-sol), M the molar mass (g/mol), i corresponds to the remaining salts (i.e. KCl, $MgCl_2$, $CaCl_2$, Na_2SO_4).

2.4. Homogeneity assessment

Homogeneity is one of the defining characteristics of reference materials and should include estimates for both within and between bottle homogeneity. Because of the amount of solution needed for one Harned cell measurement (i.e. 150mL, which is a bit less than the volume included in one bottle filled up to the brim), only the latter component was evaluated. For this purpose, six bottles were randomly selected across the entire batch, representing around 10% of the total number of produced bottles.

Harned cell measurements were carried out under repeatability conditions (i.e. same time, operator, environment conditions and protocol) and immediately after the preparation of the batch. Data acquired were used both for the homogeneity assessment and for the calculation of the pH_T value of the reference material described in Section 2.3.

2.5. Stability assessment

According to the definition, reference materials should be sufficiently stable for their intended use, so that the end user can rely on the assigned value at any point within the period of validity. Stability study should evaluate long-term storage conditions, and consider transport conditions ("ISO 17034", 2016; "ISO Guide 35", 2017).

For the feasibility study presented in this chapter, only long-term storage was evaluated. The reference material was monitored by Harned cell measurements for eight months after the preparation and characterization date.

The stability is assessed based on the acidity function value measured at 25°C, described by equation 2.2. This limits the complexity of the experimental protocol (i.e. E°* is not redetermined, although E° is), while offering the accuracy needed to highlight an eventual instability.

$$a.f. = \frac{E_{mes} - E^\circ}{k} + log\left(\frac{b_{Cl}}{b^0}\right) - \frac{1}{2} lg\left(\frac{P - p_{vap} + 0.4 \times \rho \times g \times h}{p^\circ}\right) \quad (2.2)$$

where $a.f.$ is the acidity function, E_{mes} the measured cell potential (V), E° the standard potential of Ag/AgCl electrodes (V), k the Nernstian term (V), b_{Cl} the molality of chloride (mol/kg-H_2O), b^0 equals 1 mol/kg-H_2O, P the measured ambient pressure (Pa), p_{vap} the saturation vapour pressure of the solution (Pa), ρ the density of the solution (kg/m^3), g the standard gravity (m/s^2), h the liquid height (m) and p° the standard pressure (101 325 Pa).

To evaluate the stability one must highlight with a statistical Student test (or t test) whether there is a significant trend in the evolution of the material or not ("ISO Guide 35", 2017).

This test is based on the determination of the slope, noted b1, of the regression line of the acidity function values as a function of time. It computes t_0, defined as being the ratio of the slope on its standard deviation, noted sb1, and compares it to the threshold value t_α in the Student's table with n-2 degrees of freedom (for this study, n=11) at a 95% confidence level ("ISO Guide 35", 2017; Linsinger et al., 2001).

The spectrophotometric pH_T measurement method was used as a complementary tool to assess the stability over time of the reference material. Measurements were realized with instrumentation information given in Section 2.1.2 and with the method detailed in Chapter I, Section 3.2. Spectrophotometric measurements were performed up to ten months after the reference material preparation.

2.6. Global uncertainty budget of the reference material

The overall standard uncertainty budget of the reference material pH_T value (u_{MR}) takes into account the TRIS buffer preparation and characterization carried out with the Harned cell system (u_{charac}), the homogeneity (u_{hom}) and the stability over time (u_{stab}) of the material and is thus assessed from equation 2.3 ("ISO Guide 35", 2017).

$$u_{MR} = \sqrt{u_{charac}^2 + u_{hom}^2 + u_{stability}^2} \tag{2.3}$$

The expanded uncertainty is computed from the overall standard uncertainty using a level of confidence of 95 percent, corresponding to a coverage factor of 2.

2.6.1. Preparation and characterization: u_{charac}

The term u_{charac} corresponds to the standard uncertainty obtained during preparation and characterization of the reference material. The pH_T is determined with the Harned cell system from equation 1.10.a. u_{charac} is assessed based on this equation using the law of uncertainty propagation following the Guide to the expression of Uncertainty in Measurements recommendations (Chapter I, Section 2.5; "JCGM 100:2008," 2008; Shi et al., 2021).

In order to assess the standard uncertainties of each term in equation 1.10.a, allowing a determination of u_{charac}, several steps, detailed hereafter, are followed. For each term, the uncertainty sources are identified inside their respective equations, which corresponds to the mathematical model of the term in question. The quantification of these uncertainty sources is detailed and the uncertainty corresponding to each term is obtained using the law of propagation through the equations given below.

(1) The uncertainties relative to the water mass fraction, ω_{H2O} and the chloride ion molality in the buffer solution, b_{Cl}, are obtained from the reference material gravimetric preparation. It includes weighing scales calibration and uncertainties of the molar masses.

Amount content of each stock solution

The first step, needed to assess uncertainties introduced by b_{Cl} and ω_{H2O}, is to evaluate the standard uncertainties corresponding to the amount content of each stock solution.

Following is an example for the NaCl stock solution using equation 2.4:

$$\nu_{NaCl} = \frac{m_{NaCl} \times 1000}{M_{NaCl} \times m_{total}} \tag{2.4}$$

where ν_{NaCl} is the amount content of the NaCl stock solution (mol/kg-sol), m_{NaCl} the mass of NaCl salt weighed (g) with the purity and buoyancy factor, introduced by the Archimede's principle, taken into account, m_{total} the total mass of NaCl stock solution (g) with buoyancy factor taken into account and M_{NaCl} the molar mass of NaCl (g/mol).

As the masses of NaCl and total stock solution are obtained from a subtraction (e.g. $m_{NaCl} = m_{NaCl+bottle} - m_{empty\_bottle}$); standard uncertainty of masses is calculated from equation 2.5.

$$u_m = \sqrt{(u_{m1})^2 + (u_{m2})^2} \tag{2.5}$$

All uncertainties assigned to molar masses, M_i, are taken from IUPAC (Meija et al., 2016).

The Slovak Metrology Institute certificate gives the standard uncertainty of the amount content of the stock solution of HCl purchased from SMU.

Water mass fraction: ω_{H2O}

The second step evaluates the standard uncertainty of the water mass fraction in the buffer solution, given by equation 2.1.

The standard uncertainties of ν_i and M_i are detailed in the step above.

Chloride ion molality in the buffer solution: b_{Cl}

To evaluate the standard uncertainty corresponding to the chloride ion molality of the buffer solution, equation 2.6 is used:

$$b_{Cl} = \sum \left(\frac{\nu_{i \times m_i}}{m_{buffer} \times \omega_{H2O}} \right) \tag{2.6}$$

where b_{Cl} corresponds to the molality of chloride ions in the buffer solution (mol/kg-H_2O), ν_i the amount content of NaCl, minor salts and HCl stock solutions (mol/kg-sol), m_i the mass of corresponding stock solution weighed (g) and m_{buffer} the total mass of reference material produced (g).

The standard uncertainties of ν_i, ω_{H2O} and m_i are detailed in the steps above.

(2) The temperature, pressure and density uncertainties are known from the device calibration certificates. Other terms in the Nernstian term, *k*, and in the equation allowing the correction of the measured potential to a hydrogen pressure of 1 atm (equations 1.10.b and 1.10.c, presented in Chapter I, Section 3.4), are taken from the literature or can be neglected (Pratt, 2014).

(3) The uncertainty relative to the measured potential, E_{mes} (presented in equation 1.10.b of Chapter I, section 3.4), includes the uncertainty given by the calibration ($u_{calibration}$) and the maximum standard deviation obtained between the potentials acquired during one hour for each of the six simultaneous measurements (u_{maxSD}). It is defined by equation 2.7.

$$u_{Emes} = \sqrt{(u_{calibration})^2 + (u_{maxSD})^2} \quad (2.7)$$

(4) The same methodology is applied to establish the uncertainty of the standard potential E' of Ag/AgCl electrodes in saline media for a specific chloride molality. The uncertainty evaluation of E' is calculated only for a chloride molality of 0.01 mol/kg-H_2O as it is the lowest molality used in this study for the assessment of E°*, and thus the one with the largest uncertainty on the gravimetric preparation.

E' is calculated with the equation 2.8.

$$E' = E_{mes} + k \lg (b_{Cl-} \times b_{HCl}) - \frac{k}{2} lg \left(\frac{P - p_{vap} + 0.4 \times \rho \times g \times h}{p^\circ}\right) \quad (2.8)$$

where E' is the standard potential of Ag/AgCl electrode in saline media for a given chloride molality (V), E_{mes} the measured potential (V), k the Nernstian term, b_{HCl} and b_{Cl-} are respectively the HCl and total chloride ion molalities (mol/kg-H_2O), P the measured ambient pressure (Pa), p_{vap} the saturation vapour pressure (Pa), ρ the density of the solution (kg/m^3), g the standard gravity (m/s^2), h the liquid height (m) and p° the standard pressure (101 325 Pa).

The uncertainty of the b_{Cl-}term is defined with the same method as described above for the b_{Cl-} of the buffer uncertainty evaluation.

The b_{HCl} uncertainty is calculated using equation 2.9.

$$b_{HCl} = \frac{m_{HCl} \times \nu_{HCl}}{m_{total} \times \omega_{H2O}} \quad (2.9)$$

where b_{HCl} is the HCl molality of the studied solution (mol/kg-H_2O), ν_{HCl} the HCl amount content given by SMU (mol/kg-sol), m_{HCl} the mass of HCl weighed (g), m_{total} the total mass of solution and ω_{H2O} the water mass fraction of this solution (g/kg-sol).

ω_{H2O} uncertainty is defined with the same method as above but for the E' solution with a 0.01 mol/kg-H_2O HCl molality and by taking into account the actual composition of this solution (that contains no TRIS).

(5) Finally, the E°* term uncertainty is given by equation 2.10.

$$u_{E°*} = \sqrt{\left(u_{extrapolation}\right)^2 + \left(u_{S_{E°}}\right)^2 + \left(u_{E'}\right)^2} \quad (2.10)$$

where $u_{extrapolation}$ is the uncertainty relative to the extrapolation to a zero chloride molality of E' values, $u_{S_{E°}}$ the standard deviation between standard potentials (E°) of the six Ag/AgCl electrodes used and $u_{E'}$ the uncertainty relative to E' term described above.

The standard uncertainties of each term of equation 1.10.a have been carefully assessed and described which allow the final calculation of u_{charac} using the law of uncertainty propagation.

2.6.2. Homogeneity: u_{hom}

The procedure for the assessment of the reference material homogeneity is described in Section 2.4. The standard uncertainty due to in-between bottle heterogeneity was calculated with equation 2.11.

$$u_{hom} = \frac{s^2}{N} \quad (2.11)$$

where s^2 is the standard deviation between the six pH_T values obtained from characterization and N the number of bottles analysed.

2.6.3. Stability: u_{stab}

If no significant trend is established by the t test described in Section 2.5, then the stability uncertainty contributing to the overall uncertainty budget is calculated with equation 2.12, as described in the ISO Guide 35 ("ISO Guide 35", 2017).

$$u_{stab} = s_{b1} \cdot t \quad (2.12)$$

where S_{b1} corresponds to the standard deviation of the slope and t to the time.

A material for which a significant trend is established by the t test can be suitable for certification if the degradation rate is included in the uncertainty budget. In that case, the stability uncertainty must take into account both the estimates of the degradation and the slope uncertainty (equation 2.13). The estimate of the degradation corresponds to the real degradation during half the chosen shelf life (Linsinger et al., 2001).

As the trend is considered linear, the degradation estimate is converted to an uncertainty using a rectangular law ("ISO Guide 35", 2017).

$$u_{stab} = \sqrt{(\frac{b1 \cdot \frac{t}{2}}{\sqrt{3}})^2 + (s_{b1} \cdot t)^2} \quad (2.13)$$

where t corresponds to the material shelf life considered.

2.7. Inter-laboratory comparison

The inter-laboratory comparison (ILC) was conducted on a second batch of reference material equivalent to the one presented above. The same methodologies were applied for its preparation, characterization and uncertainty evaluation, although no stability study was performed on this batch. Considering the similarity of the batches produced, the stability presented above on a different batch is used in the certification of the batch distributed for the ILC.

2.7.1. Protocol

The inter-laboratory comparison included 13 participants: 11 laboratories within the SOMLIT network and CocoriCO_2 project, Ifremer Metrology laboratory, and LNE (Table 3). Each participant received one bottle of reference material containing 160 mL of TRIS buffer.

Table 3: The 13 laboratories participating to the ILC.

Participants affiliations			
SOMLIT	*CocoriCO_2*	*SOMLIT and CocoriCO_2*	*Other*
Luc-sur-mer	Argenton	Sète	Ifremer - Metrology
Marseille		Arcachon	LNE
Banyuls		Brest (IUEM)	
Wimereux		Roscoff	
		Villefranche	
		La Rochelle	

Measurements were carried out in each laboratory within 1 month between participants and less than 2 months after the characterization date of the reference material. In each laboratory, pH_T was determined using the spectrophotometric pH_T measurement method following a shared protocol based on the Standard Operating Procedure 6b (Dickson et al., 2007), similar to the one described in Chapter I, Section 3.2.

Absorbance measurements were performed with benchtop spectrophotometers of various manufacturers using 10 cm path-length cells. The temperature at which the measurement was performed, typically between 22 °C and 25.5 °C, was recorded by

each laboratory. Each participant performed at least three measurements from a single bottle of TRIS buffer.

2.7.2. Results interpretation

The values of pH_T were calculated using equation 1.8 (presented in chapter I, section 3.2) and using the dye characterization parameters given in Liu et al. (2011).

Input information from each laboratory were the absorbances acquired at the three wavelengths, before and after dye addition, and the values of the recorded temperatures, for each measurement. All pH_T measurements were adjusted to 25 °C based on a second-degree polynomial function between pH_T and temperature, estimated from the characterization values of the reference material at three temperatures (15°C, 25°C and 30°C). The uncertainty of this adjustment is considered negligible.

Laboratories did not follow exactly the same protocol (i.e. temperature control, source of purified indicator dye solution, correction for the perturbation of the sample pH_T due to the dye addition). However, as one of the purposes of an inter-laboratory exercise is to evaluate the ability of each participant to perform the measurement, all values were taken into account, at first, in the interpretation of the inter-laboratory comparison. Two statistical tests were then applied to identify eventual outliers, following the ISO standard 5725-2 guidelines ("ISO 5725-2", 2020). The Cochran's test and Grubbs' test were used to identify, respectively, outlying within-laboratory variabilities and outlying observations.

Mean values from repeatability measurements as well as standard deviations were calculated for each laboratory. The median was then calculated from the mean values of the participants. The uncertainty associated to the median was calculating with the method given in Muller (2000).

2.7.3. Determination of the uncertainty budget of the spectrophotometric method: top-down approach

The ISO standard 21748 "Guidance for the use of repeatability, reproducibility and trueness estimates in measurement uncertainty evaluation" was used to establish an uncertainty budget with inter-laboratory comparison data (i.e. following a top-down approach) ("ISO 21748", 2017). The uncertainty budget was calculated following the top-down method detailed in Chapter I, Section 2.5, using equations 1.2 and 1.3. These equations are reintroduced below for more clarity.

$$u^2(y) = s_L^2 + s_r^2 + u^2(\hat{\delta}) \quad (1.2)$$

where $u(y)$ is the estimated measurement result uncertainty, s_L the inter-laboratory standard deviation, s_r the intra-laboratory standard deviation divided by the square

root of the mean number of replicates, and $u(\hat{\delta})$ the uncertainty associated to the estimated bias of the measurement method.

$$u^2(\hat{\delta}) = \frac{(s_L^2 + s_r^2) - \left(1 - \frac{1}{n}\right)s_r^2}{p} + u^2(\hat{\mu}) \quad (1.3)$$

where n is the number of replicates in each laboratory, p the number of laboratories and $\hat{\mu}$ the certified value.

3. Results

3.1. Reference material characterization

Table 4 summarizes the pH_T values for the reference material obtained with the Harned cell measurement method at 15°C, 25°C and 30°C. The pH_T values in Table 4 are the mean of the six values measured in step (2) of Figure .

Table 4: Results of the reference material pH_T values characterization at 15°C, 25°C and 30°C obtained with the Harned cell measurement method.

Temperature (°C)	Characterization values	
	E°* (V)	pH_T
15	0.24947	8.4136
25	0.24611	8.0915
30	0.24441	7.9375

Table 4 also gives the Ag/AgCl electrodes standard potential in saline media values (E°*) obtained from the measurements of step (1) in Figure 17 at each of the three temperatures. Figure 18 illustrates the method applied to obtain this value at 25°C (described in Chapter I, Section 3.4).

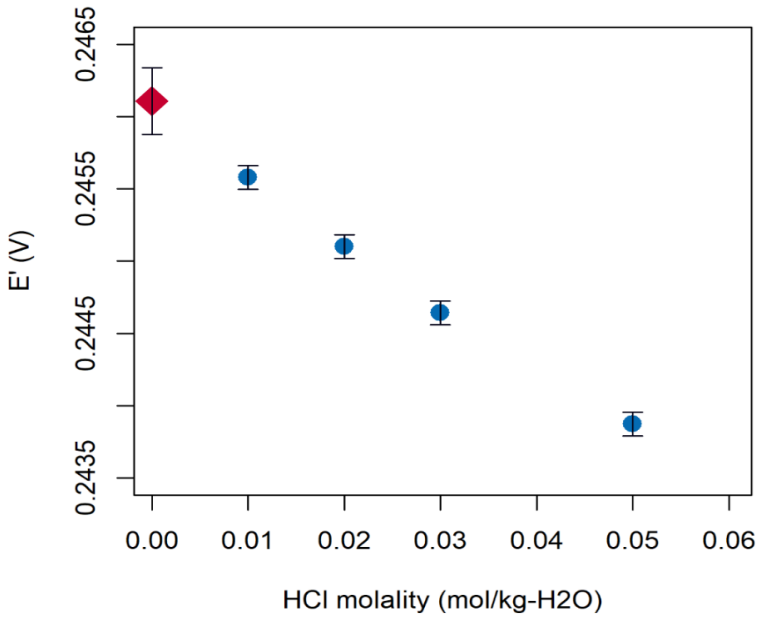

Figure 18: Determination of E°* value at 25°C. Where ● represents E' (V) of the four solutions with an HCl molality of respectively 0.01, 0.02, 0.03 and 0.05 mol/kg-H2O and ◆ represents the E°* value obtained from E' values as function of HCl molality extrapolated to an HCl molality equal to zero, with their respective expanded uncertainties (i.e. with a coverage factor of 2).

3.2. Stability assessment

Table 5 gives the results of the statistical t test described in section 2.5 allowing the determination of the material stability. Given the Harned cell measurement method (i.e. acidity function measurements as described in section 2.5), since t_0 value is higher than $t_{\alpha,}$ it can be concluded that the slope of the linear regression is statistically significant. These results highlight a clear trend showing an instability of the material. The same test applied to the data acquired by the pH_T spectrophotometric measurement method give the same conclusion. The reference material can still be certified by taking into account the instability of the material in the uncertainty budget, using equation 2.13.

Table 5: Results of the statistical t test for stability assessment of the reference material using the Harned cell and Spectrophotometric measurement methods.

Statistical t test parameters	Instrumentation	
	Harned cell[a]	Spectrophotometer[b]
Slope (b1)	-4.7E-04	-9.1E-04
Slope standard deviation (Sb1)	1.7E-04	2.4E-04
t_0 (b1 / Sb1)	2.80	3.78
t_α (Student n-2)	2.26	2.36

[a] The stability assessment performed with the Harned cell is based on acidity function measurements.
[b] The stability assessment performed with the spectrophotometer is based on pH_T measurements.

Figure 19 illustrates the evolution of the reference material assessed by Harned cell measurements (Figure 19.a) and by spectrophotometry (Figure 19.b).

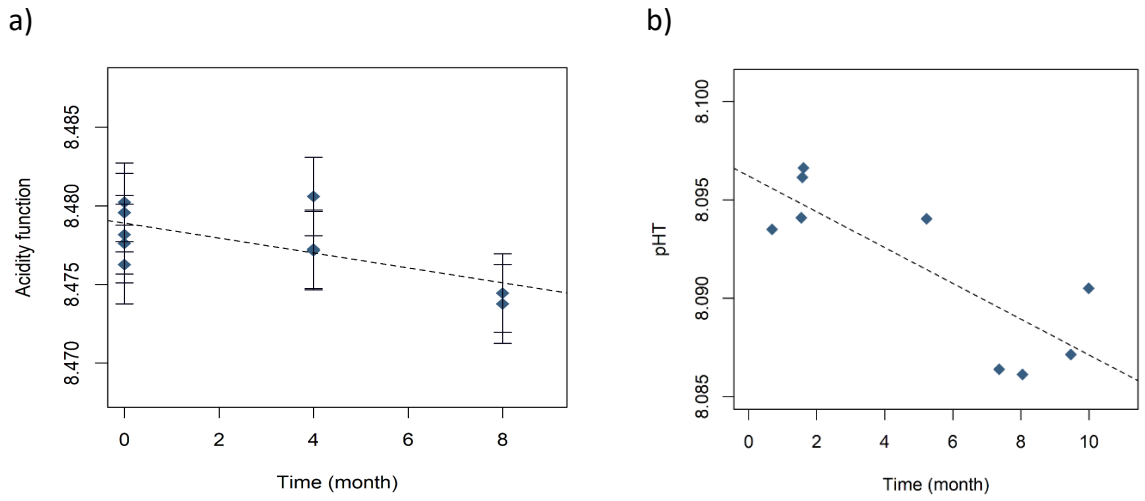

Figure 19: t test stability assessments. a) Linear regression of the acidity function measured with Harned cell at 25°C as a function of time, to each acidity function value is associated its expanded uncertainty with a coverage factor of 2. b) Linear regression of the pH_T measured by spectrophotometry at 25°C as a function of time.

3.3. Uncertainty budget of the reference material

The overall standard uncertainty budget of the pH_T values given in Table 6 is calculated from equation 2.3. The methodology employed to assess each component of equation 2.3 is described in section 2.6. The stability uncertainty is given for a chosen shelf life of six months, which allows having an overall standard uncertainty on the reference material pH_T value of maximum 0.0025, corresponding to an expanded uncertainty budget of 0.005 (i.e. with a coverage factor of 2).

Table 6: Detailed standard uncertainty budget of the reference material pH_T values obtained at 15°C, 25°C and 30°C.

Temperature (°C)	Overall standard uncertainty budget			
	u charac	u hom	u stab	u global
15	2.09E-03	9.94E-05	1.44E-03	2.54E-03
25	1.95E-03	1.28E-04	1.31E-03	2.35E-03
30	1.76E-03	1.45E-04	1.28E-03	2.18E-03

The detailed standard uncertainties of each source contributing to the preparation and characterization uncertainty, u_{charac}, are assessed following the methodology given in section 2.6.1 and are given in Table 7.

Table 7: Detailed standard uncertainties of each source contributing to the preparation and characterization uncertainty, u_{charac}.

Equations terms	Temperature (°C)	Unit	Standard uncertainty
Molality of each stock solution			
νNaCl		mol/kg-sol	4.51E-04
νminor		mol/kg-sol	3.89E-04
νNa2SO4		mol/kg-sol	5.63E-04
νTRIS		mol/kg-sol	6.21E-04
νHCl		mol/kg-sol	5.50E-05
Water mass fraction			
ω_{H2O}		g/kg-sol	9.25E-06
Chloride ion molality in the buffer solution			
b_{Cl}		mol/kg-H_2O	1.78E-04
Nernstian term			
R		J/mol.K	1.50E-05
T		K	1.10E-02
F		C/mol	8.30E-03
Hydrogen Pressure			
P		Pa	1.00E+02
ρ		kg/m3	2.00E-02
h		m	5.00E-03
Standard potential of Ag/AgCl in saline media at a chosen 0.01m HCl			
ω_{H2O}		g/kg-sol	1.12E-05
b_H		mol/kg-H_2O	1.43E-05
b_{Cl}		mol/kg-H_2O	1.87E-04
E'	15	V	3.93E-05
E'	25	V	4.09E-05
E'	30	V	4.21E-05
Standard potential of Ag/AgCl in saline media			
Extrapolation		V	4.71E-05
SD_E°	15	V	9.99E-05
E°*		V	1.17E-04
Extrapolation		V	2.08E-05
SD_E°	25	V	1.03E-04
E°*		V	1.13E-04
Extrapolation		V	8.25E-06
SD_E°	30	V	9.33E-05
E°*		V	1.03E-04

Overall characterisation and preparation uncertainty budget			
u_{charac}	15	V	2.09E-03
u_{charac}	25	V	1.95E-03
u_{charac}	30	V	1.76E-03

Figure 20.a shows the part of each uncertainty component into the overall budget at 25°C. The same pattern is obtained for the two other studied temperatures. The main source of uncertainty is the TRIS buffer preparation and characterization performed with the Harned cell (u_{charac}), which mostly arises from the determination of Ag/AgCl electrodes standard potential in saline media (E°*) (Figure 20.b).

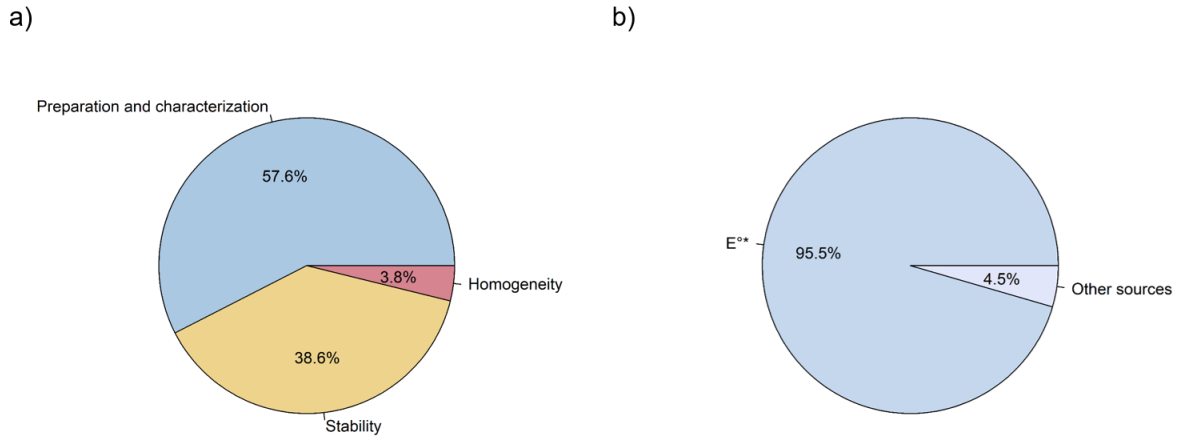

Figure 20: Uncertainty sources contribution rate to the uncertainty budget of the reference material pH_T at 25°C. a) Preparation and characterization, homogeneity and stability sources contribution to the global uncertainty budget of the reference material pH_T. b) Uncertainty sources contribution to the preparation and characterization uncertainty term (u_{charac}).

3.4. Inter-laboratory comparison results

The reference material distributed to all participants has an assigned pH_T value of 8.092 at 25°C with an expanded uncertainty (i.e. with a coverage factor, k, of 2) of 0.005. Figure 21 shows the results of the inter-laboratory comparison.

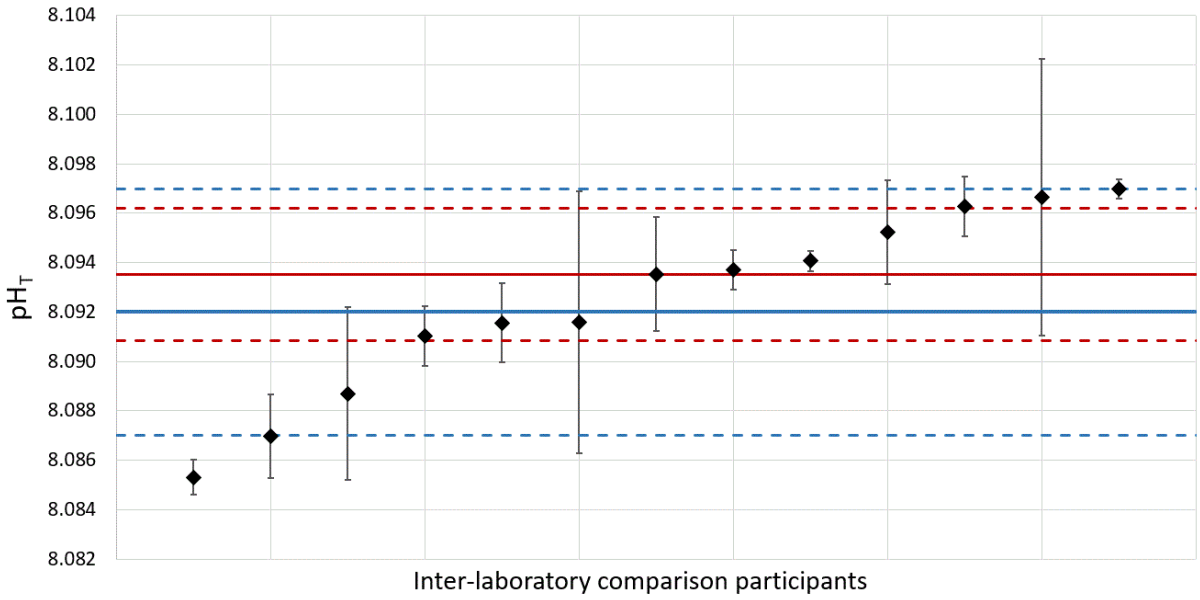

Figure 21: Inter-laboratory comparison results, where ◆ represents the mean value obtain by each participant, respectively, from at least 3 repeatability measurements. The error bars associated to the mean values correspond to standard deviation of the repeatability measurements. The solid blue line represents the reference pH_T value of the TRIS buffer reference material assigned with Harned cells, with its associated expanded uncertainty (i.e. with a coverage factor, k, of 2), in dotted blue lines. The solid red line represents the median, with its associated expanded uncertainty in dotted red lines.

Among the 13 laboratories participating to the comparison, one obtained a mean pH_T value that is outside of the pH_T range covered by the expanded uncertainty of the value of the reference material. However, Cochran's and Grubbs' tests shown no outlying laboratory and the rest of the results interpretation is thus applied for the 13 participating laboratories.

The bias of the method, estimated from the mean value of all participants, is of 0.0004 in terms of pH_T compared to the reference value.

Table 8 presents the standard uncertainties values estimated with repeatability, reproducibility and trueness information of the method drew from the inter-laboratory comparison, as described in Section 2.7.3.

Table 8: Spectrophotometric method uncertainty estimation from ILC data using equation 1.2.

Standard uncertainty estimation	
Uncertainty sources	*u (k=1)*
s_L	3.70E-03
s_r	4.90E-04
$u(\hat{\delta})$	2.60E-03
$u(y)$	4.60E-03

The overall standard uncertainty budget, estimated with equation 1.2, is of 0.0046, corresponding to an expanded uncertainty of 0.0092. Figure 22 presents the contribution to each of the parameters of equation 1.2 in the overall budget of pH_T spectrophotometric measurement method estimated with the top-down approach.

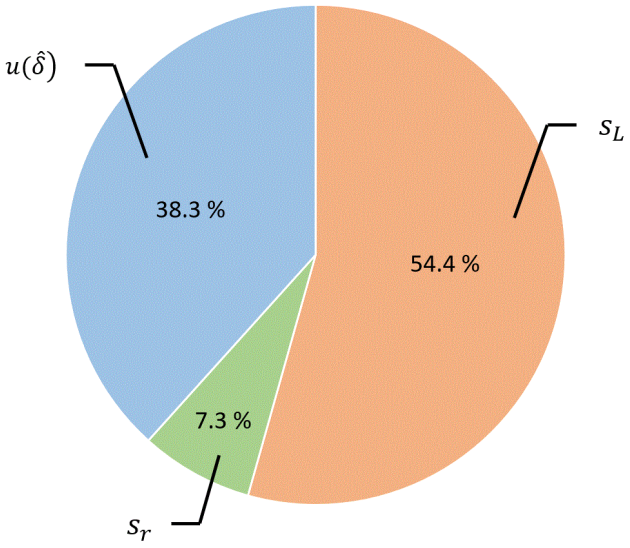

Figure 22: Relative contribution of the various components to the uncertainty of the spectrophotometric pH_T measurement method estimated from the inter-laboratory comparison data. Where s_L is the inter-laboratory standard deviation, s_r the intra-laboratory standard deviation, and $u(\hat{\delta})$ the uncertainty associated to the estimated bias of the measurement method.

4. Discussion

4.1. Comparison with existing reference materials

The pH_T values obtained with the Harned cell (Table 4) are consistent with literature values (DelValls and Dickson, 1998; Müller et al., 2018; Papadimitriou et al., 2016; Pratt, 2014), within the expanded uncertainty. Since September 2021, four other batches of TRIS buffer reference material, including the one used for the ILC presented in this chapter, were produced at LNE and characterized with Harned cells. The mean pH_T value is of 8.0944 with a standard deviation between the five batches of 0.0027. This demonstrates the reproducibility of the production of TRIS buffers.

Characterization of the reference material was performed at 15°C, 25°C and 30°C. The temperature coefficient of the produced reference material pH_T is of -0.032/°C. It is in agreement with the temperature coefficient obtained from the literature for similar TRIS buffers (DelValls and Dickson, 1998; Müller et al., 2018) and for the same range of temperatures (i.e. between 15°C and 30°C). The temperature coefficient of a natural seawater in the same range of temperatures is two times lower, around -0.015/°C

(Hunter, 1998). The temperature control is thus even more important when measuring the pH_T of a buffer solution compared to that of natural seawater samples.

4.2. Water mass fraction definition

The water mass fraction of the TRIS buffer, ω_{H2O}, used to convert pH_T expressed in molality (mol/kg-H_2O) to amount content (mol/kg-sol), was first reported by Dickson (1993) as being a function of the salinity, using equation 2.14.

$$\omega_{H2O} = 1 - 0.00106 \times S \quad (2.14)$$

where S corresponds to the nominal salinity of the buffer solution.

The S coefficient in the above expression expresses the ratio between the total mass, in kg, of salts dissolved in 1 kg of seawater of practical salinity 35, and its nominal salinity (i.e. 35). This equation well refers to the composition of a seawater solution. It doesn't refer to the actual water mass fraction of the TRIS buffer, as it doesn't take into account the TRIS and TRIS.HCl contribution.

Clegg et al. (2022) published a similar conversion equation also based on nominal salinity which has been calculated using the same approach (equation 2.15, equivalent to equation A.6 of Clegg et al., 2022). It is based on the solute content of seawater of the Reference Composition corresponding to a Practical Salinity of exactly 35 taken from Millero et al. (2008).

$$\omega_{H2O} = 1 - 0.001004715 \times S \quad (2.15)$$

Pratt (2014) and Müller et al. (2018) proposed that considering the actual water mass fraction of the buffer would be more appropriate (i.e. taking into account the TRIS and TRIS.HCl contribution). Nevertheless, to be in agreement with the final purpose of the reference material, that is to say a Quality Assurance and Quality Control (QA/QC) approach for pH_T measurements on natural seawater sample, we believe that ω_{H2O} must refer to a natural seawater composition.

One of the objectives of the present study was to provide a thorough uncertainty estimate of the ω_{H2O} term used for the pH_T calculation of the produced reference material. To that end, we calculated our own equation for water mass fraction calculation following Dickson's and Clegg's approach (equation 2.16, equivalent to equation 2.1 for the buffer considered). However, it is based on our buffer preparation (Table 2), while ignoring the TRIS component and considering the molality of HCl as being part of the NaCl amount in order to represent a pure artificial seawater composition (i.e. composition of Millero et al. (2008), simplified as described in Section 2.2). This method enables us to derive an accurate uncertainty estimate on the water mass fraction of the buffer based on gravimetric information.

$$\omega_{H2O} = 1 - 0.00099334 \times S \quad (2.16)$$

The applied equation to estimate ω_{H2O}, (equation 2.16) compared to the equations of Dickson (1993) and Clegg et al. (2022) (i.e. equations 2.14 and 2.15, respectively) gives discrepancies of respectively 0.0023 and 0.0004 in terms of water mass fraction, which results in discrepancies in term of pH_T of respectively 0.0011 and 0.0002. The maximum discrepancy is within the uncertainty of the characterization, which suggests that the applied equation is compatible with the one described in the two aforementioned papers (Clegg et al., 2022; Dickson, 1993).

Consequently, it allows us to be consistent with most studies associated to Harned cell measurements in TRIS buffers (DelValls and Dickson, 1998; Müller et al., 2018; Papadimitriou et al., 2016) and to the related studies made on the characterisation of the indicator dye (Liu et al., 2011; Loucaides et al., 2017; Müller and Rehder, 2018).

For comparison, pH_T values calculated with the water mass fraction defined on the actual buffer composition as described in Pratt (2014), (i.e. with TRIS and TRIS.HCl) are 0.0038 higher than the ones given in Table 4, calculated with equation 2.16. This discrepancy is not negligible, meaning that a consensus must be found to achieve consistency and comparability.

4.3. Uncertainty budget of the reference material

Figure 20 shows that the main contribution to the overall uncertainty budget is the E°* term. Among the uncertainty sources that are included in this term (equation 2.10), the ones coming from the extrapolation to a zero HCl molality ($u_{extrapolation}$) and from the determination of the standard potential at a given molality ($u_{E'}$) are small (Table 7). In contrast, the standard deviation of the Ag/AgCl electrodes standard potential ($u_{S_{E^\circ}}$) accounts for about 80% of the E°* term uncertainty.

The standard deviation of Ag/AgCl electrodes standard potentials determined with the Harned cell in a solution of HCl at a molality of 0.01 mol/kg-H_2O are of 100µV, 103µV and 93µV at respectively 15°C, 25°C and 30°C. The E° values obtained are in accordance with literature values (Bates and Bower, 1954).

A new batch of silver-silver chloride electrodes was produced at LNE in November 2021. A first analysis of their standard potential gave a standard deviation of 20µV between the six closest electrodes. A second standard deviation measurement was made after these electrodes were used three times in an artificial seawater matrix, which gave a standard deviation of 40µV. Pratt (2014) observed a decrease of the standard potentials after exposure of Ag/AgCl electrodes to a seawater matrix and hypothesized that bromide ion impurities in the salts used for the preparation might affect the electrodes. This could explain the larger standard deviation obtained on the older batch used for this study, especially if the electrodes have not all been exposed to artificial seawater the same amount of time in the past. A selection of Ag/AgCl electrodes with close standard potentials (i.e. below 100µV) ahead of the characterization of the reference material could help improve the overall uncertainty.

4.4. Stability over time

Stability assessment of the material is based on acidity function measurements performed over a period of 8 months with Harned cells (Figure 19.a). These measurements using the Harned cells remain complex and time-consuming, which explains the limited number of points covering the time period. Spectrophotometric measurements are easier and less time-consuming, but the quality of spectrophotometric measurements is difficult to evaluate because of the lack of a detailed uncertainty budget. Nevertheless, an estimate of the stability as a source of uncertainty to the global budget doesn't require an estimate of the single measurement uncertainty. Therefore, spectrophotometric measurements were performed up to ten months after the buffer preparation as an additional support for the stability study, allowing us to have more quantitative information (Figure 19.b). The method can be considered to have a good reproducibility. Some individual uncertainty sources (e.g., instrument, indicator dye, operator), could be cancelled out, offering perspective of achieving smaller uncertainties on pH_T variations over time.

The significant decrease of pH_T over time observed with the Harned cell measurements is confirmed with the spectrophotometric pH_T measurements (Table 5). Spectrophotometric pH_T measurements made over 10 months gave a slope of -0.00091 pH_T unit per month with a standard deviation of 0.00024 while acidity function measurements made with the Harned cell gave a slope of -0.00047 in acidity function unit per month with a standard deviation of 0.00017 for the stability assessment. The spectrophotometric measurement seems suitable for the evaluation of a material stability over time, but respective slope standard deviations demonstrate that evaluating the stability on the acidity function measured with the Harned cell system is more precise than by spectrophotometry. Moreover, as the $E^{\circ *}$ term accounts for almost all the preparation and characterization uncertainty (Figure 20.b), it makes sense to conduct the stability study on the acidity function instead of pH_T, as it does not include variability in the $E^{\circ *}$ term (equation 2.2).

Nemzer and Dickson (2005) established a stability of more than a year with potentiometric measurements for TRIS buffer sealed in borosilicate glass bottles with a greased ground-glass stopper, with a slow drift of +0.0005 in term of pH_T per year, compared to -0.0056 in this study. The instability of the material produced at LNE may come from microorganisms' development in the buffer (that could use TRIS as a source of carbon), and by the absorption of atmospheric CO_2 coming from an eventual lack of airtightness of the bottles used. In comparison, Wolfe and co-workers observed a similar drift of -0.0058 in term of pH_T per year for TRIS buffer stored in bags, that has been attributed to a CO_2 infiltration and/or microbial respiration (Wolfe et al., 2021).

After more than six months since the preparation and characterization of the buffers, a growth of mold has been observed in some bottles. This phenomenon has been observed to appear more quickly in more recently produced batches. A similar

observation in TRIS buffers has been made by Millero et al (1993). A bacteriological culture made at the Mediterranean Institute of Oceanography from aged LNE buffers demonstrated the presence of microorganisms, which could explain the pH_T drift over time.

Some solutions have been investigated to prevent microorganism development without using mercury-based additives. Mercuric chloride is still widely used to poison natural seawater samples, especially for alkalinity and pH_T measurements, but after the United Nations Minamata Convention held in Japan in 2017, it became a worldwide priority to restrict the use of all mercury compounds (UN Environment Programme, 2019). A preliminary test made by autoclaving the bottles after filling with buffer shown a small impact on the pH_T compared to another bottle of the same batch, as the pH_T discrepancy between the two bottles was lower than 0.0022. However, this method seems difficult to implement, as it requires ensuring there is no evaporation of the solutions, which could affect the pH_T. UV or gamma radiations, often used for the stabilisation of reference material, as in inorganic chemistry, aren't suitable in this case. The hydroxyl radicals formed by the radiation from water damages DNA. However, hydroxyl radicals will preferentially react with the TRIS molecule, thus compromising its buffer effect (Kejnovský and Kypr, 1993). Recommendations to prevent the growth of microorganisms are thus to autoclave the empty bottles, to sterilize the TRIS buffer by filtration, and then to perform its bottling and characterization. The TRIS buffers currently commercialised by the Scripps Institution of Oceanography are filtered (Dickson, pers. comm.).

Moreover, to prevent CO_2 absorption, the bottles could be sealed with greased ground-glass stoppers as described in Nemzer and Dickson (2005), by a crimping system or by a glass-sealed vial instead of screw cap bottles with polypropylene stoppers, which could be permeable to air.

4.5. Inter-laboratory comparison

The median and its associated expanded uncertainty obtained from data sets given by the ILC participants are within the pH_T range covered by the expanded uncertainty of the reference value (Figure 21). The bias of the method of 0.0004 in terms of pH_T compared to the reference value shows the compatibility of the spectrophotometric and potentiometric pH_T measurement results. It also gives an indication on the trueness of the spectrophotometric results, defined as the closeness of agreement between the average of an infinite number of replicate measured quantity values and a reference quantity value ("JCGM 200:2012," 2012).

The bias, of 0.0004, is below the uncertainty of the bias, $u(\hat{\delta})$ (Table 8) and can thus be neglected. This also indicates that the spectrophotometric method seems to be able to produce true values. However, demonstrating the trueness would require having more data covering a wide pH_T range, as proposed in Hammer et al. (2014).

Figure 22 allows to clearly identify that the major contribution to the uncertainty is the inter-laboratory standard deviation, s_L, corresponding to 54.4 % of the overall budget. It shows that reducing the uncertainty would require having a better agreement among participants. This might be improved as all the participants didn't follow exactly the same measurement protocol.

The second contribution comes from the uncertainty of the bias, $u(\hat{\delta})$, from which the major contribution is the uncertainty of the reference material characterized value (i.e. 0.005 at k=2). Finally, even if the uncertainty coming from the intra-laboratory standard deviation, s_r, doesn't account for much in the overall uncertainty budget (Figure 22), Figure 21 shows that some laboratories have high standard deviations between repeatability measurements (i.e. large error bars). Improving the repeatability, for example with a better temperature control system, might help improve these results.

The standard uncertainty of the spectrophotometric pH_T measurement, estimated from the ILC data and following the ISO standard 21748, is 0.0046 pH_T units. The uncertainty obtained doesn't reach the climate data quality objective required by the GOA-ON for the monitoring of ocean acidification. However, it is in accordance with the lowest uncertainties reported in the literature (Carter et al., 2013). Moreover, it seems that better agreement among the participants of the ILC, allowing to slightly decrease the uncertainty, could be reached if a common measurement procedure was to be more strictly applied by all the participants.

In order to achieve that, recommendations could be to have (1) a thorough control of the temperature during measurement (e.g. with a thermostating system), (2) carrying out the temperature measurement directly inside the spectrophotometric cell during measurement, or right after, with a calibrated temperature probe having a resolution of 0.01 °C, and (3) performing a double indicator dye addition to get rid of the perturbation of adding dye on the pH_T of the sample, especially if the sample is a natural seawater. Care must also be taken to ensure that the method used to adjust pH_T results to 25°C is harmonized.

Nevertheless, this study is encouraging in achieving a correct data quality on routine spectrophotometric pH_T measurements carried out by oceanographers.

The good results obtained in the inter-laboratory comparison also seem to indicate that the stability to transport of the reference material, not taken into account in the uncertainty budget is negligible.

4.6. pH_T measurements traceability

Up to date, seawater pH_T measurements lack established metrological traceability to the International System of Units (SI), which requires that every source of uncertainty be rigorously identified and quantified (Dickson et al., 2016). The pH_T calculated from Harned cell measurements is obtained by means of assumptions that, up to recently, have not been scrupulously investigated (Clegg et al., 2022; Dickson, 1993). The pH_T

obtained from measurements, on a molality basis, differs from the conventional thermodynamic pH_T by around 0.0045 for the studied TRIS buffer at 25°C (Clegg et al., 2022). The contribution to this discrepancy comes from the assumptions linked to chloride ion activity coefficient and hydrogen sulphate dissociation constant, this is further discussed in Chapter III. These two terms are neglected here.

This points out the complexity of the concept of pH on a total scale. Nevertheless, it is reasonable to state that the described pH_T measurement method applied for the characterization of the reference material is able to provide highly consistent and precise measurement results. If pH_T measurement traceability to the SI is not achievable, a traceability established to a common procedure, which here is the Harned cell measurement method, can be adopted. It requires the demonstration of the equivalence of the measurement procedures of the National Metrology Institutes via the participation to inter-laboratory comparisons at the International Bureau of Weights and Measures (BIPM) level. This is currently under investigation.

5. Conclusion

The present study describes the preparation, characterization and uncertainty assessment method for TRIS buffer reference material production used for seawater pH_T measurements. Detailed homogeneity and long-term stability studies are presented. The Harned cell measurements performed on the TRIS buffer allows us to estimate precisely its pH_T value, but also to thoroughly assess uncertainties coming from preparation, characterization, homogeneity and stability of the material. This complete evaluation of the reference material allows the establishment of an overall uncertainty budget following the bottom-up approach described in the GUM ("JCGM 100:2008", 2008) and in accordance with the ISO 17034 and ISO Guide 35 standards.

The t test, used to assess the stability over time of the material, shows a significant trend, which indicates an instability of the material. Considering this, the overall expanded uncertainty (i.e. with a coverage factor of 2) of the reference material is of 0.005 for a material shelf life of six months. This gives a standard uncertainty budget of 0.0025, lower than the data quality objective of GOA-ON for the monitoring of ocean acidification (i.e. GOA-ON "climate" quality objective). The produced reference material is thus suitable for oceanographic needs and can assist marine scientists in their effort to guarantee the quality of their results. Improving the stability of the material, for example with a filtration sterilization process, will be required.

The definition of the water mass fraction to be employed in the calculation of the pH_T of the reference material and, at a higher extent, the traceability of seawater pH_T measurements, are two key points that need to be discussed further within the metrological community for oceanic measurements and on which a consensus must be

found. This would allow offering a solid support to oceanographers in order to maintain the quality of their seawater pH_T measurements.

The present study showed the results of an inter-laboratory comparison carried out by 13 participants on the reference material produced for pH_T spectrophotometric measurements. The results obtained demonstrate the compatibility of the spectrophotometric measurement results with the reference value obtained by potentiometric measurements carried out with Harned cells.

The inter-laboratory comparison results allowed establishing an uncertainty budget of the pH_T spectrophotometric measurement method using the top-down approach. The overall uncertainty achieved is 0.0046. This is higher than the uncertainty expected by the GOA-ON. However, recommendations are given to try to lower these uncertainties. This ILC is thus encouraging in achieving a good data quality of end-users pH_T spectrophotometric measurements.

Finally, the work presented in this chapter demonstrates the importance of metrological principles in knowing the level of data quality achieved for a measurement method, as well as the applicability of the reference material produced at LNE in the objective of maintaining a robust quality assurance system of routine spectrophotometric pH_T measurements.

References

Bates, R.G., 1973. Determination of pH: Theory and Practice John Wiley&Sons, USA.

Bates, R.G., Bower, V.E., 1954. Standard Potential of the Silver-Silver-Chloride Electrode from 0° to 95° C and the Thermodynamic Properties of Dilute Hydrochloric Acid Solutions. J Res Nat Bur Stand 53, 283–290. https://doi.org/10.6028/jres.106.021

Breton, E., Savoye, N., Rimmelin-Maury, P., Sautour, B., Goberville, E., Lheureux, A., Cariou, T., Ferreira, S., Agogué, H., Alliouane, S., Aubert, F., Aubin, S., Berthebaud, E., Blayac, H., Blondel, L., Boulart, C., Bozec, Y., Bureau, S., Caillo, A., Cauvin, A., Cazes, J.-B., Chasselin, L., Claquin, P., Conan, P., Cordier, M.-A., Costes, L., Crec'hriou, R., Crispi, O., Crouvoisier, M., David, V., Del Amo, Y., De Lary, H., Delebecq, G., Devesa, J., Domeau, A., Durozier, M., Emery, C., Feunteun, E., Fauchot, J., Gentilhomme, V., Geslin, S., Giraud, M., Grangeré, K., Grégori, G., Grossteffan, E., Gueux, A., Guillaudeau, J., Guillou, G., Harrewyn, M., Jolly, O., Jude-Lemeilleur, F., Labatut, P., Labourdette, N., Lachaussée, N., Lafont, M., Lagadec, V., Lambert, C., Lamoureux, J., Lanceleur, L., Lebreton, B., Lecuyer, E., Lemeille, D., Leredde, Y., Leroux, C., Leynaert, A., L'Helguen, S., Liénart, C., Macé, E., Maria, E., Marie, B., Marie, D., Mas, S., Mendes, F., Mornet, L., Mostajir, B., Mousseau, L., Nowaczyk, A., Nunige, S., Parra, R., Paulin, T., Pecqueur, D., Petit, F., Pineau, P., Raimbault, P., Rigaut-Jalabert, F., Salmeron, C., Salter, I., Sauriau, P.-G., Seuront, L., Sultan, E., Valdès, R., Vantrepotte, V., Vidussi, F., Voron, F., Vuillemin, R., Zudaire, Laurent., Garcia, N., 2023. Data quality control considerations in multivariate environmental monitoring: experience of the French coastal network SOMLIT. Frontiers in Marine Science 10.

Byrne, R.H., Breland, J.A., 1989. High precision multiwavelength pH determinations in seawater using cresol red. Deep Sea Research Part A. Oceanographic Research Papers 36, 803–810. https://doi.org/10.1016/0198-0149(89)90152-0

Carter, B.R., Radich, A., Doyle, H.L., Dickson, A.G., 2013. An automated system for spectrophotometric seawater pH measurements. Limnology and Oceanography: methods 16–27. https://doi.org/10.4319/lom.2013.11.16

Clegg, S.L., Humphreys, M.P., Waters, J.F., Turner, D.R., Dickson, A.G., 2022. Chemical speciation models based upon the Pitzer activity coefficient equations, including the propagation of uncertainties. II. Tris buffers in artificial seawater at 25 °C, and an assessment of the seawater 'Total' pH scale. Marine Chemistry 244, 104096. https://doi.org/10.1016/j.marchem.2022.104096

DelValls, T.A., Dickson, A.G., 1998. The pH of buffers based on 2-amino-2-hydroxymethyl-1,3-propanediol ('tris') in synthetic sea water. Deep Sea Research Part I: Oceanographic Research Papers 45, 1541–1554. https://doi.org/10.1016/S0967-0637(98)00019-3

Dickson, A.G., 2010. Standards for Ocean Measurements. Oceanography 23, 34–47. https://www.jstor.org/stable/24860884

Dickson, A.G., 1993. pH buffers for sea water media based on the total hydrogen ion concentration scale. Deep Sea Research Part I: Oceanographic Research Papers 40, 107–118. https://doi.org/10.1016/0967-0637(93)90055-8

Dickson, A.G., Camões, M.F., Spitzer, P., Fisicaro, P., Stoica, D., Pawlowicz, R., Feistel, R., 2016. Metrological challenges for measurements of key climatological observables. Part 3: seawater pH. Metrologia 53, R26. https://doi.org/10.1088/0026-1394/53/1/R26

Dickson, A.G., Sabine, C.L., Christian, J.R. (Eds.), 2007. Guide to Best Practices for Ocean CO2 Measurements PICES Special Publication 3, 191.

GOA-ON, 2019. Global Ocean Acidification Observing Network (GOA-ON): Implementation Strategy.

Hammer, K., Schneider, B., Kuliński, K., Schulz-Bull, D.E., 2014. Precision and accuracy of spectrophotometric pH measurements at environmental conditions in the Baltic Sea. Estuarine, Coastal and Shelf Science 146, 24–32. https://doi.org/10.1016/j.ecss.2014.05.003

Hunter, K., 1998. The temperature dependence of pH in surface seawater. Deep-sea Research Part I-oceanographic Research Papers - DEEP-SEA RES PT I-OCEANOG RES 45, 1919–1930. https://doi.org/10.1016/S0967-0637(98)00047-8

ISO 5725-2, 2020. Accuracy (trueness and precision) of measurement methods and results-Part 2 : basic method for the determination of repeatability and reproducibility of a standard measurement method.

ISO 17025, 2017. General requirements for the competence of testing and calibration laboratories.

ISO 17034, 2016. General requirements for the competence of reference material producers.

ISO 21748, 2017. Guidance for the use of repeatability, reproducibility and trueness estimates in measurement uncertainty evaluation.

ISO Guide 35:2017 Reference materials — Guidance for characterization and assessment of homogeneity and stability, 2017.

JCGM 100:2008, 2008. Evaluation of Measurement Data-Guide to the Expression of Uncertainty in Measurement.

JCGM 200:2012, 2012. International vocabulary of metrology (VIM) — Basic and general concepts and associated terms.

Kejnovský, E., Kypr, J., 1993. Tris buffer protects DNA backbone against breakage upon irradiation with ultraviolet light. Gen Physiol Biophys 12, 317–324.

Lheureux, A., Savoye, N., Amo, Y.D., Goberville, E., Bozec, Y., Breton, E., Conan, P., L'Helguen, S., Mousseau, L., Raimbault, P., Rimelin-Maury, P., Seuront, L., Vuillemin, R., Caparros, J., Cariou, T., Cordier, M.-A., Corre, A.-M., Costes, L., Crispi, O., Crouvoisier, M., Latour, H. de L. de, Derriennic, H., Devesa, J., Durozier, M., Ferreira, S., Garcia, N., Grossteffan, E., Gueux, A., Lafont, M., Lagadec, V., Lecuyer, E., Leroux, C., Macé, E., Maria, E., Mornet, L., Nowaczyk, A., Parra, M., Petit, F., David, V., 2021. Bi-decadal variability in physico-biogeochemical characteristics of temperate coastal ecosystems: from large-scale to local drivers. Marine Ecology Progress Series 660, 19–35. https://doi.org/10.3354/meps13577

Linsinger, T.P.J., Pauwels, J., Lamberty, A., Schimmel, H.G., van der Veen, A.M.H., Siekmann, L., 2001. Estimating the uncertainty of stability for matrix CRMs. Fresenius J Anal Chem 370, 183–188. https://doi.org/10.1007/s002160100719

Liu, X., Patsavas, M.C., Byrne, R.H., 2011. Purification and Characterization of meta-Cresol Purple for Spectrophotometric Seawater pH Measurements. Environmental science & Technology 4862–4868.

Loucaides, S., Rèrolle, V.M.C., Papadimitriou, S., Kennedy, H., Mowlem, M.C., Dickson, A.G., Gledhill, M., Achterberg, E.P., 2017. Characterization of meta-Cresol Purple for spectrophotometric pH measurements in saline and hypersaline media at sub-zero temperatures. Sci Rep 7, 2481. https://doi.org/10.1038/s41598-017-02624-0

Meija, J., Coplen, T.B., Berglund, M., Brand, W.A., Bièvre, P.D., Gröning, M., Holden, N.E., Irrgeher, J., Loss, R.D., Walczyk, T., Prohaska, T., 2016. Atomic weights of the elements 2013 (IUPAC Technical Report). Pure and Applied Chemistry 88, 265–291. https://doi.org/10.1515/pac-2015-0305

Millero, F., Feistel, R., Wright, D., McDougall, T., 2008. The composition of Standard Seawater and the definition of the Reference-Composition Salinity Scale. Deep-Sea Research I 55, 50–72. https://doi.org/10.1016/j.dsr.2007.10.001

Millero, F.J., Zhang, J.-Z., Fiol, S., Sotolongo, S., Roy, R.N., Lee, K., Mane, S., 1993. The use of buffers to measure the pH of seawater. Marine Chemistry 44, 143–152. https://doi.org/10.1016/0304-4203(93)90199-X

Müller, J.D., Bastkowski, F., Sander, B., Seitz, S., Turner, D.R., Dickson, A.G., Rehder, G., 2018. Metrology for pH Measurements in Brackish Waters—Part 1: Extending Electrochemical pHT Measurements of TRIS Buffers to Salinities 5–20. Front. Mar. Sci. 5, 176. https://doi.org/10.3389/fmars.2018.00176

Müller, J.D., Rehder, G., 2018. Metrology of pH Measurements in Brackish Waters—Part 2: Experimental Characterization of Purified meta-Cresol Purple for Spectrophotometric pHT Measurements. Front. Mar. Sci. 0. https://doi.org/10.3389/fmars.2018.00177

Muller, J.W., 2000. Possible advantages of a robust evaluation of comparisons. J. Res. Natl. Inst. Stand. Technol. 105, 551. https://doi.org/10.6028/jres.105.044

Papadimitriou, S., Loucaides, S., Rérolle, V., Achterberg, E.P., Dickson, A.G., Mowlem, M., Kennedy, H., 2016. The measurement of pH in saline and hypersaline media at sub-zero temperatures: Characterization of Tris buffers. Marine Chemistry 184, 11–20. https://doi.org/10.1016/j.marchem.2016.06.002

Pearlman, J., Bushnell, M., Coppola, L., Karstensen, J., Buttigieg, P.L., Pearlman, F., Simpson, P., Barbier, M., Muller-Karger, F.E., Munoz-Mas, C., Pissierssens, P., Chandler, C., Hermes, J., Heslop, E., Jenkyns, R., Achterberg, E.P., Bensi, M., Bittig, H.C., Blandin, J., Bosch, J., Bourles, B., Bozzano, R., Buck, J.J.H., Burger, E.F., Cano, D., Cardin, V., Llorens, M.C., Cianca, A., Chen, H., Cusack, C., Delory, E., Garello, R., Giovanetti, G., Harscoat, V., Hartman, S., Heitsenrether, R., Jirka, S., Lara-Lopez, A., Lantéri, N., Leadbetter, A., Manzella, G., Maso, J., McCurdy, A., Moussat, E., Ntoumas, M., Pensieri, S., Petihakis, G., Pinardi, N., Pouliquen, S., Przeslawski, R., Roden, N.P., Silke, J., Tamburri, M.N., Tang, H., Tanhua, T., Telszewski, M., Testor, P., Thomas, J., Waldmann, C., Whoriskey, F., 2019. Evolving and Sustaining Ocean Best Practices and Standards for the Next Decade. Frontiers in Marine Science 6, 277. https://doi.org/10.3389/fmars.2019.00277

Pratt, K.W., 2014. Measurement of pHT values of Tris buffers in artificial seawater at varying mole ratios of Tris:Tris·HCl. Marine Chemistry 162, 89–95. https://doi.org/10.1016/j.marchem.2014.03.003

Sandifer, J.R., 1981. Effects of bromide on silver chloride electrodes. Anal. Chem. 53, 312–316. https://doi.org/10.1021/ac00225a043

Shi, C., Zhao, H., Zhang, X., Luo, Y., 2021. Evaluation of Uncertainty in Determination Methods of Seawater pH Standard Material. E3S Web Conf. 299, 02002. https://doi.org/10.1051/e3sconf/202129902002

UN Environment Programme, 2019. Minamata Convention on Mercury - Text and Annexes.

Wolfe, W.H., Shipley, K.M., Bresnahan, P.J., Takeshita, Y., Wirth, T., Martz, T.R., 2021. Technical note: Stability of tris pH buffer in artificial seawater stored in bags. Ocean Science 17, 819–831. https://doi.org/10.5194/os-17-819-2021

Chapter III: pH_T measurements of TRIS buffer solutions in artificial seawater matrix in the salinity range 5–40 and temperature range 5–40 °C. Measurements and data fitting

1. Introduction

The spectrophotometric pH_T measurement method relies on the use of the indicator dye meta-Cresol Purple (mCP). It consists of measuring the absorbance ratio at the wavelengths corresponding to the peak absorbances of the basic and acidic form of the indicator dye in a seawater sample. This, together with the second dissociation constant and molar extinction coefficients of the dye, allows for the calculation of pH_T (equation 1.8, Chapter I). To be suitable for spectrophotometric pH_T measurements on natural seawater samples, these parameters need to be characterized over appropriate ranges of salinities and temperatures (Douglas and Byrne, 2017; Liu et al., 2011; Loucaides et al., 2017; Müller and Rehder, 2018).

The characterisation of the molar extinction coefficients has been described by Liu et al. (2011) and Loucaides et al. (2017). The term $K_2^T e2$, relative to the second dissociation constant of the dye, is characterized by spectrophotometric measurements of artificial seawater solutions of known pH_T (Liu et al., 2011; Loucaides et al., 2017; Müller and Rehder, 2018).

The solutions used for that purpose are equimolal TRIS buffers (buffer of 2-Amino-2-(hydroxymethyl)-1,3-propanediol (TRIS) and TRIS hydrochloride (TRIS.HCl)) made in artificial seawater (ASW) of the desired salinities. The pH_T values of these solutions are characterized with the Harned cell potentiometric measurement method (DelValls and Dickson, 1998; Pratt, 2014; Papadimitriou et al., 2016; Müller et al., 2018, Chapter II). Harned cell measurements are the primary measurement procedures for aqueous pH measurements, they provide the lowest standard uncertainty for pH results, typically below 0.002 (Buck et al., 2002). From these measurements, a function giving the pH_T of equimolal TRIS buffers at each studied salinity and temperature can be computed and used for the subsequent determination of $K_2^T e2$. Thus, traceability of spectrophotometric pH_T results can be considered, up to now, established to the Harned cell potentiometric measurement method.

However, in TRIS buffers, TRIS and TRIS.HCl molalities contribute to a significant extent to the composition of the buffer, especially at low salinities, and do thus not represent a seawater matrix accurately. pH_T values of those buffers, which are measured with Harned cells, do not correspond to the true total pH scale in seawater, which applies to saline waters having ions ratio similar to those of open ocean (Clegg et al., 2022). To overcome this, Nemzer and Dickson (2005) recommended that the $K_2^T e2$ characterization could be made from equimolal TRIS buffers with pH_T value extrapolated to zero TRIS molality, thus to a pure artificial seawater matrix. The extrapolation is done with measurements of equimolal TRIS buffers at various TRIS molalities.

The characterization of the TRIS buffers used for the $K_2^T e2$ characterization has up to now only been made in separate ranges of salinity: 5–20 in Müller et al. (2018) and 20–40 in DelValls and Dickson (1998). It must be mentioned that Müller et al. provide an

equation for the whole salinity range 5–40 and temperature range 5–45 °C that is, however, based on measurements only made for salinities 5–20, combined with DelValls and Dickson measurements to establish the fit up to salinity 40. Furthermore, their preparation of ASW was different from the one commonly used and the extrapolation to zero TRIS molality resulted in an inconsistent ASW composition (Clegg et al., 2022).

The aim of this work is to provide pH_T results of equimolal TRIS buffers measured with the common methodology and to compute a suitable fit function for pH_T for the whole salinity and temperature range relevant for seawater spectrophotometric measurements (i.e., salinity range 5–40 and temperature range 5–40 °C). This function is suitable for the computation of pH_T values at the limit of zero TRIS molality. This work aims thus to provide a consistent function usable for the characterization of mCP in the salinity and temperature ranges most relevant for oceanography.

This chapter details the preparation and measurement of pH_T values of equimolal TRIS buffers, as well as the data processing method used to establish the fit function. Harned cell measurements of the pH_T values of the TRIS buffer solutions were conducted at three National Metrology Institutes (NMIs): the Physikalisch-Technische Bundesanstalt (PTB, Germany), the Laboratoire National de Métrologie et d'Essais (LNE, France) and the Instituto Português da Qualidade (IPQ, Portugal). Comparisons between this study and previous work available in the literature are presented. Moreover, spectrophotometric measurements have been conducted at LNE on some of the equimolal TRIS buffers to check the compatibility of the fit function presented in this study with the dye characterization of Müller and Rehder (2018), which is the only one to date giving $K_2^T e2$ for salinities as low as 5. Finally, metrological traceability of pH_T values of TRIS buffers is discussed. It has to be mentioned that the work presented in this chapter sets its focus on achieving the fit function for the pH_T of equimolal TRIS buffers in the salinity range 5-40 and temperature range 5-40 °C, whereas the estimation of the uncertainty of the fit function will be detailed in Schäfer et al. (in preparation) and will not be discussed in this chapter.

2. Materials and methods

2.1. General approach

Harned cell measurements were performed on TRIS buffer solutions of nominal practical salinities 5, 10, 15, 20, 25, 30, 35 and 40 at eight temperatures between 5 °C and 40 °C with steps of 5 °C. In accordance with former work, three equimolal TRIS buffers were measured for each salinity, having molalities of $b(\mathrm{TRIS}) = b(\mathrm{TRIS.HCl}) = 0.01$, 0.025 and 0.04 mol/kg H_2O. Measurements were shared among the three National Metrology Institutes involved in this study: PTB, LNE and IPQ (S3.1, Supplementary Material).

From these measurements, the pH_T values of equimolal TRIS buffers within the whole ranges of nominal practical salinity 5–40 and temperature 5–40 °C were calculated as described in Section 2.5. A function giving the pH_T of equimolal TRIS buffers as a function of salinity, temperature and molality of TRIS was computed by the method of least-squares. For a molality of $b(\mathrm{TRIS}) = b(\mathrm{TRIS.HCl}) = 0\ \mathrm{mol/kg\ H_2O}$, the function gives the pH_T values extrapolated to pure artificial seawater (i.e. artificial seawater matrix without TRIS and TRIS.HCl).

Spectrophotometric measurements have been conducted at LNE on equimolal TRIS buffers of nominal practical salinities 5, 20, 35 and 40 to check the equivalence of Müller and Rehder (2018) $K_2^T e2$ characterization with the pH_T values computed from the function obtained from this work. Details are given in Section 2.7.

2.2. TRIS buffer pH_T preparation

The composition of the artificial seawater used for TRIS buffers preparation was based on the reference seawater composition of the International Association for the Physical Sciences of the Ocean (IAPSO) for a practical salinity of 35 (Millero et al., 2008). From that reference composition, adjustments were made, as recommended by Dickson (1990) to simplify the composition and thus the preparation of the solutions, and to replace bromide ions that damage silver-silver chloride electrodes. The composition referring to a nominal practical salinity of 35 (i.e. same chemical environment as the reference natural seawater composition of practical salinity 35) was equivalent to the one described by Pratt (2014), and thus to the one used in Chapter II.

Table 9 presents the way of obtaining all equimolal TRIS buffers compositions for nominal practical salinities 5, 10, 15, 20, 25, 30 and 40 from the reference composition of Pratt (2014) at a nominal practical salinity of 35. They were calculated by changing the amount content of all salts proportionally, based on the ionic strength of the desired salinity.

For each salinity, three equimolal buffers were prepared at $b(\mathrm{TRIS}) = b(\mathrm{TRIS.HCl}) = 0.01$, 0.025 and $0.04\ \mathrm{mol/kg\ H_2O}$. To keep the ionic strength constant, the amount of HCl added was compensated by removing the same amount of NaCl from the initial composition (Table 9, footnote [a]).

The approach of substituting TRIS.HCl with NaCl in artificial seawater described in DelValls and Dickson (1998), and applied in this study, is applicable for the preparation of TRIS buffers with salinities as low as 5. However, it must be emphasized that the proportion of TRIS and TRIS.HCl in the artificial solution is significant for low salinities and therefore leads to changes in the acid-base properties of the solution compared to higher salinities (Clegg et al., 2022). This makes relevant the extrapolation to zero TRIS molality. A speciation model such as the one presented by Clegg and co-workers (2022) could be relevant to quantify these effects on pH_T.

The TRIS buffers were prepared gravimetrically at PTB using the compositions given in Table 9 and using the following chemical compounds: TRIS (*NIST Standard Reference Material 723e*), NaCl (*99.842 %*), KCl (*99.988 %*), Na_2SO_4 (*99.999 %*), $CaCl_2.2H_2O$, $MgCl_2.6H_2O$, HCl (*Danish Institute of Fundamental Metrology, amount content of 0.1 mol/kg sol*) and Milli-Q water.

All salts, and the stock solutions of $MgCl_2$, $CaCl_2$ and HCl, were characterized for purity or amount content, respectively, by coulometric acid-base or argentimetric titrations (S3.2, Supplementary Material)

Salts were dried before use and the buffers were prepared by gravimetry from stock solutions of the different components.

Table 9: Computation of the composition of the different TRIS buffers (i.e. various salinities, noted S, and TRIS molalities) from the reference composition of Pratt (2014). Where the Ionic strength I is calculated with the formula given in DelValls and Dickson (1998) and where b expresses molality in moles per kilogram of solvent, i.e. water in this study, noted mol/kg-H_2O. The subscript "S" corresponds to a TRIS composition at one specific salinity and the subscript "Ref" to the reference composition of Pratt (2014).

			Pure ASW reference composition (Pratt, 2014)	TRIS buffer composition (This study)
Salts	Molar mass (g/mol)		Molality b (mol/kg-H_2O)	Molality b (mol/kg-H_2O)
NaCl	58.4428		0.42753	a
Na_2SO_4	142.0421		0.02926	b
KCl	74.5513		0.01058	b
$MgCl_2$	95.2110		0.05474	b
$CaCl_2$	110.9840		0.01075	b
HCl	36.4609		-	c
TRIS	121.1352		-	d
		Salinity S	35	S
		Ionic Strength I	0.72250	I_S

[a] $b(NaCl)_{S,b(HCl)} = \frac{I_S * b(NaCl)_{Ref}}{I_{Ref}} - b(HCl)$

[b] $b(Salts)_S = \frac{I_S * b(Salts)_{Ref}}{I_{Ref}}$

[c] $b(HCl)$ of respective equimolal TRIS buffers (i.e. 0.01, 0.025 or 0.04 mol/kg-H_2O)

[d] $b(TRIS) = 2 * b(HCl)$

An offset of 0.4 % excess in the HCl molality was added unintentionally in the preparation of some TRIS buffers. Additional studies were conducted to investigate the potential impact on the pH_T values. To this end, solutions with varying excess HCl molalities (0%, 0.13%, 0.26%, 0.4%, 0.8%, 1.5% and 5%) were prepared and their pH_T

values were measured. An offset of -0.003 could theoretically be calculated for the pH_T value at 0.4% from a linear extrapolation of the results, as well as from equation 8 of Clegg et al. (2022). On the other hand, no dependence of the pH_T values on the excess HCl molality could be seen within their spread of 0.004 in the range up to 0.8%. Additionally, equimolal TRIS buffers of salinity 40 were prepared again with the correct HCl molality, and sent to LNE for comparison with the original buffers. These investigations showed that the error led to a bias of around -0.001 pH_T units, which is fairly small compared to the reproducibility of the pH_T Harned cell measurement results. As a consequence of these experimental findings, we have decided that the uncertainty of pH_T due to the excess in HCl molality of some ASW solutions is covered by the reproducibility contribution. Therefore, pH_T values obtained from ASW solutions affected from the HCl offset have not been corrected.

Each solution was stocked in 150 ml borosilicate glass bottles. Before closing with screw caps and sealing with Parafilm, the headspace was filled with Argon gas to limit exchange with CO_2, which could affect pH_T. The bottles were shipped to LNE and IPQ. The masses of the bottles were measured at PTB and at the recipient laboratory to ensure there had been no evaporation of the solutions during transport.

2.3. Definition of pH_T and potentiometric measurement model for TRIS buffers

2.3.1. Molality-based thermodynamic definition

Based on thermodynamics, the total pH scale is defined in a molality basis, noted $pH^*_{T,m}$, by equations 1.6.a and 1.6.b, reintroduced below in a molality basis. The superscript " * " is used in this chapter to indicate this thermodynamic definition of pH_T.

$$pH^*_{T,m} = -\lg\left\{\frac{b^T(H^+)}{mol/kg\ H_2O}\right\} \quad (1.6.a)$$

$$b^T(H^+) = b^f(H^+)\left(1+\frac{S_T}{K_S}\right) \approx b^f(H^+) + b(HSO_4^-) \quad (1.6.b)$$

where $b^f(H^+)$ is the molality of free protons (mol/kg H_2O), S_T is the total sulphate molality ($b(HSO_4^-) + b(SO_4^{2-})$) (mol/kg H_2O) and K_S is the dissociation constant on the same molality basis of HSO_4^- (Dickson et al., 2007).

The pH_T of TRIS buffer is measured by an electrochemical (i.e. potentiometric) method using a Harned cell. To this end, the molality-based thermodynamic potentiometric $pH^*_{T,m}$ is calculated by equation 3.1 (Clegg et al., 2022; Dickson et al., 2016), which is basically a recalculation of equation 1.6.b using the Nernst equation (see Supplementary Material S3.3 for the detailed potentiometric equations).

$$pH^*_{T,m} = \frac{E-E^{0*}}{k} + \lg(b_{Cl^-}) - 2\lg\left(\frac{\gamma HCl^{trace}}{\gamma HCl}\right) - \lg\left(\frac{1+\frac{b(SO_4^{2-})}{Kb(HSO_4^-)}}{1+\frac{b^T(SO_4^{2-})}{Kb(HSO_4^-)^{trace}}}\right) \quad (3.1)$$

The description of each term in equation 3.1 as well as their mean of determination are detailed in Chapter I, Section 3.4. Except for $\gamma\mathrm{HCl}$, being the mean activity coefficient of HCl, $b(\mathrm{SO_4^{2-}})$ the molality of sulphate ions (mol/kg-H_2O) and $Kb(\mathrm{HSO_4^-})$ the molality-based dissociation constant of bisulphate ions, equivalent to *K*s in equation 1.6.b.

2.3.2. Conversion to an amount content basis

The molality based $\mathrm{pH_{T,m}^*}$ definition must be converted to an amount content basis, noted $\mathrm{pH_T^*}$, to be suitable for oceanographers (equation 3.2).

$$\mathrm{pH_T^*} = \mathrm{pH_{T,m}^*} - \lg(\omega_{H_2O}) \tag{3.2}$$

where ω_{H_2O} is the water mass fraction (g/kg sol).

The TRIS buffer recipe is defined for a nominal practical salinity. Indeed, the artificial seawater composition of the TRIS buffer has been conceived to have the exact same chemical environment as a real seawater of the same practical salinity. This, in order to keep the same dissociation constants.

To establish the conversion in amount content, in sake of practicality for end-users, the water mass fraction must be relative to a natural seawater composition and not to the TRIS buffer composition itself. ω_{H_2O} is thus obtained from equation 3.3, based on equation A.6 of Clegg et al. (2022), itself established from the natural seawater reference composition of Millero et al. (2008).

$$\omega_{H_2O} = 1 - 0.001004715 \times S \tag{3.3}$$

where S is the nominal practical salinity.

2.3.3. Simplification for operational $\mathrm{pH_T}$

The two components with the "trace" superscripts in equation 3.1 indicate quantities in a pure artificial seawater composition and $b^T(\mathrm{SO_4^{2-}})$ is the total sulphate molality in pure ASW. If it is assumed that, in TRIS buffers, $1 + \frac{b(\mathrm{SO_4^{2-}})}{Kb(\mathrm{HSO_4^-})}$ and $\gamma\mathrm{HCl}$, which cannot be measured, are equivalent to their respective limiting values in pure ASW (Clegg et al., 2022), equation 3.1 can be simplified under this assumption to give the so-called operational potentiometric $\mathrm{pH_T}$, in an amount-content basis (equation 1.10.a, reintroduced below).

$$\mathrm{pH_T} = \frac{E - E^{0*}}{k} + \log(b_{Cl^-}) - \log(\omega_{\mathrm{H_2O}}) \tag{1.10.a}$$

2.4. Instrumentation

Harned cell measurements at LNE were conducted at 15 °C, 25 °C, and 30 °C, with instrumentation given in Chapter II, Section 2.1.1. pH_T spectrophotometric measurements were performed with the instrumentation given in Chapter II, Section 2.1.2.

2.5. TRIS buffers potentiometric characterization and pH_T values computation

The three NMIs performed the characterisation of the TRIS buffers following the method described in Chapter I, Section 3.4. The potentials E (equation 1.10.a) of the three equimolal buffers at each salinity and temperatures were measured using *cell II* (Chapter I, Section 3.4). NMIs performed duplicate or triplicate of their respective measurements.

The solutions used for the determination of the E^{0*} terms (equation 1.10.a) were prepared by each institute in its own laboratory for the salinities it had to study (S3.1, Supplementary Material). The same salts and stock solutions used by PTB for the preparation of the TRIS buffers were distributed to LNE and IPQ for the preparation of these solutions. Seven solutions with $b(HCl)$ of 0.005, 0.01, 0.012, 0.028, 0.032, 0.048 and 0.052 mol/kg-H_2O were measured for each salinity using *cell I* (Chapter I, Section 3.4). The lowest HCl molality was replaced by 0.011 mol/kg-H_2O at PTB since a drop in potential at low HCl molalities occurred. This phenomenon has also been occasionally experienced at LNE, with no clear explanation.

Homogeneity between Ag/AgCl electrodes used for the determination of E^{0*} was checked at each institute either by characterization of their standard potential E^0 in HCl solution of molality 0.01 mol/kg-H_2O, or by computing standard deviation of the potentials between the various Ag/AgCl electrodes acquired in an NaCl solution.

pH_T values were computed from equation 1.10.a from the determination of E and E°* as detailed above, while other terms in this equation are known from TRIS buffers gravimetric preparation information given by PTB, as well as temperature and pressure measurements performed by each institute. ω_{H_2O} was obtained using equation 3.3.

pH_T comparison measurements were made at 25 °C and 30 °C on the three equimolal buffers of salinities 5 and 35 to demonstrate the compatibility of the results of the three NMIs.

2.6. Data processing and fit function

2.6.1. Evaluation of anomalous results

Three equimolal TRIS buffers, $b(\mathrm{TRIS}) = b(\mathrm{TRIS.HCl}) = 0.01$, 0.025 and 0.04 mol/kg-H_2O, are used in literature up to now to extrapolate the corresponding pH_T values linearly to zero TRIS concentration (Müller et al., 2018). However, our results suggest that the assumption of linearity is not entirely justified in this molality range. The same behaviour has been observed at all salinities and temperatures studied whereas the non-linearity is more pronounced at low temperatures and high salinities. The reason for the deviation from linearity, which suggests that the pH_T values at 0.01 mol/kg-H_2O become smaller in a non-linear way for decreasing TRIS molalities, has been illustrated by Clegg et al. (2022). They suggest that for TRIS molalities lower than 0.02 mol/kg-H_2O the amount of TRIS becomes too low for an effective buffer, so that the pH_T drops and tends toward neutral pH_T. Consequently, Clegg and co-workers suggest to work at lower limit of $b(\mathrm{TRIS}) = b(\mathrm{TRIS.HCl}) = 0.02$ mol/kg-H_2O to be on the safe side. As $b(\mathrm{TRIS}) = b(\mathrm{TRIS.HCl}) = 0.01$ mol/kg-H_2O seems to be in the transition zone between increasing and decreasing pH_T, non-linearity has been observed in experiments to differing degrees. This can explain why the non-linear behaviour we have observed, which cannot be neglected but is still small in relation to the absolute pH_T value, has not always been observed in previous literature (DelValls and Dickson, 1998; Müller et al., 2018). Because of this observation, we have decided to use only the results of the TRIS buffers at 0.025 mol/kg-H_2O and 0.04 mol/kg-H_2O for the computation of the fit function. Furthermore, we suggest that future measurements should be conducted with a 0.02 mol/kg-H_2O TRIS buffer at the lower end.

The deviation of the measured pH_T values from the fit function was significantly larger at salinity 20 for all temperatures compared to the pH_T values at all other salinities (mean absolute residual of 0.0023 compared to a maximum mean absolute residual of 0.0018 for other salinities; maximum absolute residual of 0.0099 compared to 0.0040 for other salinities). This mainly arose from measurements of the TRIS buffer with $b(\mathrm{TRIS}) = b(\mathrm{TRIS.HCl}) = 0.025$ mol/kg-H_2O, however a thorough analysis of the available measurement parameters didn't reveal any obvious errors. Including the results at salinity 20 in the regression distorted the fit function significantly compared to a regression without these results, while the fit function was rather robust if the results at this salinity have been removed from the evaluation. We have therefore decided to remove the results at salinity 20, assuming unnoticed measurement errors.

Finally, the measurements at 40 °C were excluded for salinity 25 because an interference peak in the measured potential affected the results.

2.6.2. Model fitting

The equation proposed by Müller et al. (2018) (equation 9 of that publication) was used to describe the relationship between salinity, temperature, TRIS molality and pH_T. However, since the pH_T results at 0.01 mol/kg-H_2O TRIS molality were excluded, so that there are just two pH_T values at the two remaining TRIS molalities for each salinity and temperature, the quadratic $b(\mathrm{TRIS})$ terms were omitted, giving:

$$pH_T(S,T,b(TRIS)) = f\left\{\left[(1+S+S^2+S^3)*\left(1+T+\ln(T)+\frac{1}{T}\right)\right]+[b(\mathrm{TRIS})*(1+S+T+S*T)]\right\} \quad (3.4)$$

The data processing for the establishment of the fit function was performed at PTB, more details are given in Supplementary Material S3.4.

The fit function allows computing pH_T values of an ASW sample at given nominal practical salinity, temperature and TRIS molality. Additionally, it can be used to calculate the pH_T at zero TRIS molality by applying b(TRIS) = 0 mol/kg-H_2O.

Alternatively, it would have been possible to calculate a fit function pH_T(S,T) at zero TRIS molality from pH_T values received from a linear extrapolation of the pH_T values measured at molalities 0.025 and 0.04 mol/kg-H_2O for each salinity and temperature. However, this approach was less robust against statistical variations of the measurements results and was therefore discarded.

2.7. Spectrophotometric measurements

Spectrophotometric measurements were performed to check the equivalence of the $K_2^T e2$ characterisation published by Müller and Rehder (2018) with the results of this work. The measurements were performed at LNE on equimolal TRIS buffers of salinities 5, 20, 35 and 40 with $b(\mathrm{TRIS}) = b(\mathrm{TRIS.HCl}) = 0.025$ and 0.04 mol/kg-H_2O. Three replicates were performed for each buffer.

The measurements were conducted with the instrumentation given in Chapter II, Section 2.1.2, following the method given in Chapter I, Section 3.2.

The final pH_T value was calculated following the method described in Liu et al. (2011) where the $K_2^T e2$ of the indicator dye was calculated using coefficients given in Müller and Rehder (2018).

Spectrophotometric pH_T values were adjusted to 25°C from the knowledge of the pH_T dependence to temperature arising from the potentiometric characterization of the buffers at temperatures between 5°C and 40°C.

3. Results

3.1. Equivalence of results between the three NMIs

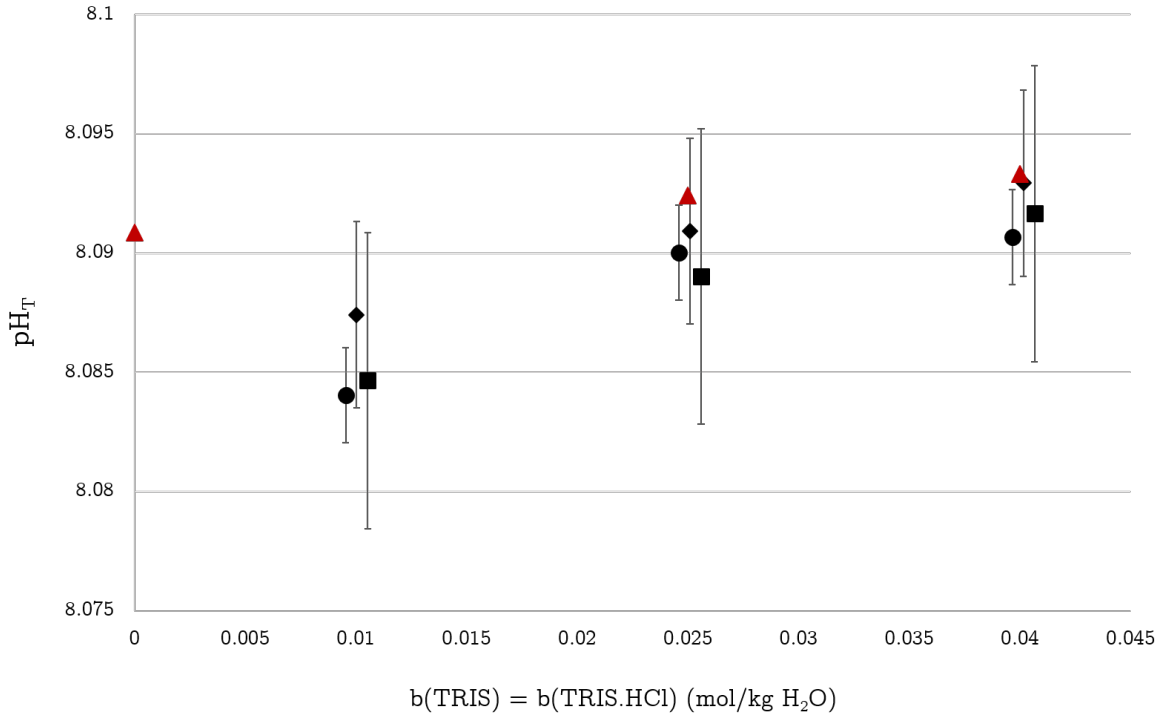

Figure 23: Harned cell measurements conducted by the three NMIs at 25 °C for the three equimolal TRIS buffers of nominal practical salinity 35. Where ●, ◆ and ■ represent measurements conducted by PTB, LNE and IPQ, respectively. Error bars correspond to their respective expanded uncertainties (i.e. with a coverage factor, k, of 2). ▲ represents the values calculated with the fit function.

Figure 23 illustrates the pH_T results at three TRIS molalities, salinity 35 and 25°C that have been measured by the three NMIs to estimate the equivalence of the measurements. Measurement points of each NMI represent the mean of repeated measurements, with its associated expanded uncertainty ($k = 2$). The expanded uncertainties were computed and given by each institute respectively. The data points are slightly staggered form the actual TRIS molality in the x axis in order to visualize the error bars correctly. From the compatibility tests performed at 25 °C and 30 °C, both for salinities 5 and 35, the maximum standard deviation between the three NMIs for specific TRIS molalities is 0.0048 with a mean standard deviation of 0.0020. These data are within the expanded uncertainties of the measurements, which demonstrates the equivalence among NMIs.

3.2. Fit function

The fit function was computed from the pH_T measurements on the TRIS buffers as described in Section 2.6. The pH_T values of equimolal TRIS buffers are given as a

function of nominal practical salinity, temperature and TRIS molality by equation 3.5 and corresponding coefficients in Table 10. Equation 3.5 shows the implementation of the coefficients in the fit function.

$$\mathrm{pH_T} = g + h_1 * S + h_2 * S^2 + h_3 * S^3 + i_1 * T + i_2 * \ln(T) + i_3 * \frac{1}{T} + j_1 * S * T + j_3 * S^3 * T + j_4 * S * \ln(T) + j_5 * S^2 * \ln(T) + j_6 * S^3 * \ln(T) + l_1 * b(\mathrm{TRIS}) \quad (3.5)$$

where T is the temperature in Kelvin in the range $278.15 \leq T \leq 313.15$ (i.e. 5–40 °C) and S the salinity in the range $5 \leq S \leq 40$.

Table 10: Coefficients to be used in the fit function given by equation 3.5.

coefficient	multiplier	value	unit
g	1	-1.60371111116E+02	–
h_1	S	-1.07922316097E+00	$\frac{\mathrm{kg}}{\mathrm{g}}$
h_2	S^2	-4.90160034300E-03	$\frac{\mathrm{kg}^2}{\mathrm{g}^2}$
h_3	S^3	3.78315116000E-04	$\frac{\mathrm{kg}^3}{\mathrm{g}^3}$
i_1	T	-4.19043463970E-02	$\frac{1}{\mathrm{K}}$
i_2	$\ln T$	2.76211128895E+01	$\frac{1}{\ln(\mathrm{K})}$
i_3	$\frac{1}{T}$	7.02080840507E+03	K
j_1	$S * T$	-9.62594719000E-04	$\frac{\mathrm{kg}}{\mathrm{g}*\mathrm{K}}$
j_3	$S^3 * T$	2.40267000000E-07	$\frac{\mathrm{kg}^2}{\mathrm{g}^2*\mathrm{K}}$
j_4	$S * \ln T$	2.39626168542E-01	$\frac{\mathrm{kg}}{\mathrm{g}*\ln(\mathrm{K})}$
j_5	$S^2 * \ln T$	8.74173653000E-04	$\frac{\mathrm{kg}^2}{\mathrm{g}^2*\ln(\mathrm{K})}$
j_6	$S^3 * \ln T$	-7.90966940000E-05	$\frac{\mathrm{kg}^3}{\mathrm{g}^3*\ln(\mathrm{K})}$
l_1	$b(TRIS)$	6.38632963020E-02	$\frac{\mathrm{kg\ H_2O}}{\mathrm{mol}}$

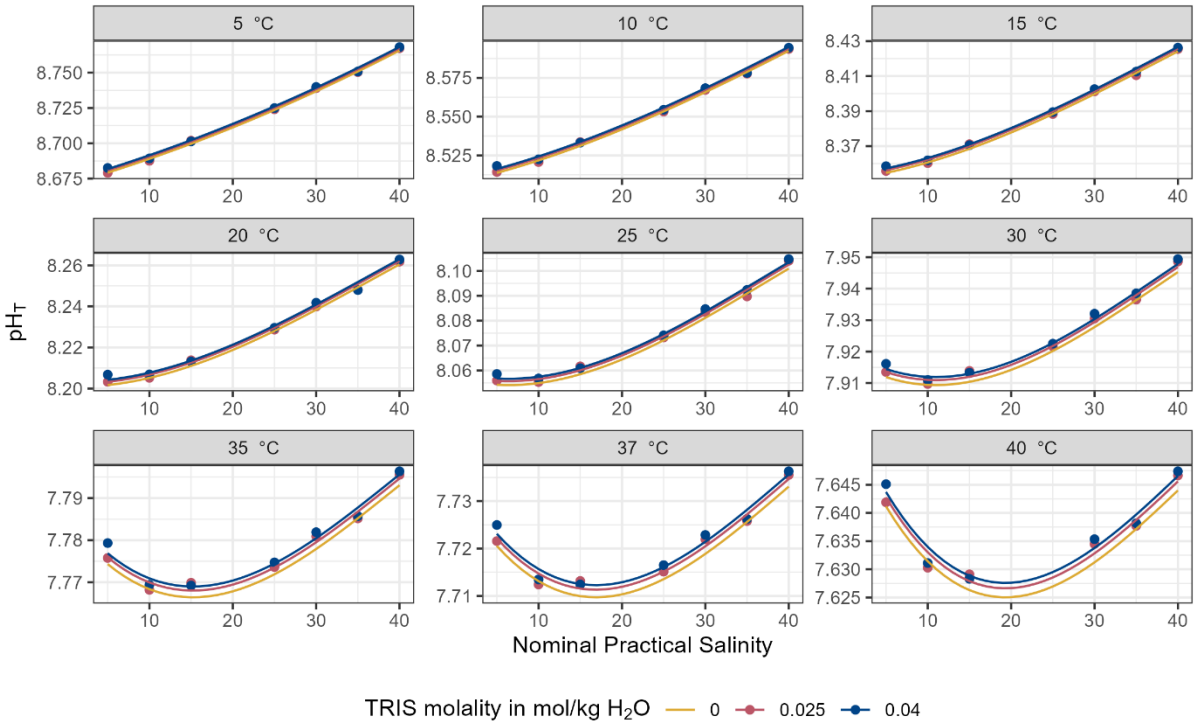

Figure 24: Fit function given by equation 3.5 and coefficients from Table 10 in dependence of temperature and nominal practical salinity. (1) pink and blue dots represent Harned cell measurements data points made for b(TRIS)=b(TRIS.HCl)=0.025 and 0.04 mol/kg H_2O, respectively. (2) yellow, pink and blue lines represent the fit function for zero TRIS molality and for $b(\mathrm{TRIS}) = b(\mathrm{TRIS.\,HCl}) = 0.025$ and 0.04 mol/kg-H_2O, respectively.

Figure 24 shows, for each temperature, the fit in function of salinity calculated with equation 3.5 for zero TRIS molality and for $b(\mathrm{TRIS}) = b(\mathrm{TRIS.\,HCl}) = 0.025$ and 0.04 mol/kg-H_2O, together with the measured pH_T values, excluding the discarded values (see section 2.6.1).

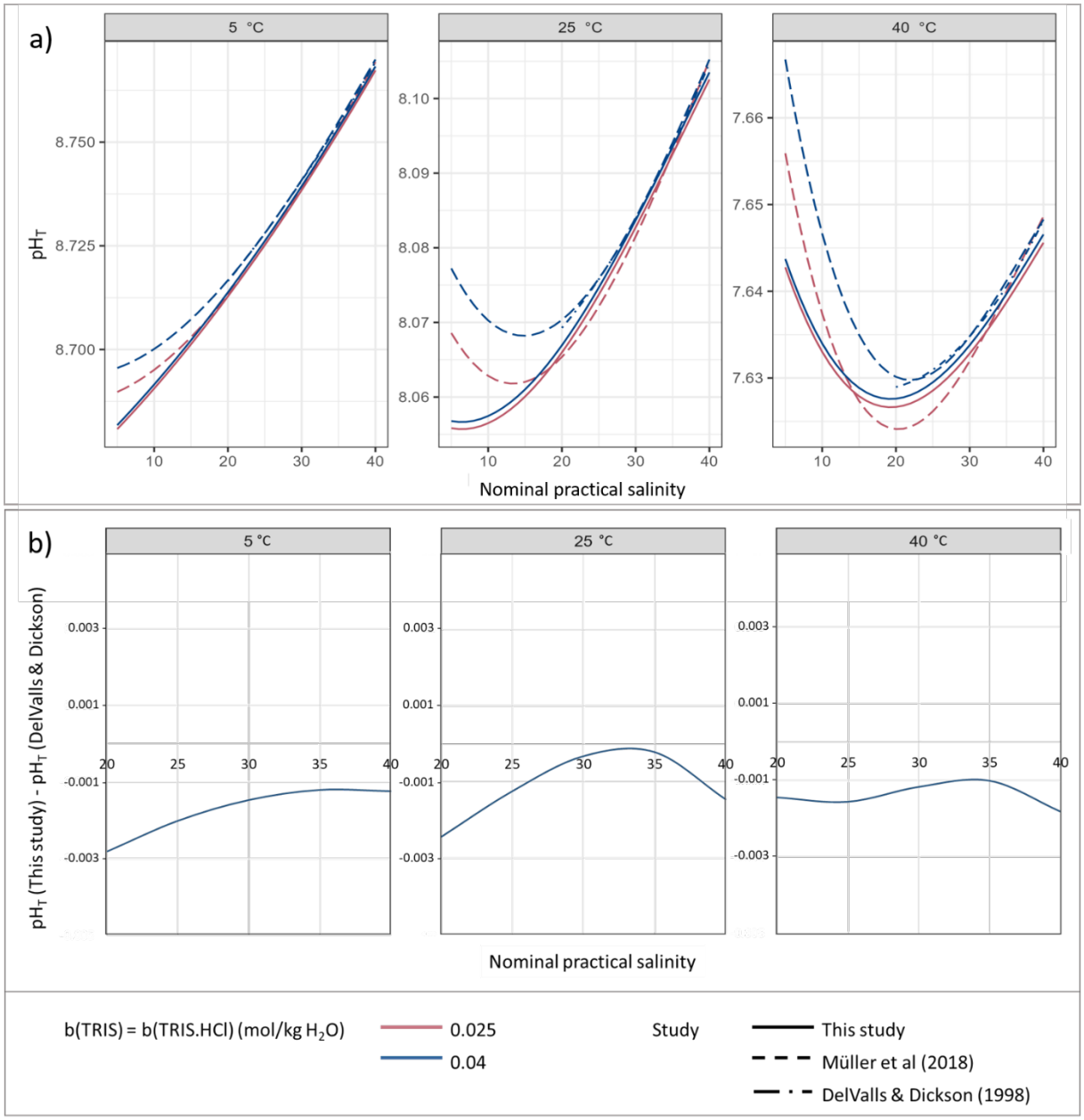

Figure 25: a) pH_T fit functions at 5 °C, 25 °C and 40 °C computed in this study, in Müller et al. (2018) and in DelValls and Dickson (1998) ; represented by the straight line, large dashes and dots, respectively. The blue and pink functions correspond to equimolal buffers of $b(TRIS) = b(TRIS.HCl) = 0.025$ and $0.04\ mol/kg\ H_2O$, respectively. b) Deviation between the pH_T fit functions at 5 °C, 25 °C and 40 °C and S 20-40 computed in this study and in DelValls and Dickson (1998) for the equimolal buffer of $b(TRIS) = b(TRIS.HCl) = 0.04\ mol/kg\ H_2O$.

Figure 25 shows, for all salinities and at 5 °C, 25 °C and 40 °C, the comparison of the fit function obtained in this study with previous work available in the literature. It shows good agreement between studies for pH_T values above salinity 20. However, discrepancies occur for lower salinities, this is further discussed in Section 4.

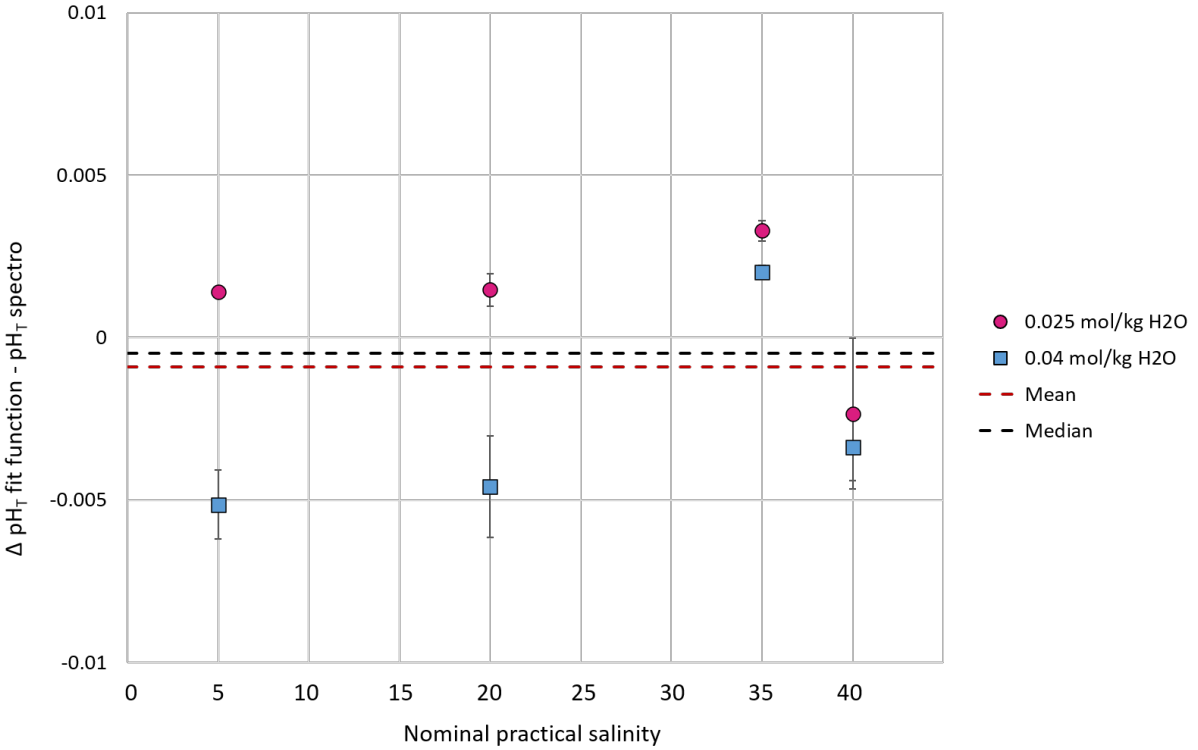

Figure 26: Difference between the pH_T value given by the fit function and the mean pH_T obtained from 3 replicates of spectrophotometric measurements made at LNE on equimolal TRIS buffers with $b(TRIS) = b(TRIS.HCl) = 0.025$ (○) and 0.04 (□) mol/kg H_2O of nominal practical salinities 5, 20, 35 and 40 at 25 °C. Error bars represent standard deviations of the three replicates. Dashed lines represent mean and median deviations computed from the eight values presented.

Figure 26 shows the difference between the fit function (equation 3.5) and spectrophotometric measurements performed at LNE at 25 °C on the two equimolal TRIS buffers of $b(\mathrm{TRIS}) = b(\mathrm{TRIS.HCl}) = 0.025$ and 0.04 mol/kg H_2O for salinities 5, 20, 35 and 40. The mean deviation between the fit function and the spectrophotometric pH_T values is of -0.0009. This is discussed further below.

4. Discussion

The fit function giving equimolal TRIS buffer pH_T as a function of salinity, temperature and TRIS molality (equation 3.5) was computed from Harned cell measurements of TRIS buffers with $b(\mathrm{TRIS}) = b(\mathrm{TRIS.HCl}) = 0.025$ and 0.04 mol/kg-H_2O. The pH_T of TRIS buffers for a pure artificial seawater matrix were then obtained by applying $b(\mathrm{TRIS}) = b(\mathrm{TRIS.HCl}) = 0$ mol/kg-H_2O to that function. Figure 25 compares the fit function obtained in this study to previous studies of DelValls and Dickson (1998) and Müller et al. (2018) at three temperatures and for all salinities. Müller and co-workers

studied pH_T of TRIS buffers, having the same TRIS molalities, but deviating ASW compositions, in the range of salinity 5–20 with an added measurement at salinity 35, and in the temperature range 5–45 °C. DelValls and Dickson (1998) studied the equimolal TRIS buffer for $b(\mathrm{TRIS}) = b(\mathrm{TRIS.HCl}) = 0.04$ mol/kg-H_2O in the salinity range 20–40 and temperature range 0–45 °C. Müller and co-workers combined their results with those of DelValls and Dickson to compute a fit function giving pH_T values of TRIS buffers as a function of salinity, temperature and molality of TRIS in the whole range of salinity 5–40. This function is illustrated by large dashes in Figure 25.a.

Mosley and co-workers (2004) also studied pH_T of TRIS buffers of $b(\mathrm{TRIS}) = b(\mathrm{TRIS.HCl}) = 0.04$ mol/kg-H_2O at 25 °C for estuarine waters, i.e. for low salinities. They computed their function with that from DelValls and Dickson (1998) for $S > 20$ and from Bates and Hetzer (1961) that performed measurements on TRIS buffers made in pure water. However, lack of in-between measurements raises questions about the robustness of the resulting fit function. It is not presented in Figure 25.a, nor further discussed.

Figure 25 shows good agreement between all fit functions for salinities between 20 and 40. Moreover, the pH_T of TRIS buffer with a molality of $b(\mathrm{TRIS}) = b(\mathrm{TRIS.HCl}) = 0.04$ mol/kg-H_2O at salinity 35 and 25 °C has been occasionally reported in literature and our fit function also shows good agreement with these studies with a maximum discrepancy of 0.002 (Papadimitriou et al., 2016; Pratt, 2014, Chapter II). However, the discrepancy between our model and the one of Müller et al. (2018) increases for salinities below 20, especially at high temperatures. Müller et al. (2018) computed, from the composition at salinity 20 of DelValls and Dickson for $b(\mathrm{TRIS}) = b(\mathrm{TRIS.HCl}) = 0.04$ mol/kg-H_2O, the composition of their two other equimolal TRIS buffers, as well as the composition of TRIS buffers at lower salinities, using equation 1 of Müller et al. (2018). However, this equation leads to a difference of the composition of ASW compared to the reference composition of artificial seawater (Clegg et al., 2022). To keep the salinity of a TRIS buffer constant when adding HCl, all salt molalities were changed to compensate for the addition of HCl instead of only changing the molality of NaCl. This results in different sulphate molalities between the three equimolal buffers at a given salinity, which affects the chemical equilibria defining pH_T (equation 1.6.b). Using those pH_T values to extrapolate to $b(\mathrm{TRIS}) = b(\mathrm{TRIS.HCl}) = 0$ mol/kg-H_2O leads to biases in the range -0.005 to -0.01 pH_T units at the extrapolated composition of pure ASW and at 25°C according to Clegg et al. (2022). The maximum bias observed for extrapolated values between the function presented in this study and the one of Müller et al. (2018) is of -0.015 for salinity 15 at 40 °C. Müller and co-workers used the same composition as DelValls and Dickson for their measurement at salinities 20 and 35, where good agreement is found. This proves the overall equivalence of the quality of the measurements of all these studies.

The present study reproduces the measurements of DelValls and Dickson (1998) for the equimolal TRIS buffer of $b(\mathrm{TRIS}) = b(\mathrm{TRIS.HCl}) = 0.04$ mol/kg-H_2O for salinities from 20 to 40 and temperatures from 5 to 40 °C. The maximum discrepancy between

pH_T values presented in Figure 25.b for this study and one of DelValls and Dickson (1998) is -0.0027, being within expanded uncertainties of measurements. No significant dependence of the discrepancy on temperature and salinity can be observed. Additionally, our results are in agreement with the measurements of DelValls and Dickson (1998) preformed on a TRIS buffer of $b(\mathrm{TRIS}) = b(\mathrm{TRIS.HCl}) = 0.01\ \mathrm{mol/kg\ H_2O}$ at salinity 35 and 25°C. Since the same procedures, i.e. regarding sample preparation, were used, this agreement validates the approach followed to obtain the pH_T values for lower salinities, giving confidence in the final fit function.

It is observed from Figure 24 and Figure 25.a that the minimum pH_T value is shifting from lower to higher salinities with increasing temperature. This could be explained by the fact that the temperature dependences of TRIS buffer pH_T values increase with salinity.

In Figure 26, the pH_T values obtained from our fit function (equation 3.5) are compared to spectrophotometric pH_T measurements. The coefficient given in Müller and Rehder (2018) for the calculation of $K_2^T e2$ seems to give pH_T values that are in agreement with the fit function presented in this paper, even for salinity 5. Indeed, the maximum discrepancy is -0.0051 pH_T units, which is lower than the estimated expanded uncertainty of the spectrophotometric pH_T results, estimated to be around 0.01 (k = 2) (Chapter II, Carter et al., 2013). However, the TRIS buffer composition made by Müller et al. (2018) is not the one commonly used, and resulting values do not extrapolate truly to pure ASW, they thus do not refer to a true pH_T scale. The use of $K_2^T e2$ values from Müller and Rehder (2018) might thus introduce an inconsistency in the subsequent spectrophotometric $\mathbf{pH_T}$ calculation. The suitability of coefficients given in Müller and Rehder (2018) must be investigated on a larger data set, for example for a TRIS buffer of salinity 15 at 40°C, where the biggest discrepancy was obtained in extrapolated $\mathbf{pH_T}$ values compared to our study, as well as on natural seawater samples. The fact that spectrophotometric pH_T values for equimolal TRIS buffers of molalities 0.025 mol/kg-H_2O seem to give systematically higher values than TRIS buffers at molalities 0.04 mol/kg-H_2O (Figure 26) also needs to be further investigated.

5. Traceability of potentiometric pH_T measurements

The work presented in this chapter, by linking TRIS buffers pH_T values to a pure artificial seawater matrix, and thus to a true pH_T scale, offers improvement of the metrological traceability of pH_T measurements.

As a reminder, metrological traceability is defined as the "property of a measurement whereby the result can be related to a reference through a documented unbroken chain of calibrations, each contributing to the measurement uncertainty" (JCGM 200:2012, 2012). Metrological traceability is ideally established to the International System of Units (SI) as it is the most stable reference. There are certain cases where this cannot

be achieved, for example, if the measurement procedure requires making approximations that are not fully mastered or do not have quantified uncertainties. In this case, the reference can either be a reference material or a common procedure.

The route of traceability of routine seawater pH_T spectrophotometric measurement results is, up to date, established to the commonly accepted measurement procedure of the primary pH potentiometric measurement method, i.e. Harned cell measurement method. This is achieved through the TRIS buffer solutions that allow the characterization of the indicator dye (Chapter I, Figure 10).

This measurement method lacks direct metrological traceability to the SI units, due to the assumptions required for the interpretation of the measurements, as expressed in Section 2.3. Indeed, the thermodynamic and operational total pH definitions (pH_T^* and pH_T, respectively) differ as shown by equation 3.6. A complete description of the potentiometric equations is given in the Supplementary Material, S3.3.

$$pH_T^* = pH_T - 2\log\left(\frac{\gamma HCl^{trace}}{\gamma HCl}\right) - \log\left(\frac{1+\frac{b(SO_4^{2-})}{Kb(HSO_4^-)}}{1+\frac{b^T(SO_4^{2-})}{Kb(HSO_4^-)^{trace}}}\right) \quad (3.6)$$

For simplicity, the terms $-2\log\left(\frac{\gamma HCl^{trace}}{\gamma HCl}\right)$ and $-\log\left(\frac{1+\frac{b(SO_4^{2-})}{Kb(HSO_4^-)}}{1+\frac{b^T(SO_4^{2-})}{Kb(HSO_4^-)^{trace}}}\right)$ are below referred to as the "γHCl term" and "$Kb(HSO_4^-)$ term", respectively.

Achieving traceability of pH_T potentiometric measurement results to SI units would require the quantification of the terms γHCl and $Kb(HSO_4^-)$ as well as their uncertainties, which cannot be achieved experimentally.

The difference between thermodynamic and operational potentiometric pH_T (equation 3.6), coming from the terms γHCl and $Kb(HSO_4^-)$, has been studied by Clegg et al. (2022) using a Pitzer based speciation model. It has been assessed to be 0.0045 ± 0.0014 for an equimolal TRIS buffer with $b(TRIS) = b(TRIS.HCl) = 0.04$ mol/kg-H_2O in artificial seawater of nominal salinity 35 at 25°C.

It was raised by Clegg et al. (2022) that for a pure artificial seawater matrix, pH_T^* and pH_T values are identical (i.e. for $b(TRIS) = b(TRIS.HCl) = 0$ mol/kg-H_2O) (see Figure 12a of Clegg et al., 2022). They also suggest that the terms γHCl and $Kb(HSO_4^-)$ are expected to tend linearly toward zero as buffer molality is reduced. SI traceability of TRIS buffers might thus be established, solely from measurements, through relation to a pure artificial seawater (i.e. without TRIS and TRIS.HCl).

The use of the speciation model may in the future assist this process by providing constraints on, for example, the slope of the relationship between pH_T and TRIS buffer molality. A sufficiently accurate and validated model would also be able to determine pH_T^* values for finite buffer molalities, including the hypothetical value for pure artificial seawater.

However, the model defined by Clegg and co-workers needs first to be validated and to be improved for key interactions. Uncertainties associated with the relevant Pitzer interaction parameters must also be thoroughly assessed (Clegg et al., 2022). The improvement and validation of this model would be an important step in the objective of achieving SI traceability of the pH_T values of TRIS buffers in artificial seawater.

6. Conclusion

This paper presents the characterization of equimolal TRIS buffers in the range of salinity 5-40 and temperature 5–40 °C with respect to their operational potentiometric pH_T values, performed with Harned cells at three National Metrology Institutes. These measurements allowed the computation of a fit function giving pH_T values of equimolal TRIS buffers depending on salinity, temperature and TRIS molality. For the first time, the experimental data covered completely the ranges of salinity and temperature that are most relevant in oceanography. This fit function allows computation of pH_T values of pure artificial seawater matrix (i.e. without TRIS and TRIS.HCl contribution) for the aforementioned salinity and temperature ranges. These values are relevant to characterize the indicator dye used for spectrophotometric measurements by better representing its response in real seawater.

The consistency with the reference work of DelValls and Dickson (1998) gives confidence in the fit function for salinities as low as 5, and the extrapolation to pure artificial seawater. This work, together with previous study of Clegg et al. (2022) is an important step to establish traceability for potentiometric pH_T measurement results of TRIS buffers, and, subsequently, for spectrophotometric measurements of natural seawater.

However, there are still a few concerns remaining regarding the establishment of traceability of routine spectrophotometric measurements: (1) reference materials used for the spectrophotometric pH_T measurement method are currently not certified for pure artificial seawater, (2) the effect of impurities in mCP aren't fully mastered and (3) the measured practical salinity of a natural seawater sample, used to calculate the pH_T, isn't itself traceable to the SI (Seitz et al., 2011).

References

Bates, R.G., Hetzer, H.B., 1961. Dissociation Constant of the Protonated Acid Form of 2-Amino-2-(Hydroxyme- thyl)-1,3-Propanediol [Tris-Hydroxymethyl)-Aminomethane] and Related Thermodynamic Quantities from 0 to 50°. J. Phys. Chem. 65, 667–671. https://doi.org/10.1021/j100822a017

Buck, R.P., Rondinini, S., Covington, A.K., Baucke, F.G.K., Brett, C.M.A., Camoes, M.F., Milton, M.J.T., Mussini, T., Naumann, R., Pratt, K.W., Spitzer, P., Wilson, G.S., 2002. Measurement of pH. Definition, standards, and procedures (IUPAC Recommendations 2002). Pure Appl. Chem. 74, 2169–2200. https://doi.org/10.1351/pac200274112169

Carter, B.R., Radich, A., Doyle, H.L., Dickson, A.G., 2013. An automated system for spectrophotometric seawater pH measurements. Limnology and Oceanography: methods 16–27. https://doi.org/10.4319/lom.2013.11.16

Clegg, S.L., Humphreys, M.P., Waters, J.F., Turner, D.R., Dickson, A.G., 2022. Chemical speciation models based upon the Pitzer activity coefficient equations, including the propagation of uncertainties. II. Tris buffers in artificial seawater at 25 °C, and an assessment of the seawater 'Total' pH scale. Marine Chemistry 244, 104096. https://doi.org/10.1016/j.marchem.2022.104096

DelValls, T.A., Dickson, A.G., 1998. The pH of buffers based on 2-amino-2-hydroxymethyl-1,3-propanediol ('tris') in synthetic sea water. Deep Sea Research Part I: Oceanographic Research Papers 45, 1541–1554. https://doi.org/10.1016/S0967-0637(98)00019-3

Dickson, A.G., 1990. Standard potential of the reaction: AgCl(s) + 12H2(g) = Ag(s) + HCl(aq), and and the standard acidity constant of the ion HSO4− in synthetic sea water from 273.15 to 318.15 K. The Journal of Chemical Thermodynamics 22, 113–127. https://doi.org/10.1016/0021-9614(90)90074-Z

Dickson, A.G., Camões, M.F., Spitzer, P., Fisicaro, P., Stoica, D., Pawlowicz, R., Feistel, R., 2016. Metrological challenges for measurements of key climatological observables. Part 3: seawater pH. Metrologia 53, R26. https://doi.org/10.1088/0026-1394/53/1/R26

Dickson, A.G., Sabine, C.L., Christian, J.R. (Eds.), 2007. Guide to Best Practices for Ocean CO2 Measurements PICES Special Publication 3, 191.

Douglas, N.K., Byrne, R.H., 2017. Spectrophotometric pH measurements from river to sea: Calibration of mCP for 0 ≤S≤ 40 and 278.15 ≤T≤ 308.15 K. Marine Chemistry 197, 64–69. https://doi.org/10.1016/j.marchem.2017.10.001

JCGM 100:2008, 2008. Evaluation of Measurement Data-Guide to the Expression of Uncertainty in Measurement.

JCGM 200:2012, 2012. International vocabulary of metrology (VIM) — Basic and general concepts and associated terms.

Liu, X., Patsavas, M.C., Byrne, R.H., 2011. Purification and Characterization of meta-Cresol Purple for Spectrophotometric Seawater pH Measurements. Environmental science & Technology 4862–4868.doi:10.1021/es200665d

Loucaides, S., Rèrolle, V.M.C., Papadimitriou, S., Kennedy, H., Mowlem, M.C., Dickson, A.G., Gledhill, M., Achterberg, E.P., 2017. Characterization of meta-Cresol Purple for spectrophotometric pH measurements in saline and hypersaline media at sub-zero temperatures. Sci Rep 7, 2481. https://doi.org/10.1038/s41598-017-02624-0

Millero, F., Feistel, R., Wright, D., McDougall, T., 2008. The composition of Standard Seawater and the definition of the Reference-Composition Salinity Scale. Deep-Sea Research I 55, 50–72. https://doi.org/10.1016/j.dsr.2007.10.001

Mosley, L.M., Husheer, S.L.G., Hunter, K.A., 2004. Spectrophotometric pH measurement in estuaries using thymol blue and m-cresol purple. Marine Chemistry 91, 175–186. https://doi.org/10.1016/j.marchem.2004.06.008

Müller, J.D., Bastkowski, F., Sander, B., Seitz, S., Turner, D.R., Dickson, A.G., Rehder, G., 2018. Metrology for pH Measurements in Brackish Waters—Part 1: Extending Electrochemical pHT

Measurements of TRIS Buffers to Salinities 5–20. Front. Mar. Sci. 5, 176. https://doi.org/10.3389/fmars.2018.00176

Müller, J.D., Rehder, G., 2018. Metrology of pH Measurements in Brackish Waters—Part 2: Experimental Characterization of Purified meta-Cresol Purple for Spectrophotometric pHT Measurements. Front. Mar. Sci. 0. https://doi.org/10.3389/fmars.2018.00177

Nemzer, B.V., Dickson, A.G., 2005. The stability and reproducibility of Tris buffers in synthetic seawater. Marine Chemistry 96, 237–242. https://doi.org/10.1016/j.marchem.2005.01.004

Papadimitriou, S., Loucaides, S., Rérolle, V., Achterberg, E.P., Dickson, A.G., Mowlem, M., Kennedy, H., 2016. The measurement of pH in saline and hypersaline media at sub-zero temperatures: Characterization of Tris buffers. Marine Chemistry 184, 11–20. https://doi.org/10.1016/j.marchem.2016.06.002

Pratt, K.W., 2014. Measurement of pHT values of Tris buffers in artificial seawater at varying mole ratios of Tris:Tris·HCl. Marine Chemistry 162, 89–95. https://doi.org/10.1016/j.marchem.2014.03.003

Schäfer, R., Capitaine, G., Bastkowski, F., Pellegrino, O., Quendera, R., Wagener, T., Achterberg, E., Fisicaro, P., Seitz, S., in preparation. Traceability of pHT measurements of TRIS buffer solutions in artificial seawater matrix in the salinity range 5-40 and temperature range 0-40°C. Part 2: uncertainty quantification.

Seitz, S., Feistel, R., Wright, D.G., Weinreben, S., Spitzer, P., De Bièvre, P., 2011. Metrological traceability of oceanographic salinity measurement results. Ocean Science 7, 45–62. https://doi.org/10.5194/os-7-45-2011

Chapter IV: Uncertainty quantification of absorbance values in the objective of assessing the uncertainty budget of seawater spectrophotometric pH_T measurement results

1. Introduction

Assessing variations of pH_T over space and time relies on the comparability of measurement results. This necessitates the application of the three essential metrological concepts. The improvement of metrological traceability and the potential for SI traceability were presented in Chapter III. The production of a reference material as well as its use in an inter-laboratory comparison, allowing procedure validation, were presented in Chapter II. However, comparing measurement results with confidence requires having an uncertainty budget associated to the result that is thoroughly assessed.

An uncertainty budget of the spectrophotometric pH_T measurement results assessed following the top-down approach have been presented in Chapter II, which gave an expanded uncertainty of 0.009 (k=2). However, the top-down approach, relying on experimental data taken from an inter-laboratory comparison, prevents us from identifying which are the main sources of uncertainty involved in a measurement process, and thus the ones it is needed to work on to reduce the uncertainty level. Moreover, the top-down approach is relatively dependent on participants' ability to perform the measurement.

Spectrophotometric pH_T measurement results are obtained from equation 1.8 below (presented in Chapter I, Section 3.2).

$$pH_T = -\log(K_2^T e2) + \log\left(\frac{R-e1}{1-R\times\frac{e3}{e2}}\right) \quad (1.8)$$

where K_2^T is the second dissociation constant of the indicator dye (meta-cresol purple, mCP), R the ratio of the absorbance at 578 nm (mCP basic form peak absorbance wavelength) A_{578} to the absorbance at 434 nm (mCP acid form peak absorbance wavelength) A_{434}, and $e1$, $e2$ and $e3$ are ratios of the molar extinction coefficients of the dye at these wavelenghts (Liu et al., 2011).

In equation 1.8, all terms (i.e. $K_2^T e2$, R, $e1$, and $\frac{e3}{e2}$) are obtained or characterized from spectrophotometric measurements. Thus, it is highly important to carefully assess the uncertainty of absorbance measurement results, in the perspective of achieving an uncertainty budget of spectrophotometric pH_T measurement results computed with the bottom-up approach (i.e. following the GUM; "JCGM 100:2008", 2008).

This chapter presents (1) the identification of uncertainty sources of the spectrophotometric pH_T measurement method, (2) a method for the calibration of a spectrophotometer and (3) the uncertainty of absorbance measurements relevant to spectrophotometric pH_T measurements. The uncertainty of the ratio R is computed and discussed.

The pH_T spectrophotometric measurement method is detailed in Chapter I, Section 3.2 while the instrumentation used is given in Chapter II, Section 2.1.2.

2.1. Identification of uncertainty sources

The identification of uncertainty sources is based on the pH_T spectrophotometric measurement model as described in Chapter I, Sections 3.2 and 3.3, which present the method to obtain each term in equation 1.8. This was completed with the sources of uncertainty identified by Carter et al. (2013) and DeGrandpre et al. (2014). It was chosen to divide the uncertainty sources into two categories: (a), the uncertainties introduced by the end-user measurement on a seawater sample (i.e. R) and (b) the uncertainties introduced by the terms appropriate to the indicator dye characteristics (i.e. $K_2^T e2$, $e1$ and $\frac{e3}{e2}$). Factors of influence that do not come directly from the measurement method, such as environmental conditions, properties of the sample, or user skills, were also included. The overall sources of uncertainties were represented with the help of an Ishikawa diagram (Liliana, 2016), given in Figure 27.

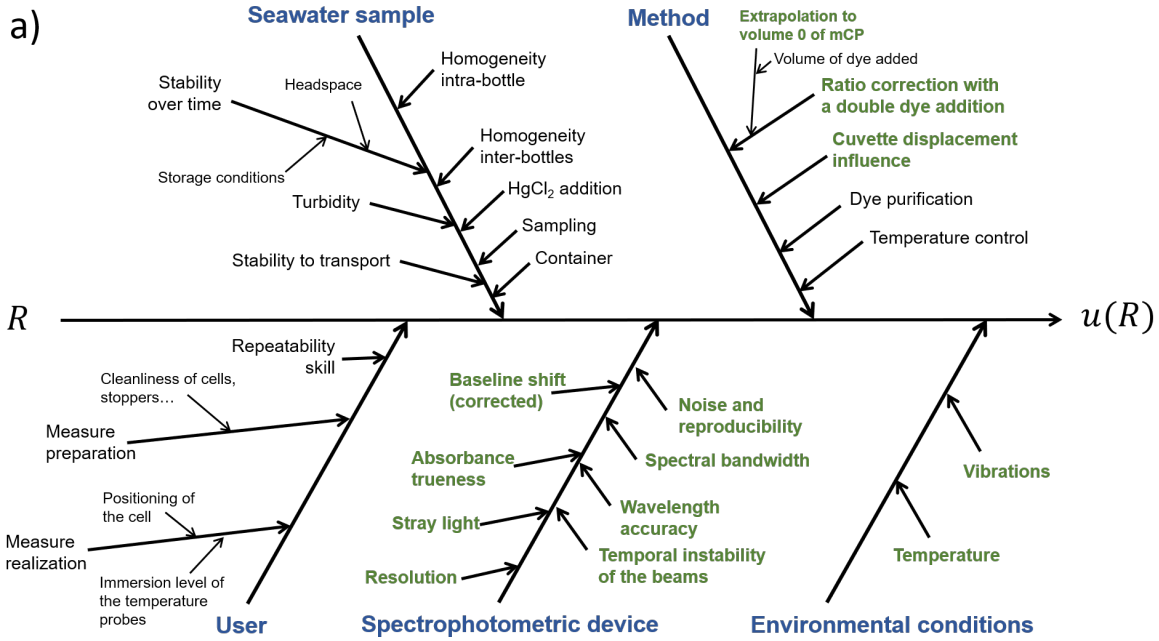

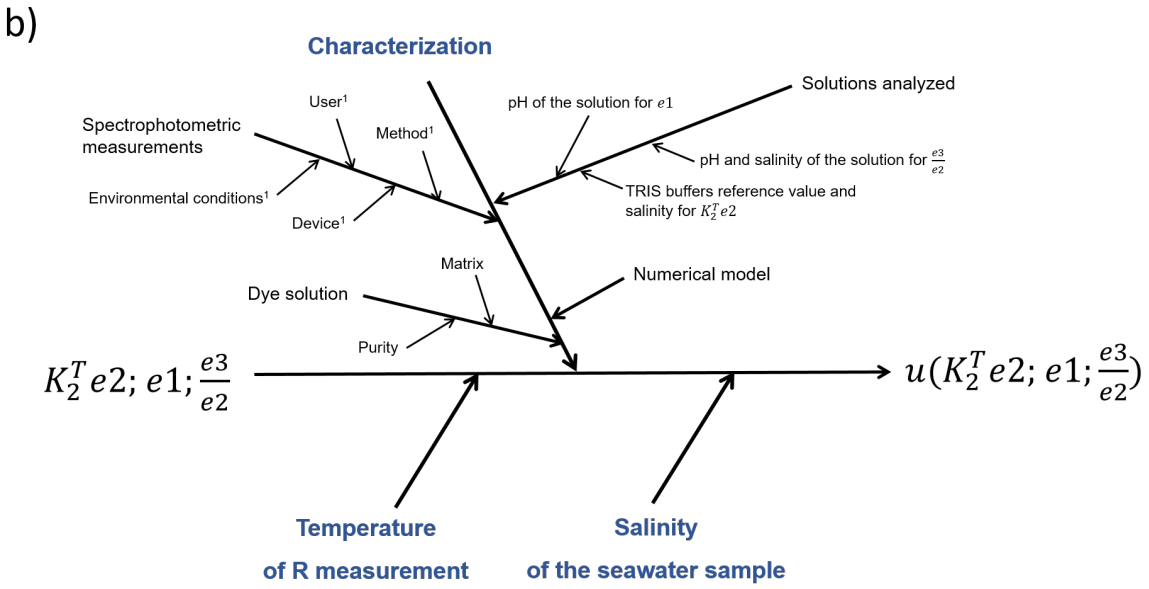

Figure 27: Ishikawa diagrams representing the uncertainty sources of the spectrophotometric pH_T measurement results with (a) uncertainties introduced by the term R in equations 1.8, and (b) uncertainty sources introduced by the terms relative to the indicator dye characterization. The sources in bold green in figure (a) are the one taken into account in the R uncertainty estimation presented in this chapter. The subscript "1" in figure (b) refers to the same sources that are more detailed in figure (a).

2.2. Calibration of the spectrophotometer

Spectrophotometer performance is commonly controlled by checking the wavelength accuracy as well as the linearity of the absorbance values, also called optical density. The wavelength accuracy was checked using holmium oxide and didymium glass filters (Allen, 2007; Burke et al., 1994) while the absorbance linearity was checked using several neutral density filters (Vega et al., 2016).

LNE's spectrophotometer (*Agilent Cary 60*) was checked using *Hellma* filters F0, F1, F2, F3, F4 and F7 that had been previously characterized by the Danish Fundamental Metrology (DFM, Danish Metrology Institute). The calibration certificate is given in Supplementary material S4.1. The calibration made at LNE was performed at 22 ± 1 °C to have the same condition as for the calibration of the filters. Indeed, temperature has an effect on spectrophotometric measurements. The procedure followed for calibration was based on the Spectrophotometer calibration guide of the French College of Metrology (CFM, 2017). Measurements were performed in transmittance and not in absorbance values, according to the CFM's guide. This facilitated the subsequent uncertainty quantification. The relation between absorbance value and transmittance is given by equation 4.1.

$$A_x = -\lg(T_x) \tag{4.1}$$

2.2.1. Optical density calibration

For the optical density calibration, four different filters were used to check photometric accuracy and linearity in the visible wavelength range. F0 represents the blank (i.e. the filter is empty). F2, F3 and F4 are three neutral density optical filters with absorbance values going from 0.2 to 1.16. Filters were characterized by DFM for the three specific wavelengths relevant for spectrophotometric pH_T measurements, i.e. 434, 578 and 730 nm.

For each filter, transmittance was acquired 10 times for the whole visible spectrum, between 400 and 800 nm, with steps of 0.2 nm. The same procedure was made with the beam light being blocked with an opaque film. The mean of the 10 replicates was computed for each filter plus for the opaque film, for the three wavelengths of interest. Optical density (OD) values were than obtained using equation 4.2.

$$OD = -\log\left(\frac{T_{Fx}-T_{F0}}{T_{F0}-T_{Fb}}\right) \quad (4.2)$$

where T_x represents the transmittance, Fx represents a specific neutral density filter (F2, F3 or F4), F0 represents the blank filter and T_{Fb} represents the transmittance acquired with the beam blocked.

A total of 9 optical density values were computed for wavelengths 434, 578 and 730 nm for the neutral density filters F2, F3 and F4. These values were then compared to the values given by DFM certificate.

Linearity was considered acceptable if the differences between absorbance values were within the expanded uncertainties of the DFM certificate and LNE's spectrophotometric results.

2.2.2. Wavelength calibration

The accuracy of the wavelengths was checked using filters F1 and F7, made respectively of holmium oxide and didymium glasses. They have the property of having many absorbance peaks in the visible range. Each of these two filters were calibrated by DFM for the three peaks closest to the wavelengths of interest for pH_T measurements, being 453.55, 536.35 and 637.60 nm for F1 and 472.00, 512.00 and 681.00 for F7 (Supplementary Material, S4.1).

For each filter, in addition to F0 and the opaque film, transmittance values of the whole visible spectrum were acquired three times with steps of 0.2 nm. The mean of the three replicates was computed and used to obtain the desired absorbance values, calculated with the same equation as for optical density (equation 4.2), with Fx representing F1 or F7, respectively. The wavelengths corresponding to the maximum of absorbance, relative to the same peaks as the ones chosen for the characterization of the filters, were then compared to the DFM certificate.

Wavelength accuracy was considered acceptable if the difference of wavelength was within the expanded uncertainties of DFM certificate and LNE's spectrophotometric results.

2.3. Quantification of the uncertainty of the ratio of absorbance *R*

The major uncertainty sources of R from the spectrophotometric device were identified. The uncertainty sources from the influence of both the environmental conditions and the method on the transmittance values acquired were also investigated. However, uncertainty components from the seawater sample, the user, the potential dye impurities and the temperature control weren't investigated.

2.3.1. Quantification of the input variables of the absorbance measurements

The quantification of the uncertainty of absorbance measurements followed the internal procedure of the LNE photonic department, and is based on the GUM approach (Dubard et al., 2016). It was computed for each of the nine transmittance values acquired based on an actual pH_T measurement performed on TRIS buffer reference material produced at LNE, equivalent to the one described in Chapter II, using a purified meta-cresol purple dye solution from GEOMAR. The nine transmittance values are therefore noted $T_{434,background}$, $T_{578,background}$, $T_{730,background}$, $T_{434,mCP}$, $T_{578,mCP}$, $T_{730,mCP}$, $T_{434,mCP*2}$, $T_{578,mCP*2}$, and $T_{740,mCP*2}$, corresponding to the three wavelength acquired at each step of the measurement process (background acquisition, first (mCP) and second ($mCP*2$) addition of dye).

The uncertainty sources of absorbance measurement considered are the following:

- Temporal instability of beams
- Wavelength accuracy
- Spectral bandwidth
- Spectrophotometric cuvette influence
- Environmental conditions
- Measurement noise and reproducibility
- Transmittance resolution
- Stray light
- Bias, or absorbance trueness
- Baseline shift

Among these sources of uncertainties, three were considered negligible. Indeed, as the spectrophotometer *Agilent Cary 60* operates in double-beam mode, the instability of the beams could be considered zero. The uncertainty linked to the bandwidth was also neglected as the device operate with a fixed bandwidth of 1.5 nm that cannot be changed. Finally, as the cuvette is thermostated during measurements and the vibrations were negligible, the influence of environmental conditions was also

considered to be zero. The method of quantification of the remaining sources are detailed below. All uncertainties are given for transmittance values.

Wavelength accuracy uncertainty

The uncertainty coming from the wavelength accuracy, also called spectral scale ($u_{spectral\ scale}$), corresponds to the impact of the error on the wavelength accuracy reported to the transmittance values measured. Indeed, when measuring a transmittance of a thin and important peak, a small error in the wavelength can induce an important error on the transmittance value. The uncertainty of the spectral scale was obtained from equation 4.3.

$$u_{spectral\ scale} = \frac{\partial T_x}{\partial \lambda} * u_{wavelength} \quad (4.3)$$

where T_x is the transmittance and λ the wavelength (in nm).

$u_{wavelength}$ was computed from the wavelength resolution of the device, the step of the scan applied for the calibration of wavelength accuracy and the uncertainty of the filter reference values used for wavelength accuracy checking. It was thus obtained from equation 4.4.

$$u_{wavelength} = \sqrt{resolution^2 + scan\_step^2 + {u_{filter}}^2} \quad (4.4)$$

The derivative $\frac{\partial T}{\partial \lambda}$ was obtained from experimental data points on either side of the wavelengths concerned. It was computed from the spectrophotometric pH_T measurement made on a TRIS buffer reference material produced at LNE (i.e. pH_T 8.1 in artificial seawater matrix of salinity 35). Nine $u_{spectral\ scale}$ values were thus computed for wavelengths 434, 578 and 730 nm and for each step of the measurement procedure: background, first and second additions of dye.

Spectrophotometric cuvette influence

During the pH_T measurement process, the 10 cm spectrophotometric cuvette is removed at each dye addition for homogenisation and then put back in the support inside the spectrophotometer. A test was performed to evaluate the impact of an eventual displacement of the cuvette occurring during this operation on the transmittance values. Transmittance values were acquired three times at 434, 578 and 730 nm for a cuvette filled with TRIS buffer and with one addition of dye, while removing and replacing the cuvette at one corner and the other of the support to exaggerate a displacement of the cell between two replicates. The maximum transmittance discrepancy (Δ_{max}) obtained was used to compute an uncertainty with equation 4.5.

$$u_{cuvette} = \frac{\Delta_{max}/2}{\sqrt{3}} \quad (4.5)$$

As this source uncertainty turned out to be in the same level as the reproducibility, it was kept in the final uncertainty budget calculation.

Noise and reproducibility

The uncertainty coming from the reproducibility, which includes the noise estimate, was obtained from the data acquired during the optical density calibration. As only repeatability measurements were performed at LNE, experimental data acquired at the laboratory of Ifremer's metrology unit (French Research Institute for Exploitation of the Sea) using the exact same filters and with the same model of spectrophotometer were used for reproducibility data. They performed the calibration with five transmittance repeatability measurements per day during three days.

For each filter (i.e. F0, F2, F3, F4 and opaque film), for each of the three wavelengths, and for each day of measurement, the maximum discrepancy between the five repeatability measurements was computed. All these discrepancy values were represented as a function of the corresponding level of transmittance, allowing us to obtain a linear relation y=ax+b. This relation was chosen in order to include all data points (Supplementary material, S4.2). It was then checked that data points obtained from the ten repeatability measurements obtained at LNE are also below that linear relation.

The uncertainty of reproducibility was obtained from equation 4.6.

$$u_{reproducibility} = \frac{aT+b}{2} \tag{4.6}$$

where T is the relevant transmittance value for a pH_T measurement (i.e. transmittance value at 434, 578 and 730 nm for each step of the measurement process). Coefficients a and b are given in S4.2.

Resolution

The resolution in transmittance was obtained from the device specification given by the manufacturer.

Stray light uncertainty

Stray light can have an influence on the value of transmittance. The uncertainty coming from the stray light corresponds to the transmittance detected when the beam is blocked (i.e. with the opaque film) for each of the three wavelengths of interest.

Bias

The uncertainty introduced by the bias ($u_{trueness}$) was quantified based on the calibration of optical density as described in Section 2.2.1. For each filter F2, F3 and F4 and for each of the three wavelengths of interest, $u_{trueness}$ was computed from equation 4.7.

$$u_{trueness} = \sqrt{\left(\frac{|\Delta_{trueness}|}{2}\right)^2 + (u_{filter})^2} \quad (4.7)$$

where $\Delta_{trueness}$ is the discrepancy between the optical density calculated with equation 4.2. and the reference value given by the filters certificate, converted in transmittance. And u_{filter} is the uncertainty of that reference value, also converted in transmittance.

This method allows to represent $u_{trueness}$ in function of the level of transmittance of the filters for the three respective wavelengths. From this representation can be computed a linear relation $u_{trueness}$ as a function of level of transmittance where $u_{trueness}$ is maximised (Supplementary material, S4.3), which allows to determine the uncertainty relative to the level of transmittance of an actual pH_T measurement.

Baseline fluctuation

The influence of the baseline fluctuation on the transmittance was assessed as the evolution of the transmittance at 730 nm during an entire process of pH_T measurement. This value was integrated into the final uncertainty budget.

2.3.2. Correlation matrix

The ratio of absorbance R in equation 1.8 (Section 1) is obtained from equations 1.9.a and 1.9.b, reintroduced below.

$$R = 2 \times R'_{(1st\ dye\ addition)} - R'_{(2nd\ dye\ addition)} \quad (1.9.a)$$

$$R' = \frac{(A_{578,dye} - A_{578,blank}) - (A_{730,dye} - A_{730,blank})}{(A_{434,dye} - A_{434,blank}) - (A_{730,dye} - A_{730,blank})} \quad (1.9.b)$$

where A represents the absorbance values.

In this mathematical model, the subtraction of absorbance values ensures that intrinsic systematic errors will be cancelled. Thus, a correlation matrix is needed to prevent the overestimation of the ratio R uncertainty. The considerations allowing for the construction of the correlation matrix are detailed below. To be consistent with the input variable uncertainty estimation, the correlation matrix is given for transmittance values.

The uncertainty of the spectral scan ($u_{spectral\ scale}$) translates the impact of the wavelength uncertainty on the measured transmittance value. It depends on the

wavelength accuracy and the shape of the transmittance peaks. The wavelength accuracy is identical for each wavelength respectively, constituting a systematic error. However, the shape of transmittance peaks depends on the measurement step (i.e. background, first addition and second addition of dye). Thus, the correlation at a wavelength is not total. A systematic error was considered for each wavelength, corresponding to the smallest variance among the three measurements for a given wavelength.

The uncertainty coming from displacement of the cuvette ($u_{cuvette}$) is completely correlated for the three transmittance values acquired simultaneously during a measurement step. But it is not correlated between two measurement steps as the cuvette is removed and put back in the support, generating an eventual displacement. Thus, a correlation of 1 was applied per measurement step, but zero correlation was considered between two measurement steps.

The uncertainties of noise and reproducibility as well as of resolution are considered completely random (correlation of zero).

For the uncertainty of the stray light, a systematic component was considered among the 9 values, corresponding to the smallest variance among them.

For the trueness uncertainty, there is a correlation by level of transmission values acquired. Thus, all values having a level of transmittance close to 1 (corresponding to an absorbance value close to 0) are considered highly correlated (correlation of 0.9). Whereas for different levels of transmission, only a systematic part was considered, corresponding to the fact that the same filters were used for the calibration (correlation of 0.5). These levels of correlation were determined with the help of LNE's photonic department experts. The correlation matrix of trueness is given in Supplementary material, S4.4.

The baseline fluctuation was considered completely systematic (correlation of 1) for the nine values as it is corrected with the baseline check at 730 nm during the whole measurement process.

From the considerations above, a covariance matrix is made using equation 4.8.

$$cov(T_a, T_b) = \sqrt{\sum u_{syst,Ta}^2} * \sqrt{\sum u_{syst,Tb}^2} \quad (4.8)$$

where $cov(T_a, T_b)$ represents the covariance between two transmittance values (a and b) and $\sum u_{syst}^2$ corresponds to the sum of the squares of all the systematic parts included in each source of uncertainty described above. For $cov(T_a, T_a)$, the random uncertainties are also included as the correlation is 1 between two exact same measurements.

The covariance matrix is given in Supplementary material, S4.5.

The correlation matrix was then obtained from equation 4.9.

$$corr(T_a, T_b) = \frac{cov(T_a, T_b)}{u_{Ta} * u_{Tb}} \quad (4.9)$$

where $corr(T_a, T_b)$ is the level of correlation between two transmittance values (ranging from 0 and 1), and u_{Ta} is the standard uncertainty budget of one transmittance value, computed from the combination of all input sources described in section 2.3.1.

2.3.3. R uncertainty budget

The uncertainty of R was computed following the principles of uncertainty propagation in equations 1.9.a and 1.9.b with the transmittance uncertainty values calculated as described in section 2.3.1, and the correlation matrix obtained as described in section 2.3.2. The absorbance values in equation 1.9.a have been replaced by transmittance using equation 4.1 to be in accordance with the uncertainties and correlation matrix that are themselves in transmittance.

3. Results

3.1. Wavelength and optical density calibrations

Table 11 presents the results of the optical density calibration of LNE's spectrophotometer performed as described in section 2.2.1. The difference of optical density values obtained at LNE compared to DFM's certificate is within the expanded uncertainties given by the certificate. The transmittance linearity of the spectrophotometer is thus considered acceptable.

Table 11: Optical density calibration results

Filter	Wavelength (nm)	Optical density	Certificate value	Difference
F2	434	0.271	0.270	0.001
	578	0.280	0.279	0.001
	730	0.234	0.233	0.001
F3	434	0.534	0.531	0.003
	578	0.539	0.535	0.004
	730	0.418	0.414	0.004
F4	434	1.078	1.078	0.000
	578	1.054	1.053	0.001
	730	0.771	0.770	0.001

Table 12 presents the results of the wavelength accuracy calibration results conducted as detailed in section 2.2.2. The wavelength difference between LNE's measurements and DFM's certificate is out of their respective expanded uncertainties for F1 at 453.4

and 637.7 nm and for F7 at 471.8 nm. These expanded uncertainties were obtained from equation 4.4 and from DFM's certificate, respectively. It seems that there is a continuing deviation over the wavelength range and that a correction is needed.

Table 12: Wavelength accuracy calibration results

Filter	Wavelength corresponding to the Absorbance peak (nm)	Certificate value (1.8nm BW)	Difference (nm)
F1	454.6	453.4	1.2
	536.6	536.3	0.3
	637.0	637.7	-0.7
F7	473.0	471.8	1.2
	513.0	512.1	0.9
	680.0	681.1	-1.1

3.2. Absorbance values and *R* uncertainty budgets

Table 13 presents the detailed uncertainty budget computed as detailed in section 2.3.1 for the nine transmittance values acquired during a pH_T measurement performed on a TRIS buffer reference material prepared at LNE, similar to the one presented in Chapter II (pH_T 8.1, artificial seawater matrix of salinity 35), using a purified meta-cresol purple dye solution from GEOMAR. The colour gradient indicates the main sources of uncertainties. Absorbance values with their uncertainties were converted using equation 4.1 and are also given in the table.

Table 13: Detailed uncertainty budget of the 9 transmittance values acquired for an actual pH_T measurement performed on a TRIS buffer reference material.

	$T_{434,background}$	$T_{578,background}$	$T_{730,background}$	$T_{434,mCP}$	$T_{578,mCP}$	$T_{730,mCP}$	$T_{434,mCPx2}$	$T_{578,mCPx2}$	$T_{730,mCPx2}$
$u_{spectral\ scale}$	3.75E-07	1.69E-06	2.10E-05	3.04E-06	1.08E-06	2.20E-05	2.40E-06	8.51E-07	2.21E-05
$u_{cuvette}$	2.02E-04	2.02E-04	2.02E-04	2.02E-04	2.02E-04	2.02E-04	2.02E-04	2.02E-04	2.02E-04
$u_{reproducibility}$	6.37E-04	6.41E-04	6.19E-04	5.46E-04	5.00E-04	6.19E-04	5.08E-04	4.83E-04	6.19E-04
$u_{resolution}$	1.00E-04	1.00E-04	1.00E-04	1.00E-04	1.00E-04	1.00E-04	1.00E-04	1.00E-04	1.00E-04
$u_{stray\ light}$	5.02E-04	5.52E-04	1.09E-03	5.02E-04	5.52E-04	1.09E-03	5.02E-04	5.52E-04	1.09E-03
$u_{trueness}$	7.17E-03	7.36E-03	6.33E-03	2.99E-03	9.16E-04	6.32E-03	1.28E-03	1.25E-04	6.33E-03
$u_{baseline\ fluctuation}$	3.00E-04	3.00E-04	3.00E-04	3.00E-04	3.00E-04	3.00E-04	3.00E-04	3.00E-04	3.00E-04
Transmittance	0.90053	0.92447	0.79558	0.37623	0.11510	0.79488	0.16132	0.01571	0.79516
u (k=1)	**7.22E-03**	**7.41E-03**	**6.46E-03**	**3.11E-03**	**1.24E-03**	**6.46E-03**	**1.52E-03**	**8.33E-04**	**6.46E-03**
Absorbance	0.04550	0.03411	0.09932	0.42455	0.93891	0.09970	0.79231	1.80377	0.09954
u (k=1)	**3.48E-03**	**3.48E-03**	**3.53E-03**	**3.59E-03**	**4.67E-03**	**3.53E-03**	**4.08E-03**	**2.31E-02**	**3.53E-03**

Table 14 presents the correlation matrix built as described in section 2.3.2 for the nine transmittance values that are acquired for a pH_T measurement. The colour gradient indicates the level of the correlation.

Table 14: Correlation matrix of the transmittance values acquired for an actual pH_T measurement

	$T_{434,background}$	$T_{578,background}$	$T_{730,background}$	$T_{434,mCP}$	$T_{578,mCP}$	$T_{730,mCP}$	$T_{434,mCPx2}$	$T_{578,mCPx2}$	$T_{730,mCPx2}$
$T_{434,background}$	1.00								
$T_{578,background}$	0.89	1.00							
$T_{730,background}$	0.88	0.88	1.00						
$T_{434,mCP}$	0.49	0.49	0.49	1.00					
$T_{578,mCP}$	0.41	0.40	0.40	0.46	1.00				
$T_{730,mCP}$	0.88	0.88	0.87	0.49	0.41	1.00			
$T_{434,mCPx2}$	0.45	0.45	0.45	0.48	0.62	0.45	1.00		
$T_{578,mCPx2}$	0.13	0.13	0.14	0.20	0.39	0.14	0.37	1.00	
$T_{730,mCPx2}$	0.88	0.88	0.87	0.49	0.40	0.87	0.45	0.14	1.00

The ratio R acquired for the TRIS buffer reference material tested is of 2.4069 with a standard uncertainty of 0.0499 computed as described in Section 2.3.3.

4. Discussion

The results on wavelength accuracy presented in Table 12 showed that a correction to the wavelength is needed. The correction was computed for the respective wavelengths according to the linear relation between wavelength and discrepancy given by Table 12. Corrections are thus of -1.53, +0.02 and +1.65 nm at respectively 434, 578, and 730 nm. This induced a correction on pH_T value of the analysed TRIS buffer of +0.0029. This difference in pH_T is lower than the uncertainty of pH_T. However, this may be larger for more acidic solution where the peak at 434 nm will be larger and for which the correction on that wavelength way induce a larger difference on the absorbance value. If no correction is applied, the uncertainty relative to spectral scale should be increased accordingly.

The ratio R acquired for the TRIS buffer reference material tested gave a value of 2.41 ± 0.05 (k=1). For comparison, without the correlation matrix, the uncertainty is of 0.08, showing the utility of identifying correlations. If only the uncertainty of R (i.e. ± 0.05) is introduced as source of uncertainty in the pH_T model (equation 1.8), it gives a pH_T value of 8.091 ± 0.010 (k=1). This is in the range of uncertainties reported in the literature, being between 0.005 and 0.02 (Carter et al., 2013; DeGrandpre et al., 2014; Loucaides et al., 2017).

However, this level of uncertainty is bigger than the standard uncertainty computed with the top-down approach presented in Chapter II, giving a standard uncertainty of 0.005 and bigger than GOA-ON climate objective (GOA-ON, 2019). This is all the more true considering that other sources of uncertainty arising from the sample, the user, the indicator dye characteristics ($K_2^T e2$, $e1$, and $\frac{e3}{e2}$), the dye impurities and the temperature control weren't taken into account (Figure 27). This later component is expected to have a low impact on the R value as, as an example, a difference of 0.05 °C only impacts the R value by 0.004, being much lower than the standard uncertainty in R. The impact of the dye could be more significant if the dye is not purified.

The main sources of uncertainty in R arise from the transmittance values $T_{434,mCP}$ (33%), $T_{434,background}$ (18%) and $T_{578,mcp*2}$ (16%), being percentage of the variances.

Within $T_{434,mCP}$ and $T_{434,background}$ uncertainty budgets, the uncertainty source that is by far the biggest comes from the bias which is itself highly dependent from the uncertainty attributed to the filter's reference values. Making the calibration with filters of higher precision might help reduce the uncertainty. A numerical test was

performed by attributing to the filters reference values the level of uncertainty achieved by LNE's photonic department for filter calibrations. The ensuing standard uncertainties on R and on pH_T are of 0.04 and 0.008, respectively. Performing the calibration with better-calibrated filters might thus improve the level of uncertainty achieved. Moreover, the fact that part of the uncertainty initially obtained comes from sources that are independent from the pH_T spectrophotometric measurement itself (e.g. filter calibration) is comforting in the possibility to decrease the level of uncertainty.

Finally, the pH_T uncertainty was also computed from the value $R'_{(1st\ dye\ addition)}$ instead of the extrapolated R to zero dye addition (equation 1.9.a). It divided by 2 the standard uncertainty on pH_T, even though the correlation between $R'_{(1st\ dye\ addition)}$ and $R'_{(2nd\ dye\ addition)}$ is integrated in the correlation matrix presented in Table 14. It might thus be interesting to investigate a way of decreasing the uncertainty introduced by the extrapolation method of R from the two dye additions. The correction of R by the extrapolation method results in a difference of 0.01 for the analyzed TRIS buffer, which is significantly lower than the uncertainty of R. Therefore, the relevance of this correction might be questioned. However, a thorough investigation is necessary, particularly for less buffered solutions such as natural seawaters.

It should be noted that the uncertainty budget presented corresponds to LNE's *Agilent Cary 60* spectrophotometer and to the measurement of a TRIS buffer with a pH_T of 8.1 and a salinity of 35. As the uncertainty budget depends on the spectrophotometer performance and the shape of the transmittance spectrum over the wavelength range, the uncertainty should be estimated for each device and type of solution analysed respectively. This means that transmittance uncertainty for the nine values as well as the correlation matrix must be adapted to one's device, measurement procedure and analysed sample.

Moreover, despite the check of the device with optical density, holmium and didymium filters, it is highly recommended to use also a TRIS buffer reference material, which would allow, from its similarity with actual seawater samples, one to check the complete pH_T spectrophotometric measurement method. It must though be noted that TRIS buffers are more sensitive to temperature fluctuations than natural seawater.

5. Conclusion

The spectrophotometric determination of pH_T depends on absorbance measurements, for the seawater sample to be analysed but also for the characterization of the indicator dye. Establishing the uncertainty of pH_T values according to the GUM approach (i.e. bottom-up approach) thus relies on the thorough quantification of the uncertainty associated with absorbance values.

This chapter presented all sources of uncertainty identified as having an influence on the pH_T measurement, the calibration procedure of spectrophotometric devices and the uncertainty quantification of the nine absorbance values involved in the determination of the ratio R, needed for the subsequent determination of the pH_T. The identified correlations between these nine values are represented under a correlation matrix.

This work allowed, for the first time, the uncertainty of R for a TRIS buffer reference material (similar to the one described in Chapter II) to be computed. The standard uncertainty achieved (0.05) leads to a minimum standard uncertainty of 0.010 on the pH_T value. This is bigger than the GOA-ON climate objective ($\pm$ 0.003) but also than the uncertainty budget determined following the top-down approach ($\pm$ 0.005). Calibrating the spectrophotometer with optical filters that have lower uncertainties, as well as studying the uncertainty attributed to the extrapolation of R to zero dye addition, should help to reduce the level of uncertainty achieved.

Other uncertainties need to be quantified in order to achieve a complete uncertainty budget of spectrophotometric pH_T measurement results. These include uncertainties attributable to the characterization of the indicator dye in order to thoroughly quantify uncertainty sources occurring during the characterization process, as mentioned by Fong (2021).

It is crucial to note that this level of uncertainty of pH_T values does not call into question the climatic trends of observed global pH_T decrease of the surface open ocean that result from a large number of studies. Moreover, time series that are assessed on decades allow for the observation of significant trends, with an overall pH_T decrease that exceeds the estimated uncertainties (Tanhua et al., 2015).

References

Allen, D.W., 2007. Holmium Oxide Glass Wavelength Standards. J Res Natl Inst Stand Technol 112, 303–306. https://doi.org/10.6028/jres.112.024

Burke, R.W., Messman, J.D., Smith, M.V., Colbert, J.C., Mavrodineanu, R., Travis, J.C., 1994. Standard Reference Materials:Glass filters as a standard reference material for spectrophotometry - selection, preparation, certification, and use of SRM 930 and SRM 1930. NIST.

Carter, B.R., Radich, A., Doyle, H.L., Dickson, A.G., 2013. An automated system for spectrophotometric seawater pH measurements. Limnology and Oceanography: methods 16–27. https://doi.org/10.4319/lom.2013.11.16

CFM, 2017. Guide d'étalonnage des spectrophotomètres. Afnor EDITIONS.

DeGrandpre, M.D., Spaulding, R.S., et al., 2014. Considerations for the measurement of spectrophotometric pH for ocean acidification and other studies. Limnology and Oceanography: Methods 12, 830–839. https://doi.org/10.4319/lom.2014.12.830

Dubard, J., Voyer, J., Hameury, J., Buteau, F., 2016. Qualification métrologique de spectrophotomètre : un guide pour les industriels. R. franç. métrol. 3–10. https://doi.org/10.1051/rfm/2016001

Fong, M.B., 2021. Uncertainty of spectrophotometric pH measurements in seawater and implications for ocean carbon chemistry. PhD Dissertation. UC San Diego.

GOA-ON, 2019. Global Ocean Acidification Observing Network (GOA-ON): Implementation Strategy.

JCGM 100:2008, 2008. Evaluation of Measurement Data-Guide to the Expression of Uncertainty in Measurement.

Liliana, L., 2016. A new model of Ishikawa diagram for quality assessment. IOP Conf. Ser.: Mater. Sci. Eng. 161, 012099. https://doi.org/10.1088/1757-899X/161/1/012099

Liu, X., Patsavas, M.C., Byrne, R.H., 2011. Purification and Characterization of meta-Cresol Purple for Spectrophotometric Seawater pH Measurements. Environmental science & Technology 4862–4868.

Loucaides, S., Rèrolle, V.M.C., Papadimitriou, S., Kennedy, H., Mowlem, M.C., Dickson, A.G., Gledhill, M., Achterberg, E.P., 2017. Characterization of meta-Cresol Purple for spectrophotometric pH measurements in saline and hypersaline media at sub-zero temperatures. Sci Rep 7, 2481. https://doi.org/10.1038/s41598-017-02624-0

Tanhua, T., Orr, J.C., Lorenzoni, L., Hansson, L., 2015. Monitoring Ocean Carbon and Ocean Acidification. WMO Bulletin 64.

Vega, G.A., Cubillos, S.D., Ruiz, J., Nunez, A., 2016. Neutral density filters calibration for spectrophotometric laboratories/Calibracion de filtros de densidad neutra para laboratorios espectrofotometricos. Visión electrónica 10, 157–170.

Part II: Development of metrological tools for the measurement of total alkalinity in seawater

Chapter V: A pilot study and uncertainty budgets toward a better route of traceability for Total Alkalinity measurements in seawater

Total alkalinity of seawater (TA) represents the excess of proton acceptors over proton donors and can be described in a simplified manner as the buffer capacity of seawater. Highly alkaline waters are indeed more likely to mitigate ocean acidification resulting from the absorption of anthropogenic carbon dioxide by seawater. The exact definition of the total alkalinity measurand is detailed in Chapter I, Section 4.1, whose representation in terms of ionic chemical model is given again here (equation 1.11).

$$\begin{aligned} TA = {} & [HCO_3^-] + 2[CO_3^{2-}] + [B(OH)_4^-] + [OH^-] + [HPO_4^{2-}] \\ & + 2[PO_4^{3-}] + [SiO(OH)_3^-] + [NH_3] + [HS^-] + [\dots] - [H^+]_F - \\ & [HSO_4^-] - [HF] - [H_3PO_4] - [\dots] \end{aligned} \quad (1.11)$$

where brackets represent amount contents (mol/kg-sol) and ellipses corresponds to minor species.

Total alkalinity is an essential variable contributing to the monitoring of changes in the ocean carbon cycle and of ocean acidification, that can be used together with pH_T, Dissolved Inorganic Carbon (DIC) or partial pressure of CO_2 (pCO_2) to compute other variables of the ocean carbonate system. Moreover, total alkalinity is a relatively simple variable to monitor thanks to the fact that (1) it is independent from temperature and pressure, unlike pH_T and pCO_2, and (2) it isn't affected by the absorption of CO_2, unlike DIC, that could come for example from the exposure of the sample to air.

The desire to monitor total alkalinity of seawater has increased in the recent years with the development of the marine Carbon Dioxide Removal technique called Ocean Alkalinity Enhancement (Ho et al., 2023; Iglesias-Rodríguez et al., 2023).

Having a sufficient data quality of total alkalinity measurement results is thus of great importance. The Global Ocean Acidification Observing Network and the World Meteorological Organization have fixed a data quality objective corresponding to a standard uncertainty in total alkalinity measurement results being of 1 and 2 µmol/kg, respectively (GOA-ON, 2019; WMO et al., 2022). These values were chosen in order to highlight climatic variations of total alkalinity relevant to the monitoring of ocean acidification.

Contributing to the objective of achieving comparable TA measurement results, the Scripps Institution of Oceanography currently distributes reference materials constituted of a stabilized natural seawater (Dickson, 2010). These materials are carefully characterized in terms of total alkalinity using the open-cell multi-step potentiometric titration method, whose accuracy has been validated with synthetic solutions constituted of bases such as sodium carbonate, borate or TRIS (Dickson *et al.,* 2003). The reference material distributed isn't however currently made available with an uncertainty budget associated to the assigned value.

The first aim of the work presented in this chapter was thus to develop a reference material produced following the international standards appropriate to the production

of reference materials ('ISO 17034', 2016; ISO Guide 35:2018, 2018). This material is made of artificial seawater with a total alkalinity reference value attributed from knowledge of the composition. The uncertainty budget associated to the reference value is determined following the Guide to the expression of Uncertainty in Measurement (GUM, 'JCGM 100:2008', 2008) and integrates information about stability and homogeneity of the material.

This developed reference material has been tested in an inter-laboratory comparison conducted with five French laboratories conducting TA measurements with the standardized method, being the multi-step potentiometric titration method, that can be performed either in an open or closed cell. Measurements were also performed on a second material, produced similarly to the one from Scripps, being a stabilized natural seawater from the Mediterranean Sea. The second aim of the work presented was, from the inter-laboratory comparison, to study the applicability in quality control for total alkalinity measurements of the artificial and natural solutions developed as reference materials.

The third objective of the work presented was to thoroughly establish the uncertainty budget of a standardized measurement method, which is up to date lacking. This chapter thus presents for the first time an uncertainty estimation for the open-cell multi-step potentiometric titration method together with Gran's data treatment, established following the GUM (i.e. bottom-up approach). A comparison with the uncertainty budget obtained from the inter-laboratory comparison results (i.e. top-down approach) is also presented.

Finally, a traceability route, involving the two reference materials developed is presented and discussed. Suggestions for the establishment of the traceability of total alkalinity measurement results to the SI units are given.

1. Materials and methods

2.1. Instrumentation for total alkalinity measurements performed at LNE

The measurement of total alkalinity was performed following the method described in Chapter I, Section 4.2, using the titration system and the 888 Titrando electroburette from *Methrom*, associated with the 801 Stirrer agitation system. A thermostated glass cell with a capacity of 50-150mL was used. The volume of the samples analysed was of 100 mL. This cell was connected to a *LAUDA* Eco Gold bath to control the temperature of the cell. The setpoint was fixed in order to obtain a temperature of 25 ± 0.2°C in the cell. The temperature was maintained stable, i.e. the temperature acquired during the whole titration had a standard deviation within 0.05°C. The potential measurement was carried out with a *Metrohm Ecotrode Plus* glass electrode (ref: 6.0262.100) and the

temperature with the *Metrohm* temperature probe (ref: 6.1110.100). The data acquisition software used was Tiamo 2.4.

The air flow for CO_2 degassing was obtained from a compressed air tank connected to an inlet system in the cell.

Figure 28 illustrates the description of the setup.

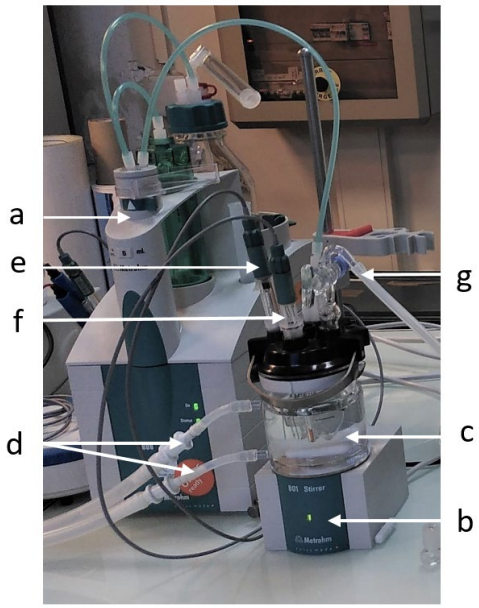

Figure 28: Description of the total alkalinity measurement setup. With a) Burette and titration system, b) Magnetic stirrer, c) Thermostated cell, d) Tubing connected to the water bath, e) Glass electrode, f) Temperature probe, and g) Air inlet for degassing.

The hydrochloric acid used was a Standard Reference Material (SRM) at 1 mol/kg-sol prepared and characterized by coulometry at the Slovenský Metrologický Ústav (Slovak Institute of Metrology, SMU). It was diluted by mass to 0.1 mol/kg-sol before its use as acid titrant; it wasn't prepared in an NaCl matrix. The density of the titrant solution was measured with a DMA 4500M *Anton Paar* densimeter.

The mass of the analyzed sample was weighed on a calibrated 2kg balance with a resolution of 0.1 mg.

The data treatment was performed as described in section Chapter I, Section 4.2, with an R routine written based on the function "alkalinity" of the package seacarb (Gattuso et al., 2021).

The glass electrode was calibrated with a TRIS buffer prepared and characterized with the Harned cell measurement method at LNE. Its linearity over a range of pH was checked with NBS buffers of pH 4, 7 and 12.

The electroburette and the temperature probe are calibrated once a year.

The accuracy of the method was controlled either with a reference material purchased from Scripps or with a synthetic solution prepared gravimetrically at LNE.

2.2. Development of reference materials

Two reference materials have been developed for the quality control of seawater total alkalinity measurement methods: a stabilized natural seawater and an artificial seawater. This section details the methods applied for the preparation, characterization, stability and homogeneity studies, as well as for the uncertainty quantification of the reference TA value assigned to the artificial solution.

2.2.1. Preparation

Stabilized natural seawater

The natural seawater was collected by the Mediterranean Institute of Oceanography (MIO) during an oceanographic field trip to the Antares station (42°48 N 6°10 E) of the Mediterranean Ocean Observation System for the Environment (MOOSE; Lefevre, 2010). Deep waters of respectively 2000, 1750, 1500 and 1000 meters depth were collected in two plastic containers and homogenized, for a total of 35 litters of seawater. The containers were stored protected from light at 4°C until filtration. 25 litters of the collected seawater were filtered with a 0.2 µm *Sartobran* filter using a *Masterflex* peristaltic pump, and gathered from the two containers to one unique container in Nalgene (polycarbonate). 10 ml of a solution of mercuric chloride at 36 g/l were added to the seawater in the Nalgene container. The container was stirred to ensure homogeneity of the seawater. The natural seawater was then bottled in 42 ground-neck borosilicate bottles of 500 ml sealed with greased glass stoppers held on with elastic bands.

Artificial seawater

The composition of the artificial seawater was chosen in order to have a total alkalinity of 2500 µmol/kg-sol, known based on gravimetric information, and with salinity and pH_T values that match those of a natural seawater. To respond to these criteria, the artificial seawater is composed of sodium bicarbonate ($NaHCO_3$), sodium carbonate (Na_2CO_3) and is made in a NaCl matrix. The ratio of $NaHCO_3$ over Na_2CO_3 amount contents to obtain a pH_T close to 8.1 was estimated based on Bjerrum plot of carbonate species and their dissociation constant in a saline media (Wolf-Gladrow et al., 2007). The composition of the artificial solution is given in Table 15.

Table 15: Composition and information about ionic strength (I), absolute salinity and theoretical pH of the artificial solution for total alkalinity reference material

	ν (mol/ kg-sol)	*b* (mol/ kg-H_2O)
$NaHCO_3$ (*Merck, 100.039 %*)	0.0022746	0.0023578
Na_2CO_3 (*Merck, 99.948 %*)	0.0001127	0.0001168
NaCl (*VWR chemicals, 99.945 %)*	0.6000000	0.6219348
I	0.625	
Absolute salinity	35	
Theoretical pH	8.1	

where ν is the amount content, expressed in mol/kg-sol, *b* is the molality, expressed in mol/kg-H_2O and I is the ionic strength. The suppliers of the salts and their purity are given in brackets.

The artificial solution was prepared from respective stock solutions of $NaHCO_3$ and Na_2CO_3. The purity of the sodium carbonate and sodium bicarbonate salts used were characterized in terms of purity as bases expressed as sodium carbonate by coulometric analysis performed at the National Metrology Institute of Japan (NMIJ), while the purity of the sodium chloride was characterized by coulometric analysis at the Slovack Metrology Institute (SMU) based on chloride content. The sodium carbonate salt was dried at 280°C for 4 hours and cooled down in a desiccator for 1h before use, to remove potential humidity. This procedure wasn't applied to sodium bicarbonate salt due to the decomposition reaction caused by heat. The same pre-treatment of the salts was applied before characterization at NMIJ and before stock solution preparation at LNE, ensuring that the purity obtained by coulometric analysis is suitable for the solution preparation.

Two batches of artificial seawater solution of respectively 12 and 7 kg were prepared. The first batch (Batch 1) was bottled in equivalent bottles to the one used for the natural seawater (i.e. ground-neck borosilicate bottles of 500 ml sealed with greased glass stoppers maintained with elastic bands). While the second batch (Batch 2) is bottled in *SCHOTT* borosilicate bottles of 500 ml with screw caps containing PTFE coated seals.

The stabilized natural seawater and Batch 1 of the artificial solution were distributed to be studied in the inter-laboratory comparison described in section 2.3. The Batch 2 of the artificial seawater was analysed at LNE, with the objective of comparing the stability of the material for the two methods of bottling.

2.2.2. Characterization

The artificial seawater was characterized in terms of total alkalinity based on gravimetric information. Given the composition of Table 15 and the total alkalinity definition (equation 1.11), the alkalinity introduced in the artificial solution is supposed to only come from carbonate and bicarbonate ions, as described by equation 4.1.

$$TA = 2\,\nu_{Na_2CO_3} + \nu_{NaHCO_3} \tag{4.1}$$

where ν represents amount contents (mol/kg-sol).

However, the impurities contained in the NaCl salt (0.055%) can also contribute to the total alkalinity of the solution. This source of alkalinity is hereafter called background alkalinity (noted $TA_{background}$, expressed in mol/kg-sol).

The final total alkalinity of the artificial solution was thus obtained from equation 4.2.

$$TA = 2\,\nu_{Na_2CO_3} + \nu_{NaHCO_3} + TA_{background} \tag{4.2}$$

The background alkalinity was quantified based on the preparation of four solutions with the same amount contents of bicarbonate and carbonate ions while varying the NaCl amount content from 0 to 3 mol/kg-sol (solutions in NaCl matrix of respectively 0, 1, 2 and 3 mol/kg-sol). The total alkalinity of each of the four solutions was determined at LNE from, respectively, the mean of at least three repeatability measurements made using the open-cell multi-step potentiometric titration method, as described in Chapter I, Section 4.2, and using the material described in Section 2.1. The difference of total alkalinity between the measured one and the theoretical value calculated with equation 4.1, was represented in function of the amount content of NaCl for each NaCl amount content present in the four solutions. From this representation was computed a linear regression passing through the origin. The linear regression was forced to pass through the origin as the background alkalinity coming from NaCl impurities is theoretically zero for a solution without NaCl matrix. The measurement results shown in Figure 29 support this theory. The linear relation obtained allowed the determination of the background alkalinity for the solution studied (i.e. for a NaCl amount content of 0.6 mol/kg-sol, Table 15). This is further discussed in section 3.1.1.

Batch 1 of the artificial reference material and the stabilized natural seawater were characterized in terms of practical salinity aboard the *Thalassa* oceanographic vessel during the 2023 PIRATA cruise (Bourles et al., 2023; Llido, 2023), using an *OSIL Portasal 8410A* salinometer.

The natural seawater was also characterized in terms of dissolved nutrients (i.e. silicates, nitrites, phosphates and nitrates) based on colorimetric determination using

a *SEAL AutoAnalyzer 3 HR* at the platform of Analysis of Basic Parameters (PAPB) of the MIO.

2.2.3. Stability and homogeneity studies

Homogeneity

Homogeneity estimations were based on TA measurements carried out at LNE, MIO and at the French National Service for Analysis of Oceanic CO_2 Parameters (SNAPO-CO_2) following the standardized multi-step potentiometric titration method. The compatibility of the measurements performed by these three institutes have first been established.

The homogeneity assessment integrates two components: (1) the between-bottle homogeneity, taking into account standard deviation between different bottles of a same batch, and (2) within-bottle homogeneity, taking into account standard deviation within one bottle.

Between-bottle homogeneity of the stabilized natural seawater and of Batch 1 of the artificial seawater was computed from standard deviation of single measurements made consecutively on three bottles of the same batch. It was conducted with the closed-cell multi-step potentiometric titration method at the SNAPO-CO_2.

The between-bottle homogeneity of the Batch 2 of the artificial seawater was obtained from the standard deviation of the mean TA values of three different bottles, themselves computed from at least three repeatability measurements. These measurements were made at LNE, using the open-cell multi-step potentiometric titration method.

The within-bottle homogeneity was computed, for the stabilized natural seawater and Batch 1 of the artificial seawater, from the mean of the standard deviations obtained at LNE and MIO, from, respectively, three repeatability measurements made in one bottle. The within-bottle homogeneity of the Batch 2 of the artificial seawater was obtained from the mean of the standard deviations obtained from repeatability measurements of the same three bottles used for between-bottle homogeneity assessment.

Stability

The stability of the stabilized natural seawater and Batch 1 of the artificial reference material, both bottled in ground-neck bottles, were followed by each participant to the inter-laboratory comparison over one year, with total alkalinity measurements performed every three months. For the results obtained at each deadline, Grubb's and Cochran's tests were applied to remove eventual outliers and the median of the remaining values are taken to establish the stability over time. The stability over time

of the Batch 2 of the artificial seawater, bottled in glass bottles with screw caps, was followed at LNE on the same schedule.

The stability was established with a statistical Student test (or t test) highlighting whether there is a significant trend in the evolution of the material or not ("ISO Guide 35", 2018, also described in Chapter II, Section 2.5).

Stability to transport was described as the discrepancy between measurements results obtained at LNE and MIO, LNE being the source laboratory of the artificial reference material and MIO the source of the natural seawater reference material. It isn't computed for the second batch of artificial solution in screw cap bottles that was only tested at LNE.

Dissolved nutrients of the stabilized natural seawater and of Batch 1 of the artificial seawater were also analysed at the end of the stability study to highlight an eventual evolution.

2.2.4. Uncertainty estimation of the artificial reference material value

The uncertainty associated to the total alkalinity reference value of the artificial solution was obtained based on the ISO Guide 35 (2018) and takes into account the uncertainties coming from the preparation and the characterization u_{charac}, the homogeneity u_{hom} and the stability u_{stab} (equation 4.3).

$$u_{MR} = \sqrt{u_{charac}^2 + u_{hom}^2 + u_{stability}^2} \quad (4.3)$$

Preparation and characterization uncertainty

The uncertainty coming from the preparation and characterization was estimated based on equation 4.2 following the law of uncertainty propagation of the Guide to the expression of Uncertainty in Measurement ("JCGM 100:2008," 2008). The evaluation of the uncertainties of the different terms in equation 4.2 requires several steps of uncertainty determination.

(1) The uncertainty of the amount contents of the stock solutions of $NaHCO_3$ and Na_2CO_3 (ν_{stock}) were determined using uncertainty propagation for the following equation (4.4).

$$\nu_{stock} = \frac{m_{salt} * p * 1000}{(m_{salt} + m_{H2O}) * M_{salt}} \quad (4.4)$$

where m_{salt} is the mass of salt of either $NaHCO_3$ or Na_2CO_3 salts (g), m_{H2O} the mass of water (g), p the purity of the salt and M_{salt} the molar mass of the salt.

The uncertainties on the masses were obtained from the weighing scales calibration, the uncertainty of the purity was known from NMIJ coulometric characterization

certificate and uncertainties on the molar masses were taken from IUPAC (Meija et al., 2016).

(2) The uncertainty of the amount content of $NaHCO_3$ and Na_2CO_3 in the artificial reference material ($v_{salt_{RM}}$) was determined using the law of uncertainty propagation for equation 4.5.

$$v_{salt_{RM}} = \frac{m_{salt^*} v_{stock}}{m_{total}} \quad (4.5)$$

where m_{total} is the total mass of the reference material ($m_{NaHCO3} + m_{Na2CO3} + m_{NaCl} + m_{H2O}$), in g.

The quantification of the uncertainties of masses and v_{stock} are detailed above.

(3) The uncertainty associated with the background alkalinity coming from the NaCl matrix also needs to be quantified. The amount content of NaCl introduced in the reference material solution and in each of the four solutions at different NaCl amount contents used to determine the background TA was obtained with equation 4.6, whose term's uncertainties quantification is detailed in the steps above.

$$v_{NaCl} = \frac{m_{NaCl}*1000}{m_{total}* M_{NaCl}} \quad (4.6)$$

The difference between measured and theoretical total alkalinity $\Delta(TA_{measured} - TA_{theoretical})$ was represented as a function of the amount content of the NaCl of the solutions used to study the background alkalinity, being respectively, 0, 1, 2 and 3 mol/kg-sol. The uncertainty estimate chosen to be attributed to the measured TA, pending a thorough assessment, was 2 µmol/kg. Indeed, it is the order of precision reported to be achievable in the literature for TA measurements. Systematic uncertainty sources, as the ones coming from the device, the operator or the procedure are here cancelled. The uncertainty is thus expected to be relatively low. The uncertainty of the theoretical total alkalinity was obtained using the law of uncertainty propagation in equation 4.1, whose term's uncertainties quantification are detailed in step (2) above.

The slope b_b giving the evolution of $\Delta(TA_{measured} - TA_{theoretical})$ in function of v_{NaCl} was obtained by linear regression passing through the origin.

The uncertainty associated to this slope was obtained using the LNE-RegPoly software. LNE-RegPoly estimates a polynomial of degree k as $y = b_a + b_b x + b_c x^2 + ... + b_k x^k$ using n pairs of points (xi, yi), taking into account the uncertainties associated with these points. It then propagates the uncertainties from the points to the coefficients of the polynomial. A second uncertainty component was added to this uncertainty to take into account for the fact that the regression is forced to pass through the origin. Indeed, the residuals were thus slightly bigger. To do so, the standard deviations of slopes (i) with regular linear regression and (ii) forced to pass through the origin, were computed from knowledge of the residuals of the regressions. The difference of the standard

deviations of regressions (i) and (ii) was added as an uncertainty component of the slope b_b.

A second approach based on weighted orthogonal distance regression was applied with help of statisticians to compute the uncertainty of the slope b_b (Boggs et al., 1992). This approach yielded a slightly lower uncertainty. To maximise the uncertainty of the slope, the first approach, described above, was adopted.

Knowing the uncertainties of, respectively, the slope b_b and the amount content of NaCl in the reference material solution ($\nu_{NaCl_{RM}}$), the uncertainty on the background total alkalinity is obtained by propagation in equation 4.7.

$$TA_{background} = b_b * \nu_{NaCl_{RM}} \quad (4.7)$$

(4) The final step is to propagate the uncertainties quantified in steps (2) and (3) in the equation 4.2, giving the total alkalinity of the reference material.

Homogeneity uncertainty

The within and between bottles homogeneities were assessed from the homogeneity study described in Section 2.2.3. This study highlighted that the determination of the homogeneity is highly dependent on the variability of the measurement method. It was chosen to neglect the within-bottle homogeneity component, supposed to be negligible, in the homogeneity uncertainty quantification. The uncertainty relative to homogeneity was obtained, based on between-bottle homogeneity assessment, as detailed in Chapter II, Section 2.6.2 and from equation 2.11, reintroduced below. It is computed for each batch respectively.

$$u_{hom} = \frac{s^2}{N} \quad (2.11)$$

where s^2 is the standard deviation between the mean TA values measured for each bottle considered in the homogeneity study and N the number of bottles analysed (i.e. 3 bottles for each batch).

Stability uncertainty

The uncertainty on the stability is presented in Chapter II, Section 2.6.3. It is obtained from equation 2.12 if no significant trend is established by the t tests described in Section 2.2.3, and by equation 2.13 if a significant trend is established. These equations are reintroduced below.

$$u_{stab} = s_{b1} \cdot t \quad (2.12)$$

$$u_{stab} = \sqrt{(\frac{b1 \cdot \frac{t}{2}}{\sqrt{3}})^2 + (s_{b1} \cdot t)^2} \quad (2.13)$$

where b_1 corresponds to the slope of the evolution over time, s_{b1} corresponds to the slope standard deviation and t to the time.

The assessment of stability to transport showed no significant discrepancy between the source and recipient laboratory, this source of uncertainty was thus neglected in the uncertainty budget.

2.3. Inter-laboratory comparison

2.3.1. Protocol of the inter-laboratory comparison

The inter-laboratory comparison (ILC) was conducted with five French laboratories conducting seawater total alkalinity measurements with the standardized measurement method, being the multi-step potentiometric measurement method (Dickson *et al.,* 2007 - SOP 3a & 3b).

Table 16 gathers information about the participants to the ILC, including affiliation and measurement methods.

Table 16: Information concerning the participants to the inter-laboratory comparison

Participants	City	TA measurement method
LNE	Paris	open-cell multi-step potentiometric titration
MIO	Marseille	open-cell multi-step potentiometric titration
SNAPO-CO_2	Paris	closed-cell multi-step potentiometric titration
IMAGO	Brest	open-cell multi-step potentiometric titration
LOV	Villefranche sur Mer	open-cell multi-step potentiometric titration

The total alkalinity measurements were performed by each participant on the two reference materials developed: the stabilized natural seawater, and the artificial seawater of known TA. The measurements were performed 2 months after the preparation of the artificial seawater, 3.5 months after sampling for the natural seawater, and all the participants completed their measurements within a 2 weeks period. Each participants performed three repeatability measurements, within one bottle for LNE, MIO, IMAGO and LOV, and using three bottles for SNAPO-CO_2 as

the closed-cell measurement method requires a larger volume of sample (around 500 ml).

The amount content of the hydrochloric acid used by MIO, SNAPO-CO_2, IMAGO and LOV was calibrated based on the analyses of a total alkalinity reference material purchased from Scripps Institution of Oceanography. LNE's hydrochloric acid was a Standard Reference Material purchased from SMU (Slovack metrology intitute, $\nu = 1$ mol/kg-sol) diluted gravimetrically.

As the artificial reference material didn't contain sulphate and fluoride ions, the data treatment applied was Gran's regression method. However, for the natural seawater samples, a correction computed from the nonlinear least-squares regression method was applied to take into account for the matrix (Chapter I, equation 1.18).

Participants also made spectrophotometric pH_T measurements on the samples following the methodology described in Dickson *et al.* (2007), similar to the method described in Chapter I, Section 3.2. To normalize every pH_T results to 25°C, the "pHinsi" function of the seacarb package (Gattuso et al., 2021) was used for the natural seawater. For the artificial seawater, a pH_T spectrophotometric analysis was performed at three temperatures between 24°C and 26°C in order to compute a relation between pH_T and measurement temperature. This relation was used to normalize pH_T values of the artificial solution to 25°C. Although the mCP parameters aren't adapted to the artificial solution that is mainly constituted of NaCl, it still provides an information on the homogeneity and stability of the solution in pH.

In addition, the SNAPO-CO_2 used the titration data from the closed-cell multi-step potentiometric titration to compute dissolved inorganic carbon values for the stabilized natural seawater reference material.

2.3.2. Treatment of the inter-laboratory comparison results

The median value of each sample analysed was obtained from means of the replicate values obtained by each of the five participants, the uncertainty associated to the median was calculated with the method given in Muller (2000).

The Cochran's and Grubbs' statistical tests were used to identify eventual isolated values or outliers due to, respectively, intra-laboratories variances and discrepancy to the mean observation. These values were removed from the ILC results treatment used to quantify trueness and precision of the method. The bias between the mean obtained on the artificial seawater and the reference value obtained with equation 4.2, gives information on the trueness of the measurement method. The precision was computed from the combination of intra- and inter-laboratory variances obtained for the two materials.

As all participants realised measurements on the two different solutions developed, the ILC results were presented under a Youden plot (Youden, 1959; 'ISO 13528', 2022,). The methodology of the Youden plot is as follows:

- The results of each participant is represented on a graph by a single point (Xi, Yi), representing its mean TA value obtained on the natural seawater in the x-axis (Xi) and its mean TA value of the artificial seawater in the y-axis (Yi).
- The medians obtained on the two samples are drawn as the centroid (X,Y). Vertical and horizontal lines are drawn from that centroid, representing x-axis and y-axis medians (i.e. natural seawater and artificial seawater median values, respectively).
- A 45° line passing through the centroid (X,Y) is then drawn.
- A 95% confidence circle is finally represented from the centroid with a radius, r, calculated with equation 4.8.

$$r = \sqrt{\frac{\sum_i^p ((X_i - Y_i) - \overline{(X_i - Y_i)})^2}{2*(p-1)}} * 2.448 \quad (4.8)$$

where $\overline{(X_i - Y_i)}$ represents the mean difference (Xi – Yi), p is the number of participants and 2.448 is the factor allowing to obtain a circle with a 95% confidence level (Youden, 1959).

Each participants having a data point (Xi, Yi) outside of the confidence circle is considered as having biased results. The shortest distance of (Xi, Yi) to the 45° line is proportional to random errors for the concerned laboratory, while the distance between that point on the 45° line to the centroid is proportional to systematic errors (Martín et al., 2017).

2.4. Uncertainty estimation of the total alkalinity measurements results

2.4.1. Top-down approach

The uncertainty of the total alkalinity measurement results was established using the top-down approach (i.e. using experimental data from the inter-laboratory comparison exercise), following the ISO standard 21748 "Guidance for the use of repeatability, reproducibility and trueness estimates in measurement uncertainty evaluation" (2017). The uncertainty budget was calculated following the method detailed in Chapter I, Section 2.5, using equations 1.2 and 1.3. These equations are reintroduced below.

As the uncertainty estimates requires information about trueness of the method, only the measurement results carried out on the artificial seawater, having a characterized reference value, can be used. Thus, the final uncertainty budget can be attributed to the results obtained with the multi-step potentiometric titration method using the Gran's data treatment. Uncertainties coming from the nonlinear least-squares regression data treatment are not included in the budget.

$$u^2(y) = s_L^2 + s_r^2 + u^2(\hat{\delta}) \quad (1.2)$$

where $u(y)$ is the estimated measurement result uncertainty, s_L the inter-laboratory standard deviation, s_r the intra-laboratory standard deviation divided by the square root of the mean number of replicates, and $u(\hat{\delta})$ the uncertainty associated to the estimated bias of the measurement method (equation 1.3).

$$u^2(\hat{\delta}) = \frac{(s_L^2 + s_r^2) - \left(1 - \frac{1}{n}\right)s_r^2}{p} + u^2(\hat{\mu}) \quad (1.3)$$

where n is the number of replicates in each laboratory, p the number of laboratories and $u(\hat{\mu})$ the standard uncertainty of the certified reference value.

2.4.2. Bottom-up approach

The bottom-up approach for the establishment of the uncertainty budget of the total alkalinity measurement results is hereafter detailed for the open-cell multi-step potentiometric titration method applied at LNE and Gran's data treatment, following the Guide to Uncertainty in Measurement ("JCGM 100:2008," 2008).

The bottom-up approach is detailed in Chapter I, Section 2.5 and involves several steps: the establishment of the measurement model, the uncertainty quantification of the input variables, the identification of eventual covariances, the propagation of the uncertainty through the established model and the final expression of the results.

Establishment of the measurement model

The measurement model is established from the measurement and Gran's data treatment methods presented in Chapter I, Section 4.2 and is represented by equations 4.9 and 4.10.

$$F1 = (m_{init} + m_{HCl}) \times \exp\left(\frac{E}{\frac{RT}{F}}\right) \quad (4.9)$$

where m_{init} is the weight of sample analysed (g), m_{HCl} the weight of HCl delivered (g), E the potential acquired by the glass electrode (mV), R the universal gas constant (J/mol.K), T the temperature of the sample (K) and F the Faraday constant (C/mol).

$$AT = \frac{-b}{a}\frac{v_{HCl}}{m_{init}} \quad (4.10)$$

where coefficients a and b represent, respectively, the slope and the intercept of the linear regression $F1 = a * m_{HCl} + b$ and v_{HCl} is the amount content of titrant HCl (mol/kg-sol).

Coefficients a and b in equation 4.10, are obtained from data points acquired during the second stage titration, representing F1 (equation 4.9) as a function of the weight of HCl added (m_{HCl}).

Identification and uncertainty quantification of input variables

Table 17 gathers all the input variables identified in the measurement model presented above. It presents also the sub-sources of uncertainty influencing these input variables and the method allowing their uncertainty quantification. The sub-sources identification together with their uncertainty quantification methods are based on the procedure conducted at LNE and instrumentation available there.

Table 17: Identification and uncertainty quantification method of the input variables involved in the measurement model of the open-cell multi-step potentiometric titration method conducted at LNE.

Input variables	Definition	Unit	Sub-sources of uncertainty	Sub-sources uncertainty quantification method
m_{HCl}	Mass of HCl delivered during the titration	g	-HCl density : Densimeter and temperature of the acid accuracies (g/cm3 and °C, respectively)	-Densimeter specification -Temperature probe calibration certificate
			-Volume delivered: burette accuracy (ml)	-Tolerance/√3
m_{init}	Mass of sample analysed	g		-Weighing scale calibration certificate
E	Potential measured by the glass electrode	mV	-Tolerance of the electrode	-Tolerance/√3
			-Repeatability	-standard deviation from experimental data
T	Temperature of the sample during the titration	°C	-Resolution	-Probe specification
			-Repeatability	- standard deviation from experimental data
			-Trueness	-Calibration with a certified temperature probe
R	Universal gas constant	J/mol.K		(Pratt, 2014)
F	Faraday constant	C/mol		(Pratt, 2014)
ν_{HCl}	Amount content of the acid titrant	mol/kg-sol	-Stock solution (HCl 1 mol/kg-sol) amount content	-SMU certificate
			-Gravimetric dilution	-Calibration certificate
a and b	Gran's regression coefficients		-m_{HCl}	-As for m_{HCl} above
			-F1	-Law of uncertainty propagation in equation 4.9
			-Gran's regression method	-LNE-RegPoly

Uncertainty propagation and expression of the results

The final uncertainty on TA results was obtained using the law of uncertainty propagation in equation 4.10. The utilisation of the software LNE-RegPoly for the quantification of the uncertainties of coefficients a and b coming from the linear regression of F1 in function m_{HCl} allowed demonstrating that these two terms are highly correlated. The factor of correlation between a and b, quantified by the software, was integrated in a correlation matrix introduced in the process of uncertainty propagation using partial derivatives.

The final uncertainty is expressed as expanded uncertainty using a coverage factor, k, of 2.

2. Results

3.1. Production of reference materials

3.1.1. Characterization

Two reference materials have been produced, an artificial seawater (2 batches) and a stabilized natural seawater. Table 18 presents the characteristics of these two reference materials, established following the methods described in section 2.2.2.

Table 18: Characteristics of the produced reference materials for total alkalinity measurements

Artificial solution		
	Batch 1 (Ground neck bottles)	Batch 2 (Screw caps bottles)
Absolute salinity[a]	35.189	35.184
Ionic strength	0.623	0.623
Reference Total Alkalinity value (µmol/kg)	2503.64	2503.78
pH_T	8.221 (0.016)[c]	8.188 (0.001)[d]

Stabilized natural seawater		
Practical salinity[b]		38.533
Dissolved nutrients (µmol/l)	Silicates	12.37
	Nitrites	0.02
	Phosphate	0.40
	Nitrates & nitrites	9.08
pH_T		7.800 (0.012)[c]

[a] The absolute salinity was calculated based on the composition of the solution (g of dissolved salts per kg of solution).

[b] The practical salinity was measured with a salinometer and is based on a conductivity ratio.

[c] The pH_T value given is the mean of the values obtained by LNE, MIO and LOV from, respectively, at least three repeatability spectrophotometric measurements performed while conducting the inter-laboratory comparison. Standard deviation are given in brackets.

[d] The pH_T value given is the mean of three repeatability spectrophotometric measurements made at LNE, with standard deviation given in brackets.

Reference values of total alkalinity for the two batches of artificial reference materials are computed from equation 4.2, giving values of respectively 2503.64 and 2503.78 µmol/kg. These values seem to indicate the reproducibility of the batches preparation. The background alkalinity has been quantified, following the method described in section 2.2.2, to be 3.53 µmol/kg for both batches, and is included in the reference values given above. Figure 29 represents the results of the quantification of the background alkalinity.

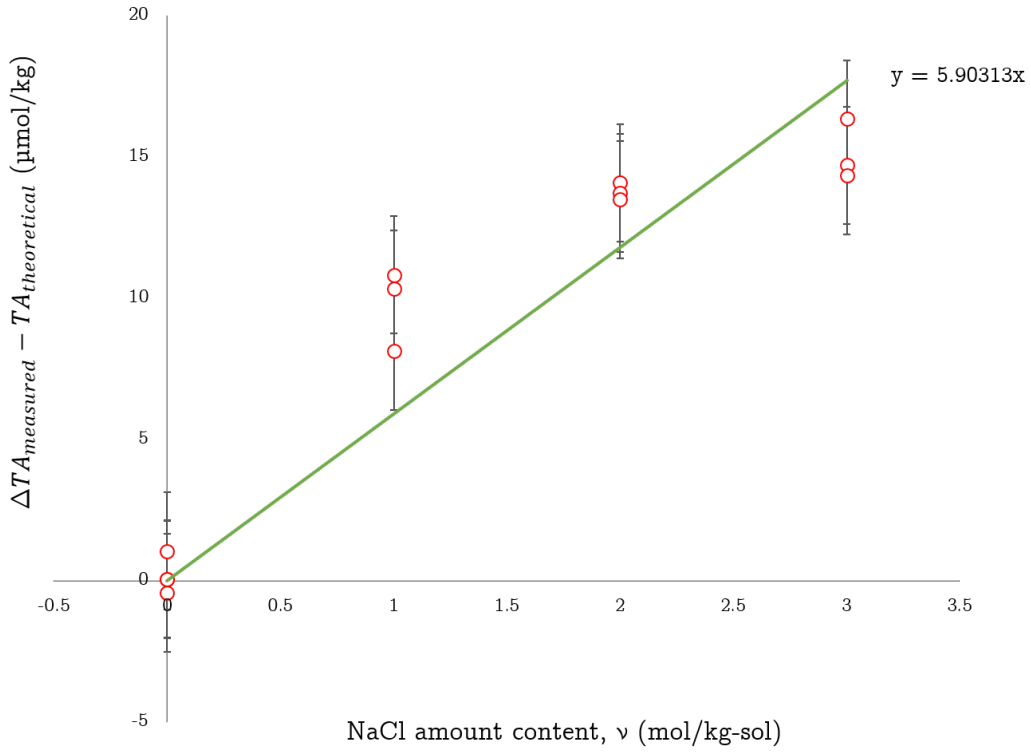

Figure 29: Quantification of background alkalinity coming from the NaCl matrix for the artificial reference material. Where red circles represent single TA potentiometric measurements with error bars representing their standard uncertainty, and green straight line represents the slope obtained from linear regression passing through the origin.

3.1.2. Homogeneity, stability studies and uncertainty quantification

Table 19 presents the results of the homogeneity and stability assessments established as described in the section 2.2.3.

Table 19: Results obtained from the homogeneity and stability assessments of the reference materials developed. Numerical values are expressed in µmol/kg.

	Artificial solution		Stabilized natural seawater
	Batch 1 (Ground neck bottles)	Batch 2 (Screw caps bottles)	
Homogeneity			
Between-bottle	1.0820	0.9915	1.6100
Within-bottle	1.3505	1.2859	1.6618
Stability over time			
Slope (b1)	0.8065	0.9325	0.2219
Slope standard deviation (Sb1)	0.2735	0.1341	0.4366
t0 (b1 / Sb1)	2.9485	6.9528	0.5081
tα (Student n-2)	4.3027	3.1824	3.1824
Stability to transport	1.2052	/	1.1781

The between and within bottles standard deviations are in the range 1.0 – 1.7 µmol/kg, and seems to be slightly greater for the natural seawater than for the artificial solutions.

Assessments of stability over time show a significant trend ($t0 > t\alpha$) only for Batch 2 of the artificial reference material. Its stability has been studied up to fourteen months after the preparation, however, the significant trend, and thus instability of the material, was already established after eleven months. The stability study of the stabilized natural seawater and of the 1st batch of artificial seawater doesn't show a significant trend, which seems to indicate a better stability. The stability study on the Batch 1 of the artificial solution had to be interrupted before due to lack of remaining bottles to pursue the study, it was conducted up to eleven months. The stability study of the natural solution was conducted up to sixteen months after sampling at the ANTARES station. The detail of the alkalinity values used to establish the stability of the materials are given in Supplementary Material S5.1.

The stability to transport is negligible (discrepancies are in the level of within and between bottles homogeneities reported) and is thus not taken into account in the final uncertainty budget. It is expected that the second batch of artificial solution behaves similarly to transportation as the other materials. Thus, the uncertainty of the second batch is also computed, even if stability to transport study wasn't performed.

Table 20 presents the uncertainty budget attributed to the reference values of the artificial reference materials as detailed in section 2.2.4.

Table 20: Uncertainties involved in equation 4.3 for the assessment of total alkalinity reference value's uncertainty of the artificial reference material

	Batch 1 (Ground neck bottles)	Batch 2 (Screw caps bottles)
Characterization and preparation		
ν_{NaHCO_3} (µmol/kg)	5.11E-01	8.06E-01
$\nu_{Na_2CO_3}$ (µmol/kg)	5.53E-02	7.77E-02
Background TA (µmol/kg)	3.09E-01	3.09E-01
Combined u	6.00E-01	8.67E-01
Homogeneity	3.61E-01	3.30E-01
Stability	8.21E-01	9.02E-01
Total		
u (k=1)	1.08E+00	1.29E+00
U (k=2)	2.16E+00	2.59E+00

The standard uncertainties of the terms in equations 4.2 are assessed following the method given in Section 2.2.4 and are given in Table 20, corresponding to the "characterization and preparation" uncertainty. The difference of uncertainty coming from the preparation and characterization between the two batches is explained by the fact that the volume of the Batch 1 is higher, allowing to reduce the relative uncertainty of gravimetric preparation.

The uncertainty of stability of the Batch 1 and Batch 2 of the artificial reference material are computed from equations 2.12 and 2.13, respectively, using the t-test information given in Table 19 and for a material shelf life of 3 months (chosen as the ILC was conducted within 3 months after the preparation of the solutions).

The standard uncertainty attributed to the TA reference values of Batch 1 and Batch 2 of the artificial reference material are of 1.08 and 1.29 µmol/kg, respectively, and were computed from equation 4.3. Which gives a global expanded uncertainty budget (i.e. with a coverage factor, k, of 2) of respectively 2.16 and 2.59 µmol/kg.

3.2. Inter-laboratory comparison results

Figure 30 represents, following the method detailed in section 2.3.2, the Youden plot obtained from the results of the inter-laboratory comparison conducted with five laboratories (Table 16) for total alkalinity measurements on the two reference materials developed: a stabilized natural seawater and an artificial solution. The total alkalinity values obtained by each participant are presented in Supplementary Material S5.1, corresponding to the measurements made at the first deadline.

The median value obtained on the stabilized natural seawater is of 2581.43 ± 2.19 µmol/kg (k=2). The median obtained on the artificial solution is of 2501.61 ± 2.78 µmol/kg (k=2).

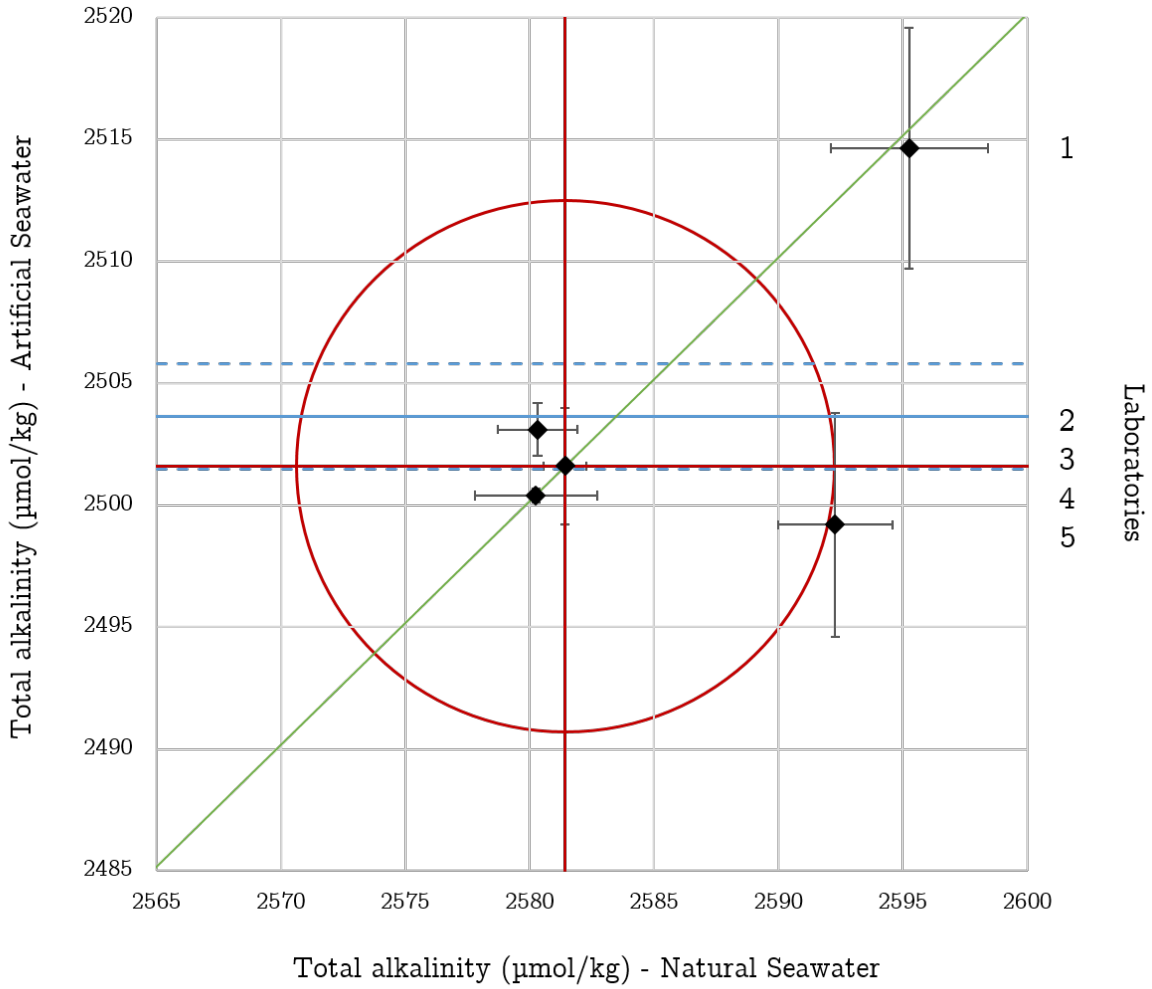

Figure 30: Youden plot of the inter-laboratory comparison conducted on the Stabilized natural seawater (X-axis) and the Artificial seawater, Batch 1 (Y-axis). Where diamonds correspond to the data point (Xi, Yi) of each participant, green line corresponds to the 45° line graphical marker, the two red horizontal and vertical lines represent the median of total alkalinity results obtained from the five laboratories on the artificial solution and the stabilized natural seawater, respectively, and the red circle represents the 95% confidence level circle. The blue line represents the artificial reference material reference value together with its expanded uncertainty in blue dotted lines.

The Youden plot shows that three laboratories out of five obtained really closed results that are centred around the medians of the two samples (laboratories, 2, 3 and 4). The standard deviation (represented by error bars) obtained by the laboratory 5 on the natural seawater show that this laboratory obtained results that could be considered compatible according to the 95% confidence circle. Moreover, its error bars obtained on the artificial reference material are compatible with the TA reference value. The laboratory 1, on the other hand, is considered as having biased results according to the 95% confidence circle drawn on the plot. Its proximity with the 45° line clearly indicates

that the source of error is systematic (i.e. similar bias to the medians for the two samples).

The value of the laboratory 1 obtained on the artificial seawater was also isolated by Grubb's test. This laboratory was thus not taken into account in the computation of the precision and bias of the measurement method.

The bias between the reference value and the mean value obtained by the four participants selected for the artificial solution is of -2.56 ± 2.44 µmol/kg (k=2). The precision of the method, s_R, given by the computation of s_L and s_r, being, respecpectively, inter and intra laboratory variation, is of 1.99 µmol/kg on the artificial seawater. This precision reaches level of precision reported in the literature (Millero *et al.,* 1998; Bockmon and Dickson, 2015). However, the precision on the natural seawater is of 5.85 µmol/kg, which mostly arises from the laboratory 5 random error highlighted by the Youden plot in Figure 30.

3.3. Uncertainty of total alkalinity measurements results with Gran's data treatment

Table 21 presents the uncertainty budget of the total alkalinity measurement results obtained from the inter-laboratory comparison, i.e. following the top-down approach, as described in section 2.4.1. The uncertainty budget corresponds to the multi-step potentiometric measurement method and Gran's data treatment, as it was computed from measurements made on the artificial solution. As laboratory 1 was isolated, the uncertainty budget is obtained from results of the four remaining laboratories. The uncertainties attributed to inter and intra laboratory variation are of, respectively, 1.67 and 1.09 µmol/kg. The uncertainty attributed to the bias is of 1.22 µmol/kg. The global standard uncertainty budget is thus of 2.33 µmol/kg; giving an expanded uncertainty of 4.67 µmol/kg.

Table 21: Uncertainty budget of total alkalinity measurement results computed with the top-down approach. Where s_L and s_r represent respectively inter and intra laboratory variation, $u(\hat{\delta})$ the uncertainty of the bias and $u(y)$ the global standard uncertainty.

Standard uncertainty estimation	
Uncertainty sources	*u (k=1)*
s_L	1.67E+00
s_r	1.09E+00
$u(\hat{\delta})$	1.22E+00
$u(y)$	2.33E+00

Table 22 presents the uncertainty quantification of all input variables involved in the measurement model of the multi-step open-cell potentiometric titration procedure with Gran's data treatment. The uncertainty quantification is detailed in section 2.4.2 and is based on LNE's measurement method and apparatus as described in section 2.1. The overall total alkalinity uncertainty budget gives a standard uncertainty of 2.63 µmol/kg, thus an expanded uncertainty (i.e. with a coverage factor, k, of 2) of 5.26 µmol/kg.

Table 22: Quantification of the uncertainty sources involved in the Total Alkalinity measurement method and Gran's data treatment following the bottom-up approach.

Input variables	Definition	Unit	Sub-sources of uncertainty	Standard uncertainty (k= 1)	
m_{HCl}	Mass of HCl delivered during the titration	g	- Densimeter accuracy (g/cm3)	2.00E-05	2.89E-03
			- Acid temperature (°C)	1.25E-01	
			-Volume delivered (ml), burette tolerance	2.89E-03	
m_{init}	Mass of sample analysed	g			1.70E-03
E	Potential measured by the glass electrode	mV	-Tolerance of the electrode	1.15E-01	1.16E-01
			-Repeatability	1.11E-02	
T	Temperature of the sample during the titration	°C	-Resolution	1.00E-01	1.00E-01
			-Repeatability	2.95E-03	
			-Trueness	5.66E-03	
R	Universal gas constant	J/mol.K			1.50E-05
F	Faraday constant	C/mol			8.30E-03
C_{HCl}	Amount content of the acid titrant	mol/kg-sol	- Stock solution (HCl 1 mol/kg-sol) amount content	6.00E-05	1.08E-05
			- Gravimetric dilution: weighing scale calibration	5.09E-03	
a and b	Gran's regression coefficients		- m_{HCl}		2.89E-03
			- F1	= 0.0055 * F1 - 76.39097	
			- Gran's regression method	a	5.33E+03
				b	1.59E+04
				corr(a,b)	-0.99889

Total uncertainty budget of total alkalinity (µmol/kg)	u (k=1)	2.63E+00
	U (k=2)	5.26E+00

The two uncertainty quantification approaches, i.e. top-down and bottom-up approaches, gave the same level of uncertainty for the total alkalinity measurement results obtained with the standardized measurement method and the Gran's data treatment, being an expanded uncertainty of 5 µmol/kg (k=2).

3. Discussion

4.1. Development of the artificial reference material

4.1.1. Composition of the artificial solution

The artificial solution developed for use as a reference material for total alkalinity measurements differs slightly from synthetic solution described in the literature for accuracy checking. Previous studies by Dickson *et al.* (2003) used solutions composed of either sodium carbonate, TRIS, or borax in an NaCl matrix. In this study, a decision was made to use a combination of sodium carbonate and sodium bicarbonate for two main reasons: (1) to mimic the alkalinity source found in natural seawater, which primarily arises from carbonate and bicarbonate ions, and (2) to achieve a pH level representative of seawater, ensuring that the potential measured by the glass electrode during titration is similar to that of a natural sample.

The addition of NaCl to the solution background helps maintain an ionic strength similar to that of natural seawater. However, it introduces background alkalinity, which complicates the determination of the total alkalinity reference value of the material. Moreover, the zero level of protons defined to measure TA in seawater is based on seawater acid-base chemical equilibria (Schulz et al., 2023). The impact of using a reference material with a simplified matrix must be further investigated, even though the good results obtained in the ILC seems to show that the artificial RM could be adequate.

For the artificial solution, the practical salinity was also measured with a salinometer, highlighting a difference of +2.05 compared to the absolute salinity obtained from knowledge of the composition. The significant discrepancy between both comes from the difference in definition. Absolute salinity is defined as the mass fraction of dissolved material in solution while the practical salinity is defined as the ratio of the conductivity of the solution on the conductivity of a standard KCl solution. For a natural seawater,

the discrepancy between both is in the order of 0.2 (Pawlowicz, 2013). The composition of the artificial seawater being composed in high majority of NaCl, explains the higher discrepancy between practical and absolute salinity observed. The definition of absolute salinity may not be really adequate for the artificial solution, where it is probably more relevant to compare ionic strengths. For the natural solution, only the practical salinity is given due to a lack of knowledge of its exact composition.

Developing an artificial reference material also served as a step forward in eliminating the use of mercuric compounds, which are currently employed to inhibit the growth of microorganisms in natural seawater solutions. This is however tied to the stability of the RM achievable.

4.1.2. Reference value determination

The total alkalinity reference value is determined through the gravimetric preparation of the solution, which is composed of salts previously characterized in terms of base amount content via coulometric analysis. Both the gravimetry and coulometry methods provide SI traceable results. Since the background alkalinity ($TA_{background}$) is carefully quantified, along with its associated uncertainty, the reference TA value assigned to the material may also be considered traceable to the SI units. It however necessitates that NaCl is the only significant source of background alkalinity and the purity of $NaHCO_3$ is correctly assessed.

The determination of background alkalinity resulting from NaCl impurities involves the gravimetric preparation of artificial solutions with varying NaCl concentrations, coupled with TA potentiometric measurements. This approach establishes a relationship between NaCl concentration and background alkalinity, along with its uncertainty (as described in equation 4.7). The linear regression was forced to pass through the origin as the background alkalinity coming from NaCl impurities is zero for a solution without NaCl matrix, this is confirmed by the measurements made with $\nu_{NaCl} = 0$ mol/kg-sol (Figure 29). Initially, an uncertainty of 2 µmol/kg was chosen for the TA potentiometric results to quantify $TA_{background}$, which closely matches the final estimated uncertainty obtained through the bottom-up approach (2.63 µmol/kg). Attributing this final uncertainty to the TA measurements for determining $TA_{background}$ would only marginally increase the uncertainty of the reference value of the material by 1 to 2%, which is negligible. Additionally, considering the presence of systematic errors between measurements (such as the same operator, device, method, acid titrant, etc.), 2 µmol/kg can be deemed a realistic uncertainty for this purpose.

However, to simplify the determination of the TA reference value, it may be considered to purify the NaCl before use, as suggested by Dickson *et al.* (2003), who estimated that the resulting $TA_{background}$ could be negligible. Alternatively, removing completely the NaCl background may be a final solution but it should first be investigated whether

the difference in salinity with natural samples would introduce other mechanisms that could hinder the artificial solution's applicability for quality control.

4.1.3. Other considerations

Having a reference material such as the developed artificial solution, with a potential for a SI traceable reference value provided alongside a comprehensive uncertainty budget, offers several advantages:

(1) It enables the validation of experimental protocols and the Gran's determination of the TA value.
(2) It facilitates the control of device accuracy
(3) It assists in qualifying new operators
(4) It allows for the quantification of acid titrant amount content for laboratories that do not have access to coulometric methods.

Another benefit of having an artificial reference material is the ability to provide reference materials for a wide range of total alkalinity values. This is important for end-users to verify that there isn't a linear bias in the measurement method across the studied range of alkalinity.

However, it does not allow for the accuracy verification of TA values obtained using the nonlinear least-squares regression method, which is yet widely applied to natural seawater samples to correct the value considering the acid-base system in the solution. Therefore, it is highly recommended to distribute a second material being a stabilized seawater, as the one from Scripps or the one developed in this study, to ensure the comparability of TA measurements on natural seawater samples.

Having a natural seawater reference material, that is easy to collet during open ocean oceanographic cruises, also offers the availability of a reference material that can be a bit cheaper than the artificial one, which has to be produced in the lab from high purity compounds.

4.2. Homogeneity and stability of the materials

The homogeneity of the material was assessed through potentiometric total alkalinity measurements. However, due to the method's limited precision, it was challenging to detect significant within- and between-bottle inhomogeneity (Table 19). It is anticipated that the homogenization step during material preparation ensures sufficient homogeneity for the intended use. Only the estimation of between-bottle homogeneity was included in the uncertainty budget of the TA reference value of the artificial materials, accounting for 6 to 7% of the final budgets.

The stability studies presented in Table 19 revealed a significant trend in Batch 2 of the artificial solution bottled with screw caps borosilicate bottles, indicating instability.

Conversely, Batch 1 of the artificial solution and the stabilized natural seawater, both bottled in ground neck borosilicate bottles, did not exhibit significant instability based on the t-test results (Table 19). This suggests potential better stability with the latter bottles. However, it should be noted that the standard deviation of corresponding slopes is not negligible compared to the slopes themselves. Further stability studies with longer durations could provide clearer insights into the stability of Batch 1 of the artificial solution and the stabilized natural seawater.

Dissolved inorganic carbon (DIC) analyses conducted at SNAPO-CO_2 on the natural seawater solution after 4, 10, and 13 months since sampling indicated a mean DIC value of 2385 µmol/kg with no significant evolution over time. Similarly, pH_T measurements performed on the solutions over time showed relatively dispersed results among laboratories and did not reveal any discernible trend. These results are presented in Supplementary Material S5.2 and S5.3.

However, nutrients analysis performed at MIO revealed an increase in silicate content from 12.1 to 23.2 µmol/kg-sol for the stabilized natural seawater in the ground neck bottles, representing an increase of about 11 µmol/kg-sol between months 4 and 16 post-sampling (Supplementary Material S5.4). Additionally, nutrient analysis on Batch 2 of the artificial seawater indicated a silicate content of 26.5 µmol/kg-sol 14 months after preparation, despite an initial supposed content of zero. This suggests a release of silicate ions from the borosilicate glass containers, as previously suggested by Mos *et al.* (2021). The release appears to be more significant from glass bottles with screw caps, which may align with the findings that Batch 2 of the artificial solution was less stable. However, the fact that silicates are also released in glass bottles with ground necks suggests that Batch 1 of the artificial solution and stabilized natural seawater may also lack stability. The increase in alkalinity measured by potentiometric measurements for both solutions is lower than the amount of silicates released, indicating potential secondary processes influencing alkalinity. Improving the stability of the developed materials likely necessitates using different bottling methods, such as employing glass with specific treatments to prevent silicate release. The reference materials distributed by Scripps Institution of Oceanography are known to be more stable, possibly due to differences in glass bottle suppliers. It could also be worthwhile to test storing solutions in polypropylene bottles, as investigations by Mos *et al.* (2021) suggested better stability, although this may compromise eventual stable DIC and pH_T values simultaneously.

4.3. Results of the inter-laboratory comparison

The results of the inter-laboratory comparison indicate an acceptable agreement among four out of five participants, even though the random error highlighted for laboratory 5 seems to affect the estimated precision of the method. Also, laboratory 1 exhibits a systematic error in Figure 30, evidenced by an equivalent bias compared to the median

for both analysed samples: 13.64 µmol/kg for the artificial solution and 13.82 µmol/kg for the stabilized natural seawater.

More broadly, the results of this inter-comparison suggest that:

(1) The TA reference value assigned to the artificial material based on knowledge of its composition aligns well with TA values measured using the standardized potentiometric titration method. The bias between the two, being of -2.56 ± 2.44 µmol/kg (k=2), falls within the expanded uncertainties of the bias and of the reference value (which is of 2.16 µmol/kg).
(2) In the case of a laboratory showing a systematic bias, the artificial material with a well-characterized reference value might be employed to correct potentiometric measurements by calculating the trueness bias, however this needs further careful investigation.
(3) The closed-cell measurement method, being employed by one of the laboratories among laboratories 2, 3, and 4 in Figure 30, yields results that are compatible with those obtained using the open-cell measurement method.

These seem to demonstrate that both developed materials could be considered suitable for use in quality controls of the multi-step potentiometric titration method for total alkalinity measurements in seawater.

4.4. Uncertainty estimation

The bottom-up and top-down approaches applied for uncertainty quantification of total alkalinity measurement results obtained from the standardized method and Gran's data treatment yielded really close results, with standard uncertainties of 2.63 and 2.33 µmol/kg, respectively. This level of uncertainty is coherent regarding the precision of the method reported in the literature, typically ranging between 2 and 4 µmol/kg (Millero *et al.,* 1998; Bockmon and Dickson, 2015). Moreover, it is close to the data quality objective required by the GOA-ON for monitoring ocean acidification, indicating promising prospects for achieving good data quality for TA results.

However, the uncertainty budget detailed in this chapter does not include uncertainty arising from the nonlinear least-squares (NLLS) regression typically applied to natural seawater samples (equation 1.18, Chapter I). This remains to be quantified and may slightly increase the uncertainty budget. Quantifying this uncertainty will entail considering several aspects and input variables from the NLLS equation, including:

(1) The uncertainty of practical salinity measurements
(2) Possible discrepancies between total fluoride and total sulphate amount contents computed from salinity and the actual composition of natural seawaters worldwide
(3) The uncertainty of dissociation constants of fluoride and sulphate ions

The Monte Carlo approach, as described in GUM Supplement 1 ("JCGM 101:2008," 2008), might be pertinent for computing the uncertainty of the NLLS regression as it enables uncertainty computation from the distribution of the regression.

Although the top-down approach appears to provide a realistic evaluation of the uncertainty of TA measurement results, conducting an inter-laboratory comparison with more participants could lead to a more robust uncertainty budget. According to the top-down uncertainty budget (Table 21), reducing uncertainty would necessitate mitigating the contributions of inter-laboratory deviation and bias uncertainty. This could be achieved through better harmonization of measurement procedures and reducing uncertainty in the reference value of the material, which requires improving material stability.

The bottom-up approach, which relies on a detailed identification and quantification of sources of uncertainty in the measurement process, helps identify the main contributions to the overall budget.

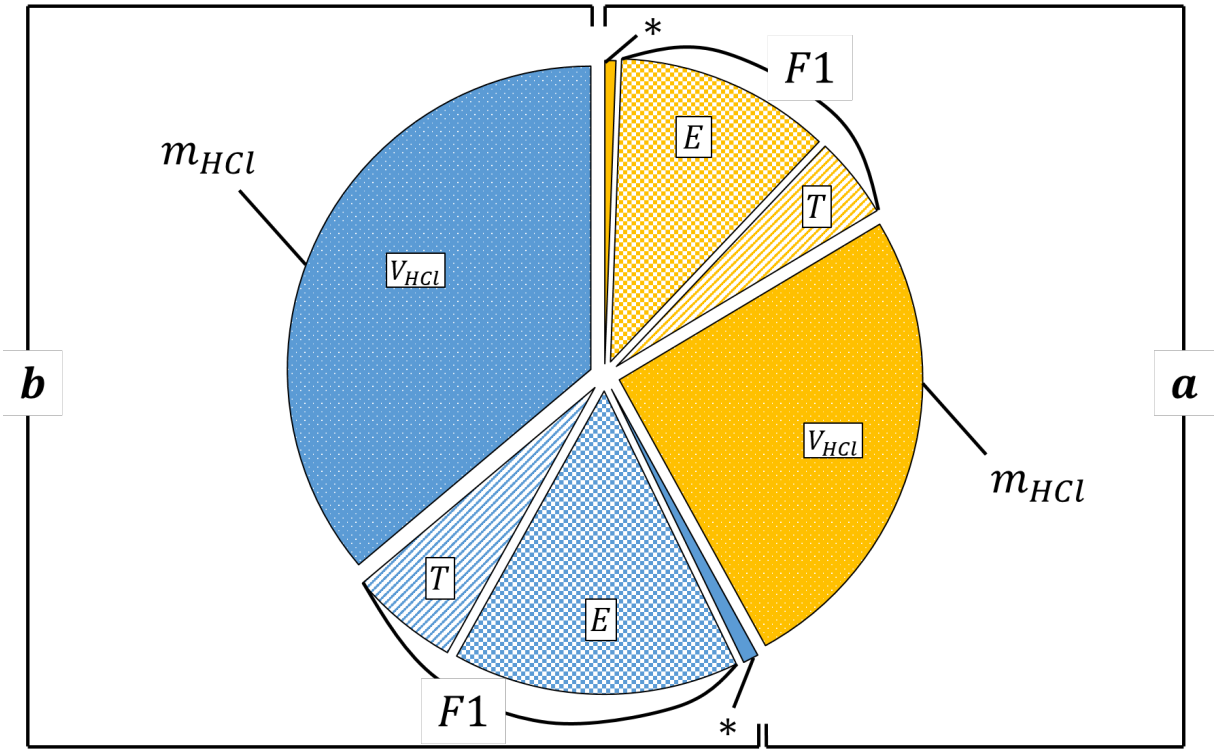

Figure 31: Main sources of uncertainty contributing to the overall budget of total alkalinity measurement results obtained with the open-cell titration measurement method together with Gran's data treatment. With uncertainty sources coming from a and b represented in yellow and blue, respectively. The symbol * corresponds to the residuals of Gran's regression.

In Table 22, the main sources identified are the coefficients a and b of Gran's regression, contributing 42% and 58%, respectively, to the uncertainty budget. These components are computed from F1 (equation 4.9) and from the weight of HCl added during titration (m_{HCl}). The main sources of uncertainty influencing F1 are the measured potential

(≈72.5%) and temperature (≈27.5%). The main source of uncertainty influencing m_{HCl} is the volume of acid delivered by the burette (nearly 100%). The weight of all of these sources in the overall budget are presented in Figure 31. Reducing uncertainties in these three components can help diminish the overall budget. However, this is heavily reliant on device resolution and tolerance, and thus depends on the choice of the device and manufacturer. The similarity of the sources of uncertainty influencing a and b in Figure 31 well illustrates the high correlation between both (corr(a,b) = -0.999).

4.5. Route of traceability proposition

Figure 32 presents a proposed route of traceability for seawater total alkalinity measurements results obtained with the standardized potentiometric titration measurement method, which includes the two reference materials developed, being the artificial solution and the stabilized natural seawater.

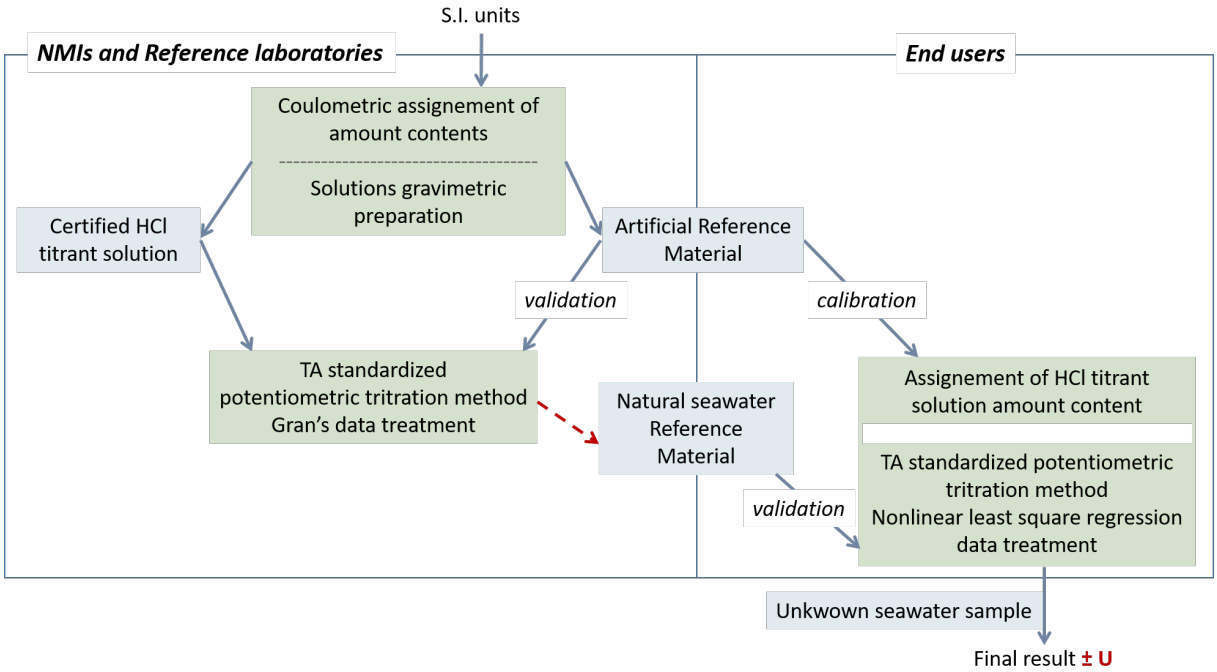

Figure 32: Proposed route of traceability for the total alkalinity measurement results. Where blue boxes correspond to solutions and green boxes to measurement processes. Signs in red highlight remaining tasks in the objective of establishing traceability to the SI units of end user's results.

Starting from the top-left of the scheme presented in Figure 32, on one hand, the HCl titrant solution used by reference laboratories for total alkalinity measurements is characterized in terms of base amount content through coulometric measurements. Gravimetric dilution may additionally be necessary to achieve the desired amount content. Results obtained from both coulometry and gravimetry are directly traceable to the SI units.

On the other hand, the artificial solution is prepared by gravimetry from sodium carbonate and sodium bicarbonate salts whose bases amount contents have previously been characterized by coulometry. The total alkalinity background ($TA_{background}$) introduced by the NaCl matrix of the artificial solution is quantified by TA potentiometric measurements with a thorough uncertainty estimation. Accurate knowledge of the composition permits the attribution of a TA reference value together with an uncertainty that could be considered traceable to the SI units. The artificial solution could thus be described as a Certified Reference Material (CRM).

The artificial CRM, along with the HCl titrant solution, serves as means for reference laboratories to validate the accuracy of their experimental protocols as well as Gran's data treatment for potentiometric determination of total alkalinity. This validation process enables reference laboratories to robustly assign a TA reference value to a stabilized natural seawater reference material, adding the nonlinear least-squares regression data treatment to correct for the acid-base system present in seawater.

However, the lack of uncertainty estimation stemming from the nonlinear least-squares regression prevents the stabilized natural seawater reference material from being considered certified or traceable to SI units. The red arrow on Figure 32 identifies this remaining issue. Having a stabilized natural seawater reference material remains essential in ensuring the comparability of end users' measurements. The stabilized natural seawater could be described as a secondary standard.

The artificial CRM could also be used as a calibrant by end users to assess the amount content of their HCl titrant solution in a more robust manner compared to using stabilized natural seawater reference material. The artificial reference material is used once to validate the measurement method of reference laboratories (i.e. without applying a correction), and is only used as a calibrant by end-users. Both uses of this RM in the traceability route can thus be considered independent. Alternatively, end users can obtain HCl titrant solution directly characterized by coulometry, for example, from the Scripps Institution of Oceanography. However, a survey conducted by Acquafredda *et al.* (2022) highlighted that among the laboratories purchasing reference materials for total alkalinity and dissolved inorganic carbon from Scripps, less than one quarter purchased also certified HCl titrant solution. Meaning an alternative approach must be found to accurately characterize amount contents of end users' titrant solution.

Ensuring the comparability of TA measurements on natural seawater samples then necessitates the use of the secondary standard in quality control, being a stabilized natural seawater such as those available at Scripps or those developed in this study.

To enhance the traceability route of standardized total alkalinity measurement results, the following tasks remain:

(1) Finding a more straightforward method to quantify the background alkalinity introduced by the NaCl matrix in the artificial CRM.
(2) Quantifying the uncertainty arising from the nonlinear least-squares regression method, which could enable traceability of the stabilized natural

seawater reference material to SI units and provide a complete uncertainty budget for end users' TA measurement results on unknown natural samples. These points are highlighted in red in Figure 32.

(3) Improving the stability of both materials.

4. Conclusion

This chapter explores the application of various metrological tools to measurements of total alkalinity (TA) of seawater using the standardized multi-step potentiometric titration method.

Two batches of an artificial certified reference material with reference TA values of, respectively, 2503.6 ± 2.2 µmol/kg and 2503.8 ± 2.6 (k=2) for a shelf-life of three months have been produced, alongside a second reference material comprising stabilized natural seawater. These materials underwent homogeneity and stability studies to comply with ISO standard 17034 "General requirements for the competence of reference material producers" (2016). While the homogeneity study requires more precise measurements to obtain significant information, stability was evaluated to be unsatisfactory due to an increase in TA over time. This might be partly attributed to the release of silicates from the glass container but needs further investigation. Using a different type of bottling is suggested to enhance stability.

An inter-laboratory comparison involving five laboratories indicated that both reference materials could be suitable for quality control of the standardized total alkalinity measurement method.

A route of traceability integrating these two reference materials is proposed in this study in the objective of getting further the establishment of the traceability to the SI units of end users measurement results. However, remaining tasks such as establishing the overall uncertainty budget of TA measurements need completion.

As a first step, the uncertainty of the multi-step potentiometric measurement method with Gran's data treatment was quantified through both bottom-up and top-down approaches, yielding expanded uncertainties of 5.26 and 4.67 µmol/kg, respectively. Although slightly higher than required by the GOA-ON for monitoring ocean acidification, these results are encouraging for achieving good data quality of TA measurement results. The bottom-up approach helps identify key sources of uncertainty to prioritize for improvement.

Quantification of the nonlinear least-squares regression is necessary to establish the overall uncertainty budget of seawater TA measurement results needed in the objective of achieving traceability to the SI units.

The results presented in this chapter represent progress towards ensuring compatibility and accuracy of seawater total alkalinity measurement results.

References

Acquafredda, M., Cochran, C., Busch, D.S., Jewett, L., Edmonds, H., Dickson, A.G., 2022. Understanding the Current Use and Future Needs of CO2 in Seawater Certified Reference Materials NOAA Technical Memorandum OAR-OAP-5. https://doi.org/10.25923/ANC4-GJ33

Bockmon, E.E., Dickson, A.G., 2015. An inter-laboratory comparison assessing the quality of seawater carbon dioxide measurements. Marine Chemistry 171, 36–43. https://doi.org/10.1016/j.marchem.2015.02.002

Boggs, P.T., Byrd, R.H., Rogers, J.E., Schnabel, R.B., 1992. User's reference guide for ODRPACK version 2.01::software for weighted orthogonal distance regression. NIST.

Bourles, B., Baurand, F., Hillion, S., Rousselot, P., Grelet, J., Bachelier, C., Roubaud, F., Gouriou, Y., Chuchla, R., Cariou, T., Llido, J., 2023. French PIRATA cruises: CHEMICAL ANALYSIS data. https://doi.org/10.17882/58141

Dickson, A.G., 2010. Standards for Ocean Measurements. Oceanography 23, 34–47. https://www.jstor.org/stable/24860884

Dickson, A.G., Afghan, J.D., Anderson, G.C., 2003. Reference materials for oceanic CO2 analysis: a method for the certification of total alkalinity. Marine Chemistry 80, 185–197. https://doi.org/10.1016/S0304-4203(02)00133-0

Dickson, A.G., Sabine, C.L., Christian, J.R. (Eds.), 2007. Guide to Best Practices for Ocean CO2 Measurements PICES Special Publication 3, 191.

Gattuso, J.-P., Epitalon, J.-M., Lavigne, H., Orr, J., 2021. seacarb: seawater carbonate chemistry. R package: version 3.3.1. https://doi.org/10.5281/zenodo.595096

GOA-ON, 2019. Global Ocean Acidification Observing Network (GOA-ON): Implementation Strategy.

Ho, D.T., Bopp, L., Palter, J.B., Long, M.C., Boyd, P., Neukermans, G., Bach, L., 2023. Monitoring, Reporting, and Verification for Ocean Alkalinity Enhancement (preprint). https://doi.org/10.5194/sp-2023-2

Iglesias-Rodríguez, M.D., Rickaby, R.E.M., Singh, A., Gately, J.A., 2023. Laboratory experiments in ocean alkalinity enhancement research. State of the Planet 2-oae2023, 1–18. https://doi.org/10.5194/sp-2-oae2023-5-2023

ISO 13528, 2022. Statistical methods for use in proficiency testing by interlaboratory comparison.

ISO 17034, 2016. General requirements for the competence of reference material producers.

ISO 21748, 2017. Guidance for the use of repeatability, reproducibility and trueness estimates in measurement uncertainty evaluation.

ISO Guide 35:2017 Reference materials — Guidance for characterization and assessment of homogeneity and stability, 2017.

JCGM 100:2008, 2008. Evaluation of Measurement Data-Guide to the Expression of Uncertainty in Measurement.

JCGM 101:2008, 2008. Evaluation of measurement data — Supplement 1 to the "Guide to the expression of uncertainty in measurement" — Propagation of distributions using a Monte Carlo method.

Lefevre, D., 2010. MOOSE (ANTARES). https://doi.org/10.18142/233

Llido, J., 2023. PIRATA-FR33 cruise, RV Thalassa. https://doi.org/10.17600/18002398

Martín, J., Velázquez, N., Asuero, A.G., 2017. Youden Two-Sample Method Quality Control and Assurance-An Ancient Greek Term Re-Mastered. https://doi.org/10.5772/66397

Meija, J., Coplen, T.B., Berglund, M., Brand, W.A., Bièvre, P.D., Gröning, M., Holden, N.E., Irrgeher, J., Loss, R.D., Walczyk, T., Prohaska, T., 2016. Atomic weights of the elements 2013 (IUPAC Technical Report). Pure and Applied Chemistry 88, 265–291. https://doi.org/10.1515/pac-2015-0305

Millero, F.J., Lee, K., Roche, M., 1998. Distribution of alkalinity in the surface waters of the major oceans. Marine Chemistry 60, 111–130. https://doi.org/10.1016/S0304-4203(97)00084-4

Mos, B., Holloway, C., Kelaher, B.P., Santos, I.R., Dworjanyn, S.A., 2021. Alkalinity of diverse water samples can be altered by mercury preservation and borosilicate vial storage. Sci Rep 11, 9961. https://doi.org/10.1038/s41598-021-89110-w

Muller, J.W., 2000. Possible advantages of a robust evaluation of comparisons. J. Res. Natl. Inst. Stand. Technol. 105, 551. https://doi.org/10.6028/jres.105.044

Pawlowicz, R., 2013. TEOS-10 Primer.

Pratt, K.W., 2014. Measurement of pHT values of Tris buffers in artificial seawater at varying mole ratios of Tris:Tris·HCl. Marine Chemistry 162, 89–95. https://doi.org/10.1016/j.marchem.2014.03.003

Schulz, K.G., Bach, L.T., Dickson, A.G., 2023. Seawater carbonate chemistry considerations for ocean alkalinity enhancement research: theory, measurements, and calculations. State of the Planet 2-oae2023, 1–14. https://doi.org/10.5194/sp-2-oae2023-2-2023

WMO, United Nations Environment Programme (UNEP), International Science Council (ISC), Scientific and Cultural Organization (IOC-UNESCO) Intergovernmental Oceanographic Commission of the United Nations Educational, 2022. The 2022 GCOS Implementation Plan (GCOS-244) [WWW Document]. URL https://library.wmo.int/records/item/58104-the-2022-gcos-implementation-plan-gcos-244 (accessed 1.4.24).

Wolf-Gladrow, D.A., Zeebe, R.E., Klaas, C., Körtzinger, A., Dickson, A.G., 2007. Total alkalinity: The explicit conservative expression and its application to biogeochemical processes. Marine Chemistry 106, 287–300. https://doi.org/10.1016/j.marchem.2007.01.006

Youden, W.J., 1959. Graphical diagnosis of Interlaboratory Test Results. Industrial Quality Control, National Bureau of Standards, Washington, D. C. XV.

Conclusion and perspectives

1. Conclusion

1.1. Summary

Changes in the seawater carbonate system, induced by the absorption of anthropogenic CO_2, result in acidification of the ocean and alteration of the ocean carbon cycle. These changes are already impacting marine ecosystems. Mitigating further impacts requires international strategies for mitigation, adaptation, and redress (Harrould-Kolieb and Hoegh-Guldberg, 2019; United Nations, 2015). Observing the chemical parameters of the carbonate system is essential to establish long-term trends and support these strategies. Therefore, it is crucial to ensure the high quality and comparability of measurement results for reliable assessments. This necessitates the application of metrological tools to the measurement methods. The main metrological concepts required are (1) a clear definition of the measurand, (2) established traceability to the highest international standard, (3) comprehensive uncertainty estimation, and (4) validation of measurement methods using reference materials or participating in inter-laboratory comparisons. This thesis focused on developing or improving these concepts for measuring the pH and total alkalinity of seawater.

Chapter I presented definitions of the most widely recognized measurands for both parameters. The definitions chosen and applied throughout this work are those that have become established in the oceanographic community over the years.

The traceability route for total pH is currently established to the potentiometric Harned cell measurement method, used to characterize TRIS buffers. By linking the pH_T values of TRIS buffers to a pure artificial seawater matrix, thereby establishing a true pH_T scale, across the relevant range of salinity and temperature for oceanographic measurements (S 5-40 and T 5°C-40°C), the work presented in Chapter III improved the traceability route. An improved traceability route for total alkalinity measurements is also proposed in Chapter V, based on the development of two reference materials.

Indeed, for both parameters, reference materials have been produced (Chapters II and V). The suitability of these materials for quality control in end-users' measurement methods was investigated through inter-laboratory comparison exercises. Artificial reference materials for each parameter were produced according to international standards ("ISO 17034", 2016; "ISO Guide 35", 2018). The reference values of these artificial materials are (1) traceable to the highest international standard established to date and (2) provided with comprehensive uncertainty budgets established using the bottom-up approach (GUM, "JCGM 100:2008", 2008).

The uncertainty budgets for the standardized measurement methods of pH_T and TA were investigated using both bottom-up and top-down approaches (Chapters II, IV, and V). Uncertainties established following the top-down approach ("ISO 21748", 2017) provided an estimation of the uncertainty budget for the complete measurement method. It must be noted though, that the uncertainty budget for TA measurement

corresponds to the standardized measurement method with Gran's data treatment method.

Only partially complete budgets were established using the bottom-up approach due to lack of estimation of uncertainty sources coming from users or samples. Moreover, there is missing information from the dye characterization step for the total pH uncertainty budget. This approach still provided valuable information about the minimum level of uncertainty achieved and the main sources contributing to the overall budgets. This highlights the crucial areas that require further work.

The application and enhancement of metrological tools for measuring pH_T and total alkalinity of seawater, as investigated throughout this thesis, have led to significant advances in data quality and the comparability of measurement results. The key outcomes are summarized below.

1.2. Main results

1.2.1. Metrological tools for the measurement of pH_T

Chapter II

The widely accepted reference material, and the only one available for the oceanographic community to date, is an equimolal TRIS buffer with a pH_T of 8.1 in an artificial seawater matrix of salinity 35. This reference material was reproduced at LNE and characterized using the Harned cell potentiometric measurement method. The stability and homogeneity of the produced material were also rigorously studied with Harned cell measurements. The material was found to be instable, with a decrease in the acidity function of -0.0005 per month. This work still allowed for the first comprehensive uncertainty budget to be attributed to the reference pH_T value of the TRIS buffer, considering preparation, characterization, stability, and homogeneity of the material. The uncertainty budget was established based on the GUM ("JCGM 100:2008", 2008), i.e. bottom-up approach. All steps were conducted in accordance with international standards for the production of reference materials. The achieved level of uncertainty is 0.005 in pH_T (k=2) for a shelf-life of six months. This level of uncertainty, being below the requirements of GOA-ON for ocean acidification monitoring (GOA-ON, 2019), makes the reference material suitable for quality control of the routine spectrophotometric pH_T measurement method performed by oceanographers.

The main source of uncertainty was identified as being the determination of silver-silver chloride electrodes standard potential in saline media, $E^{\circ *}$. To lower this uncertainty, care must be taken on the homogeneity of the batch of electrodes used. Moreover, the definition of the water mass fraction was identified as a key point on which a consensus must be found, as differences in the definition can lead to discrepancies around 0.004 in pH_T.

This reference material was also tested in an inter-laboratory comparison involving thirteen participants, demonstrating good precision and trueness (precision of 0.0037 and a bias of 0.0004). The results of the inter-laboratory comparison were used to compute an uncertainty estimation of spectrophotometric pH_T measurement results following the top-down approach, resulting in an expanded uncertainty of 0.009 in pH_T.

Chapter III

Spectrophotometric pH_T measurements rely on the characterization of the second dissociation constant of the indicator dye, which is obtained from measurements on solutions with known pH_T. To achieve this, Harned cell potentiometric measurements were performed on several equimolal TRIS buffers. These buffers, prepared at various TRIS molalities, were made in an artificial seawater matrix with salinities ranging from 5 to 40, and Harned cell measurements were conducted at temperatures between 5°C and 40°C. This approach provided, for the first time, TRIS buffer pH_T values that are consistent across the entire range of salinity and temperature relevant to oceanographic measurements.

The presented work included a reproducibility assessment conducted in collaboration with two other metrology institutes, giving a mean standard deviation of 0.002 in pH_T among the three NMIs, as well as a function that provides equimolal TRIS buffer pH_T values based on salinity, temperature, and TRIS molality. This function can be used to derive pH_T values for zero TRIS molality, recommended to represent pure artificial seawater (i.e., without TRIS and TRIS.HCl), thus referring to a true total pH scale in seawater.

There is a good agreement between the fit function presented and previous work reported in the literature for salinities above 20. However, significant discrepancy was found with the previous work of Müller et al. (2018) for lower salinities below, which likely comes from an inconsistent composition of their artificial seawater. The consistency of our results with the reference work of DelValls and Dickson (1998) gives confidence in the fit function for salinities as low as 5, and the extrapolation to pure artificial seawater.

The fit function provided, by referring to a true total pH scale, is a step further in improving the traceability of pH_T measurements. Additionally, the study gives insights on the remaining work needed to establish TRIS buffer pH_T values traceability to the SI units. This will require the help of a speciation model as the one developed by Clegg et al. (2022) to quantify the assumptions applied while performing potentiometric measurements and link the pH_T values to their thermodynamic definition.

Chapter IV

Spectrophotometric pH_T measurement results have, until now, lacked an uncertainty budget established using the bottom-up approach. To address this, the sources of uncertainty affecting the measurement were identified. It was raised that the measurement process is highly dependent on absorbance values. Therefore, the uncertainty budget for the nine absorbance values relevant to pH_T measurement in a seawater sample was quantified, using data from the spectrophotometer's calibration. The correlation between these nine values was thoroughly investigated. This analysis enabled the computation of the uncertainty of the absorbance ratio R, which is used for the subsequent determination of pH_T.

From this information, a preliminary minimal uncertainty level for pH_T measurement results was computed, yielding an expanded uncertainty of 0.02. The bias in absorbance measurements was identified as the main source of uncertainty in the ratio R. Performing the calibration of the spectrophotometer with optical density filters having lower uncertainties should help in reducing this uncertainty. The uncertainty introduced by the correction method arising from the dye perturbation should also be further investigated.

1.2.2. Metrological tools for the measurement of total alkalinity

Chapter V

Two reference materials were produced for the total alkalinity (TA) measurement method:

(1) An artificial reference material which consists of carbonate and bicarbonate ions in a NaCl matrix, with a characterized reference value potentially traceable to the SI units. The reference value is provided with a complete uncertainty budget established according to international recommendations for the production of reference materials. This uncertainty budget integrates the uncertainty arising from the background alkalinity introduced during the preparation of the reference material. The reference value is 2503.6 ± 2.2 µmol/kg (k=2), for a shelf-life of three months.
(2) A stabilized natural seawater sampled in the Mediterranean sea. The reference value of that material can be assigned by reference laboratories.

Both materials underwent homogeneity and stability studies and were tested in an inter-laboratory comparison involving five laboratories, demonstrating their applicability in quality control of TA measurements. The bias was of -2.56 ± 2.44 µmol/kg (k=2) and the precision of 1.99 µmol/kg on the artificial material.

The uncertainty budget for the multi-step potentiometric titration method using Gran's data treatment was investigated using both the bottom-up and top-down approaches

for uncertainty quantification. Both approaches yielded similar uncertainty levels for TA results, with an expanded uncertainty of 5 µmol/kg.

Additionally, a proposed traceability route for TA measurement results, involving the two developed reference materials, was detailed. In this traceability route, the artificial reference material can be used to validate the measurement method used with Gran's data treatment of reference laboratories, allowing them to robustly assign a reference TA value to a natural seawater reference material. End-users can then use, on one hand the artificial reference material to assign the amount content of their HCl titrant solution, and on the other hand the natural seawater reference material to validate their measurement method together with the nonlinear least-squares (NLLS) regression data treatment. The establishment of the uncertainty arising from the NLLS regression is one key point that will be required to complete the traceability route.

1.3. To go further

The monitoring of ocean acidification relies on the knowledge of different variables of the oceanic carbonate system that are computed from two measured parameters. Moreover, data quality requirements for the monitoring of ocean acidification have been set on the carbonate ions concentration. It is thus also crucial to know the level of uncertainty achieved on these variables. The computation of the other variables are based on solution chemical equilibrium and are generally calculated with computer programmes, which often lack of uncertainties in the input parameters. Recently, uncertainty propagation have been added to these programmes (Humphreys et al., 2022; Orr et al., 2018).

Based on (1) the total alkalinity and pH_T measurements carried out on the stabilized natural seawater reference material for TA, presented in Chapter V, and (2) the estimated uncertainty levels for both parameters, the uncertainties of other parameters of the carbonate system were propagated. The functions "carb" and "errors" from the seacarb package (version 3.3.3) were used for this purpose (Gattuso et al., 2021; Orr et al., 2018). The "errors" function integrates the standard uncertainties of the input variables as well as the default standard uncertainties from the dissociation constants. Uncertainties on the salinity and temperature were set by default to 0.01 and relative uncertainties on the nutrients were fixed to 5%. The results are presented in Table 23.

The relative standard uncertainty of carbonate ion concentration is 3.2% when derived from pH_T and TA uncertainties estimated using the top-down approach (a), and 3.6% from minimum uncertainties estimated using the bottom-up approach (b). A sensitivity analysis revealed that the uncertainty in output parameters is significantly more dependent on the uncertainty in pH_T than in TA. Therefore, it is crucial to continue developing a comprehensive uncertainty budget for pH_T measurement results using the bottom-up approach.

Moreover, the default uncertainty from constants, as estimated by Orr et al. (2018), also appears to be a limiting factor in reducing the uncertainty for the dataset presented in Table 23. The uncertainties of the salinity, temperature and nutrients were, on the contrary, observed to have a very small impact on the overall budget.

The GOA-ON recommendations for monitoring ocean acidification, which set a climate goal of 1% standard uncertainty for the dissolved carbonate ions concentration, refer to differences in $[CO_3^{2-}]$ for establishing trends. Therefore, systematic errors, such as uncertainties in constants, can be cancelled out (Orr et al., 2018). With this consideration, the relative standard uncertainty of carbonate ion concentration is 1% when derived from pH_T and TA uncertainties estimated using the top-down approach (a), and 2% from minimum uncertainties estimated using the bottom-up approach (b). While work remains to establish complete and thoroughly assessed uncertainty budgets, these findings are highly encouraging for achieving sufficient data quality to robustly monitor ocean acidification.

Table 23: Uncertainty propagation to other parameters of the carbonate system, from estimated uncertainties of total alkalinity and pH_T measurement results. The hydrostatic pressure was set to zero.

Input parameters	TA (µmol/kg)	pH_T	Practical salinity	Temperature (°C)	Total phosphate (µmol/kg)	Total silicate (µmol/kg)
Value	2581.4	7.800	38.53	25.00	0.40	12.10
Standard uncertainty						
(1) Top-down approach	2.3	0.005	0.01	0.01	0.02	0.61
(2) Bottom-up approach, minimum uncertainty	2.6	0.010				

Output parameters	$[CO_2]$ (µmol/kg)	$[HCO_3^-]$ (µmol/kg)	$[CO_3^{2-}]$ (µmol/kg)	DIC (µmol/kg)	pCO_2 (µatm)	fCO_2 (µatm)	Aragonite saturation state	Calcite saturation state
Value	23.8	2188.5	161.4	2373.75	856.2	853.5	2.49	3.77
Relative standard uncertainty (%)								
(1)	2.2%	0.5%	3.2%	0.3%	2.3%	2.3%	5.6%	5.6%
(2)	3.2%	0.6%	3.6%	0.3%	3.2%	3.2%	5.9%	5.8%

1.4. Graphical summary

Figure 33 summarizes the key outcomes of the work presented in this thesis, with the metrological tools developed or improved for pH_T and total alkalinity measurement results.

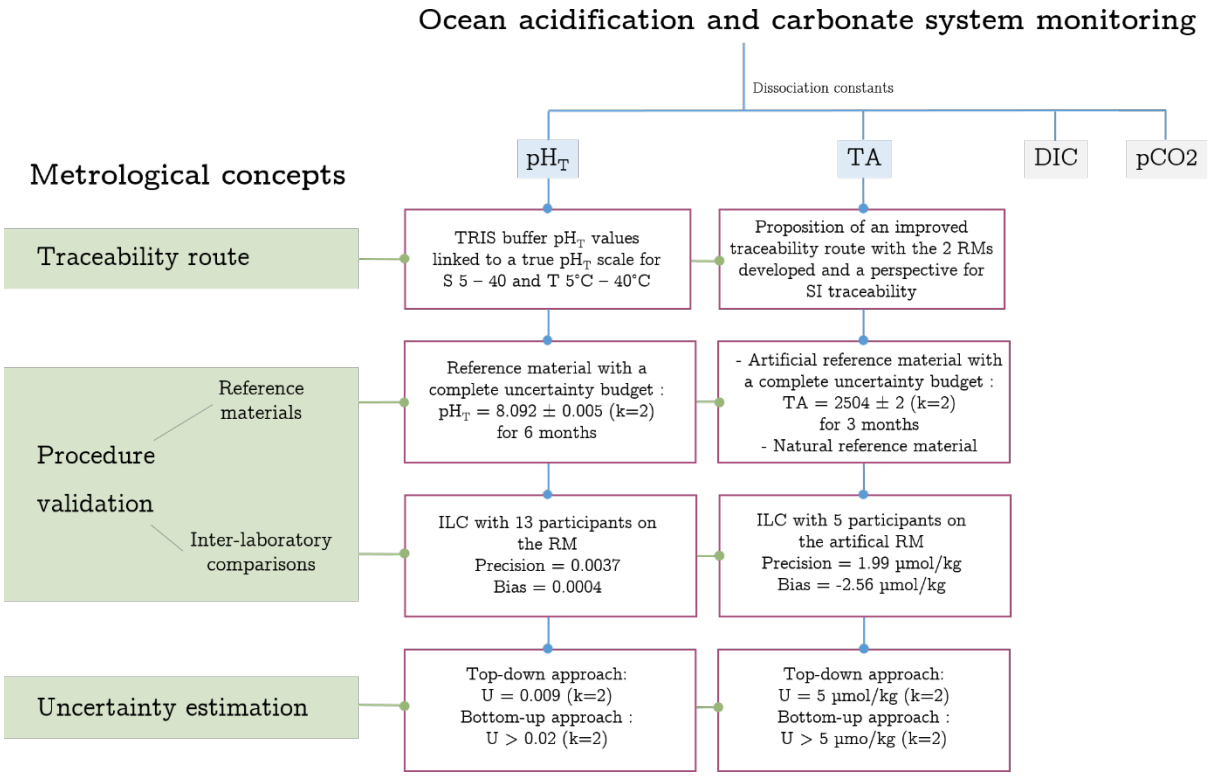

Figure 33: Graphical summary of the key outcomes of the work presented in the thesis.

2. Perspectives

For both studied parameters, total pH and total alkalinity, work remains to robustly establish metrological traceability and comparability of measurement results.

2.1. Reference materials transfer to field laboratories

Making the developed reference materials available for the oceanographic community will be one crucial step. Above the need of production capacity, the first step will be to find a way of improving the stability of the materials.

For the TRIS buffer reference material produced, the improvement of the stability may be achieved by adding a filtration step before bottling and characterization to prevent microorganism development, thereby enhancing stability. Moreover, developing non-equimolal TRIS buffers as reference materials would be beneficial, as they would allow

checking measurement methods across the entire range of pH_T relevant for oceanographers.

For total alkalinity reference materials, it could be interesting to find a different type of bottling that prevents the release of silicates into the solution to enhance the stability. Moreover, a better method for quantifying background alkalinity must be adopted.

2.2. Towards improved data quality of pH_T results

The complete uncertainty budget for spectrophotometric pH_T measurement results, established following the GUM (i.e., bottom-up approach), must be finalized. A crucial step in this process is evaluating the uncertainties arising from the indicator dye characterization. This requires re-characterizing the dye, which is a significant task. Within the SapHTies project (EMPIR 20NRM06), a software has been developed to propagate uncertainties from (1) dye characterization and (2) absorbance, salinity, and temperature values acquired by end-users to the pH_T result. This software will be made available. Further investigation into dye purity and its effect on pH_T measurements is also necessary.

Establishing SI traceability of TRIS buffers pH_T values requires quantifying errors introduced by neglecting terms related to HCl activity coefficients and sulphate dissociation constants in Harned cell potentiometric measurements, thus linking the measured pH_T to its thermodynamic definition. This will require the assistance of speciation models such as the one developed by Clegg et al. (2022). Several metrological challenges also remain unsolved to achieve traceability to the SI for final seawater pH_T spectrophotometric measurements:

(1) The pH_T spectrophotometric measurements are currently validated using a TRIS buffer that is certified for a specified TRIS molality. Consequently, the reference pH_T value obtained is not linked to a pure artificial seawater matrix and is neither linked to the thermodynamic definition of pH_T.
(2) The commercially available indicator dye used for seawater pH_T spectrophotometric measurements may contain impurities that affect the pH_T measurement. Methods have been developed to purify the dye, generally using High-Performance Liquid Chromatography (DeGrandpre et al., 2014; Liu et al., 2011; Patsavas et al., 2013). The impact of impurities is not yet fully understood, and it is essential to ensure that remaining impurities in the mCP, as well as batch-to-batch variations, do not affect the measured pH_T.
(3) The definition of salinity is another issue in achieving SI traceability for seawater spectrophotometric pH_T measurements. The salinity of a natural seawater sample is needed to calculate the indicator dye parameters, and the Practical Salinity is used for this purpose. It is defined on the Practical Salinity Scale of 1978 in terms of the conductivity ratio K15, which is the electrical conductivity of the sample at 15°C and one standard atmosphere, divided by

the conductivity of a standard potassium chloride solution at the same temperature and pressure (IOC et al., 2010). However, this definition lacks metrological traceability to SI units (Seitz et al., 2011). Additionally, a different definition, nominal salinity known from the artificial seawater composition, is applied for the salinity of TRIS buffers. Although the low difference between the two definitions does not significantly impact the final pH_T value, the lack of traceability to the SI, combined with the difference in salinity definitions between TRIS buffers and natural seawater samples, complicates establishing rigorous SI traceability for seawater spectrophotometric pH_T measurement methods.

2.3. Rising metrological challenges for Total Alkalinity measurements

For total alkalinity measurements, it is crucial to quantify the uncertainty arising from nonlinear least squares (NLLS) regression. One effective approach could be using the Monte Carlo method for uncertainty quantification. Additionally, uncertainties stemming from the sample and user need to be investigated. The influence of the method itself, such as the impact of residual bicarbonate ions at the end of the titration, must also be considered (Dickson et al., 2003). Addressing these issues will help establish a thorough uncertainty budget and identify the main sources of uncertainty, thereby improving the method's accuracy.

Ensuring the comparability of measurement results over time and space will also require improving metrological traceability with an established link to SI units, which provide the most stable reference. Developing a more straightforward way of quantifying background alkalinity in the artificial reference material, along with the uncertainty estimation of NLLS regression, will be crucial steps toward this goal.

With the development of marine carbon dioxide removal (mCDR) methods, such as ocean alkalinity enhancement (OAE), specific requirements for high data quality and a role for metrology institutes could emerge. This is further discussed in the box below.

Focus on Ocean Alkalinity Enhancement

The Paris agreement, signed at the Conference of the Parties of 2015, aims to limit global warming to 1.5°C. This goal requires a net zero balance between greenhouse gas emissions and removal by sinks. In that objective, carbon dioxide removal (CDR) techniques are being investigated for their potential to sequester anthropogenic CO_2 and mitigate climate change. Ocean Alkalinity Enhancement (OAE), is a marine CDR with an important CO_2 sequestration potential (Oschlies et al., 2023).

OAE involves adding alkalinity to the marine environment, either in the form of crushed-rock feedstock or as a dissolved substance. This addition can come from natural minerals, human-made chemicals, or industrial waste products (NASEM, 2022). This process modifies seawater composition and carbonate system chemical equilibria, leading to a decrease in seawater partial pressure of CO_2. This allows seawater, by equilibrating with air, to absorb more CO_2 from the atmosphere. Additionally, OAE can help mitigate ocean acidification.

However, in addition to technical and logistical challenges, it is essential to address also social, environmental, and ethical considerations before implementing mCDR technologies. Several researchers have raised concerns about deploying such technologies. Few of them are reported below.

(1) The industry associated with ocean alkalinity enhancement relies on mining to provide alkaline mineral feedstock. The expansion of mining activities is suspected to cause several social and environmental impacts (NASEM, 2022).
(2) The effectiveness of mCDR, particularly whether net air-to-sea CO_2 transfer is higher with mCDR than without, called "additionality", still needs to be guaranteed for OAE. It has been suggested by Bach (2024) that anthropogenic alkalinity could reduce the generation of natural alkalinity. Additionally, the carbon footprint of the OAE industry must be thoroughly quantified.
(3) It is crucial that the deployment of mCDR technologies does not detract from the urgent need to drastically reduce CO_2 emissions, to fight climate change and meet the Paris Agreement targets (Anderson et al., 2023). Voget-Kleschin et al. (2024) have emphasized that policy measures promoting societal changes toward lifestyles with lower greenhouse gas emissions are not necessarily ethically problematic and offer important co-benefits. The authors suggest that this consideration should be factored into discussions about how to respond to climate change, potentially leading to a reassessment of the need for carbon dioxide removal techniques, thus reducing the need for large-scale CDR.

These social, environmental and ethical considerations must be thoroughly investigated before an eventual implementation of OAE and other CDR techniques, however, the discussion will here focus on the metrological needs that may arise with the development of OAE.

Indeed, implementing an Ocean Alkalinity Enhancement system is complex and requires thorough investigation before large-scale deployment. It is crucial to ensure (1) the efficiency of long-term CO_2 sequestration, (2) the absence of secondary precipitation, and (3) the absence of biochemical and ecological side effects.

To address these considerations and determine the amount of CO_2 removed from the atmosphere, a robust monitoring, reporting, and verification (MRV) system for

marine carbon dioxide removal needs to be designed, with explicit uncertainty budgets (Ho et al., 2023). Total alkalinity measurements are recommended for assessing ocean alkalinity enhancement for several reasons (Iglesias-Rodríguez et al., 2023). They allow a short-term check to quantify background alkalinity before implementation and to evaluate the efficient addition of alkalinity to seawater. Combined with another variable of the carbonate system, they can also help computing essential carbonate chemistry parameters, which are useful for validating numerical models used in OAE efficiency assessments.

Acquiring accurate and robust data on seawater total alkalinity is thus highly relevant, and the MRV system should rely on comparable measurement results and integrate metrological considerations. Furthermore, OAE may necessitate measuring alkalinity levels above the usual natural TA values (Schulz et al., 2023). Having an artificial reference material that can be produced for any desired total alkalinity reference value might, therefore, be relevant. The diffusion of the added alkalinity in the open ocean will lead to very small variations in total alkalinity. These variations will be assessed using numerical models but should also be confirmed as much as possible with measurements to validate and give confidence in the models, representing a real metrological challenge.

OAE activities and mCDR, in general, will be subject to legal frameworks to ensure safe and responsible implementation. These frameworks will vary across national legal systems, but international laws such as the London Convention and Protocol offer a minimal set of rules (Steenkamp and Webb, 2023). Legal considerations will depend on whether the OAE is used for research or commercial purposes, an issue that is becoming increasingly urgent with the growing number of field trials, as experienced within the Ocean Alk-Align project (Oberlander et al., 2024). In the perspective of large-scale OAE implementation, legal metrology may play a role in ensuring compliance.

Legal metrology aims to enable states to establish effective, mutually compatible, and internationally recognized infrastructures, facilitating trade and harmonizing levels of protection for citizens and the environment. Legislation on legal metrology is one of the pillars of the single market for goods.

Given these considerations, the application of metrological tools to total alkalinity measurements may become increasingly important in the coming years.

References

Anderson, K., Buck, H.J., Fuhr, L., Geden, O., Peters, G.P., Tamme, E., 2023. Controversies of carbon dioxide removal. Nat Rev Earth Environ 4, 808–814. https://doi.org/10.1038/s43017-023-00493-y

Bach, L.T., 2024. The additionality problem of ocean alkalinity enhancement. Biogeosciences 21, 261–277. https://doi.org/10.5194/bg-21-261-2024

Clegg, S.L., Humphreys, M.P., Waters, J.F., Turner, D.R., Dickson, A.G., 2022. Chemical speciation models based upon the Pitzer activity coefficient equations, including the propagation of uncertainties. II. Tris buffers in artificial seawater at 25 °C, and an assessment of the seawater 'Total' pH scale. Marine Chemistry 244, 104096. https://doi.org/10.1016/j.marchem.2022.104096

DeGrandpre, M.D., Spaulding, R.S., et al., 2014. Considerations for the measurement of spectrophotometric pH for ocean acidification and other studies. Limnology and Oceanography: Methods 12, 830–839. https://doi.org/10.4319/lom.2014.12.830

DelValls, T.A., Dickson, A.G., 1998. The pH of buffers based on 2-amino-2-hydroxymethyl-1,3-propanediol ('tris') in synthetic sea water. Deep Sea Research Part I: Oceanographic Research Papers 45, 1541–1554. https://doi.org/10.1016/S0967-0637(98)00019-3

Dickson, A.G., Afghan, J.D., Anderson, G.C., 2003. Reference materials for oceanic CO2 analysis: a method for the certification of total alkalinity. Marine Chemistry 80, 185–197. https://doi.org/10.1016/S0304-4203(02)00133-0

Gattuso, J.-P., Epitalon, J.-M., Lavigne, H., Orr, J., 2021. seacarb: seawater carbonate chemistry. R package: version 3.3.1. https://doi.org/10.5281/zenodo.595096

GOA-ON, 2019. Global Ocean Acidification Observing Network (GOA-ON): Implementation Strategy.

Harrould-Kolieb, E.R., Hoegh-Guldberg, O., 2019. A governing framework for international ocean acidification policy. Marine Policy 102, 10–20. https://doi.org/10.1016/j.marpol.2019.02.004

Ho, D.T., Bopp, L., Palter, J.B., Long, M.C., Boyd, P., Neukermans, G., Bach, L., 2023. Monitoring, Reporting, and Verification for Ocean Alkalinity Enhancement (preprint). https://doi.org/10.5194/sp-2023-2

Humphreys, M.P., Lewis, E.R., Sharp, J.D., Pierrot, D., 2022. PyCO2SYS v1.8: marine carbonate system calculations in Python. Geoscientific Model Development 15, 15–43. https://doi.org/10.5194/gmd-15-15-2022

Iglesias-Rodríguez, M.D., Rickaby, R.E.M., Singh, A., Gately, J.A., 2023. Laboratory experiments in ocean alkalinity enhancement research. State of the Planet 2-oae2023, 1–18. https://doi.org/10.5194/sp-2-oae2023-5-2023

IOC, SCOR, UNESCO, 2010. The international thermodynamic equation of seawater – 2010: Calculation and use of thermodynamic properties [WWW Document]. URL https://www.teos-10.org/ (accessed 2.13.24).

ISO 17034, 2016. General requirements for the competence of reference material producers.

ISO 21748, 2017. Guidance for the use of repeatability, reproducibility and trueness estimates in measurement uncertainty evaluation.

ISO Guide 35:2017 Reference materials — Guidance for characterization and assessment of homogeneity and stability, 2017.

JCGM 100:2008, 2008. Evaluation of Measurement Data-Guide to the Expression of Uncertainty in Measurement.

Liu, X., Patsavas, M.C., Byrne, R.H., 2011. Purification and Characterization of meta-Cresol Purple for Spectrophotometric Seawater pH Measurements. Environmental science & Technology 4862–4868.

Müller, J.D., Bastkowski, F., Sander, B., Seitz, S., Turner, D.R., Dickson, A.G., Rehder, G., 2018. Metrology for pH Measurements in Brackish Waters—Part 1: Extending Electrochemical pHT Measurements of TRIS Buffers to Salinities 5–20. Front. Mar. Sci. 5, 176. https://doi.org/10.3389/fmars.2018.00176

NASEM, 2022. A Research Strategy for Ocean-based Carbon Dioxide Removal and Sequestration. National Academies Press, Washington, D.C. https://doi.org/10.17226/26278

Oberlander, J., Atamanchuk, D., Bach, L., Fennel, K., Hartmann, J., Keller, D.P., Mihailova, B., Musgrave, R., Oschlies, A., Riebesell, U., Schulz, K.G., Wallace, D., 2024. Ocean Alk-Align: an international research project to assess the potential of Ocean Alkalinity Enhancement for marine Carbon Dioxide Removal (No. EGU24-438). Presented at the EGU24, Copernicus Meetings. https://doi.org/10.5194/egusphere-egu24-438

Orr, J.C., Epitalon, J.-M., Dickson, A.G., Gattuso, J.-P., 2018. Routine uncertainty propagation for the marine carbon dioxide system. Marine Chemistry 207, 84–107. https://doi.org/10.1016/j.marchem.2018.10.006

Oschlies, A., Bach, L.T., Rickaby, R.E.M., Satterfield, T., Webb, R., Gattuso, J.-P., 2023. Climate targets, carbon dioxide removal, and the potential role of ocean alkalinity enhancement. State of the Planet 2-oae2023, 1–9. https://doi.org/10.5194/sp-2-oae2023-1-2023

Patsavas, M.C., Byrne, R.H., Liu, X., 2013. Purification of meta-cresol purple and cresol red by flash chromatography: Procedures for ensuring accurate spectrophotometric seawater pH measurements. Marine Chemistry 150, 19–24. https://doi.org/10.1016/j.marchem.2013.01.004

Schulz, K.G., Bach, L.T., Dickson, A.G., 2023. Seawater carbonate chemistry considerations for ocean alkalinity enhancement research: theory, measurements, and calculations. State of the Planet 2-oae2023, 1–14. https://doi.org/10.5194/sp-2-oae2023-2-2023

Seitz, S., Feistel, R., Wright, D.G., Weinreben, S., Spitzer, P., De Bièvre, P., 2011. Metrological traceability of oceanographic salinity measurement results. Ocean Science 7, 45–62. https://doi.org/10.5194/os-7-45-2011

Steenkamp, R.C., Webb, R., 2023. Legal considerations relevant to research on ocean alkalinity enhancement. State of the Planet 2-oae2023, 1–19. https://doi.org/10.5194/sp-2-oae2023-10-2023

United Nations, 2015. Transforming our world: the 2030 Agenda for Sustainable Development A/RES/70/1.

Voget-Kleschin, L., Baatz, C., Heyward, C., Vuuren, D.V., Mengis, N., 2024. Reassessing the need for carbon dioxide removal: moral implications of alternative climate target pathways. Global Sustainability 7, e1. https://doi.org/10.1017/sus.2023.21

Appendix

S.3. Supplementary material of chapter III

S3.1: Repartition of Harned cell measurements among the three NMIs

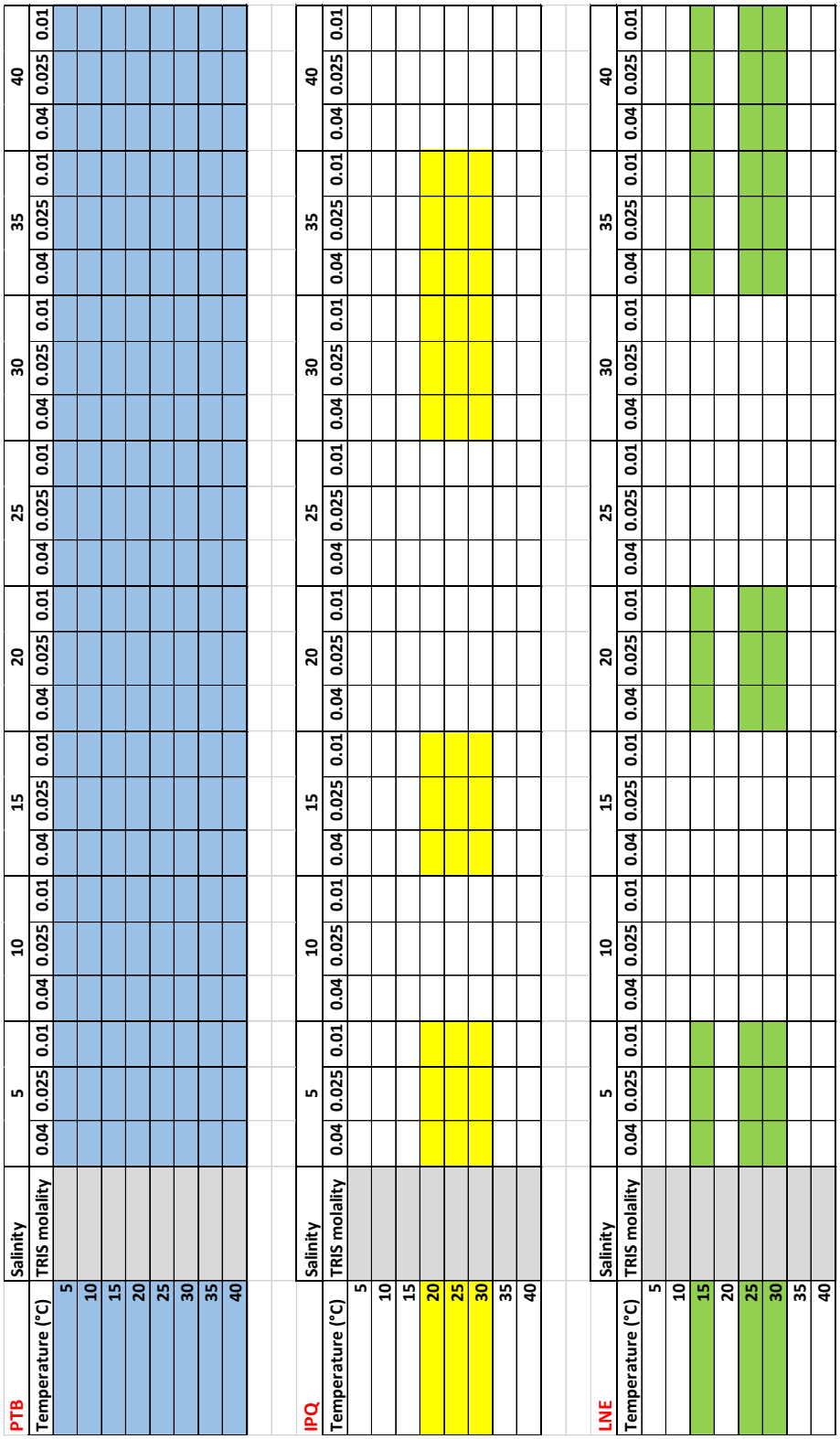

S3.2: Information from coulometric characterization of the salts used for the TRIS buffers preparation

Material for ASW preparation	Mass fraction/ %, or molar amount content/ mol/ kg ± uncertainty (k= 2)	Impurities/ mg/ kg ± uncertainty (k= 2)	Method/ Comments/ Instructions
NaCl, dried 3 h at 110 °C	99.842 ± 0.036 % (chloride coulometry)	Br^-: 25 ± 14 mg/kg SO_4^{2-}: 7 ± 4 mg/kg	Coulometric argentimetric titration. Mass fraction based on halide content See certificate of analysis 03947-640-045-22,
KCl, dried 3 h at 110 °C	99.880 ± 0.036 %	Br^-: 3.3 ± 8 mg/kg SO_4^{2-}: 0 ± 4 mg/kg	Coulometric argentimetric titration. Mass fraction based on halide content See certificate of analysis 03948-640-045-22,
Na_2SO_4, dried 3 h at 110 °C	99.999 ± 0.027 %	Cl^-: 0 ± 4 mg/kg Br^-: 0.5 ± 3 mg/kg	Coulometric acid-base titration. See certificate of analysis 03951-640-45-22,
$CaCl_2$ stock solution	1. charge: 0.51586 ± 0.00018 $mol \cdot kg^{-1}$ 2. charge: 0.58727 ± 0.00022 $mol \cdot kg^{-1}$	Br^-: 1.0 ± 0.6 mg/kg SO_4^{2-}: 1.3 ± 0.6 mg/kg	Coulometric argentimetric titration. See certificate of analysis 03949-640-045-22 (1. charge) and 05417-640-045-23 (2. charge),
$MgCl_2$ stock solution	1. charge: 1.42294 ± 0.00058 $mol \cdot kg^{-1}$ 2. charge: 1.46098 ± 0.00052 $mol \cdot kg^{-1}$	Br^-: 2.6 ± 1.9 mg/kg SO_4^{2-}: 0.3 ± 1 mg/kg	Coulometric argentimetric titration. See certificate of analysis 03950-640-045-22 (1. charge) and 05418-640-045-23 (2. charge),
HCl	1. batch: 0.106494 ± 0.000038 $mol \cdot kg^{-1}$ 2. batch: 0.106470 ± 0.000038 $mol \cdot kg^{-1}$	not investigated	Coulometric acid-base titration at DFM
TRIS SRM 723e	99.925 ± 0.054 %		See certificate of analysis SRM 723e

S3.3: Description of pH_T thermodynamic Harned Cell equations

Electrochemical cell: Pt | H_2 (g) | H^+, Cl^- in ASW | AgCl | Ag

Cathode: $AgCl_{(s)} + e^- \rightarrow Ag_{(s)} + Cl^-_{(aq)}$

Anode: $\frac{1}{2} H_{2(g)} \rightarrow H^+_{(aq)} + e^-$

Nernst: $E = E^\circ + \frac{RT\ ln10}{nF} \lg \left(\frac{a(Ox)}{a(Red)}\right)$

$$E\ cathode = E^\circ_{Ag/AgCl} + \frac{RT\ ln10}{nF} \lg \left(\frac{1}{a(Cl^-)}\right)$$

$$= E^\circ_{Ag/AgCl} + k \lg \left(\frac{1}{b_{Cl^-} \times \gamma_{Cl^-}}\right) \qquad k = \frac{RT\ ln10}{nF}\ for\ n = 1$$

$$= E^\circ_{Ag/AgCl} - k \lg \left(b_{Cl^-} \times \gamma_{Cl^-}\right)$$

$$E\ anode = E^\circ_{H_2} + \frac{RT\ ln10}{n\,F} \lg \left(\frac{a(H^+)}{\frac{p(H_2)1}{2}}\right)$$

$$= k \lg \left(a(H^+) - (pH_2^{1/2})\right) \qquad E^\circ_{H_2} = 0$$

$$= k \lg(b_{H+} \times \gamma_{H+}) - \frac{k}{2} (\lg pH_2) \qquad pH_2 = \frac{p measured - pH_2O + 0.4\,\rho gh}{P^\circ}$$

$$\Delta E = E\ cathode - E\ anode$$

$$= E^\circ_{Ag/AgCl} - k \lg \left(b_{Cl^-} \times \gamma_{Cl^-}\right) - k \lg(b_{H+} \times \gamma_{H+}) + \frac{k}{2} (\lg pH_2) \quad \gamma_{Cl^-} \times \gamma_{H+} = \gamma_{HCl}^{\ 2}$$

$$= E^\circ_{Ag/AgCl} - k \lg \left(b_{Cl^-} \times b_{H+}\right) - 2k \lg(\gamma_{HCl}) + \frac{k}{2} (\lg pH_2) \qquad (S3.3.1)$$

In an ionic medium (noted: *) the following equilibrium occurs: $HSO_4^- \leftrightarrow H^+ + SO_4^{2-}$, this equilibrium is ruled by the dissociation constant $K_b(HSO_4^-)$

$$b^*_{H+} = b_{H+} \times \left(1 + \frac{b^T_{SO_4^{2-}}}{K_b(HSO_4^-)}\right) \qquad \approx b_{H+} + b_{HSO_4^-}$$

where: $K_b(HSO_4^-) = \lim_{b_{H+} \to 0} \left(\frac{b_{H+} \times b_{SO_4^{2-}}}{b_{HSO_4^-}}\right)$

$$\rightarrow b_{H+} = \frac{b^*_{H+}}{\left(1+\frac{b^T_{SO_4^{2-}}}{K_b(HSO_4^-)}\right)} \qquad \text{(S3.3.2)}$$

(S3.3.2) → (S3.3.1)

$$E = E°_{Ag/AgCl} - k \lg \left(b_{Cl-} \times \frac{b^*_{H+}}{\left(1+\frac{b^T_{SO_4^{2-}}}{K_b(HSO_4^-)}\right)}\right) - 2k \lg(\gamma_{HCl}) + \frac{k}{2} (\lg pH_2)$$

$$= E°_{Ag/AgCl} - k \lg (b_{Cl-} \times b^*_{H+}) + k \lg \left(1 + \frac{b^T SO_4^{2-}}{K_b(HSO_4^-)}\right) - 2k \lg(\gamma_{HCl}) + \frac{k}{2} (\lg pH_2)$$

(S3.3.3)

Unknown in the equation: $E°_{Ag/AgCl} + k \lg \left(1 + \frac{b^T SO_4^{2-}}{K_b(HSO_4^-)}\right) - 2k \lg(\gamma_{HCl})$

Step to determine the unknowns in the equation (S3.3.3) : E°* determination

In a solution of known HCl molality, b_{HCl}, in ASW matrix we have:

$b_{HCl} = b_{H+} + b_{HSO_4^-} - b_{OH^-}$ $\qquad b_{OH^-} = 0$ in acidic solution $\qquad$ (S3.3.4)

$b_{H+} = b_{HCl} - b_{HSO_4^-}$

We note $Q_b(HSO_4^-)$ the molality ratio $\frac{b_{H+} \times b_{SO_4^{2-}}}{b_{HSO_4^-}}$

$$b_{HSO_4^-} = \frac{b_{H+} \times b_{SO_4^{2-}}}{Q_b(HSO_4^-)} \qquad \text{(S3.3.5)}$$

(S3.3.5) → (S3.3.4)

$$b_{HCl} = b_{H+} + \frac{b_{H+} \times b_{SO_4^{2-}}}{Q_b(HSO_4^-)} = b_{H+} \times \left(1 + \frac{b_{SO_4^{2-}}}{Q_b(HSO_4^-)}\right)$$

$$b_{H+} = \frac{b_{HCl}}{1+\frac{b_{SO_4^{2-}}}{Q_b(HSO_4^-)}} \qquad \text{(S3.3.6)}$$

(S3.3.6) → (S3.3.1)

$$E = E°_{Ag/AgCl} - k \lg \left(b_{Cl-} \times \frac{b_{HCl}}{1+\frac{b_{SO_4^{2-}}}{Q_b(HSO_4^-)}}\right) - 2k \lg (\gamma_{HCl}) + \frac{k}{2} (\lg pH_2)$$

$$= E°_{Ag/AgCl} - k \lg (b_{Cl-} \times b_{HCl}) + k \lg \left(1 + \frac{b_{SO_4^{2-}}}{Q_b(HSO_4^-)}\right) - 2k \lg (\gamma_{HCl}) + \frac{k}{2} (\lg pH_2)$$

(S3.3.7)

For a molality of HCl tending towards 0 ($b_{HCl} \to 0$) we have:

- $Q_b(HSO_4^-) = K_b(HSO_4^-)^{trace}$
- $b_{SO_4^{2-}} = b^T_{SO_4^{2-}}$
- $\gamma_{HCl} = {\gamma_{HCl}}^{trace}$

$\to$ (S.3.3.7).

$$E = E^\circ_{Ag/AgCl} - k \lg (b_{Cl^-} \times b_{HCl}) + k \log \left(1 + \frac{b^T_{SO_4^{2-}}}{K_b(HSO_4^-)^{trace}}\right) - 2k \lg ({\gamma_{HCl}}^{trace}) + \frac{k}{2} (\lg pH_2)$$

$$E + k \lg (b_{Cl^-} \times b_{HCl}) - \frac{k}{2} (\lg pH_2) = \lim_{bH \to 0} \left(E^\circ_{Ag/AgCl} + k \lg \left(1 + \frac{b^T_{SO_4^{2-}}}{K_b(HSO_4^-)^{trace}}\right) - 2k \lg ({\gamma_{HCl}}^{trace})\right)$$

E' (at a given bHCl) $\qquad$ E°*

$$E^{0*} - k \lg \left(1 + \frac{b^T_{SO_4^{2-}}}{K_b(HSO_4^-)^{trace}}\right) + 2k \lg({\gamma_{HCl}}^{trace}) = E°Ag/AgCl \qquad (S3.3.8)$$

(S3.3.8) $\to$ (S3.3.3)

$$E = E^{0*} - k \lg \left(1 + \frac{b^T_{SO_4^{2-}}}{K_b(HSO_4^-)^{trace}}\right) + 2k \lg({\gamma_{HCl}}^{trace}) - k \lg (b_{Cl^-} \times b^*_{H+}) + k\, lg\left(1 + \frac{b^T_{SO_4^{2-}}}{K_b(HSO_4^-)}\right) - 2k \lg (\gamma_{HCl}) + \frac{k}{2} (\lg pH_2)$$

$$E - \frac{k}{2} (\lg pH_2) - E^{0*} = -k \lg (b_{Cl^-} \times b^*_{H+}) + 2k \lg \left(\frac{{\gamma_{HCl}}^{trace}}{\gamma_{HCl}}\right) + k\, lg\left(\frac{1 + \frac{b^T_{SO_4^{2-}}}{K_b(HSO_4^-)}}{1 + \frac{b^T_{SO_4^{2-}}}{K_b(HSO_4^-)^{trace}}}\right)$$

$\div$ k

$$\frac{E - \frac{k}{2} (\lg pH_2) - E^{0*}}{k} = -\lg (b_{Cl^-} \times b^*_{H+}) + 2 \lg \left(\frac{{\gamma_{HCl}}^{trace}}{\gamma_{HCl}}\right) + lg\left(\frac{1 + \frac{b^T_{SO_4^{2-}}}{K_b(HSO_4^-)}}{1 + \frac{b^T_{SO_4^{2-}}}{K_b(HSO_4^-)^{trace}}}\right)$$

$$\frac{E - \frac{k}{2} (\lg pH_2) - E^{0*}}{k} + \lg (b_{Cl^-}) - 2 \lg \left(\frac{{\gamma HCl}^{trace}}{\gamma HCl}\right) - lg\left(\frac{1 + \frac{b^T_{SO_4^{2-}}}{K_b(HSO_4^-)}}{1 + \frac{b^T_{SO_4^{2-}}}{K_b(HSO_4^-)^{trace}}}\right) = -\lg (b^*_{H+}) = pH_T$$

b^*_{H+} is defined here in mol/kg H_2O. To be comparable with the pH_T measured spectrophotometrically, it must be defined in mol/kg sol.

b^*_{H+} (mol/kg H_2O) = $b^*_{H+} \times \omega_{H2O}$ (mol/kg sol)

$$pH_T = \underbrace{\frac{E-\frac{k}{2}(\lg \mathrm{pH2})-E^{0*}}{k} + \lg\,(b_{Cl^-}) - 2\lg\left(\frac{\gamma HCl^{trace}}{\gamma HCl}\right) - lg\left(\frac{1+\frac{b^T SO_4^{2-}}{Kb(HSO_4^-)}}{1+\frac{b^T SO_4^{2-}}{Kb(HSO_4^-)^{trace}}}\right)}_{\text{Operational } pH_T,m} - \lg\,(\omega_{H2O})$$

Conventional thermodynamic $pH^*_{T,m}$

Established based on:

Clegg, S.L., Humphreys, M.P., Waters, J.F., Turner, D.R., Dickson, A.G., 2022. Chemical speciation models based upon the Pitzer activity coefficient equations, including the propagation of uncertainties. II. Tris buffers in artificial seawater at 25 °C, and an assessment of the seawater 'Total' pH scale. Marine Chemistry 244, 104096. https://doi.org/10.1016/j.marchem.2022.104096

Dickson, A.G., 1993. pH buffers for sea water media based on the total hydrogen ion concentration scale. Deep Sea Research Part I: Oceanographic Research Papers 40, 107–118. https://doi.org/10.1016/0967-0637(93)90055-8

Dickson, A.G., 1990. Standard potential of the reaction: AgCl(s) + 12H2(g) = Ag(s) + HCl(aq), and and the standard acidity constant of the ion HSO4− in synthetic sea water from 273.15 to 318.15 K. The Journal of Chemical Thermodynamics 22, 113–127. https://doi.org/10.1016/0021-9614(90)90074-Z

Dickson, A.G., 1984. pH scales and proton-transfer reactions in saline media such as sea water. Geochimica et Cosmochimica Acta 48, 2299–2308. https://doi.org/10.1016/0016-7037(84)90225-4

Dickson, A.G., Camões, M.F., Spitzer, P., Fisicaro, P., Stoica, D., Pawlowicz, R., Feistel, R., 2016. Metrological challenges for measurements of key climatological observables. Part 3: seawater pH. Metrologia 53, R26. https://doi.org/10.1088/0026-1394/53/1/R26

Khoo, K.H., Ramette, R.W., Culberson, C.H., Bates, R.G., 1977. Determination of Hydrogen Ion Concentrations in Seawater from 5 to 40 °C: Standard Potentials at Salinities from 20 to 45‰. Analytical Chemistry 49, 29–34.

S3.4: Data processing of the fit function

The data processing used for the computation of the fit function was done with R (R Core Team, version: 4.3.2 (R Core Team, 2023)). Key packages with their versions are listed in Table S3.4. A custom R package, that combined many of the functions needed, was developed.

Table S3.4 Overview of the key packages used in R with their version number and respective main use. AIC – Akaike Information Criterion, RMSE – root-mean-squared-error.

Package	Use	Version	Citation
MASS	Stepwise model selection by AIC	7.3.61	Venables and Ripley (2002)
metafor	Uncertainty of extrapolations	4.6.0	Viechtbauer (2010)
metRology	Uncertainties following GUM ("JCGM 100:2008," 2008)	0.9.28.1	Ellison (2018)
mltools	Weighted RMSE	0.3.5	Gorman (2018)
tidymodels bundle	Leave-one-out cross-validation	1.1.1	Kuhn and Wickham (2020)
tidyverse bundle	Data processing	2.0.0	Wickham et al. (2019)

For the determination of E°*, each measured potential E'_m with *cell I*, corrected to a pressure of H_2 equal to 1 atm, was used to calculated E' from equation (S3.4.1).

$$E' = E'_m + \frac{R*T*\ln(10)}{F} * \log\frac{b(\mathrm{HCl})*b(\mathrm{Cl})}{b_0} \quad \text{(S3.4.1)}$$

where F is the Faraday constant (C/mol), R the Gas constant (J/mol.K), T the measured temperature (K), $b(\mathrm{HCl})$ the molality of HCl, $b(\mathrm{Cl})$ the molality of Cl^- and b_0 the standard molality (mol/kg H_2O) (Müller et al., 2018).

Each E^{0*} value was determined from a quadratic fit function fitted through the E' values and the corresponding molalities b(HCl):

$$E' = \alpha_0 + \alpha_1 * b(\mathrm{HCl}) + \alpha_2 * b(\mathrm{HCl})^2 \quad \text{(S3.4.2)}$$

with α_0, α_1, and α_2 being the fit parameters. E^{0*} was then determined as the value of the fit function at $b(HCl) = 0\ \mathrm{mol/kg}$. The E' values were weighted with $\frac{1}{u(E')^2}$, and $u(E')$ being the standard uncertainties of the measured *E'* values. Equation S3.4.2 was fitted with *metafor::rma* (Viechtbauer, 2010)

The pH_T values were calculated at each salinity and temperature with equation 1.10.a (DelValls and Dickson, 1998). Additional to the input values needed to calculate pH_T, salinity and temperature must be assigned to each pH_T value for the subsequent fitting. Temperatures were measured during the Harned cell measurements and salinities were calculated from gravimetric preparations.

Finally, the uncertainty weighted mean pH_T value was calculated to get a single value for the regression of the fit function if more than one institute had measured at the same salinity and temperature.

For the fit we used the *glm* function and weighted the pH_T values with $\frac{1}{u(pH_T)^2}$. The *stepAIC* function was used to do stepwise model selection based on the Akaike Information Criterion (AIC) (Venables and Ripley, 2002). The number of necessary digits in the coefficients given in Table 10 was determined by checking with how many digits the calculated pH_T value of the function stabilised.

The robustness of the function was tested by doing a leave-one-out cross-validation and using all fits to calculate the predicted values under each initial condition. The spread of those predicted values was compared to the root-mean-squared-error (RMSE) of the fits. These fits were based on the stepwise selected model.

Established based on:

Ellison, S.L.R., 2018. metRology: Support for Metrological Applications. r package version 0.9-28-1.

Gorman, B., 2018. mltools: Machine Learning Tools. r package version 0.3.5.

JCGM 100:2008, 2008. Evaluation of Measurement Data-Guide to the Expression of Uncertainty in Measurement.

Kuhn, M., Wickham, H., 2020. Tidymodels: a collection of packages for modeling and machine learning using tidyverse principles.

R Core Team, 2023. R: A Language and Environment for Statistical Computing. R Foundation for Statistical Computing Vienna, Austria.

Venables, W.N., Ripley, B.D., 2002. Modern Applied Statistics with S. Springer, New York., iSBN 0-387-95457-0. Fourth ed.

Viechtbauer, W., 2010. Conducting Meta-Analyses in R with the metafor Package. Journal of Statistical Software 36, 1–48. https://doi.org/10.18637/jss.v036.i03

Wickham, H., Averick, M., Bryan, J., Chang, W., McGowan, L.D., François, R., Grolemund, G., Hayes, A., Henry, L., Hester, J., Kuhn, M., Pedersen, T.L., Miller, E., Bache, S.M., Müller, K., Ooms, J., Robinson, D., Seidel, D.P., Spinu, V., Takahashi, K., Vaughan, D., Wilke, C., Woo, K., Yutani, H., 2019. Welcome to the Tidyverse. Journal of Open Source Software 4, 1686. https://doi.org/10.21105/joss.01686

S4.1: Calibration certificate of Hellma filters F1, F2, F3, F4 and F7 issued by DFM (Danish Metrology Institute)

DFM
Danish National Metrology Institute

DFM A/S
Kogle Allé 5, 2970 Hørsholm, Denmark
Tlf. +45 7730 5800 | www.dfm.dk

DANAK
CAL Reg nr. 255

Calibration certificate

Calibration of regular absorbance

Customer	Sappties Consortium

Device ID	
Device type	Hellma filters F2, F3, F4

The measurements were performed at a room temperature of 22 °C ± 1 °C.

The calibration is performed using the illuminance ratio method defined in CIE 130-1998.

The calibration is verified with reference standards for regular absorbance calibrated at MIKES in Finland.

The wavelength calibration is traceable to DFM's realization of the meter.

The reported uncertainty is given as the standard uncertainty multiplied with a coverage factor k= 2, which for a normal distribution results in a coverage factor of approximately 95%. The standard uncertainty is determined in accordance with EAL-R2.

Measurements at wavelengths 434 nm, 578 nm and 730 nm were performed with a measurement bandwidth of 1,8 nm.

Absorbance [OD]

	Wavelength		
Filter	434 nm	578 nm	730 nm
F2	0,270 ± 0,005	0,279 ± 0,005	0,233 ± 0,005
F3	0,531 ± 0,005	0,535 ± 0,006	0,414 ± 0,005
F4	1,078 ± 0,019	1,053 ± 0,010	0,770 ± 0,008

Date: 2023-10-09

Ph.D. Anders Brusch

DFM
Danish National Metrology Institute

DANAK
CAL Reg nr 265

DFM A/S
Kogle Allé 5, 2970 Hørsholm, Denmark
Tlf. +45 7730 5800 | www.dfm.dk

Measurements at wavelengths 434 nm, 578 nm and 730 nm were performed with a measurement bandwidth of 1,8 nm.

Measurements at of wavelength references F1 and F7 were performed with a measurement bandwidth of 1,0 and 1,8 nm

The uncertainty on the wavelength calibration of the F1 Holmium filter is ± 0,2 nm.

The uncertainty on the wavelength calibration of the F7 Didynium filter is ± 0,5 nm.

Wavelength calibration

Holmium glass filter F1			
Nominal wavelength	453,55 nm	536,35 nm	637,6 nm
Measured 1 nm BW	453,5 nm	536,4 nm	637,8 nm
Measured 1,8 nm BW	453,4 nm	536,3 nm	637,7 nm

Didymium glass filter F7			
Nominal wavelength	472 nm	512 nm	681 nm
Measured 1 nm BW	472,0 nm	512,2 nm	681,2 nm
Measured 1,8 nm BW	471,8 nm	512,1 nm	681,1 nm

S4.2: Transmittance maximum discrepancy between reproducibility measurements (conducted at Ifremer for the calibration of a Cary 60 spectrophotometer) represented in function of the corresponding level of transmittance. The maximised linear relation was used for the determination of the uncertainty of noise and reproducibility.

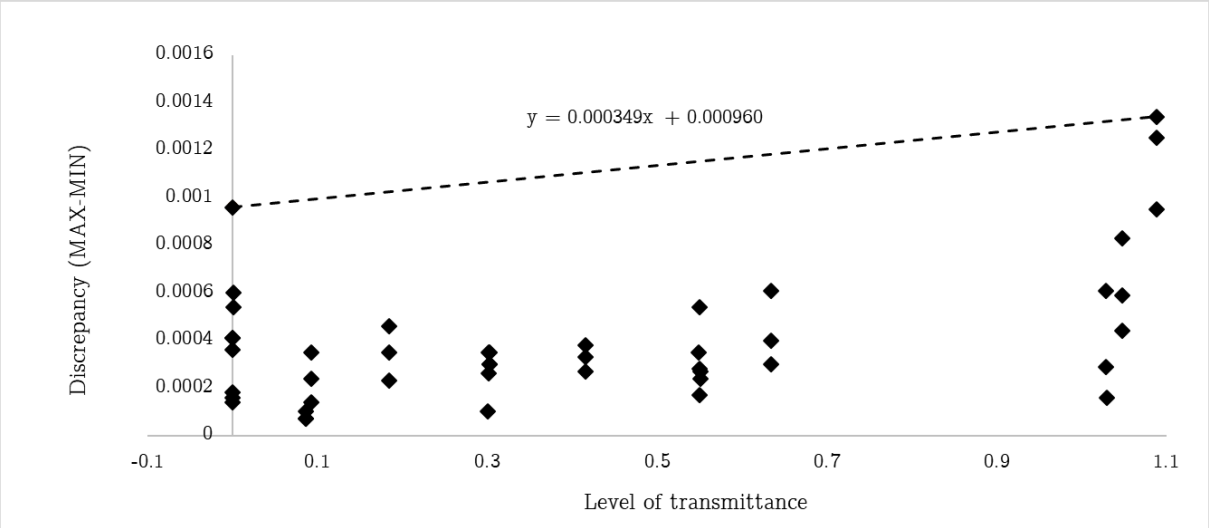

S4.3: Bias uncertainty in function of the level of transmittance obtained from LNE spectrophotometer optical density calibration. The maximised linear relation computed from these results was used for the determination of the bias uncertainty for transmittance values corresponding to an actual pH_T measurement.

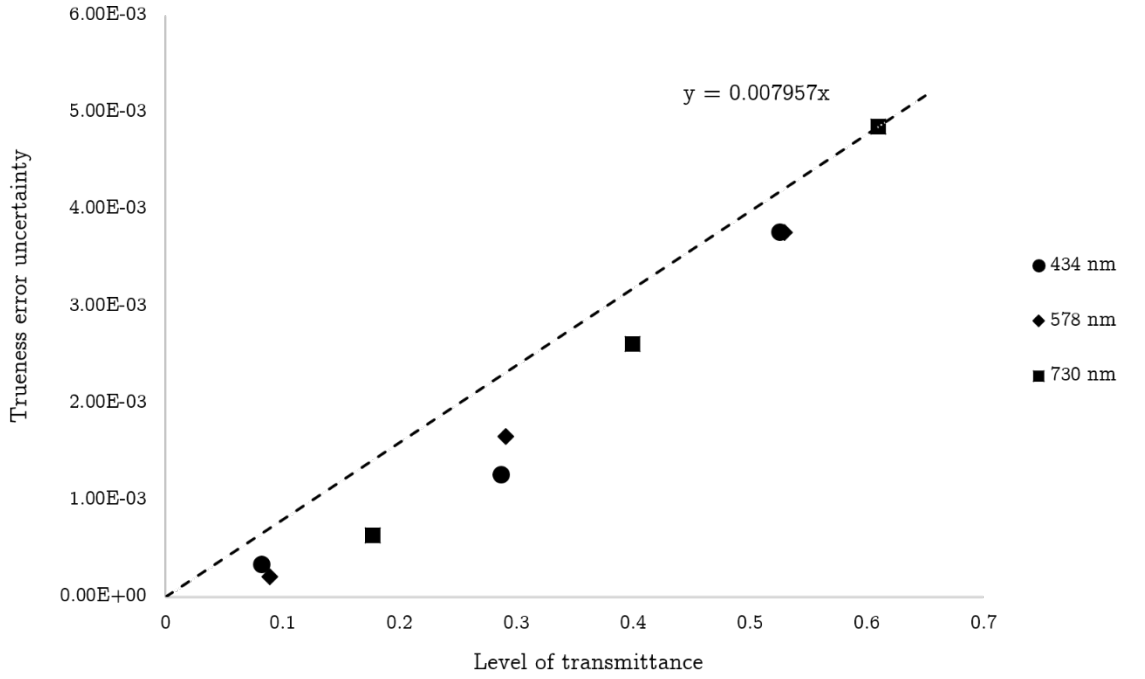

S4.4: Correlation matrix of the trueness. Where the colour gradient gives the importance of the correlation, with 1 being a complete correlation.

	T434,background	T578,background	T730,background	T434,mCP	T578,mCP	T730,mCP	T434,mCPx2	T578,mCPx2	T730,mCPx2
T434,background	1.00								
T578,background	0.90	1.00							
T730,background	0.90	0.90	1.00						
T434,mCP	0.50	0.50	0.50	1.00					
T578,mCP	0.50	0.50	0.50	0.50	1.00				
T730,mCP	0.90	0.90	0.90	0.50	0.50	1.00			
T434,mCPx2	0.50	0.50	0.50	0.50	0.70	0.50	1.00		
T578,mCPx2	0.50	0.50	0.50	0.50	0.50	0.50	0.50	1.00	
T730,mCPx2	0.90	0.90	0.90	0.50	0.50	0.90	0.50	0.50	1.00

S4.5: Global covariance matrix of the nine transmittance values to be considered for a pH_T measurement performed at LNE on an equimolal TRIS buffer (pH_T 8.1, S35).

	$T_{434,background}$	$T_{578,background}$	$T_{730,background}$	$T_{434,mCP}$	$T_{578,mCP}$	$T_{730,mCP}$	$T_{434,mCPx2}$	$T_{578,mCPx2}$	$T_{730,mCPx2}$
$T_{434,background}$	5.21E-05								
$T_{578,background}$	4.78E-05	5.50E-05							
$T_{730,background}$	4.12E-05	4.23E-05	4.18E-05						
$T_{434,mCP}$	1.11E-05	1.14E-05	9.82E-06	9.65E-06					
$T_{578,mCP}$	3.62E-06	3.71E-06	3.24E-06	1.75E-06	1.53E-06				
$T_{730,mCP}$	4.11E-05	4.22E-05	3.64E-05	9.85E-06	3.28E-06	4.17E-05			
$T_{434,mCPx2}$	4.94E-06	5.06E-06	4.41E-06	2.26E-06	1.17E-06	4.40E-06	2.30E-06		
$T_{578,mCPx2}$	7.90E-07	8.02E-07	7.38E-07	5.29E-07	3.99E-07	7.38E-07	4.63E-07	6.95E-07	
$T_{730,mCPx2}$	4.11E-05	4.22E-05	3.64E-05	9.81E-06	3.24E-06	3.64E-05	4.44E-06	7.79E-07	4.17E-05

S.5. Supplementary material of chapter V

S5.1: Total Alkalinity measurement results of all participants to the ILC (µmol/kg-sol)

	Laboratory	1		2		3		4		5	
Artificial reference material - Batch 1	Time after solution preparation (months)	Mean	SD	Mean	SD	Mean	SD	Mean	SD	Mean	SD
	2	2514.6	4.9	2503.1	1.1	2501.6	2.4	2500.4	0.3	2499.2	4.6
	5	2516.8	0.7			2502.1	1.6	2499.2	1.8	2487.5	0.5
	8	2506.5	0.7			2506.5	0.6	2510.5	1.2	2522.5	3.4
	11	2507.1	1.9			2510.2	1.9	2505.4	1.3	2502.8	5.8

	Laboratory	LNE	
Artificial reference material - Batch 2	Time after solution preparation (months)	Mean	SD
	2	2503.7	0.6
	5	2504.6	1.5
	8	2509.3	0.6
	11	2512.9	0.7
	14	2513.5	2.3

	Laboratory	1		2		3		4		5	
Natural Reference Material	Time after solution sampling (months)	Mean	SD	Mean	SD	Mean	SD	Mean	SD	Mean	SD
	3.5	2595.3	3.2	2580.3	1.6	2581.4	0.9	2580.2	2.5	2592.3	2.3
	6.5	2593.3	0.4			2583.5	0.9	2582.0	1.4	2573.5	1.4
	9.5	2592.5	0.6	2583.7	1.6	2581.2	0.4	2588.13	0.57	2603.4	5.9
	12.5	2590.5	0.6	2590.3	1.0	2589.7	1.4	2587.0	0.7	2573.5	0.3
	15.5	2580.3	1.8			2582.0	1.8	2585.1	2.2	2577.4	0.8

S5.2: pH_T spectrophotometric measurement results of all participants to the ILC

	Laboratory	1		3		4		5	
Artificial reference material - Batch 1	Time after solution preparation (months)	Mean	SD	Mean	SD	Mean	SD	Mean	SD
	2	8.2371	0.0052	8.2221	0.0034	8.2044	0.0017		
	5	8.2205	0.0009	8.2260	0.0004	8.2234	0.0086	8.1940	0.0020
	8	8.2210	0.0060	8.2253	0.0005	8.2063	0.0012	8.1960	0.0000
	11	8.2204	0.0105	8.2109	0.0005	8.2019	0.0051		

	Laboratory	LNE	
Artificial reference material - Batch 2	Time after solution preparation (months)	Mean	SD
	2	8.188	0.0007
	5	8.190	0.0012
	8	8.185	0.0028
	11	8.163	0.0032
	14	8.181	0.0014

	Laboratory	1		3		4		5	
Natural Reference Material	Time after solution sampling (months)	Mean	SD	Mean	SD	Mean	SD	Mean	SD
	3.5	7.7863	0.0007	7.8042	0.0008	7.8100	0.0017		
	6.5	7.7961	0.0005	7.8032	0.0004	7.8044	0.0009	7.7930	0.0030
	9.5	7.8071	0.0009	7.7980	0.0003	7.8033	0.0006	7.7840	0.0010
	12.5	7.7898	0.0002	7.7947	0.0015	7.8023	0.0002		
	15.5	7.7816	0.0011	7.7986	0.0009	7.7990	0.0040	7.7890	0.0010

S5.3: Dissolved Inorganic Carbon measurement results performed at the SNAPO-CO_2 (µmol/kg-sol)

	Laboratory	SNAPO-CO_2	
Natural Reference Material	Time after solution sampling (months)	Mean	SD
	3.5	2384.9	1.2
	9.5	2384.4	2.2
	12.5	2385.5	1.1

S5.4: Nutrients measurement results performed at the MIO (µmol/L)

	Laboratory	MIO							
		silicates		nitrites		phosphates		nitrates+nitrites	
Natural Reference Material	Time after solution sampling (months)	Mean	SD	Mean	SD	Mean	SD	Mean	SD
	3.5	12.37	0.10	0.02	0.00	0.40	0.01	9.08	0.03
	12.5	21.94		0.00		0.75		9.32	
	15.5	23.83	0.00	0.01	0.00	0.45	0.01	8.79	0.09

	Laboratory	MIO			
		silicates	nitrites	phosphates	nitrates+nitrites
Artificial Reference Material - Batch 2	Time after solution preparation (months)	Mean	Mean	Mean	Mean
	14	27.13	0.03	0.03	0.4

B: Table of acronyms

ASW	Artificial Seawater
BIPM	International Bureau of Weights and Measures
CBA	Charge Balance Alkalinity
CDR	Carbon Dioxide Removal
CEN	European Committee for Standardisation
CFM	French College of Metrology
CGPM	General Conference of Weights and Measures
CRM	Certified Reference Material
DFM	Danish National Metrology Institute
DIC	Dissolved Inorganic Carbon
EMPIR	European Metrology Programme for Innovation and Research
EURAMET	European Association of National Metrology Institutes
fCO_2	Fugacity of carbon dioxide
GCOS	Global Climate Observing System
GOA-ON	Global Ocean Acidification – Observing Network
GUM	Guide to the expression of Uncertainty in Measurement
Ifremer	French Research Institute for Exploitation of the Sea
ILC	Inter-laboratory comparison
IMAGO	Instrumentation, Analytical Methods, Observatories in Geophysics and Oceanography of the French Institute of Research and Development (IRD)
IOC	Intergovernmental Oceanographic Commission
IPCC	Intergovernmental Panel on Climate Change
IPQ	Instituto Português da Qualidade, Portuguese NMI
ISO	International Organization of Standardisation
IUPAC	International Union of Pure and Applied Chemistry
JCGM	Joint Committee for Guides in Metrology
LNE	Laboratoire National de Métrologie et d'Essais, French NMI

LOV	Villefranche Oceanography Laboratory
mCP	meta-Cresol Purple
MIO	Mediterranean Institute of Oceanography
MRV	Monitoring, Reporting and Verification system
NBS	National Bureau of Standards
NLLS	Nonlinear Least-Squares regression
NMI	National Metrology Institute
NMIJ	National Metrology Institute of Japan
OA	Ocean Acidification
OAE	Ocean Alkalinity Enhancement
pCO_2	Partial pressure of carbon dioxide
pH_T	pH on the total scale
pH_T^*	Thermodynamic definition of the pH on the total scale, amount content-based (Chapter III)
$pH_{T,m}^*$	Thermodynamic definition of the pH on the total scale, molality-based (Chapter III)
PTB	Physikalisch-Technische Bundesanstalt, German NMI
QA/QC	Quality Assurance / Quality Control
RM	Reference Material
RMO	Regional Metrology Organization
SapHTies	Metrology for standardised seawater pH_T measurements in support of international and European climate strategies
SDG	Sustainable Development Goal
SI	International System of units
SMU	Slovak Institute of Metrology
SNAPO-CO_2	French National Service for Analysis of Oceanic CO_2 Parameters
SOMLIT	French National Observation Service for Coastal Environment
TA	Total Alkalinity
TA_{ec}	Explicitly conservative form of total alkalinity
TRIS	2-Amino-2-(hydroxymethyl)-1,3-propanediol

TRIS.HCl	TRIS hydrochloride
VIM	International Vocabulary of Metrology
WMO	World Meteorological Organization

C: Glossary of symbols

General symbols	
K	Dissociation constants
Ω	Saturation state of calcium carbonate
u	Standard uncertainty
k	Coverage factor in the expression of uncertainty
s_L	Inter-laboratory standard deviation
s_r	Intra-laboratory standard deviation divided by the square root of the mean number of replicates
$\hat{\delta}$	Bias of a measurement method
n	Number of replicates
p	Number of laboratories
r	Radius of the 95% confidence circle in the Youden plot
$\hat{\mu}$	Certified reference value
b	Molality, expressed as moles per kilogram of water (mol/kg-H_2O)
ν	Amount content, expressed as moles per kilogram of solution (mol/kg-sol)
T	Temperature (in °C or K, specified in the text)
S	Salinity (the definition used is specified in the text)
I	Ionic strength
b	Slope
t	Time
s	Standard deviation
M	Molar mass (g/mol)
m	Mass (g)
$cov(a,b)$	Covariance between two values
$corr(a,b)$	Correlation between two values
p	Purity of salts (%)

Symbols specific to pH_T measurements	
$e1$, $e2$, $e3$	meta-Cresol Purple molar extinction coefficient ratios
R	Ratio of the absorbance values (equations 1.9)
T_x	Transmittance values
λ	Wavelength (nm)
E	E_{mes} corrected to a pressure of H_2 equal to 1 atm (V)
E_{mes}	Measured potential between Standard Hydrogen electrode and silver-silver-chloride electrode (V)
$E^{\circ *}$	Standard potential of silver-silver chloride electrode in saline media (V)
k	Nernstian term (equation 1.10.c)
P	Measured Pressure (Pa)

p_{vap}	Saturation vapour pressure (Pa)
ρ	Density of the solution (kg/m^3)
g	Standard gravity (m/s^2)
h	Liquid height in the Hydrogen electrode compartment (m)
p°	Standard pressure (101 325 Pa)
E'	Potential of silver-silver chloride electrode in saline media at a given chloride molality ($>$ 0 mol/kg H_2O) (V)
E°	Standard potential of silver-silver chloride electrode in HCl 0.01 mol/kg H_2O (V)
ω_{H2O}	Water mass fraction, expressed as grams per kilogram of solution (g/kg-sol)
$a.f.$	Acidity function
γ	Activity coefficient
γHCl term	$-2\log\left(\frac{\gamma\mathrm{HCl}^{trace}}{\gamma\mathrm{HCl}}\right)$
$Kb(\mathrm{HSO_4^-})$ term	$-\log\left(\frac{1+\frac{b(\mathrm{SO_4^{2-}})}{Kb(\mathrm{HSO_4^-})}}{1+\frac{b^T(\mathrm{SO_4^{2-}})}{Kb(HSO_4^-)^{trace}}}\right)$

Symbols specific to total alkalinity measurements

C_H	Amount content of hydrogen ions (mol/kg-sol)
m_{HCl}	Mass of acid added during titration (g)
C_{HCl}	Acid amount content (mol/kg-sol)
m_{init}	Mass of sample analysed (g).
E	Potential measured by the glass electrode (mV)
E°	Standard potential of the glass electrode (mV)
R	Gas constant (J/molK)
F	Faraday constant (C/mol)
$F1$	$(m_{init} + m_{HCl}) \times \exp\left(\frac{E}{\frac{RT}{F}}\right)$ (equation 4.9)
m_{HCl_GRAN}	Mass of HCl added for which F1 is equal to zero (g), determined with Gran's method.
Z	$1 + \frac{S_T}{K_s}$ (equation 1.18)
f	$[H^+]_T/[H']_T$ (equation 1.18)

Introduction

Depuis le début de la révolution industrielle, dans les années 1800, il est estimé que la concentration en dioxyde de carbone (CO_2) dans l'atmosphère a augmenté de 50%, passant de 280 parties par million (ppm) à 421 ppm (NOAA, 2022). Cette hausse de la concentration en CO_2 est directement liée aux activités humaines : combustion des ressources fossiles, industrie du ciment, changement d'affectation des sols. L'océan est un allié majeur dans la crise climatique actuelle, puisqu'il absorbe chaque année 26% de nos émissions de CO_2 (Friedlingstein et al., 2023). De surcroit, il absorbe 90% de l'excès de chaleur issu du renforcement de l'effet de serre causé par la hausse de la concentration en CO_2 dans l'atmosphère (IPCC, 2019). Cependant, la dissolution du CO_2 dans les eaux marines entraîne des changements dans le système océanique des carbonates, conduisant à l'acidification de l'eau de mer et à la diminution de la concentration en ions carbonate. En impactant la stabilité des formes minérales du carbonate de calcium, ces deux effets entraînent une baisse du taux de biocalcification, une malformation et une dissolution des structures carbonatées, et ont donc un impact sur la biodiversité marine (Rastelli et al., 2020). De nombreuses espèces ayant des structures en carbonate de calcium sont déjà impactées. Parmi celles-ci, on retrouve les coraux, les mollusques, ou les ptéropodes : une espèce de plancton, à la base de la chaîne alimentaire marine.

L'acidification des océans étant un phénomène climatique, il doit être évalué sur des périodes suffisamment longues. Il est estimé que le pH de l'océan de surface a diminué d'au moins 0,1 par rapport aux niveaux préindustriels et le Groupe d'experts intergouvernemental sur l'évolution du climat (GIEC) a estimé une diminution potentielle d'environ 0,4 unité d'ici à 2100 (IPCC, 2019). Ce phénomène est considéré comme l'une des neuf limites planétaires, un concept qui soutient les systèmes de gouvernance internationaux dans un objectif de durabilité mondiale (Rockström et al., 2009).

L'ampleur internationale des causes et des impacts de l'acidification des océans nécessite un système de gouvernance internationale afin de traiter ce problème par des actions politiques. En 2015, les États membres des Nations Unies ont adopté l'Agenda 2030 pour le développement durable, incluant 17 objectifs de développement durable (ODD). Un indicateur de l'ODD 14, « Conserver et exploiter de manière durable les océans, les mers et les ressources marines aux fins du développement durable », vise à réduire au maximum l'acidification des océans et à lutter contre ses effets, notamment en renforçant la coopération scientifique à tous les niveaux (ODD 14.3)(United Nations, 2015).

Les mesures océanographiques in-situ sont à la base du système d'observation du carbone inorganique des océans, conduisant aux évaluations climatiques grâce aux traitement de ces données et au développement de modèles. C'est sur ces éléments que

se basent les rapports des Nations Unies et la prise de décision en matière de stratégies d'atténuation et d'adaptation (Jiang et al., 2023).

L'étude de l'acidification des océans repose sur la surveillance de différentes variables, parmi lesquelles on retrouve la concentration en ions carbonate ou la saturation du carbonate de calcium (sous forme d'aragonite ou de calcite). Ces variables peuvent être calculées à partir de la connaissance de deux des quatre variables du système des carbonates qui sont indépendamment mesurables : le carbone inorganique dissous, l'alcalinité totale, le pH_T et la pression partielle de dioxyde de carbone.

Afin d'établir des tendances à long terme qui soient significatives et avec une confiance suffisante, des recommandations internationales et des guides de bonnes pratiques ont été mis à disposition au cours des dernières décennies. À titre d'exemple, le Réseau mondial d'observation de l'acidification des océans (GOA-ON) a fixé un objectif de qualité des données pour la surveillance de l'acidification des océans, appelé objectif de qualité « climatique ». Il repose sur des cibles d'incertitude pour chacune des variables mesurables afin d'avoir une incertitude standard de 1% sur la concentration en ions carbonate (GOA-ON, 2019). Les exigences de haute qualité des données deviennent d'autant plus importantes que ces données sont partagées dans des bases internationales et sont collectées à des échelles spatiales et temporelles diverses, provenant de nombreuses sources et avec une grande variété d'instruments. Le travail présenté dans cette thèse s'intègre dans ce contexte d'un besoin de haute qualité des données pour la surveillance de l'acidification des océans.

L'objectif global de la thèse est de soutenir les océanographes avec des outils métrologiques permettant de garantir la comparabilité des résultats de mesure. La thèse se concentre sur les mesures de deux des quatre variables mesurables du système des carbonates : le pH_T et l'alcalinité totale. Ces deux paramètres ont été sélectionnés car ils sont déjà largement étudiés et mesurés en laboratoire. Les observations de pH_T ont également été renforcées grâce au développement de capteurs in situ. La nécessité de mesurer l'alcalinité totale pourrait, elle, également augmenter avec le développement des techniques de séquestration du dioxyde de carbone telles que l'alcalinisation des océans. Pour ces deux variables, plusieurs problématiques métrologiques subsistent.

La métrologie est essentielle pour répondre à l'objectif de qualité des données requis par le GOA-ON. En effet, l'évaluation de tendances à long terme implique plusieurs défis métrologiques, tels que la comparabilité des résultats de mesure et l'obtention de faibles incertitudes de mesure. Cet aspect est d'autant plus important compte tenu de la variabilité saisonnière des variables permettant la surveillance de l'acidification des océans. Parmi les principes métrologiques, la traçabilité métrologique est la notion selon laquelle les résultats de mesure peuvent être reliés à une référence unique ("JCGM 200:2012", 2012). Cette référence est de préférence les unités du Système International (SI), représentant la référence la plus stable. Dans certains cas, cela ne peut pas être atteint, par exemple lorsque la procédure de mesure nécessite de faire des approximations qui ne sont pas totalement maîtrisées et dont l'incertitude n'est pas quantifiée. Dans ce cas, la référence à laquelle les mesures finales sont traçables peut

être soit un matériau de référence, soit une procédure de mesure harmonisée. En outre, la validation des procédures de mesure, réalisée par des comparaisons inter-laboratoires (CIL) ou l'utilisation de matériaux de référence, ainsi que l'évaluation des incertitudes de mesure, sont des principes essentiels. L'application de ces trois principes : chaîne de traçabilité, validation des procédures, et estimation des incertitudes, garantit des résultats de mesure fiables et comparables dans le temps et l'espace pour permettre l'évaluation des tendances à long terme. Le but de la thèse est donc d'appliquer ces trois principes à la mesure du pH_T et de l'alcalinité totale de l'eau de mer.

Partie I : Concepts métrologiques appliqués à la mesure du pH_T

La mesure du pH dans l'eau de mer se fait une une échelle totale, notée pH_T, et est décrite par les équations suivantes :

$$pH_T = -\log [H^+]_T \quad (1.6.a)$$

$$[H^+]_T = [H^+]_F \ (1 + S_T/K_S) \approx [H^+]_F + [HSO_4^-] \quad (1.6.b)$$

Où $[H^+]_F$ est la concentration d'ions hydrogène libres en moles par kg de solution, noté mol/kg-sol, S_T la concentration totale d'ions sulfate ($[HSO_4^-] + [SO_4^{2-}]$) (mol/kg-sol), et K_S la constante de dissociation de HSO_4^-.

La mesure du pH_T utilisée par les océanographes est une mesure spectrophotométrique. Elle repose sur l'ajout d'un indicateur coloré, le pourpre de méta-crésol (mCP), dont le spectre d'absorbance varie avec le pH_T de l'échantillon analysé (Clayton and Byrne, 1993; Dickson et al., 2007).

La mesure du rapport des absorbances R aux longueurs d'onde correspondant aux formes basiques et acides de l'indicateur coloré dans l'échantillon permet le calcul du pH_T en utilisant l'équation 1.8.

$$pH_T = -\log(K_2^T e2) + \log\left(\frac{R - e1}{1 - R \times \frac{e3}{e2}}\right) \quad (1.8)$$

Où K_2^T est la seconde constante de dissociation de l'indicateur coloré, et e1, e2 et e3 sont les rapports des coefficients d'extinction molaire de l'indicateur (Liu et al., 2011).

Les mesures de routine reposent sur l'acquisition des valeurs d'absorbance permettant de calculer le rapport R, tandis que les termes $K_2^T e2$, e1 et e3/e2 sont calculés à partir de la caractérisation de l'indicateur coloré disponible dans la littérature (Liu et al., 2011; Loucaides et al., 2017; Müller and Rehder, 2018) pour la salinité et la température correspondant à l'échantillon analysé.

La caractérisation de l'indicateur coloré utilisé pour la mesure spectrophotométrique nécessite l'utilisation de solutions de pH_T connu, qui sont des solutions tampon TRIS, elles-mêmes caractérisées en pH_T par la méthode de mesure potentiométrique réalisée avec des cellules de Harned. Cette méthode de mesure dans l'eau de mer n'étant pas traçable aux unités du Système International (SI), la traçabilité des mesures

spectrophotométrique du pH_T de l'eau de mer est à ce jour établi à la mesure potentiométrique par cellule de Harned (Figure 10).

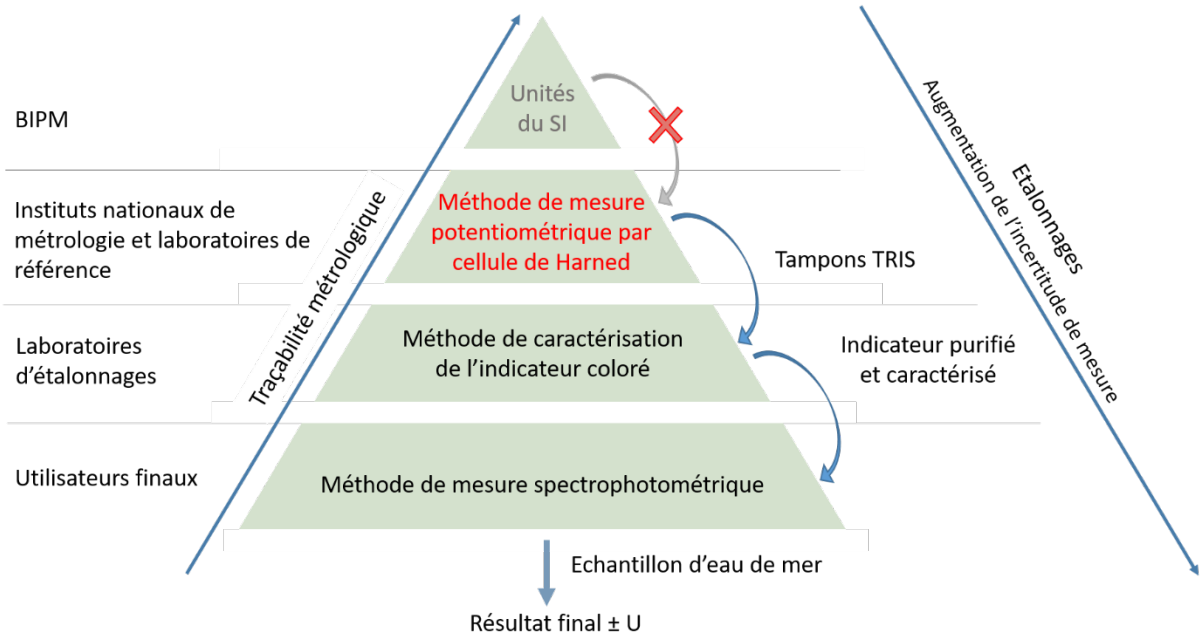

Figure 10 : Chaîne de traçabilité des mesures de pH_T des eaux marines.

Des avancées métrologiques importantes ont été réalisées sur les dernières décennies pour établir la comparabilité des résultats spectrophotométriques du pH_T de l'eau de mer. Cela a été rendu possible par le développement et la distribution de tampons TRIS comme matériaux de référence, la réalisation de comparaisons inter-laboratoires, la standardisation des procédures de mesure et l'estimation préliminaire des incertitudes des résultats de mesure de routine du pH_T. Afin de garantir pleinement la comparabilité de ces résultats, il est nécessaire d'établir de manière approfondie les budgets d'incertitude de (1) la valeur de pH_T attribuée au matériau de référence, en tenant compte de son homogénéité et de sa stabilité, et (2) la valeur de pH_T attribuée aux échantillons d'eau de mer par la méthode spectrophotométrique. De plus, un travail métrologique est également nécessaire pour établir la traçabilité de la méthode spectrophotométrique au SI. Le travail effectué au cours de cette thèse, relatif aux besoins métrologiques mentionnés ci-dessus, est détaillé dans les chapitres II, III et IV.

Chapitre II

Le matériau de référence largement accepté, et le seul disponible à ce jour pour la communauté océanographique, est un tampon TRIS équimolaire avec un pH_T de 8,1 dans une matrice d'eau de mer artificielle de salinité 35. Ce matériau de référence a été reproduit au LNE et caractérisé en utilisant la méthode de mesure potentiométrique avec cellule de Harned. La stabilité et l'homogénéité du matériau produit ont également

été rigoureusement étudiées avec des mesures effectuées à l'aide de cellules de Harned. Le matériau s'est révélé instable, avec une diminution de la fonction d'acidité de -0,0005 par mois. Ce travail a néanmoins permis d'attribuer pour la première fois un budget d'incertitude complet à la valeur de référence de pH_T du tampon TRIS, en tenant compte de la préparation, de la caractérisation, de la stabilité et de l'homogénéité du matériau. Le budget d'incertitude a été établi selon la méthode GUM (Guide to the expression of uncertainty in measurement, "JCGM 100:2008", 2008), c'est-à-dire une approche bottom-up, qui permet d'identifier et quantifier chaque source d'incertitude intervenant dans le processus de mesure. Toutes les étapes ont été réalisées conformément aux normes internationales pour la production de matériaux de référence ("ISO 17034", 2016; "ISO Guide 35", 2018). Le niveau d'incertitude élargie obtenu est de 0,005 en pH_T ($k = 2$) pour une durée de vie de six mois. Ce niveau d'incertitude, étant inférieur aux exigences du GOA-ON pour la surveillance de l'acidification des océans (GOA-ON, 2019), rend le matériau de référence adapté au contrôle de qualité de la méthode de mesure spectrophotométrique de routine du pH_T effectuée par les océanographes.

La principale source d'incertitude a été identifiée comme étant la détermination du potentiel standard des électrodes au chlorure d'argent en milieu salin, $E°^*$. Pour réduire cette incertitude, il est essentiel de veiller à l'homogénéité du lot d'électrodes utilisé. De plus, la définition de la fraction massique d'eau a été identifiée comme un point clé sur lequel un consensus doit être trouvé, car des différences dans la définition peuvent conduire à des écarts de l'ordre de 0,004 en pH_T.

Ce matériau de référence a également été testé lors d'une comparaison interlaboratoire impliquant treize participants, démontrant une bonne précision et justesse (précision de 0,0037 et justesse de 0,0004). Les résultats de la comparaison interlaboratoire ont été utilisés pour calculer une estimation de l'incertitude des résultats de mesure spectrophotométrique du pH_T en suivant l'approche top-down, qui repose sur l'estimation de la justesse et de la précision de la mesure ("ISO 21748", 2017), donnant une incertitude élargie de 0,009 en pH_T.

Chapitre III

Les mesures spectrophotométriques du pH_T reposent sur la caractérisation de la deuxième constante de dissociation de l'indicateur coloré, $K_2^T e2$, obtenue à partir de mesures sur des solutions de pH_T connu. Pour ce faire, des mesures potentiométriques avec cellule de Harned ont été réalisées sur plusieurs tampons TRIS équimolaires. Ces tampons, préparés à diverses molalités de TRIS, ont été réalisés dans une matrice d'eau de mer artificielle avec des salinités allant de 5 à 40, et des mesures avec cellule de Harned ont été effectuées à des températures comprises entre 5°C et 40°C. Cette approche a fourni, pour la première fois, des valeurs de pH_T pour les tampons TRIS cohérentes sur l'ensemble de la gamme de salinité et de température pertinentes pour les mesures océanographiques.

Le travail présenté a compris une évaluation de la reproductibilité réalisée en collaboration avec deux autres instituts de métrologie, donnant un écart-type moyen de 0,002 en pH_T parmi les trois instituts, ainsi qu'une fonction fournissant les valeurs de pH_T des tampons TRIS équimolaires en fonction de la salinité, de la température et de la molalité de TRIS. Cette fonction peut être utilisée pour dériver des valeurs de pH_T pour une molalité de TRIS nulle, recommandée pour représenter de l'eau de mer artificielle pure (c'est-à-dire sans molécule tampon TRIS), se référant ainsi à une véritable échelle de pH total dans l'eau de mer.

Il y a une bonne concordance entre la fonction présentée et les travaux antérieurs rapportés dans la littérature pour des salinités supérieures à 20. Cependant, une divergence significative a été trouvée avec les travaux antérieurs de Müller et al. (2018) pour des salinités plus basses, probablement due à une composition différente de leur eau de mer artificielle. La cohérence de nos résultats avec les travaux de référence de DelValls and Dickson (1998) conforte la validité de cette fonction pour des salinités aussi basses que 5, ainsi que pour l'extrapolation à l'eau de mer artificielle pure.

La fonction fournie, en se référant à une véritable échelle de pH total, constitue une avancée pour améliorer la traçabilité des mesures de pH_T. De plus, l'étude présentée donne des indications sur le travail restant à accomplir pour établir la traçabilité des valeurs de pH_T des tampons TRIS aux unités du SI. Cela nécessitera l'aide d'un modèle de spéciation comme celui développé par Clegg et al. (2022) pour quantifier les approximations appliquées lors des mesures potentiométriques et relier les valeurs de pH_T à leur définition thermodynamique.

Chapitre IV

Les résultats des mesures spectrophotométriques de pH_T n'ont jusqu'à présent pas de budget d'incertitude établi en utilisant l'approche du GUM. Pour remédier à cela, les sources d'incertitude affectant la mesure ont été identifiées. Il a été souligné que le processus de mesure dépend fortement des valeurs d'absorbance. Par conséquent, le budget d'incertitude pour les valeurs d'absorbance utilisées pour la mesure de pH_T dans un échantillon d'eau de mer a été quantifié, en utilisant les données de la calibration du spectrophotomètre. La corrélation entre ces valeurs a été soigneusement étudiée. Cette analyse a permis de calculer l'incertitude du rapport d'absorbance R, qui est utilisé pour la détermination ultérieure du pH_T (équation 1.8).

À partir de ces informations, un niveau d'incertitude minimal préliminaire pour les résultats de mesure de pH_T a été calculé, donnant une incertitude élargie de 0,02 ($k = 2$). La justesse des mesures d'absorbance a été identifié comme la principale source d'incertitude dans le rapport R. La calibration du spectrophotomètre avec des filtres de densité optique ayant des incertitudes plus faibles devrait aider à réduire cette incertitude. L'incertitude introduite par la méthode de correction, appliquée pour prendre en compte la perturbation du pH_T de l'échantillon lors de l'ajout de l'indicateur coloré, doit également être examinée.

Partie II : Concepts métrologiques appliqués à la mesure de l'alcalinité totale

L'alcalinité totale peut être décrite de façon simplifiée comme étant la capacité tampon de l'eau de mer, soit sa capacité à absorber les variations d'acidité. Elle est précisément définie comme le nombre de moles d'ions hydrogène équivalant à l'excès de d'accepteurs de protons (bases formées à partir d'acides faibles avec une constante de dissociation $K \leq 10^{-4,5}$, à 25°C et à force ionique nulle) sur les donneurs de protons (acides avec $K > 10^{-4,5}$, mêmes conditions) dans un kilogramme d'échantillon. L'alcalinité totale est décrite par l'équation suivante :

$$TA = [HCO_3^-] + 2[CO_3^{2-}] + [B(OH)_4^-] + [OH^-] + [HPO_4^{2-}] + 2[PO_4^{3-}] + [SiO(OH)_3^-] + [NH_3] + [HS^-] + [\dots] - [H^+]_F - [HSO_4^-] - [HF] - [H_3PO_4] - [\dots] \quad (1.11)$$

Où les crochets représentent les concentrations (mol/kg-sol) et les points de suspension les espèces mineures, non-identifiées ou négligeables.

La méthode de mesure standard pour la détermination de l'alcalinité totale de l'eau de mer est un titrage potentiométrique en plusieurs étapes. Elle consiste à suivre le pH de l'échantillon d'eau de mer analysé, titré avec un acide fort (HCl), afin d'identifier le point d'équivalence où tous les accepteurs de protons ont été consommés (Wolf-Gladrow et al., 2007). À ce point d'équivalence, la concentration des accepteurs de protons est donc égale à celle des donneurs de protons et l'alcalinité totale est égale à zéro. L'alcalinité totale est finalement reliée à la quantité d'acide ajoutée pour atteindre le point d'équivalence. La méthode de Gran est utilisée pour calculer l'alcalinité totale à partir des données de la titration, à laquelle peut être ajoutée une régression non linéaire des moindres carrés permettant de prendre en compte la matrice et les systèmes acide-base de la solution.

Le développement de matériaux de référence par le Scripps Institution of Oceanography a permis d'établir une organisation robuste pour la production, la caractérisation et la distribution de matériaux de référence (MR) qui soutiennent la communauté océanographique mondiale dans l'amélioration de la qualité et de la comparabilité des résultats de mesure de l'alcalinité totale. Cependant, les MR distribués ne sont pas totalement traçables et ne sont pas accompagnés d'une incertitude associée à la valeur de référence. Développer un matériau de référence fabriqué dans une eau de mer artificielle, caractérisé par une méthode de référence traçable, et avec une incertitude rigoureusement quantifiée, qui pourrait être distribué conjointement avec une eau de mer naturelle comme celle de Scripps, pourrait aider à améliorer la justesse des résultats. De plus, le budget d'incertitude des résultats de la méthode de mesure est nécessaire pour assurer la comparabilité des mesures d'alcalinité totale. Les travaux

relatifs à ces défis métrologiques menés pendant la thèse sont présentés dans le Chapitre V.

Chapitre V

Deux matériaux de référence ont été produits pour la méthode de mesure de l'alcalinité totale (AT) :

(1) Un matériau de référence artificiel, composé d'ions carbonate et bicarbonate dans une matrice NaCl, avec une valeur de référence caractérisée étant potentiellement traçable aux unités SI. La valeur de référence est fournie avec un budget d'incertitude complet établi selon les recommandations internationales pour la production de matériaux de référence. Ce budget d'incertitude intègre l'incertitude provenant de l'alcalinité résiduelle provenant des impuretés du NaCl, introduite lors de la préparation du matériau de référence. La valeur de référence est de 2503,6 ± 2,2 µmol/kg (k = 2), pour une durée de vie de trois mois.
(2) Une eau de mer naturelle stabilisée prélevée en Méditerranée. La valeur de référence de ce matériau peut être attribuée par des laboratoires de référence.

Les deux matériaux ont fait l'objet d'études d'homogénéité et de stabilité et ont été testés dans le cadre d'une comparaison inter-laboratoires impliquant cinq laboratoires, démontrant leur applicabilité aux contrôles qualité des mesures d'AT. Le biais obtenu est de -2,56 ± 2,44 µmol/kg (k = 2) et la précision de 1,99 µmol/kg pour le matériau artificiel.

Le budget d'incertitude pour la méthode de titration potentiométrique multi-étapes utilisant le traitement des données de Gran a été examiné en utilisant à la fois les approches top-down et bottom-up pour la quantification de l'incertitude. Les deux approches ont donné des niveaux d'incertitude similaires pour les résultats d'AT, avec une incertitude élargie de 5 µmol/kg.

De plus, une route de traçabilité proposée pour les résultats de mesure d'AT, impliquant les deux matériaux de référence développés, a été détaillée (Figure 32). Dans cette route de traçabilité, le matériau de référence artificiel peut être utilisé pour valider la méthode de mesure utilisée avec le traitement des données de Gran des laboratoires de référence, leur permettant d'attribuer de manière robuste une valeur de référence d'AT à un matériau de référence d'eau de mer naturelle. Les utilisateurs finaux peuvent ensuite utiliser, d'une part, le matériau de référence artificiel pour attribuer une concentration à leur acide titrant, et d'autre part, le matériau de référence d'eau de mer naturelle pour valider leur méthode de mesure, conjointement avec le traitement des données par régression non linéaire des moindres carrés. L'établissement de l'incertitude provenant de cette régression sera nécessaire pour compléter la route de traçabilité.

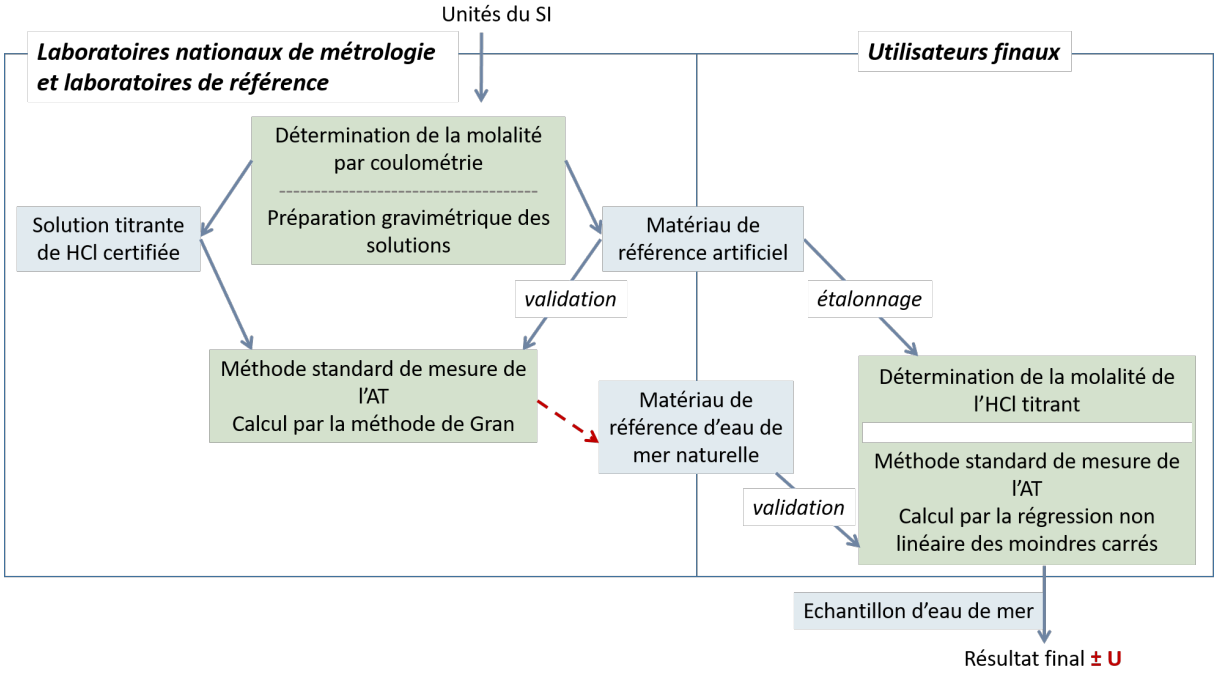

Figure 32 : Chaîne de traçabilité proposée pour les résultats de la mesure de l'alcalinité totale. Les cases bleues correspondent aux solutions et les cases vertes aux processus de mesure. Les signes en rouge mettent en évidence les tâches restantes dans l'objectif d'établir la traçabilité aux unités SI des résultats des utilisateurs finaux.

Conclusion et perspectives

Les routes de traçabilités du pH_T et de l'alcalinité totale ont été améliorées. La route de traçabilité pour le pH total est actuellement établie par la méthode de mesure potentiométrique avec les cellules de Harned, utilisée pour caractériser les tampons TRIS. En reliant les valeurs de pH_T des tampons TRIS à une matrice d'eau de mer artificielle pure, établissant ainsi une véritable échelle de pH_T, sur la plage de salinité et de température pertinente pour les mesures océanographiques (S 5-40 et T 5°C-40°C), le travail présenté au chapitre III a amélioré la route de traçabilité. Une route de traçabilité améliorée pour les mesures d'alcalinité totale est également proposée au chapitre V, basée sur le développement de deux matériaux de référence. Assurer la comparabilité des résultats de mesure dans le temps et l'espace nécessitera d'établir la traçabilité métrologique aux unités SI, fournissant la référence la plus stable.

Pour les deux paramètres, des matériaux de référence ont été produits (chapitres II et V). L'adéquation de ces matériaux pour le contrôle qualité des méthodes de mesure des utilisateurs finaux a été étudiée par le biais d'exercices de comparaison inter-laboratoires. Les matériaux de référence artificiels pour chaque paramètre ont été produits selon les normes internationales. Les valeurs de référence de ces matériaux artificiels sont (1) traçables au plus haut standard international établi à ce jour et (2) fournies avec des budgets d'incertitude complets établis selon l'approche du GUM. Mettre les matériaux de référence développés à la disposition de la communauté océanographique est une perspective cruciale. Au-delà de la nécessité d'une capacité de

production, la première étape consistera à trouver un moyen d'améliorer la stabilité des matériaux.

Les budgets d'incertitude pour les méthodes de mesure standardisées de pH_T et d'AT ont été étudiés en utilisant à la fois les approches bottom-up et top-down (chapitres II, IV et V). Les incertitudes établies selon l'approche top-down ont fourni une estimation du budget d'incertitude pour la méthode de mesure complète. Il faut noter que le budget fourni pour la mesure d'AT correspond à la méthode de mesure standardisée avec le traitement des données de la méthode de Gran. Seuls des budgets partiellement complets ont été établis en utilisant l'approche bottom-up en raison de l'absence actuelle d'estimation des incertitudes provenant des échantillons et des utilisateurs. De plus, des informations supplémentaires correspondant à l'étape de caractérisation de l'indicateur coloré seront nécessaires à l'établissement du budget d'incertitude de la mesure du pH_T. L'approche bottom-up a tout de même fourni des informations précieuses sur le niveau minimal d'incertitude atteint et les principales sources contribuant aux budgets globaux. Cela met en évidence les points qui nécessitent des travaux supplémentaires. La propagation de ces niveaux d'incertitude a conduit à une incertitude standard sur la concentration en ions carbonates de 1% pour les budgets évalués avec l'approche top-down et de 2% avec les niveaux minimaux établis selon l'approche bottom-up. Il sera nécessaire de finaliser l'évaluation rigoureuse des incertitudes, cependant ce résultat est très encourageant dans l'obtention d'une qualité des données suffisante pour le suivi de l'acidification des océans.

Le développement et l'amélioration des outils métrologiques pour mesurer le pH_T et l'alcalinité totale de l'eau de mer ont conduit à des avancées significatives pour la qualité des données et la comparabilité des résultats de mesure. Avec l'éventualité du développement de l'alcalinisation des océans, une technique de géo-ingénierie étudiée pour son potentiel de séquestration du dioxyde de carbone, des besoins spécifiques en matière de qualité des données et d'outils métrologiques pourraient également émerger.

Références

Clayton, T.D., Byrne, R.H., 1993. Spectrophotometric seawater pH measurements: total hydrogen ion concentration scale calibration of m-cresol purple and at-sea results. Deep Sea Research Part I: Oceanographic Research Papers 40, 2115–2129. https://doi.org/10.1016/0967-0637(93)90048-8

Clegg, S.L., Humphreys, M.P., Waters, J.F., Turner, D.R., Dickson, A.G., 2022. Chemical speciation models based upon the Pitzer activity coefficient equations, including the propagation of uncertainties. II. Tris buffers in artificial seawater at 25 °C, and an assessment of the seawater 'Total' pH scale. Marine Chemistry 244, 104096. https://doi.org/10.1016/j.marchem.2022.104096

DelValls, T.A., Dickson, A.G., 1998. The pH of buffers based on 2-amino-2-hydroxymethyl-1,3-propanediol ('tris') in synthetic sea water. Deep Sea Research Part I: Oceanographic Research Papers 45, 1541–1554. https://doi.org/10.1016/S0967-0637(98)00019-3

Dickson, A.G., Sabine, C.L., Christian, J.R. (Eds.), 2007. Guide to Best Practices for Ocean CO2 Measurements PICES Special Publication 3, 191.

Friedlingstein, P., O'Sullivan, M., Jones, M.W., Andrew, R.M., Bakker, D.C.E., Hauck, J., Landschützer, P., Le Quéré, C., Luijkx, I.T., Peters, G.P., Peters, W., Pongratz, J., Schwingshackl, C., Sitch, S., Canadell, J.G., Ciais, P., Jackson, R.B., Alin, S.R., Anthoni, P., Barbero, L., Bates, N.R., Becker, M., Bellouin, N., Decharme, B., Bopp, L., Brasika, I.B.M., Cadule, P., Chamberlain, M.A., Chandra, N., Chau, T.-T.-T., Chevallier, F., Chini, L.P., Cronin, M., Dou, X., Enyo, K., Evans, W., Falk, S., Feely, R.A., Feng, L., Ford, D.J., Gasser, T., Ghattas, J., Gkritzalis, T., Grassi, G., Gregor, L., Gruber, N., Gürses, Ö., Harris, I., Hefner, M., Heinke, J., Houghton, R.A., Hurtt, G.C., Iida, Y., Ilyina, T., Jacobson, A.R., Jain, A., Jarníková, T., Jersild, A., Jiang, F., Jin, Z., Joos, F., Kato, E., Keeling, R.F., Kennedy, D., Klein Goldewijk, K., Knauer, J., Korsbakken, J.I., Körtzinger, A., Lan, X., Lefèvre, N., Li, H., Liu, J., Liu, Z., Ma, L., Marland, G., Mayot, N., McGuire, P.C., McKinley, G.A., Meyer, G., Morgan, E.J., Munro, D.R., Nakaoka, S.-I., Niwa, Y., O'Brien, K.M., Olsen, A., Omar, A.M., Ono, T., Paulsen, M., Pierrot, D., Pocock, K., Poulter, B., Powis, C.M., Rehder, G., Resplandy, L., Robertson, E., Rödenbeck, C., Rosan, T.M., Schwinger, J., Séférian, R., Smallman, T.L., Smith, S.M., Sospedra-Alfonso, R., Sun, Q., Sutton, A.J., Sweeney, C., Takao, S., Tans, P.P., Tian, H., Tilbrook, B., Tsujino, H., Tubiello, F., van der Werf, G.R., van Ooijen, E., Wanninkhof, R., Watanabe, M., Wimart-Rousseau, C., Yang, D., Yang, X., Yuan, W., Yue, X., Zaehle, S., Zeng, J., Zheng, B., 2023. Global Carbon Budget 2023. Earth System Science Data 15, 5301–5369. https://doi.org/10.5194/essd-15-5301-2023

GOA-ON, 2019. Global Ocean Acidification Observing Network (GOA-ON): Implementation Strategy.

IPCC, 2019. 2019: Technical Summary In: IPCC Special Report on the Ocean and Cryosphere in a Changing Climate [H.-O. Pörtner, D.C. Roberts, V. Masson-Delmotte, P. Zhai, M. Tignor, E. Poloczanska, K. Mintenbeck, A. Alegría, M. Nicolai, A. Okem, J. Petzold, B. Rama, N.M. Weyer (eds.)]. Cambridge University Press, Cambridge, UK and New York, NY, USA, pp. 39–69. https://doi.org/10.1017/9781009157964.002

ISO 17034, 2016. General requirements for the competence of reference material producers.

ISO 21748, 2017. Guidance for the use of repeatability, reproducibility and trueness estimates in measurement uncertainty evaluation.

ISO Guide 35:2017 Reference materials — Guidance for characterization and assessment of homogeneity and stability, 2017.

JCGM 100:2008, 2008. Evaluation of Measurement Data-Guide to the Expression of Uncertainty in Measurement.

JCGM 200:2012, 2012. International vocabulary of metrology (VIM) — Basic and general concepts and associated terms.

Jiang, L.-Q., Kozyr, A., Relph, J.M., Ronje, E.I., Kamb, L., Burger, E., Myer, J., Nguyen, L., Arzayus, K.M., Boyer, T., Cross, S., Garcia, H., Hogan, P., Larsen, K., Parsons, A.R., 2023. The Ocean

Carbon and Acidification Data System. Sci Data 10, 136. https://doi.org/10.1038/s41597-023-02042-0

Liu, X., Patsavas, M.C., Byrne, R.H., 2011. Purification and Characterization of meta-Cresol Purple for Spectrophotometric Seawater pH Measurements. Environmental science & Technology 4862–4868.

Loucaides, S., Rèrolle, V.M.C., Papadimitriou, S., Kennedy, H., Mowlem, M.C., Dickson, A.G., Gledhill, M., Achterberg, E.P., 2017. Characterization of meta-Cresol Purple for spectrophotometric pH measurements in saline and hypersaline media at sub-zero temperatures. Sci Rep 7, 2481. https://doi.org/10.1038/s41598-017-02624-0

Müller, J.D., Bastkowski, F., Sander, B., Seitz, S., Turner, D.R., Dickson, A.G., Rehder, G., 2018. Metrology for pH Measurements in Brackish Waters—Part 1: Extending Electrochemical pHT Measurements of TRIS Buffers to Salinities 5–20. Front. Mar. Sci. 5, 176. https://doi.org/10.3389/fmars.2018.00176

Müller, J.D., Rehder, G., 2018. Metrology of pH Measurements in Brackish Waters—Part 2: Experimental Characterization of Purified meta-Cresol Purple for Spectrophotometric pHT Measurements. Front. Mar. Sci. 0. https://doi.org/10.3389/fmars.2018.00177

NOAA, 2022. Carbon dioxide now more than 50% higher than pre-industrial levels [WWW Document]. noaa.gov. URL https://www.noaa.gov/news-release/carbon-dioxide-now-more-than-50-higher-than-pre-industrial-levels (accessed 11.18.22).

Rastelli, E., Petani, B., Corinaldesi, C., Dell'Anno, A., Lo Martire, M., Cerrano, C., Danovaro, R., 2020. A high biodiversity mitigates the impact of ocean acidification on hard-bottom ecosystems. Sci Rep 10, 2948. https://doi.org/10.1038/s41598-020-59886-4

Rockström, J., Steffen, W., Noone, K., Persson, Å., Chapin, F.S.I., Lambin, E., Lenton, T., Scheffer, M., Folke, C., Schellnhuber, H.J., Nykvist, B., de Wit, C., Hughes, T., van der Leeuw, S., Rodhe, H., Sörlin, S., Snyder, P., Costanza, R., Svedin, U., Falkenmark, M., Karlberg, L., Corell, R., Fabry, V., Hansen, J., Walker, B., Liverman, D., Richardson, K., Crutzen, P., Foley, J., 2009. Planetary Boundaries: Exploring the Safe Operating Space for Humanity. Ecology and Society 14 (2), art32. https://doi.org/10.5751/ES-03180-140232

United Nations, 2015. Transforming our world: the 2030 Agenda for Sustainable Development A/RES/70/1.

Wolf-Gladrow, D.A., Zeebe, R.E., Klaas, C., Körtzinger, A., Dickson, A.G., 2007. Total alkalinity: The explicit conservative expression and its application to biogeochemical processes. Marine Chemistry 106, 287–300. https://doi.org/10.1016/j.marchem.2007.01.006